Clinical delineation and immunopathogenesis of autoimmune encephalitis

James Alexander Varley

A thesis submitted for the degree of Doctor of Philosophy



Somerville College

University of Oxford

Hilary Term 2019

Abstract

CLINICAL DELINEATION AND IMMUNOPATHOGENESIS OF AUTOIMMUNE ENCEPHALITIS by JAMES A VARLEY, SOMERVILLE COLLEGE, HILARY TERM 2019. Submitted for the degree of DPhil.

Neuroglial surface antibody (NSAb)-mediated diseases are autoimmune brain diseases including autoimmune encephalitis (AE). Early immunotherapy improves outcome making prompt diagnosis crucial. In N-methyl D-aspartate receptor antibody encephalitis (NMDAR-AbE), improved description of the associated movement disorder (MD) should aid early recognition. Similarly, clarifying the purported association between NMDAR-antibodies and systemic lupus erythematosus (SLE) would help clinicians. Finally, the underlying immunology in patients with AE secondary to leucine-rich glioma inactivated protein-1 (LGI1) and contactin-associated protein-like 2 (CASPR2) antibodies remains unexplored and a likely source of novel, targeted immunotherapies.

To improve recognition, MD experts rated 76 videos of 34 patients with NMDAR-AbE. The associated MD was described as a characteristic triad of dystonia, chorea and stereotypy, distributed across the body and variable over time. Patients with NMDAR-AbE are defined by the presence of conformationally-sensitive autoantibodies, these were not found in patients with neuropsychiatric SLE. In fact, existing linear protein assay techniques demonstrated high artefact rates. This suggested a lack of autoantibodies with pathogenic potential in NPSLE.

In a different form of AE, a novel class II HLA association was demonstrated in 48% of CASPR2-antibody patients (HLA-DRB1*11:01, n=31) and a known association was confirmed in 91% of LGI1-antibody patients (HLA-DRB1*07:01, n=68). This suggested an important role for T helper cells and, experimentally, evidence was found of antigen-specific T cells in these patients. Individuals with CASPR2-antibodies and HLA-DRB1*11:01 had higher autoantibody titres and less clinical improvement with immunotherapy. Lymphocytes from these patients, when cultured, produced CASPR2-antibody matching serum CASPR2-antibody subclass and epitope-specificity. However, a marker of germinal centre activity, serum CASPR2-IgM, was seen only rarely. CASPR2-antibody patients carrying HLA-DRB1*11:01 produced more autoantibody in culture and to a wider range of CASPR2-epitopes in culture and serum. This may explain the poorer response to immunotherapy seen in these patients, highlighting the B-T cell interface as a key therapeutic target.

Acknowledgments

As a clinician, being able to spend three and a half years working towards a higher scientific degree has been a huge privilege and I am grateful to the ABN, Guarantors of Brain and OBRC for their funding and support. This involved a steep learning curve and I was greatly aided in my early days by Beth Lang, Angela Vincent, Mark Woodhall and Matteo Gastaldi. They were generous with their time despite not having much, so thank you.

As the project became more immunology-focussed, I was lucky enough to be part of a growing B cell laboratory with world class colleagues like Mateusz Makuch, Bob Wilson, Valentina Damato, Anne-Kathrin Kienzler, Adam Al-Diwani, Sophie Binks, Andrew Fower, Ronan McGinty and Jenny Taylor. Special thanks must go to Mateusz, Anne-Kathrin and Bob for being so kind, patient and selfless in their sharing of the mysteries of Immunology with me. In the latter phases of my DPhil I worked closely with Sophia Michael, Selina Thomsen and Melanie Ramberger, all of whom were brilliant, kind and fun colleagues and a pleasure to spend time in the laboratory with.

Sarosh Irani, my principal supervisor, has dedicated hundreds of hours to my development and I will always owe him a debt of gratitude for his generosity. Sarosh, as well as my other supervisor Patrick Waters, have provided hard work, support and intelligence which has helped me to produce a body of work I feel very proud of and it is certainly something I could not have done without them.

I would like to thank my parents, for getting me interested in science and supporting me always. Finally, I would like to thank Freya, for her congratulations in the good times, commiseration in the bad times and all the Rolo Yoghurts.

Table of contents

1 GENERAL INTRODUCTION 14

1.1 Autoimmune disease 14
1.2 Antibody mediated autoimmune brain disease 22
1.3 N-methyl-D-aspartate receptor antibody encephalitis (NMDAR-AbE) 23
1.3.1 Original description and demographics 23
1.3.2 Clinical presentation 24
1.3.3 Investigations 24
1.3.4 Immunology 25
1.3.5 Antibody mediated pathogenesis 27
1.3.6 Treatment 29
1.3.7 Controversies over the spectrum of NSAb mediated disease 29
1.4 Leucine-rich glioma inactivated-1 (LGI1) and contactin-associated protein-like 2 (CASPR2) antibodies 30
1.5 LGI1-antibody patients 32
1.5.1 Demographics 32
1.5.2 Clinical presentation 32
1.5.3 Pathogenesis 33
1.5.4 Treatment 34
1.6 CASPR2-antibody patients 35
1.6.1 Demographics 35
1.6.2 Clinical presentation 35
1.6.3 Mechanism of action 36
1.6.4 Treatment 38
1.7 Summary and aims 39

2 METHODS 41

2.1 Cell Culture 41
2.1.1 Human Embryonic Kidney 293 cells 41
2.1.2 Primary hippocampal neuronal cultures 41
2.2 Transfection of HEK293 cells 42
2.3 Immunocytochemistry 43
2.3.1 CBA 43
2.3.2 Neuronal staining 44
2.4 Fluorescent immunoprecipitation assay (FIPA) 44
2.5 Peripheral blood mononuclear cell (PBMC) isolation, cryopreservation and resuspension 45

3 THE UNIQUE MOVEMENT DISORDER ASSOCIATED WITH NMDA RECEPTOR ANTIBODY ENCEPHALITIS 47

3.1 Introduction 47
3.2 Methods 49
3.2.1 Patient Selection 49
3.2.2 Video Editing 49
3.2.3 Movement disorder classification 50
3.2.4 Statistical Analysis 50
3.3 Description of cohort 50
3.4 Video evaluation of MD 52
3.4.1 Phenomenologies predominant in NMDAR-AbE MD 52
3.4.2 Co-association of MDs in NMDAR-AbE 53
3.5 Temporal variability 56
3.6 Regional distribution of movement disorder 57
3.7 Discussion 58

4 THE ROLE OF ANTIBODIES IN NEUROPSYCHIATRIC SYSTEMIC LUPUS ERYTHEMATOSUS 62

4.1 Introduction 62
4.2 Methods 65
4.2.1 Patient selection 65
4.2.2 DWEYS Enzyme Linked Immunosorbent Assay (ELISA) 65
4.2.3 IFN-α SIMOA 66
4.3 Cohort description 66
4.4 Screening for binding on native conformational epitopes 68
4.4.1 Antibodies in cohort plasma or CSF do not bind extracellular domains of natively expressed NR1, NR2A or NR2B on CBA 68
4.4.2 SLE plasma/CSF does not bind cultured primary rodent hippocampal neurons 69
4.5 DWEYS ELISA assay experiments 71
4.5.1 DWEYS ELISA set up and optimisation 71
4.5.2 DWEYS ELISA Plasma/CSF results in cohorts 72
4.5.3 Cohort plasma/CSF results on IgG ELISA without peptide coating and on scrambled peptide 75
4.6 IFN-α in SLE and NPSLE 77
4.6.1 IFN-α SIMOA results in plasma and CSF 77
4.6.2 Clinical and paraclinical correlations with IFNα results 80
4.7 Discussion 81

5 HLA ASSOCIATIONS IN LGI1- AND CASPR2-ANTIBODY MEDIATED NEUROLOGICAL DISEASES 86

5.1 Introduction 86
5.2 Methods 87
5.2.1 Patients 87
5.2.2 Genotyping, HLA imputation, verification and multi-locus haplotype-block construction. 88
5.2.3 Statistical analyses 89
5.3 CASPR2-, LGI1- and VGKC-antibody patient clinical description 89
5.4 CASPR2- and LGI1-antibody patient HLA associations 93
5.4.1 HLA allelic associations in LGI1-, CASPR2-, VGKC- and double-antibody positive patients. 93
5.4.2 HLA haplotype associations in CASPR2- and LGI1-antibody patients 96
5.5 Associations between HLA and clinical features in CASPR2- and LGI1-antibody patients 97
5.6 Associations between HLA and biochemical features in patients with CASPR2-antibody mediated neurological disease 100
5.6.1 CASPR2-antibody live CBA 100
5.6.2 FIPA 102
5.7 Discussion 106

6 THE B CELL IMMUNOLOGY OF PATIENTS WITH CASPR2-ANTIBODIES 111

6.1 Introduction 111
6.2 Methods 114
6.2.1 Patients 114
6.2.2 PBMC culture 114
6.2.3 B cell subclass sorting and culture 115
6.2.4 Pan IgG and subclass ELISAs 116
6.2.5 Multiplex flow cytometry assay 116
6.2.6 CXCL13 ELISA 117
6.2.7 Statistics 117
6.3 CASPR2-antibody subclass flow cytometry assay optimisation and cohort results 117
6.3.1 Subclass flow assay optimisation 117
6.3.2 CASPR2-antibody patient serum IgG subclass analysis 124
6.3.3 CASPR2-antibody patient serum IgM and IgE antibodies 126

6.4 CASPR2-antibody patient PBMC matrix cultures – Total, specific IgG and clinical correlations 128
6.5 CASPR2-antibody patient PBMC matrix cultures – IgG subclass characteristics and comparisons 135
6.6 CASPR2-antibody patient PBMC matrix cultures - Serial cultures 143
6.7 CASPR2-antibody patient PBMC matrix cultures - Epitope specificities and effect of HLA allele expression 146
6.8 CASPR2-antibody patient serum epitope quantification in the context of HLA allele expression 151
6.9 Discussion 154

7 CASPR2- AND LGI1-ANTIBODY PATIENT T CELL IMMUNOLOGY 165

7.1 Introduction 165
7.2 Methods 167
7.2.1 HLA-peptide binding prediction 167
7.2.2 Patient recruitment 167
7.2.3 T cell proliferation assay 168
7.3 In silico peptide prediction 169
7.4 Clinical description of cohort 171
7.5 Optimisation of T cell proliferation assay 173
7.5.1 T cell proliferation protocol – optimisation 173
7.5.2 Successful T cell proliferation to LGI1 peptides in an LGI1-antibody patient 175
7.6 Cohort-wide responses to relevant stimulating peptides 179
7.7 Discussion 184

8 CONCLUSIONS 187

9 REFERENCES 191

10 APPENDIX 206

10.1 Appendix A 206
10.2 Appendix B 211

List of figures

Figure 1-1 Recombination of heavy and light chain variable regions 16
Figure 1-2 B cell maturation and activation via germinal centre reaction..... 21
Figure 1-3 CASPR2 associates with dimerised contactin-2 to contribute to clustering of voltage-gated potassium channels in the juxtaparanode..... 37
Figure 3-1 Symptom onset and offset in NMDAR-AbE 52
Figure 3-2 Expert classification of dominant MD phenomenology in NMDAR-AbE 53
Figure 3-3 Co-occurrence of NMDAR-AbE MD phenomenologies in dominant MDs 55
Figure 3-4 NMDAR AbE predominant MDs and co-occurrences - dominant and associated MDs included 56
Figure 3-5 Temporal variation in NMDAR AbE MD 57
Figure 3-6 Regional distribution of MD in NMDAR-AbE 58
Figure 4-1 Crystal Structure of NMDAR, with location of DWEYS (AA284-287) sequence highlighted in red. 64
Figure 4-2 Cell based assay of serum and CSF from patients with NPSLE and SLE 69
Figure 4-3 Antibodies in SLE plasma and CSF do not bind primary rodent hippocampal neurons 70
Figure 4-4 Optimisation of DWEYS IgG ELISA..... 72
Figure 4-5 Plasma and CSF DWEYS IgG ELISA results from cohorts 74
Figure 4-6 Cohort binding on uncoated ELISA plates vs DWEYS coated ELISA plates 75
Figure 4-7 Scrambled peptide ELISA results using cohort SLE samples 76
Figure 4-8 Plasma vs CSF DWEYS 77
Figure 4-9 IFNα SIMOA results from SLE cohort: correlation between plasma and CSF 78
Figure 4-10 IFNα full cohort results, plasma and CSF 79
Figure 4-11 Correlation between plasma and CSF DWEYS and IFNα 80
Figure 4-12 Clinical and paraclinical associations of plasma and CSF IFNα. 81
Figure 5-1 Comparison of HLA alleles between LGI1-, CASPR2-antibody and healthy control (HC) cohorts..... 95
Figure 5-2 Comparison between LGI1- and CASPR2-antibody double positive antibody patients, VGKC only patients and HCs. 96
Figure 5-3 Comparison of HLA haplotypes between LGI1-, CASPR2-antibody and healthy control (HC) cohorts..... 97
Figure 5-4 Improvement in mRS compared between CASPR2-antibody associated HLA allele and haplotypes 99
Figure 5-5 Cell based assay end titre in CASPR2-antibody patients, compared by HLA risk allele or haplotype expression 101
Figure 5-6 Optimisation of CASPR2-antibody fluorescent immunoprecipitation assay (FIPA)..... 103
Figure 5-7 CASPR2-antibody FIPA correlation with CBA and comparison of quantification by HLA allele and haplotype 104
Figure 5-8 CBA end titre versus FIPA FU in low positive or non-immune patients 106
Figure 6-1 Literature review of cytokines associated with autoimmune encephalitis 113
Figure 6-2 Multiplex versus separate IgG subclass flow cytometry assay 118
Figure 6-3 Multiplex IgG subclass flow cytometry assay gating example 119

Figure 6-4 Multiplex flow cytometry assay optimisation – assessment of steric inhibition of multiplexed IgG subclass secondaries. 120
Figure 6-5 Multiplex flow cytometry assay - cell number and titration optimisation . 122
Figure 6-6 Comparison of multiplex flow cytometry assay to established methods of antibody quantification 123
Figure 6-7 Cohort serum CASPR2-IgG subclasses 125
Figure 6-8 CASPR2 IgM flow cytometry assay gating and example plots 127
Figure 6-9 Serum CASPR2 IgM over time 128
Figure 6-10 Production of CASPR2 IgG from cultured PBMCs 131
Figure 6-11 The effect of In vitro inhibition of MTX using folinic acid (FA) on the production of total IgG and CASPR2 specific IgG MTX-treated CASPR2-antibody patient's PBMCs. 132
Figure 6-12 Comparison of total IgG production in culture between CASPR2-antibody patients and HCs 134
Figure 6-13 Clinical correlations of CASPR2 IgG production in vitro 135
Figure 6-14 Subclass comparison between serum and supernatant produced CASPR2 specific IgG and total IgG 136
Figure 6-15 Total IgG subclass ratio across different stimulating cytokine conditions 138
Figure 6-16 Total IgG subclass production from subclass sorted B cells 140
Figure 6-17 CASPR2 IgG subclass comparison between serum and SN, corrected for total subclass IgG 142
Figure 6-18 Serial PBMC matrix cultures from CASPR2-antibody patients (n=4) 146
Figure 6-19 CASPR2 N-terminal domain and C-terminal domain mutant constructs .. 147
Figure 6-20 CASPR2 IgG N-terminal domain and C-terminal domain reactivity in serum and SN 148
Figure 6-21 Relationship between CASPR2 IgG epitopes over time in individuals 150
Figure 6-22 HLA DRB1*11:01 associations and amounts of CASPR2-antibody in serum measured by multiplex flow cytometry assay. 151
Figure 6-23 CASPR2-antibody epitope specificities divided by HLA DRB1*11:01 carrier status against FL CASPR2, NTD CASPR2 and CTD CASPR2 153
Figure 7-1 Dendritic cell uptake of antigen, processing and presentation to T cells via Class II HLA molecules 166
Figure 7-2 In silico LGI1 and CASPR2 peptide-HLA associations 170
Figure 7-3 T cell proliferation assay protocol 174
Figure 7-4 Gating strategy for flow cytometry analysis of proliferated T cells 174
Figure 7-5 Optimisation of media used for T cell proliferation assay and assessment of the effect of DMSO on cell viability 175
Figure 7-6 Successful expansion of CD4+ memory T cells with LGI1 peptides 176
Figure 7-7 Fresh versus frozen PBMC T cell proliferation assay comparison 177
Figure 7-8 T cell proliferation in the presence of anti-HLA DR antibody 178
Figure 7-9 Cohort responses to stimulating peptides derived from FL LGI1 (L1-9) and CASPR2 (C1-8) 181
Figure 7-10 Comparison of the proliferation of CD4+ T cells in DMSO only conditions 183
Figure 7-11 Effects of clinical and sample conditions on T cell proliferation 183

List of tables

Table 3-1 Description of MD associated with NMDAR-AbE in different series. 48
Table 3-2 Clinical and paraclinial details of NMDAR-AbE MD cohort 51
Table 4-1 American College of Rheumatology definition of syndromes associated with SLE.[172] 64
Table 4-2 Description of SLE cohort from Karolinska Institute Sweden 68
Table 5-1 Clinical features of recruited CASPR2-antibody cohort, all ethnicities included. 90
Table 5-2 Clinical features of Caucasian patients with antibodies to LGI1, CASPR2, both LGI1 and CASPR2 and VGKC only. Adapted from Binks, Varley, Lee et al[195] 92
Table 5-3 Clinical associations of both CASPR2-antibody associated HLA allele (DRB1*11:01) and haplotype (DRB1*11:01-DQA1*05:01-DQB1*03:01) expression. ... 98
Table 6-1 Demographics and clinical characteristics of CASPR2-antibody patients and age matched healthy controls (HC) used in matrix cell culture experiments. 129
Table 7-1 LGI1 and CASPR2 derived peptides selected for use in T cell stimulation experiments 171
Table 7-2 Characteristic of cohort used for T cell stimulation experiments 172

Abbreviations

AA – amino acid
ABC – antibody binding capacity
AChR - acetyl-choline receptor
ADAM22 - a disintegrin and metalloproteinase domain-containing protein 22
ADAM23 - a disintegrin and metalloproteinase domain-containing protein 23
AED – anti-epileptic drug
AF – Alexa-Fluor
AMPA - α-amino-3-hydroxy-5-methyl-4-isoxazolepropionic receptors
ANA – anti-nuclear antibody
APCs – antigen presenting cells
AQP4 – aquaporin-4
BCM – B cell medium
BSA- bovine serum albumin
CASPR2 - contactin-associated protein-like 2
CBA – based assay
CDI – cell division index
CFSE - carboxyfluorescein succinimidyl ester
CNS – central nervous system
CRP – C-reactive protein
CSF – cerebrospinal fluid
CTD – C-terminal domain
CV – coefficient of variation
DAPI - 4',6'-diamidino-2-phenylindole
DIV – day *in vitro*
DMEM - Dulbecco's Modified Eagle medium
DMSO - dimethyl sulfoxide
ΔMFI – delta median fluorescence intensity
DNA – deoxyribonucleic acid
dsDNA – double stranded DNA
DTX – dendrotoxin
EDTA - ethylenediaminetetraacetic acid
EEG – electroencephalogram
eGFP – enhanced green fluorescent protein
ELISA – enzyme-linked immunosorbent assay
ES – epitope spread
ESR – erythrocyte sedimentation rate
FBDS - faciobrachial dystonic seizures
FCS – fetal calf serum
FIPA – fluorescent immunoprecipitation assay
FL – full-length
FU – fluorescent units
H+L – heavy and light chain
$GABA_AR$ – γ-aminobutyric acid A receptor
GFAP – glial fibrillary acid protein

HBSS - Hank's balanced salt solution
HLA – human leukocyte antigen
HSVE – herpes simplex virus encephalitis
HEK293 - human embryonic kidney 293 cells
IFN – interferon
IgA – immunoglobulin A
IgG – immunoglobulin G
IgM – immunoglobulin M
ITU – Intensive care unit
IVIG – intravenous immunoglobulin
LE – limbic encephalitis
LGI1 - leucine-rich glioma inactivated-1 (LGI1)
NMDAR - N-methyl-D-Aspartate Receptor
NMDAR-AbE - N-methyl-D-Aspartate Receptor antibody encephalitis
NMOSD – neuromyelitis spectrum disorder
NMT - neuromyotonia
NSAbs – neuroglial surface targeted antibodies
NPSLE – neuropsychiatric systemic lupus erythematosus
NTD – N-terminal domain
MD – movement disorder
MEM - minimal essential medium
MoS – Morvan's syndrome
MRI – magnetic resonance imaging
mRS – modified Rankin scale
MS – multiple sclerosis
PBMC – peripheral blood mononuclear cell
PBS – phosphate buffered saline
PCP – phencyclidine
PCR – polymerase chain reaction
PCR-SSP – polymerase chain reaction sequence specific primers
PEI – polyethyleneimine
PHA - phytohaemagglutinin
PLEX – plasma exchange
PLL – poly-L-lysine
PSA - penicillin/streptomycin/amphotericin
PSD95 - post-synaptic density protein 95
OR – odd's ratio
RNA - ribonucleic acid
SIADH - syndrome of inappropriate anti-diuretic hormone secretion
SIMAO – single molecule array
SLE – systemic lupus erythematosus
SLEDAI – systemic lupus erythematosus disease activity index
SN – supernatant
TCR – T-cell receptor
TLR – toll-like receptor
TTX- tetanus toxin
VGKC - voltage-gated potassium channel

1 General introduction

1.1 Autoimmune disease

The role of the immune system is to protect an individual from invasive foreign organisms and harmful material. It is divided into two functional arms: the innate and adaptive immune response. The innate immune response comprises physical barriers, such as the skin, as well as phagocytic cells and chemical substances which are active prior to exposure to foreign material. There is little enhancement of this response with experience of foreign material. Adaptive immunity has the capacity to distinguish between structures present on foreign organisms versus self and therefore target foreign particles specifically. Based on this ability to discriminate it is permissible for the adaptive immune response to 'remember' prior encounter with foreign material and generate a more potent and efficient immune response upon re-exposure. Indeed, this memory response is crucial to normal human immune function and underlines the practice of vaccination against common pathogens.

Adaptive immunity has several characteristics important to consider. Antigen is a conceptual description of any substance which is stimulant to the immune system, such as bacterial cell wall particles. B and T cells, the core cellular components of the adaptive immune system, express receptors which are specific for particular aspects of antigens, known as epitopes. An individual cell and its receptor are specific for a single epitope or group of structurally related epitopes. This requires a huge diversity of receptors in order to give adequate protection against the broad range of potential immune challenges an individual can encounter. In B cells there are thought to be at least 10^{11} antibody specificities in the human immunoglobulin repertoire. This is greater than the

number of genes in a cell. To circumvent this problem the antigen binding variable region is composed of more than one gene segment. Heavy chain segments are comprised of V (variable), D (diversity) and J (joining) segments. Light chain variable regions contain only V and J segments. There are multiples copies of each gene segment with 65 heavy chain V segments, 27 D segments and 6 heavy chain J segments. There is comparable diversity in the light chain V and J segment genes. As each end-product variable region requires transcription of a single VDJ gene, the differential selection of these germ line genes in the cell is a mechanism to generate diversity in antigen specificity. This is known as VDJ recombination (Figure 1-1) and it takes place during assembly of the T or B Cell receptor (TCR or BCR). Further diversity in B cells arises from the combination of heavy and light chain variable regions. A final source of diversity is via somatic hypermutation (SHM) in germinal centres whereby point mutations are introduced into rearranged V-region genes during B cell activation which allows for positive or negative selection. This is discussed in more detail later on.

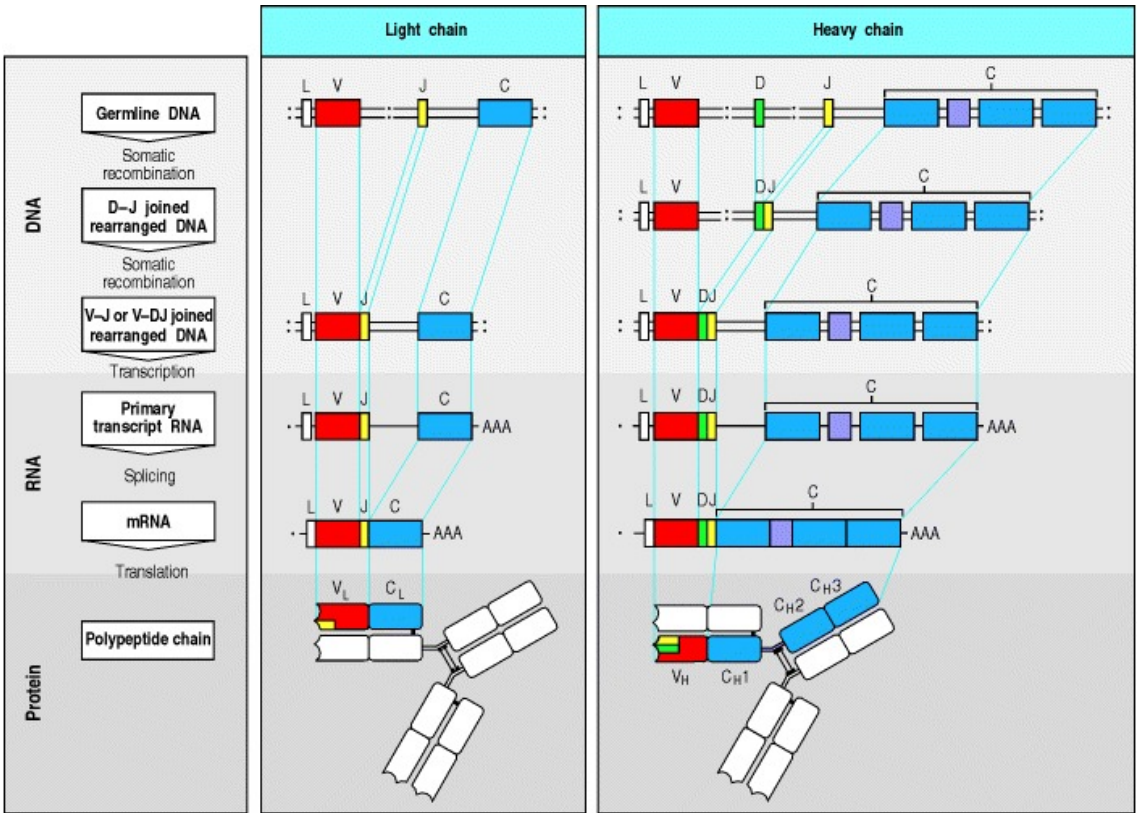


Figure 1-1 Recombination of heavy and light chain variable regions

Adapted from Janeway's Immunobiology[1] this demonstrates the sequential cleaving of introns between the exons coding for the VDJ and constant regions, leading to the assembly of an intact variable region for both heavy and light chains on immunoglobulins.

Generation of this broad diversity challenges a fundamental, albeit nuanced, requirement of the immune response: that of accurate self versus non-self discrimination. In order to prevent the generation of B and T cells with self-reactivity, editing of the adaptive immune repertoire occurs in the form of tolerance. One way to define tolerance is the acquisition of non-reactivity towards a particular antigen. Tolerance is acquired during foetal development when the immune system is maturing. If allogeneic tissue is infused into foetal mice *in utero*, once matured, these mice show markedly reduced reactivity to tissue from the allogeneic mouse strain but not to a third-party graft.[2] This suggests a tolerance mechanism which selects against "self"-reactive

lymphocytes that does not affect the ability to respond to foreign tissue. This is an ongoing process carried out by central and peripheral arms.

Central tolerance takes place in the primary lymphoid organs. Namely the bone marrow for B cells and the thymus for T cells. Developing lymphocytes are exposed to self-antigens in these sites and if self-reactivity is detected then they are destroyed in a process called clonal deletion. Medullary thymic epithelial cells are present in the thymus and are central to T cell central tolerance as they express a wide variety of tissue-specific antigens. Crucial to their function is a nuclear regulatory protein entitled autoimmune regulator (AIRE) and mutation in this protein gives rise to a debilitating multi-organ autoimmune disease called autoimmune polyendocrinopathy candidiasis ectodermal dystrophy syndrome (APECED).[3] Nevertheless, a significant proportion of cells escape clonal deletion and enter peripheral circulation creating a requirement for peripheral mechanisms of tolerance. T regulatory cells (Tregs) are an important aspect of this response. These are T cells which have been identified to be self-directed and are clonally 'diverted' into a cellular phenotype which reduces immune activation. They do this by producing anti-inflammatory cytokines, direct cell-cell inhibition and modulating activation states of antigen presenting cells (APCs).[4] Mutations in a crucial Treg transcription factor, Foxp3, give rise to human immunodysregulation, polyendocrinopathy and enteropathy, X-linked syndrome (IPEX). A further important mechanism of peripheral tolerance is anergy. In T cells, anergy occurs when an antigen is encountered without co-stimulatory CD28 ligation leading to downregulation of both TCR signalling and interleukin-2 (IL-2) expression. APCs can be tolerogenic in this way by presenting antigen without co-stimulatory molecules. B cell anergy is less fully understood but follows similar principles whereby if antigen encounter is not followed

by a second co-stimulatory signal in the form of T-cell help and CD40 ligation then B cells become anergic and unreactive.[5] Finally there can be peripheral deletion of chronically stimulated self-reactive clones by apoptosis.

One way of conceptualising the process of how antigen-driven autoimmune disease arises is by dividing it into three distinct phases.[6] First, there is initiation of an autoimmune response governed by genetic factors, environmental triggers and defective regulation of the early phase of this response. Second, there is propagation where a self-reactive response gathers momentum and autoreactive B and T cells proliferate, co-stimulate and traffic to various immune system niches. Antigen can persist and B and T cell receptors are mutated to target self-antigen more broadly and efficiently, encouraged by an ongoing pro-inflammatory response. Finally, there is a failure of the systems designed to resolve autoimmunity. Tregs are crucial in this aspect, supported also by altered expression of receptors in activated lymphocytes designed to trigger homeostatic downregulation of immune activity, such as CTLA-4 and PD-1.

In terms of the development and propagation of a B cell mediated response, germinal centres are central. These are transient structures which form within peripheral lymphoid organs in response to an antigen-driven immune response. Lymph nodes are composed of follicles of antigen inexperienced IgM+ and IgD+ naïve B cell bordered by T cell-rich zones. Follicular dendritic cells (FDCs) are located in the centre of a follicle and this is where germinal centres arise. Formation occurs when naïve B cells encounter antigen then begin to proliferate and traffic to the border of the T cell zone. Here, they interact with antigen-specific T cells who provide further stimulation in the form of CD40 ligation, IL-2, IL-21 and TNFα.[7] At this point activated B cells fate is defined by their affinity to specific antigen. The highest affinity B cells enter the germinal centre

pathway due to interclonal competition for T cell help. [8] Antigen specific T cells, through expression of B cell lymphoma 6 (BCL-6) and upregulation of CXC-chemokine receptor 5 (CXCR5), differentiate into T-follicular helper cells (TFH). Activated B cell blasts displace inactivated naïve B cells which form the mantle zone around the germinal centre. The germinal centre itself becomes polarised into a dark zone and a light zone. These zones are defined by their expression of CXCR4 and CXCR5 respectively. Developing B cell blasts cycle between dark and light zone by varying their expression of CXCR4 and CXCR5.

Once germinal centres have formed polarised light and dark zones, the process of somatic hypermutation (SHM) begins. In the dark zone, B cells rapidly proliferate and undergo point mutations within their antigen-specific VDJ regions. This process requires activation-induced cytidine deaminase (AID) and produces B cell clones with variable affinity for target antigen. These clones then traffic into the light zone where higher affinity clones are positively selected. Positive selection takes place first by interaction with FDCs which present antigen to B cell clones. High affinity clones are able to capture more antigen and therefore present higher densities of peptide-major histocompatibility (MHC) complexes to TFHs, receiving a greater share of T cell help, and driving positive selection.[9] By this process, high-affinity clones are then transferred back to the dark zone for further proliferation, SHM and further cycling to light zone with resultant affinity maturation.

Whilst in germinal centres, B cells can undergo class switch recombination (CSR) in light zones where immunoglobulin isotype changes from IgM or IgD to IgG, of which there are four subtypes. These different antibodies have different effector functions and allow for a more effective immune response. AID is also important in CSR where it serves

to induce mismatch and base-excision repair in B cell DNA, juxtaposing assembled VDJ exons to heavy chain constant region exons downstream of IgM and IgD coding region, such as IgG1-4. [10] AID mutations in humans cause hyper-IgM syndrome characterised by the absence of class switch recombination, the lack of SHM and lymph node hyperplasia due to giant germinal centre formation, showing how central this protein is to these core immunological functions.[11]

Post-germinal centre B cells can either have a memory (CD27+, CD38-) or plasmablast (CD27++, CD38++) phenotype, which can be switched (IgG+, IgD-) or unswitched (IgD+, IgG-). Plasmablasts secrete antibody at a prolific rate and are characterised by decreasing expression of classical B cell markers CD19 and CD20. They can further differentiate into niched plasma cells (CD138+). Memory B cells continue to circulate in the periphery where they secrete less specific antibody than plasmablasts, have ongoing expression of CD19 and CD20 and underpin the ability to generate a pronounced antibody response upon antigen re-experience (Figure 1-2).

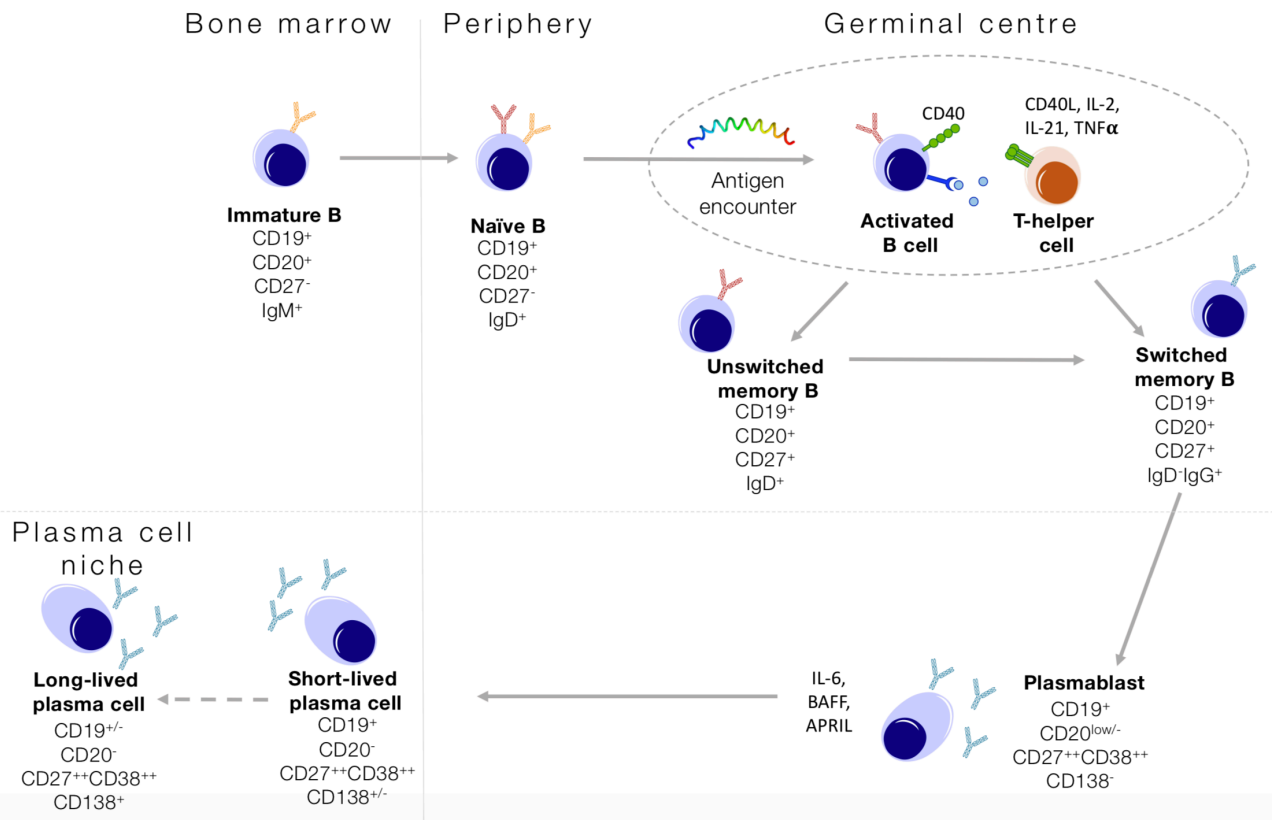


Figure 1-2 B cell maturation and activation via germinal centre reaction

Reproduced from Wilson et al[12]. This diagram shows the journey of a B cell from the bone marrow into the periphery and its activation to become a mature memory B cell or plasmablast. Eventually, a proportion of plasmablasts migrate back into the bone marrow. Expression of cluster of differentiation (CD) markers immunoglobulin receptors (M, D and G) at various points is denoted, as is the influence of various cytokines at each stage

Autoantibodies are antibodies directed against self-antigen and can either be tissue specific, such as those seen in autoimmune thyroid or adrenal disease, or non-tissue specific, targeting widely distributed antigen, such as rheumatoid factor, associated with Rheumatoid arthritis, or anti-nuclear antibodies, seen in systemic lupus erythematosus (SLE). Autoantibodies can be the primary drivers of an immune response or an epiphenomena of a CD8+ T effector cell driven immune response, creating widespread tissue destruction and exposing intracellular antigen to the adaptive immune system, such as anti-Jo antibodies in polymyositis.[13]

1.2 Antibody mediated autoimmune brain disease

A number of neurological diseases are thought to be caused by the immune system including multiple sclerosis, neuromyelitis optica, para-infectious conditions, myasthenia gravis and encephalitis. Across this wide range of conditions, data exists to support effector roles for innate immunity as well as a role for adaptive immunity involving T and B cell populations. The prototypic autoantibody mediated neurological disease is myasthenia gravis, described over 40 years ago in association with acetylcholine receptor antibodies.[14] More recently a new paradigm of neuroglial surface targeted antibodies (NSAbs) has emerged, where pathogenic autoantibodies causing disease of the central nervous system are being discovered annually.[15, 16] The crucial aspect of these antibodies is that they are directed towards extracellular protein domains and can therefore access their target epitope at the neuroglial cell surface *in vivo*. A further key characteristic of NSAbs is their sensitivity to the conformational integrity of antigen. They bind conformationally intact antigen presented in a cell based assay (CBA) or cultured neurons but do not reliably bind denatured, linearised antigen in systems such as Western blot or enzyme linked immunosorbent assay (ELISA).[17] The recognition of this fact was central to the development of assays to effectively diagnose and categorise these conditions, with the CBA being the current gold standard.

Evidence of NSAb pathogenicity is demonstrated by a number of *in vitro* and *in vivo* models, close phenotype to antibody correlations and patient response to immunotherapy.[15, 18-20] NSAbs contrast with classical neoplasm-associated 'paraneoplastic' antibodies which are directed against intracellular epitopes and are often also expressed by associated neoplasms.[21] These antibodies cannot access their antigen *in vivo* and any resulting associated neuronal dysfunction is thought to arise

from cytotoxic T cell mediated neuronal death, explaining the poor response to immunotherapies in these patients.[22] NSAb-mediated diseases are described by their antibody specificity and three of the most common make up the main clinical subjects in this thesis and are explored in more detail below.

1.3 N-methyl-D-aspartate receptor antibody encephalitis (NMDAR-AbE)

1.3.1 Original description and demographics

Though the incidence of N-methyl-D-aspartate receptor antibody encephalitis (NMDAR-AbE) is not precisely described it appears to be most common of the antibody-mediated encephalitidies.[23] The first clinical description of an immunotherapy-responsive, teratoma associated encephalitis was made in 2005,[24] with NMDAR as the antigenic target described a few years later in a small cohort.[25] Serum and cerebrospinal fluid (CSF) from patients was shown to bind in a characteristic pattern to immunohistochemical preparations of rodent hippocampus and cell membrane of hippocampal neuronal cultures. The NR1 subunit of the NMDAR was found to be the specific antigen a year later.[26]

Further description of NMDAR-AbE demonstrated that men could be affected but that it predominantly affects children and young women (median age 21 [range 1 – 95], 81% female).[27] Over time it has also become clear that it is predominantly a non-paraneoplastic disease, with case-series now showing tumour rates of 21-38%, which are almost exclusively ovarian teratoma.[27, 28] There is also some evidence of seasonal onset in paediatric cases.[29]

1.3.2 Clinical presentation

The clinical presentation of adult NMDAR-AbE is highly characteristic with a stereotyped temporal evolution. There is often a viral prodrome, 10-20 days prior to disease onset, with fever, myalgia, headache and coryzal symptoms. This is followed by the abrupt onset, over a few days, of an acute neuropsychiatric presentation including psychosis, seizures and cognitive impairment. Later features include a characteristic movement disorder,[30] dysautonomia and coma.[28] Due to these later effects, many patients require intensive care unit admission and there is a mortality rate of 7%.[27]

The NMDAR-AbE associated movement disorder (MD) has very striking phenomenology and is variably described in the literature, with frequently used terms including catatonia, chorea, dystonia, akathisia, and orofacial dyskinesias.[31-33] A consensus description of this MD could aid neurologists in making a prompt clinical diagnosis and feel, therefore, more confident in starting immunotherapy early, something which is known to improve outcomes in these patients.

1.3.3 Investigations

CSF sampling demonstrates lymphocytic pleocytosis in over 80% of patients,[26-28] with an elevated IgG index and CSF-specific oligoclonal bands [26, 28] supporting intrathecal antibody synthesis. Surprisingly, given the clinical severity of the disorder, clinical magnetic resonance imaging (MRI) is often normal or only shows non-specific changes in around 30% of patients.[27] Research level MRI, however, shows a number of abnormalities. On diffusion tension imaging (DTI) gross abnormalities in the white matter tracts are seen and on functional MRI, reduced functional connectivity in the default mode network anteriorly is evident.[34] Diffuse encephalopathy is seen on electroencephalogram (EEG) in 90%, with background slowing.[27] Extreme delta brush

has been described as a characteristic EEG pattern in 30% of patients requiring ITU care.[35] This is defined as diffuse delta rhythms of 1 – 3 Hz, with superimposed rhythmic bursts of faster beta activity. The specificity of this pattern is debated but NMDAR hypofunction has been postulated as a major contributor, with an NMDAR antagonist, ketamine, recapitulating some of the observed EEG characteristics.

1.3.4 Immunology

The frequent, but not dominant, association with teratoma gives a clue as to how a break in tolerance may occur, allowing an autoimmune response to propagate. Ovarian teratomas have been described to express ectopic neural tissue, including the NMDAR.[25, 36] Furthermore, lymphocytic inflammatory infiltrates (particularly B cells) in teratomas from patients with encephalitis [37] have been described, with some closely resembling germinal centre-like structures.[38] Amounts of NMDAR antibody were measured and found to have the highest concentration in teratoma fluid, then blood, then CSF, giving a suggestion as to the original source of NMDAR antibody in these patients. The fact that these structures, crucial to the maturation of an immune response, have been found in teratomas suggests they are important sites of antibody production in this autoimmune condition. However, as noted previously, the majority of patients do not have teratoma associated disease. This suggests that, while the concept of the germinal centre has been demonstrated to be important in the context of teratomas, further exploration of pathogenic mechanisms is required.

NMDAR-AbE post herpes simplex virus encephalitis (HSVE) is now well appreciated. Initially, a proportion of post-HSVE patients were found to have serum and CSF NMDAR-antibodies, with unclear clinical significance.[39] A choreoathetoid MD and symptoms of encephalopathy in children several weeks post-HSVE have long been

described, but were not associated with relapse in HSV viral load.[40]. The demonstration of *de novo* generation of NMDAR-antibodies during this relapsing choreoathetoid-encephalopathy suggested the relapse in these children was driven by NMDAR-antibodies.[41-43] Further support of this hypothesis was that immunotherapy gave a better treatment response than antiviral agents in this context. More recently, it has been described that these antibodies do not always cause a full-blown NMDAR-AbE like presentation but can be seen as part of a subtly evolving neuropsychiatric sequelae post-HSVE in adults and to a lesser extent, children.[44]

The appearance of these antibodies post-HSVE a provides a potential mechanism for NMDAR antibody generation. HSVE is a profoundly inflammatory and destructive brain pathology leading to the release of a large quantity of brain proteins into the periphery where tolerance mechanisms to these relatively infrequently encountered proteins could be overwhelmed, allowing NMDAR reactive B and T cells proliferate. This hypothesis is supported by the fact that other brain-reactive antibodies can be generated at the same time, such as those to γ-aminobutyric acid A receptor ($GABA_AR$)[45] and glial fibrillary acid protein (GFAP) antibodies.[46] It could be theorised that these antibodies arise as a result of molecular mimicry, whereby an HSV epitope overlaps with the NMDAR receptor and the antibody-mediated response to HSV has off target effects. This appears unlikely, however, given HSV-1 IgG seroprevalence is 60% in adults and the rarity of NMDAR-AbE in the general population,[47] compared to the significantly higher prevalence of NMDAR-AbE and NMDAR antibodies post HSV-encephalitis.

Further to this, little is known about the underlying immunobiology of NMDAR-AbE and represents an area requiring further study. Current knowledge on the cellular immunology of NMDAR-AbE and other NSAbs is discussed in more detail in chapter six.

1.3.5 Antibody mediated pathogenesis

NMDARs are crucial actors in central nervous system (CNS) excitatory transmission and plasticity via long term potentiation. It is a ligand-gated ion channel formed of a 'dimer of dimers', composed of two obligate NR1 subunits and two NR2 (A – D) subunits. Dual agonisation with glutamate and glycine binding is required for channel opening, influx of cations including Ca^{2+} and downstream activation of signal transduction cascades.[48] Glycine binds the NR1 subunit and glutamate binds the NR2 subunit. NMDARs are predominantly located on neurons in the hippocampus, cerebellum and cortex.[49]

NMDAR-AbE antibodies target the extracellular, N-terminal domain of the NR1 subunit of the NMDAR.[26, 50] Both patient sera and CSF antibody binding co-localise with NR1 commercial antibody staining.[51] *In vitro* studies demonstrate that patient sera and CSF reduce NMDAR cluster density with resulting impaired glutamatergic transmission, which is largely reversible upon antibody removal.[26, 50, 52] NMDAR-antibodies are predominantly complement-fixing IgG1 subclass antibodies[28] and surprisingly, though patient brain tissue demonstrates IgG deposition, there is no associated complement deposition. This suggests, in combination with the lack of frank inflammation on MRI, that functional downmodulation of NMDARs is the predominant mechanism. In human post-mortem brain tissue, B cells and plasma cells have been observed in perivascular regions and interstitial spaces and may provide a local source antibody production, explaining the observed intrathecal synthesis.[53-55]

In vivo passive transfer of patient CSF via continuous, low-level intraventricular infusion recapitulates aspects of the neuropsychiatric presentation of NMDAR-AbE in mice,[56] with an associated reduction in NMDAR hippocampal clusters. No inflammatory

infiltrates, complement deposition or neuronal apoptosis were seen, again suggesting NMDAR hypofunction and not frank inflammation was responsible for generating the observed phenotype. This must be interpreted with the caveat that this animal model is a partial phenotype capturing only aspects of the human NMDAR-AbE disease, with notably no seizures or MD seen. In addition, mice have been shown to be more susceptible to seizures after infusion of NMDAR-antibodies.[57] An informative model of human *in vivo* pathogenicity is represented by maternal to foetal transmission of NMDAR-antibodies, giving rise to a transient foetal encephalitic syndrome.[58]

Experimental evidence suggests disruption of NMDAR clusters is due to two related but distinct processes: internalisation and lateral dispersion. NMDAR antibodies cross-link extrasynaptic NMDARs inducing endocytosis, whereas antibody binding to synaptic NMDAR initiates lateral dispersion of these receptors. The synaptic dispersion is likely due to interruption of the Ephrin-B2-NMDAR interaction, as synaptic NMDAR composition is regulated by Ephrin-B2 expression.[59, 60] In mice, infusion of Ephrin-B2 alongside patient CSF IgG prevented manifestation of the previously observed neurocognitive phenotype and while IgG binding to brain was not altered, NMDAR cluster density was preserved.[61]

Finally, humans provide further evidence that NMDAR hypofunction gives rise to the clinical features and extent of reversibility seen in this disease. Ingestion of NMDAR-antagonists ketamine and phencyclidine (PCP) give rise to similar clinical features, including a MD with facial involvement, agitation, hallucinations, delusions and autonomic dysfunction.[62-64]

1.3.6 Treatment

Current practice in the treatment of NMDAR-AbE, and for all NSAb-mediated diseases, is based on expert opinion and retrospectively collected data as no clinical trial of treatment in these patients currently exists. Treatment involves supportive therapy, often in an intensive care unit to manage autonomic crises and reduced consciousness. Immunotherapy given first-line is usually a combination of steroids with either plasma exchange (PLEX) or intravenous immunoglobulin (IVIG) or both. Second-line treatments can include either cyclophosphamide and rituximab.[27] Second-line treatment is often required as only around 50% of patients respond to first-line treatment and of the remaining 50%, there is evidence to suggest second-line treatment significantly alters final outcome.[27] Earlier treatment gives clear benefits in terms of outcome, stressing the need to make a diagnosis accurately and quickly. Despite immunotherapy, relapse rates remain at around 5-10% and only 50% of patients have no disability at two years.[27] This strongly makes the case for better therapies to improve outcomes for patients, perhaps employing a more targeted approach based on an improved understanding of the immunobiology of this condition.

1.3.7 Controversies over the spectrum of NSAb mediated disease

Since their discovery, defining the scope of NSAb mediated diseases has been a core theme of much of the work in the field. An informative example is that of NSAbs in association with psychiatric disease. Psychiatric features are a core early manifestation of NMDAR-AbE, with as many as 77% of patients being seen first by a psychiatrist in early series.[26] The glutamate hypothesis is central in current conceptions of schizophrenia,[65] with both pharmacological and genetic disruption of NMDAR reproducing aspects of the

disease. The question arose, therefore, as to whether antibody-mediated NMDAR-hypofunction was responsible for a proportion of schizophrenia cases.

Evidence to date is mixed, with some studies finding small differences between the number of controls and patients with psychiatric illness with serum NMDAR antibodies,[66-68] and others finding no difference.[69, 70] These results are difficult to interpret due to differences in sample timing and the assay methodology employed. Demonstration of CSF NMDAR antibody is important in making a diagnosis of NMDAR-AbE. Therefore, a key finding is the absence of NMDAR antibodies in CSF from patients with schizophrenia.[71] While mono and oligo-symptomatic presentations of NMDAR-AbE are acknowledged, particularly in relapse, these are the minority of presentations and the consensus still stands that each NSAb is associated with a core syndrome that matches well to the underlying biology of the antibody target. Indeed, recent work has demonstrated that a relatively unique psychiatric phenotype exists in NMDAR-AbE which is sensitive for this disease.[72]

A further challenge to this consensus comes with the association of antibodies to the NMDAR in association with neuropsychiatric systemic lupus erythematosus (NPSLE), an extremely broadly defined clinical manifestation. The biology of this supposition and the experiments to explore this are presented in chapter four.

1.4 Leucine-rich glioma inactivated-1 (LGI1) and contactin-associated protein-like 2 (CASPR2) antibodies

Antibodies against voltage-gated potassium channels (VGKCs) were described predominantly in association with the following immunotherapy responsive conditions: Limbic encephalitis (LE),[73, 74] some forms of epilepsy including faciobrachial dystonic

seizures (FBDS),[75, 76] Morvan's syndrome (MoS)[77] and neuromyotonia (NMT).[78] The VGKC radioimmunoprecipitation assay employed to the describe these syndromes made use of digitonin solubilised brain tissue, with iodinated alpha-dendrotoxin utilised to label Kv1.1, Kv1.2 and Kv1.6. Human serum or CSF was then added to assess for binding and consequent immunoprecipitation. Based on this assay, Kv1.1, Kv1.2 and Kv1.6 were thought to be the antigenic targets.[79] In 2010, however, biochemical studies revealed that proteins which complex with the VGKC - LGI1 and CASPR2, rather than the channel itself, were the targets of antibodies from patients with LE, FBDS, MoS and NMT.[80-82] Because of this, there was a change in nomenclature from VGKC antibodies to VGKC-complex antibodies in order to reflect the frequent co-immunoprecipitation of LGI1 or CASPR2 alongside radiolabelled VGKCs. The patients with VGKC-antibodies, without LGI1 or CASPR2-reactivities ("double-negative"), had a broad mixture of phenotypes were often non-responsive to immunotherapy. It was then discovered that double-negative autoantibody target epitopes could either be intracellular, especially aspects of VGKCs, or the non-neuronal protein dendrotoxin (DTX). Antibodies to either of these targets are unlikely to be pathogenic autoantibodies. Furthermore, these antibodies did not bind to the surface of live hippocampal neurons.[83] Conversely, LGI1- and CASPR2-antibodies have been robustly demonstrated to target the cell surface of neurons, are associated with clearly defined, immunotherapy responsive syndromes and are more sensitive than VGKC-complex antibody determination.[84, 85] Therefore, the terms LGI1- and CASPR2-antibodies are used in preference to VGKC-complex antibodies. Further explanation of patients with LGI1- and CASPR2-antibodies follows.

1.5 LGI1-antibody patients

1.5.1 Demographics

That patients with LGI1-antibodies are predominantly older men, with a median age of onset in the seventh decade,[86, 87] is in contrast to many classical autoimmune diseases. Most cases are non-paraneoplastic, with most frequently associated tumours including skin and prostate cancers.[86]

1.5.2 Clinical presentation

The majority of patients with LGI1-antibodies present with a variety of focal seizures, by far the most common and certainly the most specific of these are the pathognomonic FBDS. FBDS are brief (<3s), stereotyped, posturing movements of the hand and ipsilateral hemi-face characterised by their high frequency (median 50/day).[76] FBDS precede LE in around two-thirds of cases.[76, 85, 88] Other semiologies are also present such as medial temporal lobe seizures, including bradycardia,[89] thermal sensations or autonomic features such as piloerection.[90] Rarely patients can present with MoS.[81, 82, 88, 91]

In patients with LGI1-antibodies, FBDS or other forms of seizure are nearly always followed by progression to an established LE.[87] The clinical picture at this point is of subacute memory disturbance, ongoing seizures and psychiatric disturbances.[81, 82] Accompanying this progression is an accumulation of abnormal investigations, with hippocampal high signal on T2-weighted MRI, ictal discharges on EEG and serum hyponatraemia, most often due to syndrome of inappropriate anti-diuretic hormone secretion (SIADH). Patients with LGI1-antibodies and FBDS only do not show these abnormal investigations.[81, 82, 87] In rarer cases, cognitive impairment can be present at disease onset.[76, 85, 92] Once a patient has had LE they often then develop hippocampal

atrophy associated with a fixed memory deficit causing long-term disability, as well as occasional ongoing seizures.[93, 94] A number of other residual cognitive deficits are also recognised.[95]

A final interesting observation of these patients is their intolerance of older AEDs, in particular phenytoin and carbamazepine, with 25-30% having a reaction to these drugs and five out of 103 patients exhibiting a severe, Stevens-Johnson spectrum reaction.[87] The observation of this sensitivity led members of our laboratory to hypothesise a possible human leukocyte antigen (HLA) association in these patients. This is explored in chapter five.

1.5.3 Pathogenesis

LGI1 is a 64kDa, secreted protein expressed mainly in the hippocampus and neocortex.[81, 96] It forms a trans-synaptic complex with pre-synaptic a disintegrin and metalloproteinase domain-containing protein 23 (ADAM23), and post-synaptic ADAM22. ADAM22 interacts with post-synaptic α-amino-3-hydroxy-5-methyl-4-isoxazolepropionic (AMPA) receptors, post-synaptic density protein 95 (PSD95), and ADAM23 with presynaptic Shaker Kv1-potassium channels. How these proteins are differentially affected by LGI1 antibodies is not known, however, murine mutations of LGI1 disrupt the formation of this complex and specifically abrogate AMPA-mediated synaptic signalling. [97] Indeed, *in vitro* and *in vivo* work showed that LGI1-antibodies inhibit the binding of LGI1 to ADAM22 and 23, giving a reversible reduction of synaptic AMPA receptors and a loss of function of inhibitory interneurons, with consequent excess neuronal-network excitation and seizures.[98, 99] Therefore, although LGI1 is not a channel itself, loss of function of LGI1 gives rise to secondary channel dysfunction.

LGI1-antibodies in human disease are predominantly of the IgG4 subclass[77, 91] and therefore do not fix complement. This is intriguing as despite the demonstration of complement deposition in post-mortem tissue,[55] significant symptomatology, particularly in the form of seizures, can occur without CSF or MRI evidence of inflammation. This suggests that similarly to NMDAR-AbE, it is the functional effect of these antibodies driving clinical manifestations as opposed to a more generalised inflammatory process.[76, 85, 88, 91]

1.5.4 Treatment

Convincing evidence now exists that FBDS respond poorly to anti-epileptic drugs (AEDs) but rapidly to immunotherapy, with further clear evidence that prompt treatment of FBDS can prevent the onset of cognitive impairment and improves outcome.[87] Any delay to starting immunotherapy reduces the odds of achieving seizure freedom. First-line treatment, similar to NMDAR-AbE, is with steroids and plasma exchange or IVIG. Response to treatment in LGI1-antibody patients is better, however, with nearly all patients who are treated early enough responding to first line treatment and achieving good outcomes without second-line therapies.[76] Rituximab has been used LGI1-antibody encephalitis to mixed effect but this is based on very small sample sizes.[100] Relapse rates in LGI1- or CASPR2-antibody encephalitis currently lack consensus, with estimates varying from 5%[76] to 20%.[88, 91] Possible reasons for this include differing immunotherapy regimens as well as relative lags to recognition and treatment in different healthcare settings.

1.6 CASPR2-antibody patients

1.6.1 Demographics

As with patients with LGI1-antibodies, there is a male predominance in patients with CASPR2-antibodies with similar onset later in life.[77, 80, 81, 101] In the largest comparative series of these patients, the male predominance in CASPR2-antibody mediated syndromes (74%) is slightly more pronounced than in LGI1-antibody patients (59%).[86]

1.6.2 Clinical presentation

Clinical syndromes more often involve the peripheral nervous system in patients with CASPR2-antibodies when compared to patients with LGI1-antibodies. This can take the form of NMT, a syndrome of peripheral nerve hyperexcitability with cramps, stiffness and fasciculations.[78] This can be present as NMT alone or in combination with LE, along with prominent sleep and autonomic disturbance in the form of MoS. Patients can also present with a LE phenotype without NMT but with more subtle autonomic features, peripheral nerve pain or cerebellar symptoms that are not as severe as seen in patients with MoS.[77, 80, 86, 102] As with NMDAR antibodies, rare monosymptomatic cases of patients with CASPR2-antibodies exist, with patients presenting with isolated epilepsy, ataxia or cognitive impairment.[77, 81, 101] Thymomas are present in around 40% of patients with MoS[103] and in around 10% with other presentations.[101] Probably partly driven by this tumour association, it is possible to have dual NSAb positivity to CASPR2 and acetyl-choline receptor (AChR)-antibodies[104] or CASPR2- and LGI1-antibodies, though further reasons for this specific co-occurrence are explored in chapter five.[77]

1.6.3 Mechanism of action

CASPR2 is a 148 kDa transmembrane protein with an extracellular domain over 1,200 amino acids long, expressed predominantly in the juxtaparanodal region of myelinated axons in the brain and the peripheral nervous system.[105] It is a neuronal cell adhesion molecule, responsible for clustering of Kv1.1 and Kv1.2 at the juxtaparanode (Figure 1-3),[106] though its role in synaptic function remains unclear. CASPR2 protein has been found at low levels in the parathyroid glands and there is evidence of ribonucleic acid (RNA) expression in the adrenal and prostate glands, as well as the rectum and ovaries.[107] Mutations in the gene encoding CASPR2 are linked to autistic spectrum disorders, seizures, attention-deficit hyperactivity disorder and schizophrenia.[108]

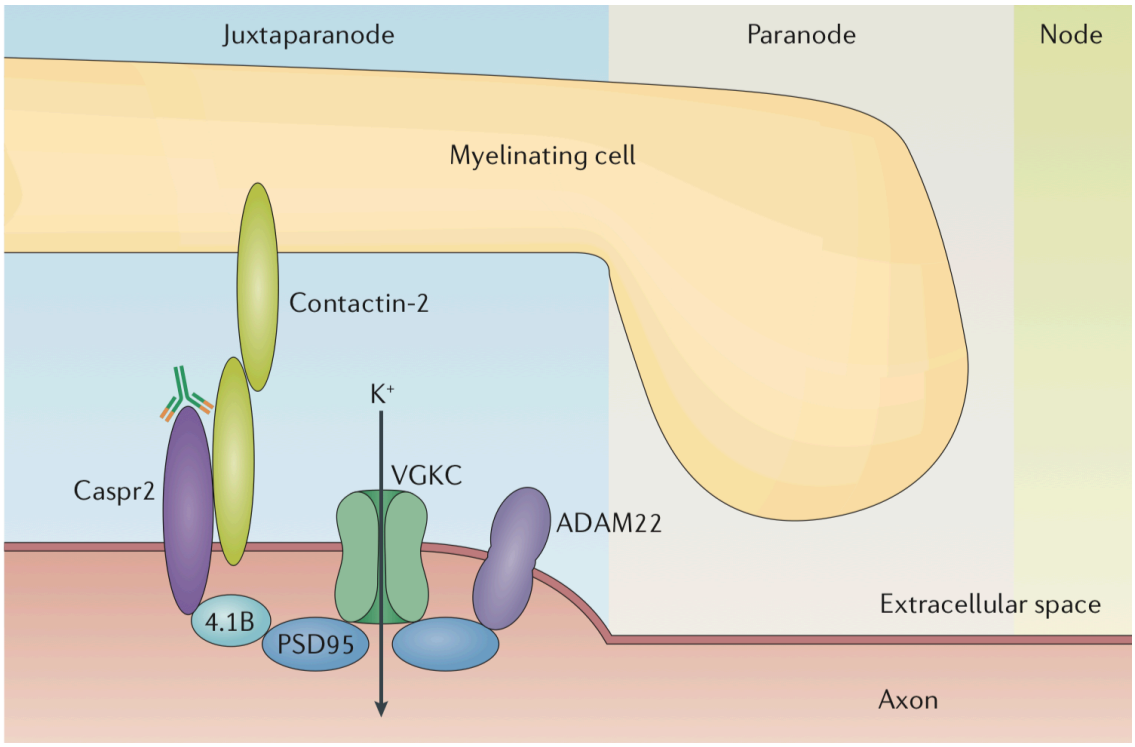


Figure 1-3 CASPR2 associates with dimerised contactin-2 to contribute to clustering of voltage-gated potassium channels in the juxtaparanode

This schematic is adapted from van Sonderen et al[109] and demonstrates a myelinated axon, with emphasis on the juxtaparanodal region. Here, CASPR2 associates with contactin-2 which is expressed by oligodendrocytes. CASPR2 is anchored to disk large homologue 4 (PSD95) via 4.1B and this allows for clustering of voltage gated potassium channels (VGKCs) in the juxtaparanode where they facilitate repolarisation after action potential firing. Pathogenic CASPR2 antibodies (shown in green) are thought to disrupt the CASPR2-contactin-2 interaction therefore preventing VGKC clustering.

Antibodies to CASPR2 have been demonstrated to be mainly of the IgG4, and less so IgG1, subclass [102, 110, 111] and predominantly target epitopes concentrated at the N-terminus of CASPR2.[112] The mechanism of action of antibodies remains controversial, with the same theoretical lack of complement fixing and Fc-receptor binding applying as with LGI1-antibodies due to the IgG4 subclass predominance. *In vitro* work utilising limited conditions did not show any internalisation of CASPR2 in response to CASPR2-antibodies, but they were shown to disrupt the nanomolar affinity interaction between CASPR2 and contactin-2. Interestingly, titre alone did not predict the degree of

disruption of this interaction, with precise epitope specificity thought to play a role.[111] Binding between CASPR2 and contactin-2 is central to clustering Kv1.1 and Kv1.2 at juxtaparanodes, stabilising conduction at the nodes of Ranvier and maintaining resting potential.[113] Very little is known about the underlying cellular immunology of CASPR2-antibody mediated diseases. A report of a single case demonstrated an excellent clinical response to Rituximab, an anti-CD20 monoclonal antibody which predominantly targets circulating B cells.[114] This suggests these cells are making an ongoing contribution to disease in some patients. This, as well as other work on other NSAb-mediated diseases, forms the basis of the exploration of the B cell immunology of CASPR2-mediated diseases in chapter six.

1.6.4 Treatment

The treatment strategy is similar to LGI1-antibody encephalitis with a similar response to immunotherapy observed, irrespective of central or peripheral presentation.[86] A variability in relapse rate is also seen in patients with CASPR2-antibody mediated neurological diseases.[77, 86, 102] More specific, targeted therapies are an important research priority for patients with NSAb mediated diseases as current immunosuppressive therapies have a broad mechanism of action with many off-target side-effects which contribute significantly to disease associated morbidity.[85] A neuroscience-centred approach to the channel dysfunction caused by antibodies in these diseases is informative and is exemplified by the work in NMDAR-antibody encephalitis and Ephrin B2. An important, and thus far neglected, area is the study of the immunology of NSAb mediated diseases. Identification of populations of cells responsible for the generation of pathogenic antibodies, how this varies between different patients and antigens as well as over time, will enable a more scientific and

specific approach to the treatment of these disorders, therefore improving clinical recovery and reducing drug-related side effects.

1.7 Summary and aims

NSAb-mediated diseases remain a novel group of diseases and knowledge is expanding rapidly. Three of the most common brain-targeted NSAbs-mediated diseases have been described and this gives a sense in the variation between them in terms of the characteristics of antigenic targets, clinical phenotypes, antibody-mediated pathology, cancer association and treatment responses. The pathogenesis of these antibodies is firmly established by *in vitro* and *in vivo* evidence and discovery of new targets is ongoing but appears to be slowing, with more recently described syndromes being of very rare diseases.[115, 116] Given the burden of evidence pointing to the benefit of early treatment, a key priority is to improve the description and recognition of these disorders, in order to allow early and confident diagnosis, facilitating prompt treatment. This underlines the work undertaken in chapter three to create a better description of the characteristic MD seen in association with NMDAR-AbE. Another key research priority is to ensure NSAb testing is used appropriately in the correct clinical context, hence the work in chapter four to explore the reported association between NMDAR antibodies and NPSLE.

Optimal treatments in NSAb-mediated diseases are increasingly understood but remain untargeted and with a significant side effect burden. Excellent neuroscience work has already been undertaken but the underlying immunology remains mostly unexplored and represents an excellent source of potential novel treatment strategies. The remainder of this thesis focusses on immunogenetic associations in patients with

LGI1- and CASPR2-antibodies (chapter five), the B cell immunology of CASPR2-antibody patients (chapter six) and the T cell immunology of LGI1- and CASPR2-antibody patients (chapter seven).

2 Methods

Methods relating to techniques used recurrently in various chapters are described below. Methods which are specific to each chapter, including recruitment of patient cohorts, are detailed within individual chapters for ease of reference.

2.1 Cell Culture

2.1.1 Human Embryonic Kidney 293 cells

All cell culture was conducted in a sterile class II tissue culture hood, cleaned before and after every use. Cells were incubated in a humidified 37 ˚C, 5% CO_2 incubator. Human embryonic kidney 293 (HEK) cells were grown in Dulbecco's Modified Eagle medium (DMEM, Sigma) plus 10% foetal calf serum (FCS, Biosera) and 1% penicillin/streptomycin/amphotericin (PSA, Sigma) in either a Corning T75 cm^2 or a T175 cm^2 flask. Passaging of cells was carried out every 3-4 days when 90% confluency was reached. At this point medium was aspirated, cells were detached from the flask from manual shaking and then they were re-suspended in fresh DMEM, at set proportions to allow them to reach useable confluency at an appropriate time point.

2.1.2 Primary hippocampal neuronal cultures

Wistar rats were kept in an animal facility on site. An appointed lab member would manage the rats and determine when they were pregnant. At embryonic day 19, the dam was sacrificed by CO_2 inhalation and the pups dissected out and stored on ice. Pups were then decapitated in in a class II tissue culture laboratory under sterile conditions for further procession. Using sterile dissection tools, the skin was cut along the superior midline aspect of the head, the skull removed and the brain extracted and placed into a petri dish containing ice cold Hank's balanced salt solution (HBSS, Gibco). Next, brains

were hemisected, hippocampi identified and dissected out, with care taken to ensure full removal of the meninges. Once all hippocampi had been dissected from the litter (with hippocampi kept in ice-cold HBSS during the processing of the whole litter), they were then dissociated in HBSS supplemented with 1% trypsin for 20 minutes in an incubator at 37 °C. HBSS containing trypsin was gradually replaced with complete Minimal Essential Medium (MEM [Gibco], 450 ml, supplemented with 10% FCS and 1% PSA) by changing the media three times with a 3 ml sterile hand pastette. Washed cells were then gently triturated in complete MEM forty times with a P1000 and then a P200 pipette tip until all tissue was in solution. This suspension was then centrifuged (300 ×g, 5 minutes) and the supernatant discarded. The cell pellet was resuspended in 3ml of MEM and then plated onto 13 mm PLL-coated sterile coverslips in a six-well plate at a density of two hippocampi per plate and then incubated as described. Five to six hours later, media was replaced with 3 ml per well of Neurobasal medium (Gibco), accompanied with 1% B-27 serum free supplement [Gibco], 200 mM L-glutamine [Gibco] and 1% PSA. Neurons were stained at day *in vitro* (DIV) 12-16, with replacement of 1.5 ml of Neurobasal media every three to four days during culture.

2.2 Transfection of HEK293 cells

CBAs were carried out on coverslips coated with transfected HEK cells grown in six well plates. In each well, 13 mm glass coverslips were incubated in sterile poly-L-lysine (PLL) for 15 minutes, this was then aspirated and the plates were dried in a culture hood for two hours. Day one, $8x10^5$ HEK cells were seeded per well in 2 ml of medium, with counting performed using 0.04% Trypan Blue and a haemocytometer. On day two, early in the morning, each well was transfected with a mix containing 3 μg of DNA (either a

3:1 ratio of NR1 to NR2A/2B to a total of 2.8 µg, along with 0.2 µg of an eGFP expression vector, or 3µg of CASPR2-eGFP DNA) and 1.5 µl of polyethyleneimine (PEI) made up in 50 µl of unsupplemented DMEM per well in 2 ml of medium. After 8-10 hours, the transfection medium was removed from the well and replaced with fresh media (supplemented with 1.4 µl/ml of ketamine if transfected with NMDAR subunits).

2.3 Immunocytochemistry

2.3.1 CBA

Transfected coverslips were inspected under a fluorescent microscope 24 hours after transfection to check for an eGFP signal indicating successful transfection. Serum or plasma was used at a dilution of 1:20 in NMDAR assays or 1:100 for CASPR2-antibody assays. CSF and B cell culture supernatant were used at 1:5 diluted in DMEM supplemented with 1% BSA (bovine serum albumin) and 200 mM HEPES. Coverslips containing successfully transfected cells were then placed into wells containing diluted patient sample for an hour-long primary incubation at room temperature, protected from light on an agitation device. Appropriate antigen and sample specific positive and negative controls were included in each assay run for calibration. After primary incubation, coverslips were washed with wash buffer (DMEM and 200 mM HEPES) three times and then fixed at room temperature in 4% formaldehyde in PBS for 10 minutes. Fixative was then washed three times. A polyclonal goat anti-human IgG Fc Alexa Fluor 594-conjugated secondary antibody (Jackson, 109-586-008) was diluted 1:750 and incubated with the cells for 45 minutes. Final wash steps included two washes in wash buffer and two in PBS. Coverslips were then mounted on labelled glass slides with mounting medium (DakoCytomation, Cambridge, UK) supplemented with 1:1000 4',6'-diamidino-2-phenylindole (DAPI). Results were viewed on the same fluorescent

microscope using MacProbe v4.3 digital imaging system. Scoring was based on a semi-quantitative 0-4 scoring system, in serum any score above 2 was deemed positive and in CSF and supernatant, due to lower background, any score greater than 1 was deemed positive.

2.3.2 Neuronal staining

This process was similar to that of the CBA. Key differences included the use of conditioned Neurobasal medium for the primary incubation, 2% formaldehyde used for fixation and secondary stain with Alexa Fluor goat anti-human IgG heavy and light chain (H+L) 488 (A-11013) diluted 1:1000. Otherwise, assay procedure was identical to the primary and secondary incubation in a CBA. After secondary staining, coverslips were washed as previously and then permeabilised in PBS 0.3% Triton-X-100 for 15 minutes. Permeabilisated coverslips were incubated with a mouse monoclonal anti-MAP2 antibody diluted 1:1000 in PBS 0.1% Triton-X100 and 5% normal goat serum, in order to label neurons. One hour later, coverslips were washed and incubated with goat anti-mouse Alexa Fluor 568 IgG (H+L) for 45 minutes, then washed, mounted and read as previously described.

2.4 Fluorescent immunoprecipitation assay (FIPA)

To make CASPR2-eGFP protein extract for FIPA, the quantity of cells was scaled up based on numbers used in a six well plate for CBA. $1.2x10^7$ HEK cells were seeded in T175 cm^2 culture flasks in DMEM, 10% BSA, 1% PSA, checked for 80% confluency the next day and then transfected with a mixture of 60 µg of CASPR2-eGFP DNA, 30 µl PEI and 1 ml of unsupplemented DMEM per flask. Culture medium was replaced on the evening of day two. 24 hours after transfection, culture media was aspirated from the flask, a single layer cell suspension was washed twice in ice cold PBS and the cells were

extracted in 3 ml of FIPA buffer (20 mM Tris pH 8.0, 100 mM NaCl, 1 mM EDTA) supplemented with 1% triton-X-100 and protease inhibitor cocktail (1:1000, Sigma). After gentle agitation the supernatant was collected, rotated at 4 ˚C for 1 hour before being centrifuged at 13,000 ×g for 10 minutes. Extracted proteins in the supernatant were collected and the eGFP content was assessed from a 100 µl of extract on a fluorescent plate reader (Victor3, Perkin Elmer). EGFP was quantified fluorescent units (FU). Protein extract was stored at -80 ˚C until required.

Serum was used at a dilution of 1:100 in FIPA buffer and extract optimisations were carried out by titrating the amount of extract in used in combination with FIPA buffer and serum. Primary incubation was either two hours at 4 ˚C or overnight at 4 ˚C, where specified. Immunocomplexes were precipitated using 50 µl of anti-human secondary antibody (RSR limited) secondary antibody after a two-hour, room temperature incubation, washed three times in FIPA buffer (1600 ×g for 10mins) with FU quantified on a fluorescent plate reader (Victor3, Perkin Elmer). Final figures are given as fluorescence units in FU.

2.5 Peripheral blood mononuclear cell (PBMC) isolation, cryopreservation and resuspension

Whole blood was taken in heparinised tubes and PBMCs were isolated by Ficoll gradient separation (Ficoll-Paque, GE Healthcare). Once washed and layered, phases were separated via centrifugation at 400 ×g for 30 min, at room temperature with a slow deceleration. The buffy coat layer was isolated with a sterile hand pastette and transferred into a sterile 50 ml conical tube. Cells were then washed twice with PBS/1%BSA (200 g, 10 minutes, RT).

0.04% trypan blue exclusion was used to count cells and at this point, PBMCs were either used fresh in experiments as described or frozen at 10–20 × 10^6 cells per mL per tube in B cell medium (BCM), consisting of RPMI 1640 without phenol red, 5% FBS, 1% PSA, 1% Glutamax, 0.1% beta-mercaptoethanol, 0.1% IgG-depleted transferrin (20 µg/ml), supplemented with 40% FBS and 10% DMSO. PBMCs suspended in this medium in cryovials were then placed in a CoolCell® Cell Freezing Container (BioCision), to allow freezing at a controlled rate, and kept at −80 °C for 24-48 hours before storage in liquid nitrogen.

To thaw and resuspend PBMCs, cryovials were transferred onto dry ice from liquid nitrogen tanks. Vials were quick thawed by immersion in a lukewarm water bath with agitation. As soon as the ice had thawed, 1 ml of the cell suspension was pipetted dropwise into a 50 mL conical tube containing 9 ml cold BCM. This 10 ml suspension was washed twice in 50 ml BCM (200 ×g, 10 minutes) and counted using trypan blue. Counted cells were then re-suspended at target PBMC concentrations.

3 The unique movement disorder associated with NMDA receptor antibody encephalitis

3.1 Introduction

NMDAR-AbE since its original description over ten years ago,[24] is an increasingly-recognised and treatable cause of encephalitis, predominantly affecting children and young adults.[26-28, 117, 118] As with other conditions in the NSAb paradigm,[87] it is firmly established that early immunotherapy improves outcomes and, therefore, prompt and accurate recognition of NMDAR-AbE will optimise patient recovery.[26-28, 118]

NMDAR-AbE has a stereotyped presentation, with early neuropsychiatric symptoms, seizures and MD, and with later onset of autonomic dysfunction and reduced consciousness, often requiring intensive care support.[26-28, 117, 118] The MD, present in around 90% of patients, can dominate the initial presentation, especially in paediatric cases.[27, 117] It is typically hyperkinetic, occurs during both obtundation and wakefulness and predominates in the limbs, often with marked orofacial involvement.[26-28, 30-32, 117-119] Currently, elegant descriptions exist in a few patients.[30] However, these series have used a variety of phenomenological terms to describe this MD, including choreoathetosis, chorea, stereotypies, myorhythmia, ataxia, and the broad term dyskinesia (Table 3-1).[26-28, 30-32, 117, 119] To date, there is no consensus on the most accurate phenomenological description of this characteristic MD and many studies rely on one or two movement disorder experts from the same centre. A better agreement on its description will better define the disorder, aid clinicians in confident recognition, thus enabling earlier immunotherapy administration as well as potentially providing insights into the neural networks involved in NMDAR-AbE.

Expert-rater descriptions are the current gold-standard used to define phenotypes in the field of movement disorders. In this study, ratings from seven experts, from seven centres around the world, across 76 videos were used to create a consensus definition of the MD in NMDAR-AbE

Study	Number of cases	Terms used to describe NMDAR-AbE movement disorder
Dalmau et al, 2008	100	Dyskinesia, Orofacial dyskinesia, choreoathetoid, ballism, rigidity, dystonia, myoclonus, tremor.
Kleinig et al, 2008	4	Repetitive semirhythmic ocular, jaw, facial, lingual, limb and trunk movements, with oculogyric deviation, opisthotonous and dystonic limb posturing. Bulbar movements – bruxism, chewing, facial grimacing, frowning, lip pouting and tongue protrusion. Limb – range from undulating movement. Variable and influenced by sensory stimulation, even during depressed consciousness.
Florance et al, 2009	81	Orofacial dyskinesia, choreoathetoid, dystonia, chorea, complex stereotyped movements, rigidity, catatonia, opisthotonous.
Irani et al, 2010	44	Choreoathetoid orofacial movements, parkinsonian, ridigity, myoclonus, oculogyric crises, opisthotonous.
Stamelou et al, 2012	1	Stereotyped antigravity movements of the arms and mouth, present during unresponsive state. Stereotyped perioral dyskinetic movements.
Baizabal-Carvallo, 2013	9	Chorea, stereotypic movements, ataxia, limb dystonia, limb myorhythmia, oromandibular dystonia, facial myorhythmia, blepharospasm, opisthotonous, athetosis and tremor.
Titulaer et al, 2013	577	Orofacial dyskinesia and choreoathetosis.
Mohammad et al, 2014	10	Stereotypy, dystonia, chorea, perseveration, akinesia, ballism and tremor.

Table 3-1 Description of MD associated with NMDAR-AbE in different series.

Cases were collected from the literature. [26-28, 30-32, 117, 119] The number of NMDAR-AbE antibody positive patients shown in the second column and terms used to describe MD in the third column. Note the variation in terms used.

3.2 Methods

3.2.1 Patient Selection

Autoimmune neurology researchers from three international centres contributed 44 videos of 20 patients who met diagnostic criteria for NMDAR-AbE (Ethical Approval numbers, Sydney 09/CHW/56, Milan 10/6/15 VN19, Oxford 16/YH/0013).[120] A literature search using the following terms "NMDAR-antibody encephalitis" and "anti-NMDAR encephalitis" plus associated references, yielded eight papers and another 32 videos of 14 patients.[31, 32, 41, 121-125] Clinical features, onset and offset data, outcomes and paraclinical findings were collected via case note review and from data in published papers. Disease control videos were also taken from the literature, yielding twenty videos of 18 age- and sex-matched cases (age range 2-41 years, median 12, 50% female),[32, 126-136] selected to represent some predicted MD phenomenological overlaps with the NMDAR-AbE associated MD. These included a mixture of relatively pure MDs including chorea (Sydenham's, n=3), stereotypies (Rett's syndrome n=2; Autism, n=1) and dystonia (DYT1, n=2; DYT16, n=2), as well as complex mixed MDs (ADCY5, n=3; FOXG1, n=3; Ataxia Telangiectasia, n=1; Myoclonus Dystonia, n=2; Neuroacanthocytosis, n=1).

3.2.2 Video Editing

Videos were standardised, anonymised and had time stamps removed to give as unbiased view of the video as possible. Video files which were of the same subject at different time points were cut into separate videos to allow for analysis of patients in as full a way as possible.

3.2.3 Movement disorder classification

Seven movement disorder experts (Kailash Bhatia, Victor Fung, Tony Lang, Tim Lynch, Nardo Nardocci, Kapil Sethi and Marina Tijssen) agreed to participate in a study entitled 'Autoimmune movement disorders'. Initially, these experts established a consensus glossary of MD terms (Appendix A, modified from Mohammad et al[32]). Next, they each blindly, and separate from each other, rated 76 videos from 34 NMDAR-AbE patients (median 2 videos per patient, range 1-7) plus 20 disease control videos, using a standardised proforma (Appendix B) containing forced-choice glossary-derived MD terms. This also included the evaluation of the dominant and associated MD,[137] the anatomical distribution of the MD (face, upper limb, lower limb, neck and trunk) and free-text for comment on specific videos. The results of this study have been published and the data presented below is derived from this work.[138]

3.2.4 Statistical Analysis

Statistics included inter-rater reliability (Fleiss-kappa) and Mann-Whitney U test. Analyses were performed in GraphPad Prism v7 and Microsoft Excel.

3.3 Description of cohort

As shown in Table 3-2, there were 34 patients with a median age of 7 years (range 0.2 – 32 years) and 59% females. The cohort was young and consistent with this, only 6% (2/34) had an ovarian teratoma. Peak modified Rankin scale (mRS) illustrated that this is a severe illness (median 5; range 2-5), and, other than the fact patients were selected on the basis of having a MD, the clinical features and investigation findings are similar to other published series of patients with NMDAR-AbE.[26-28, 117, 118]

Clinical and paraclinical Details	Patients (N = 34)
Median Age (range)	7 (0.2-32 years)
Female	20/34 (59%)
Median peak mRS (range)	5 (2-5)
Tumor	2/34 (6%)
Psychiatric	33/34 (97%)
Cognitive Symptoms	32/34 (94%)
Seizures	30/34 (88%)
Autonomic	17/34 (50%)
EEG Abnormal	28/30 (93%)
CSF Abnormal	19/33 (58%)
MRI Abnormal	9/34 (27%)

Table 3-2 Clinical and paraclinial details of NMDAR-AbE MD cohort

Clinical and investigation findings from the 34 patients whose videos were rated. To be included in the study, patients were required to have a movement disorder, therefore this information is not displayed. Abnormal CSF findings was classified as any of pleocytosis, oligoclonal bands or a raised protein. Tumours noted were two ovarian teratomas, seen in adult women (25 and 32 years old). Datasets were obtained by co-authors and denominators <34 represent instances where certain details were not available from videos taken from the literature.

Based on data collected from collaborators, onset and offset of major symptoms groups were plotted, the offset data in a cohort of this size is novel in this condition. As expected, the MD was an early feature (Figure 3-1-A) and persisted for a median of 112.5 days (range 30-1482, Figure 3-1-B), with offset at a similar time to the psychiatric features (median 90, range 5-1482 days). In contrast, seizures and dysautonomia had a median offset in the first 50 days of illness. In addition to the established prolonged presence of psychiatric symptoms,[139] the MD was similarly an enduring problem in this population.

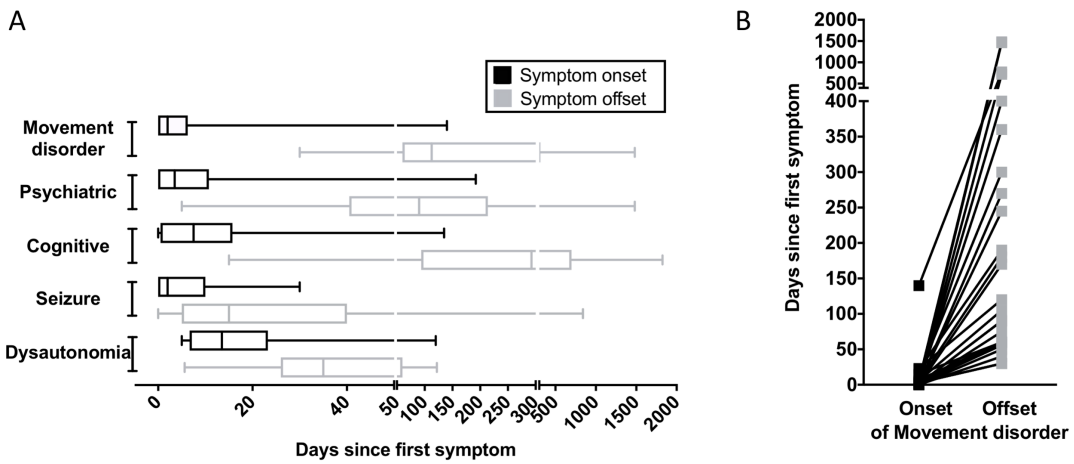


Figure 3-1 Symptom onset and offset in NMDAR-AbE

(A) Day of onset (black) and offset (grey) of the main five symptom categories after first symptom (day 1; median, box hinges are 25th and 75th percentile and whiskers go to minimum and maximum values), (B) with a particular focus on the timing of the movement disorder (MD) in individual patients.

3.4 Video evaluation of MD

3.4.1 Phenomenologies predominant in NMDAR-AbE MD

Videos of NMDAR-AbE patients were rated by seven experts, with patients sampled at a range of time points since disease onset (median 28 days, range 1-690 days). Dominant MD phenomenologies were examined initially and three predominated (Figure 3-2): dystonia (20%), chorea (20%) and stereotypies (19%). A number of other hyperkinetic phenomenologies were observed as well, including, in order of decreasing frequency: clonic perseveration (6%), ballism (6%), myoclonus (5%), tonic perseveration (3%), and tremor (1%). Terms relating to hypokinetic MDs including catatonia (6%), and bradykinesia (5%) were less frequent.

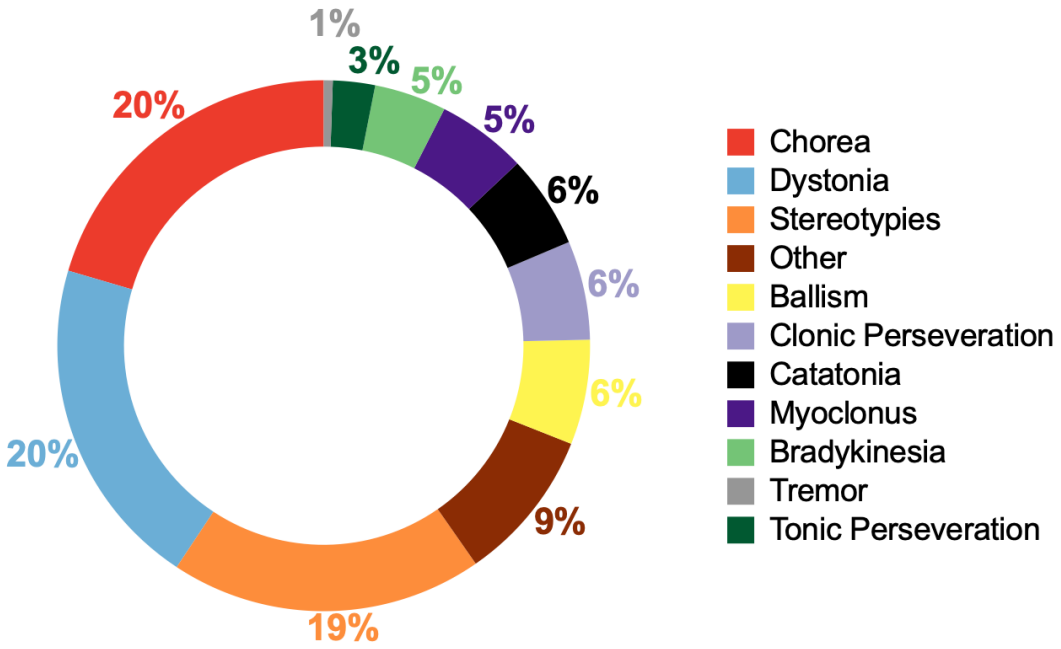


Figure 3-2 Expert classification of dominant MD phenomenology in NMDAR-AbE

This is the distribution of the dominant MD terms used by experts across all 76 videos. Dystonia, chorea and stereotypies were the most commonly used terms. For the 'other' category, raters used terms including mutism, stupor, myorhythmia, myokymia, tics, opisthotonus, cerebellar syndrome/ataxia, orofacial dyskinesia, waxy flexibility, oculogyric crises, athetosis, agitation, seizure, startle and vocal perseveration.

Overall, experts used fewer phenomenological descriptors when describing the MD in controls (mean 1.9 per video, range 1-4) compared to NMDAR-AbE (mean 3.4 per video, range 1-7; $p<0.0001$, Mann-Whitney U-test). This complex appearance was further emphasised in free-text feedback from expert-raters (see discussion). This was also consistent with the more robust inter-rater reliability seen across the 20 control videos compared to the 76 NMDAR-AbE videos, for the dominant phenomenology as dystonia (κ= 0.65 vs 0.39, controls vs NMDAR-AbE), chorea (κ=0.63 vs 0.39) or stereotypies (κ= 0.91 vs 0.22).

3.4.2 Co-association of MDs in NMDAR-AbE

The next question was to see how these MD interacted with each other, for example, whether there were three distinct populations of patients with predominant

dystonia, chorea or stereotypy respectively, or if these phenomenologies were occurring together and if so, what these relationships were. A co-occurrence matrix was plotted based on how often MDs occurred together in single videos and then represented using a chord diagram constructed with Circos.[140] This demonstrated marked co-occurrence of chorea, dystonia and stereotypies, represented by the thickness of chords connecting these three MDs (Figure 3-3-A). Looking at patients individually, 97% (33/34) of them and 79% (60/76) of videos were described as having two of dystonia, chorea and stereotypies and 76% (26/34) of patients and 46% (35/76) of videos containing all three phenomenologies. This, and further co-occurrence analyses (Figure 3-3-B-D) where videos were selected based on having predominance of either dystonia, chorea or stereotypy and then the associated MDs were plotted, confirmed their co-occurrence and revealed other interesting associations. These included the frequent overlaps of stereotypies with clonic perseveration and catatonia but its disassociation from bradykinesia, (Figure 3-3-C), the lack of catatonia in patients with predominant chorea, (Figure 3-3-D), and the less common triad of tonic perseverations-catatonia-bradykinesia (Figure 3-3-A). It also confirmed reassuring overlaps, such as the expected co-occurrence of chorea with ballism. Overall, very similar patterns were observed with the inclusion of associated disorders (Figure 3-4).

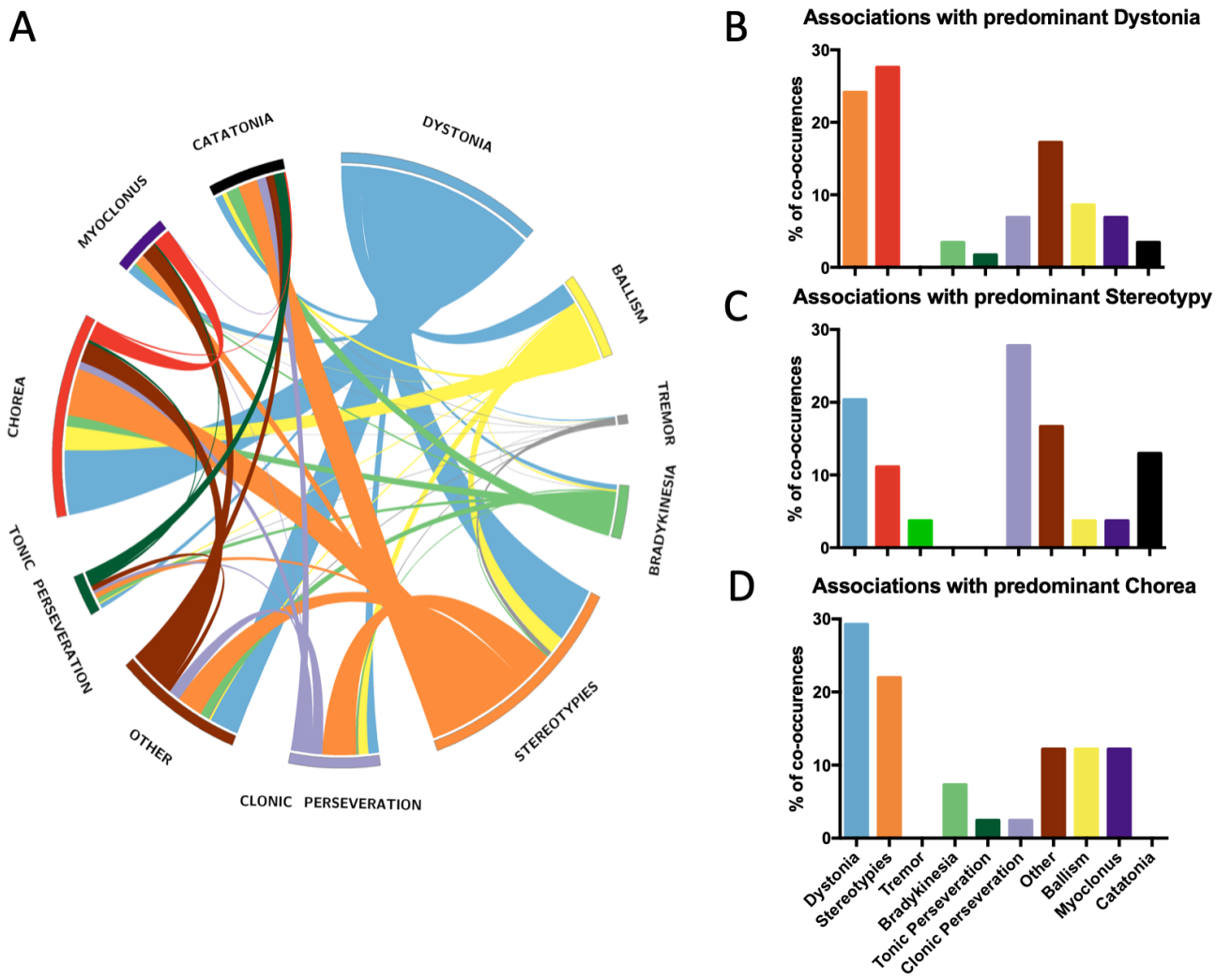


Figure 3-3 Co-occurrence of NMDAR-AbE MD phenomenologies in dominant MDs

(A) The interactions between phenomenologies in NMDAR-AbE with striking co-occurrence of stereotypies, chorea and dystonia shown in a chord diagram based on a co-occurrence matrix within single video ratings. The most common MD rated within a video was used to compare co-occurrence of other phenomenologies within that video, for dystonia (B), stereotypies (C) and chorea (D).

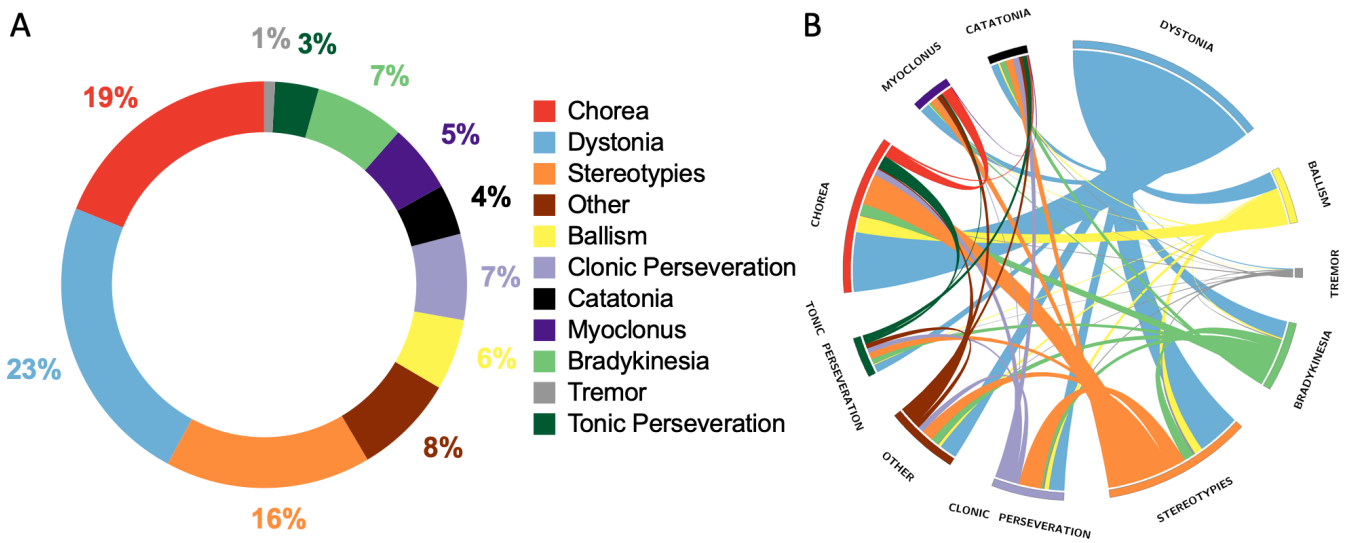


Figure 3-4 NMDAR AbE predominant MDs and co-occurrences - dominant and associated MDs included

Overall, the patterns and proportions are strikingly similar to the dominant disorders alone. Slightly lower overall kappa values were noted, likely due to the sensitivity of Fleiss-kappa values to an increased number of responses from multiple raters: dystonia (κ= 0.44 vs 0.46, controls vs NMDAR-AbE), chorea (κ=0.48 vs 0.34), and stereotypy (κ= 0.74 vs 0.17). (A) The summarised data for expert-ratings for 76 videos from patients with NMDAR-AbE. For other, raters used terms including mutism, stupor, myorhythmia, myokymia, tics, opisthotonus, cerebellar syndrome/ataxia, orofacial dyskinesia, waxy flexibility, oculogyric crises, athetosis, agitation, seizure, startle and vocal perseveration. (B) Striking co-occurrence of stereotypies, chorea and dystonia shown in a chord diagram plot, based on a co-occurrence matrix within single video ratings.

3.5 Temporal variability

A longstanding clinical observation is the rapid variability in this MD over time in patients and therefore, in order to explore this, several patients were rated longitudinally. Patients with multiple videos from the same day were scored (Figure 3-5-A), as well as those with videos sequentially over different days (median=21 days, range 0–360 days; Figure 3-5-B). Dystonia, stereotypies and chorea remained prominent but this clinical observation was confirmed with both marked variability in the MD within an individual patient over a single day, as well as over a number of weeks.

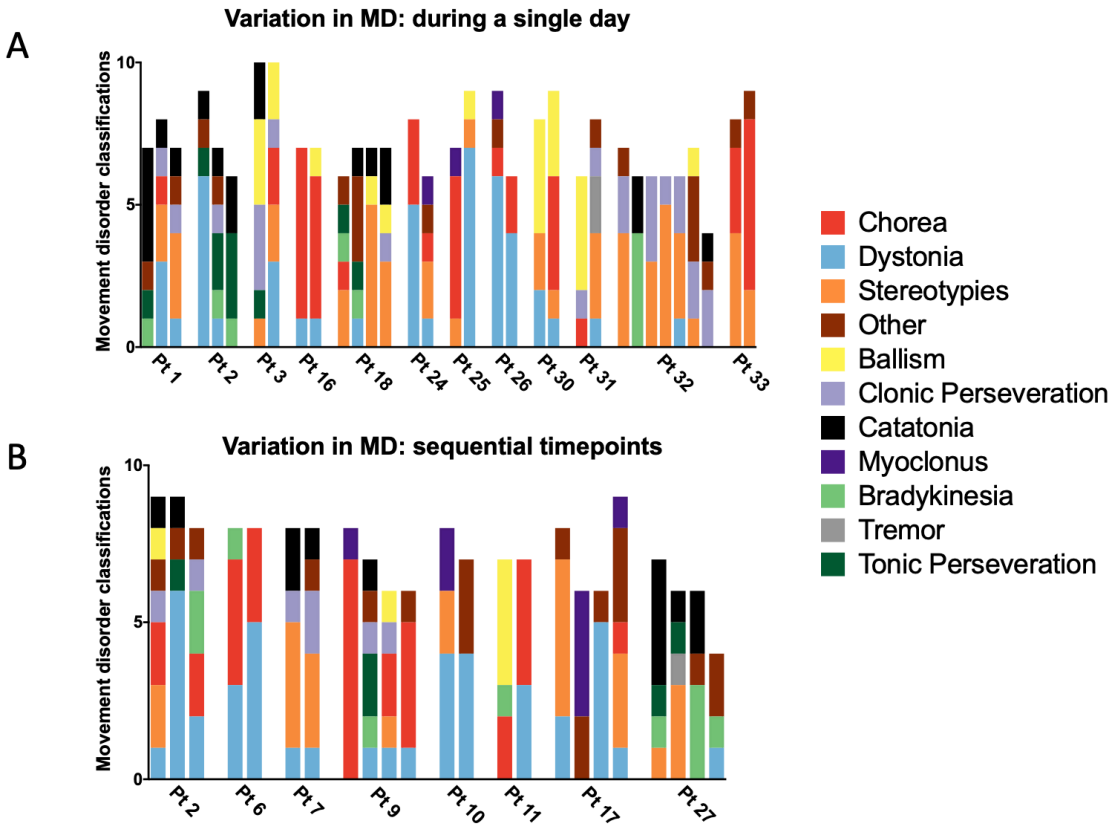


Figure 3-5 Temporal variation in NMDAR AbE MD

(A) Sequential videos of the same patient (Pt), filmed on the same day. (B) Videos of the same patient filmed over a range of time points (median= 21 days, range 0-360 days). The movement disorder is highly variable over minutes and hours as well as over days to weeks. These figures show the dominant movement disorder calls made by each expert where more than one video was available for a patient. Each bar displays the different movement disorders described by experts and gaps between clusters of bars allow distinction between groups of videos from a single patient.

3.6 Regional distribution of movement disorder

Finally, as part of their description, raters were requested to ascribe an anatomical distribution to the MD observed. This demonstrated similar rates of dystonia, chorea and stereotypies in the face, arm and leg (Figure 3-6).

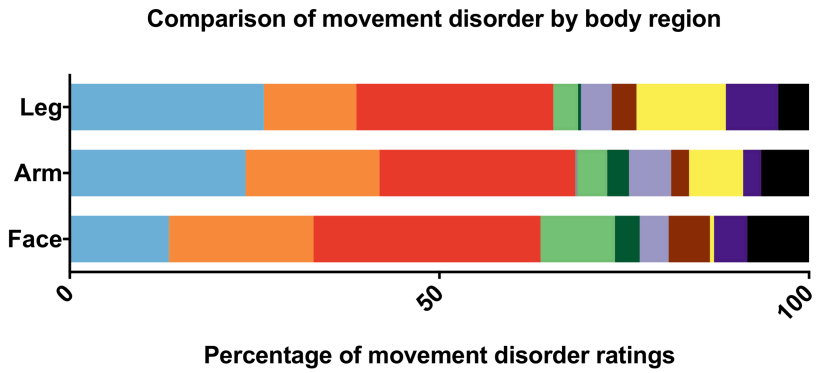


Figure 3-6 Regional distribution of MD in NMDAR-AbE

For each region, MDs were summed, a percentage of total MDs was derived and these were plotted side by side. Stereotypies, chorea and dystonia were equally represented in the face, arm and leg.

3.7 Discussion

NMDAR-AbE is a severe neurological disorder which is treatable and the earlier immunotherapy is given, the better the outcomes.[26-28] The MD is a commonly appreciated and well-emphasised feature of descriptions of NMDAR-AbE, however, its classification remains highly-variable, with no expert consensus.[26-28, 30-32, 117, 119] In order to recognise a MD closely associated with a disease, there must be informed and accurate phenomenological characterisation. This is especially important in paediatric NMDAR-AbE where the MD manifests early.[117] Therefore, we aimed to create a consensus description of the MD from some of the leading international experts in the field of MD phenomenology. Our data show that the MD associated with NMDAR-AbE occurs early in disease and is a persistent feature, characterised by a variety of widely-distributed hyperkinetic phenomenologies, with dystonia, chorea and stereotypies especially prominent. It remains, however, a complex entity to describe in conventional MD terminology.

Expert-rater assessment of our large collection of videos categorised the MD associated with NMDAR-AbE as a combination of chorea, stereotypies and dystonia with a marked absence of tremor and tics, and a relative paucity of myoclonus. This triad was seen in the limbs and face and may be a more accurate description than the imprecise term dyskinesia, often used in particular to describe the orofacial movements seen in patients with NMDAR-AbE. These characteristics highlight distinctive features of this complex, mixed movement disorder and aid differentiation from key differential diagnoses in routine clinical practice including primary psychiatric disorders, childhood metabolic disturbances, drug intoxication and Sydenham's chorea.[62, 129, 134, 141, 142] Indeed, the coexistence of widely-distributed chorea, dystonia and stereotypies is very rare in any other neurological conditions, making this combination highly characteristic of NMDAR-AbE (expert panel, unpublished observations).

The gold-standard in the classification of MDs is still provided by expert-raters. In this study, they struggled to classify the MD associated with NMDAR-AbE, with their feedback stating: "*our definition and description of hyperkinetic movements do not cover some of these patients*" and "*reviewing all of these videotapes was a challenge particularly to preconceived and established phenomenological categorizations. Not infrequently I was dissatisfied with the final category that I chose*". This difficulty in classifying patients with existing terms is reflected in the poorer inter-rater kappa statistics seen in the patients with NMDAR-AbE compared to controls, and the greater numbers of terms required to describe these patients. While these kappa values could be interpreted as reflecting intrinsic variability between expert-raters, they showed good agreement across other varied disorders and many terms are not interchangeable. For example, the distinction between stereotypies, with seemingly planned and

purposeful movements, versus irregular, non-purposeful chorea is clear, especially to MD experts.[143, 144] There are, however, a number of limitations inherent in our study. These include the lack of accompanying clinical histories and standardised video assessments to systematically assess bradykinesia, awareness and arousal, the young age of the cohort, an intrinsic bias towards recording the most unusual observations when creating videos of patients and the use of forced-choice descriptors. A future study would ideally be prospective, with a standardised video assessment at fixed time points of a patient's illness to better map the evolution of the MDs over time and its response to treatment. It could also incorporate a more exhaustive list of control mixed movement disorders.

Nevertheless, the above distinctive combination of features may give some sense of the dysfunctional neural circuits underlying NMDAR-AbE. For example, stereotypies associate with few disorders including autism-spectrum disorder, Rett's syndrome and fronto-temporal dementia,[144-146] and chorea often localises to the striatum.[147] Furthermore, at a molecular level, it is especially striking that the movement disorders seen in patients with NMDAR hypofunction, such as GRIN1A mutations and users of drugs which inhibit NMDARs such as ketamine and PCP, share close phenomenological similarities to the patients in our study.[62, 148, 149] Indeed, the common mechanism of diffuse down-regulation of NMDARs in all these disorders may modulate downstream circuits and decrease signalling of cortico-striatal projections allowing disinhibition of central pattern generators to produce this characteristic MD.[30, 119]

There is an apparent contradiction in suggesting the down regulation of NMDARs, an excitatory receptor, gives an increased propensity to seizures and hyperkinetic MD. This was addressed a recent study using dynamic causal modelling based on EEG of

paediatric NMDAR-AbE cases and mice infused with NMDAR antibodies. They found diffusely disrupted networks, giving altered dynamics of spontaneous EEG activity introducing a susceptibility to 'paroxysmal abnormalities' in the form of seizures and MD.[150] Given the striking similarity in the onset and offset timings of psychiatric features and the MD, this NMDAR hypofunction likely explains the psychiatric phenomenology also.

In summary, this study provides the largest multi-expert, multi-centred, in-depth, gold-standard analysis of the NMDAR-AbE MD. The MD, in conjunction with psychiatric and cognitive symptoms, has been found to be a prolonged feature of the syndrome, in contrast to seizures and autonomic dysfunction. Expert-raters classified the MD as a complex, hyperkinetic disorder dominated by the triad of chorea, stereotypies and dystonia occurring together, in addition to other less-frequently associated phenomenologies. This characteristic combination should provide clinicians with greater confidence in diagnosing this common cause of encephalitis, allowing earlier immunotherapy administration and improved patient outcome

4 The role of antibodies in neuropsychiatric systemic lupus erythematosus

4.1 Introduction

SLE is a multi-system autoimmune disease primarily affecting young women.[151] A common and particularly debilitating aspect of this disease are its neuropsychiatric sequelae, grouped together as NPSLE. These manifestations are extremely broadly defined, ranging from headache to aseptic meningitis (Table 4-1), and are therefore difficult to classify.[152] Efforts have therefore been made to identify biomarkers of NPSLE, and antibodies to the DWEYS peptide have received much attention due to their ability to recognise linearised NMDARs and for monoclonal antibodies targeting DWEYS to cause hippocampal neuronal loss in both *in vitro* and *in vivo* models.[153] DWEYS is pentapeptide sequence similar to the amino acid sequence 283 -287 on the extracellular domain of NMDA receptor subunit 2A (DWDYS) and 2B (DEWDY) and thought, therefore, to represent a feasible antigenic substrate (Figure 4-1). The sequence was derived from a phage display library using the monoclonal antibody R4A[154], previously described as an antibody to double stranded DNA (dsDNA) and known to reproduce aspects of SLE pathology in mouse models.

The literature is, however, inconsistent on whether the DWEYS antibody, as measured by ELISA, reliably associates with NPSLE in humans, with evidence for[155-157] and against.[158-160] A recent meta-analysis suggested serum/plasma DWEYS antibodies are present in a higher proportion in SLE versus disease controls and in NPSLE versus SLE.[161] CBA uses NR2A/B in its natural, conformational state with the extracellular portion of the molecule freely available, therefore these antibodies should be detectable using this system as well as in live cultured

primary rodent hippocampal neurons, which express a broad range of neuronal surface proteins, including NMDARs.

The pathogenesis of SLE is complex and remains only partially understood, with genetic, environmental and immunological abnormalities all thought to contribute. There is a growing literature on the role of type 1 interferons (IFN) in association with SLE. IFNs are antiviral molecules secreted by cells of the innate and adaptive immune system. There are numerous IFN molecules and these have been divided into three families; type 1, type 2 and type 3. Type 1 interferons include IFN$\alpha/\beta/\delta/\varepsilon/\kappa/\tau/\omega/\zeta$. Cells of the innate immune system, such as dendritic cells, express proteins called pattern recognition receptors (PRRs). The purpose of these proteins is to respond to viruses, viral particles, foreign organism nucleic acids or host cell components release during cell damage or death. Type I IFN is one secretory response to PRR stimulation.[162] Of the type 1 IFNs, IFNα is most robustly associated with SLE and is secreted by plasmacytoid dendritic cells. Several patients have been shown to develop SLE in response to IFNα therapy[163] and elevated serum levels of type 1 IFN was noted in SLE,[164] and in CSF of patients with NPSLE,[165] though this was not reproduced in another study using different assay methodology.[166]

In general, measurement of IFNα protein has been methodologically challenging and surrogate markers have been employed such as the type 1 IFN induced gene transcription signature from SLE PBMCs which is widely established.[167, 168] Furthermore, in a large, longitudinal study looking at blood biomarkers which correlated with SLE disease activity, the type 1-IFN response was the best predictor.[169] Crucially this response was localised functionally to IFNα as it was demonstrated that inhibition with an IFNα neutralising antibody, abrogated the ability of patient plasma to induce a type 1 interferon genetic signature.[170] The pan-IFNα digital single molecule array (SIMOA) is a novel, validated assay,[171]

utilised by collaborators to measure IFNα levels in the plasma and CSF of a mixed cohort of SLE and NPSLE to see if this could predict NPSLE.

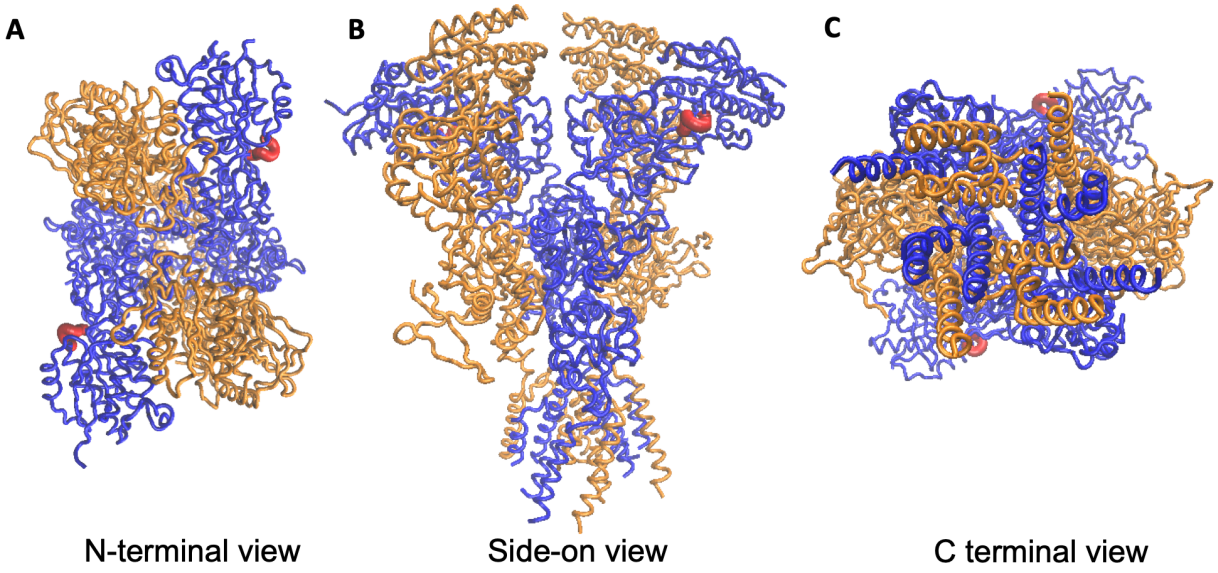


Figure 4-1 Crystal Structure of NMDAR, with location of DWEYS (AA284-287) sequence highlighted in red.

NR1 subunit in yellow and NR2A subunit in blue. Views represented from three angles.

Central Manifestations	**Peripheral Manifestations**
Aseptic meningitis	Acute inflammatory demyelinating polyradiculoneuropathy
Myelopathy	Autonomic disorder
Demyelinating syndrome	Mononeuropathy, single/multiplex
Cerebrovascular disease	Myasthenia gravis
Headache (including migraine and benign intracranial hypertension)	Plexopathy
Movement disorder (chorea)	Neuropathy, cranial
Seizure disorders	Polyneuropathy
Cognitive dysfunction	
Acute confusional state	
Mood disorder	
Anxiety disorder	
Psychosis	

Table 4-1 American College of Rheumatology definition of syndromes associated with SLE.[172]

4.2 Methods

4.2.1 Patient selection

Healthy controls, SLE patients and disease controls were obtained via a collaboration with Dr Frederik Piehl and Dr Magnus Andersson from the Karolinska institute, Sweden, who provided paired plasma and CSF samples as well as clinical results based on retrospective case note review. SLE patients were a mixture of NPSLE and SLE. Basic laboratory results included in this study were provided and based on measurements from local laboratories from Sweden (dsDNA, C-reactive protein [CRP] and erythrocyte sedimentation rate [ESR]). Disease controls were 32 patients with multiple sclerosis (MS) and 4 patients with 'neuroinflammation'. 36 additional antibody controls were patients with known antibody mediated central nervous system disorders, recruited from our laboratory; 12 aquaporin-4 (AQP4) antibody seropositive NMOSD, 13 LGI1-antibody positive patients and 11 with NMDAR-AbE.

4.2.2 DWEYS Enzyme Linked Immunosorbent Assay (ELISA)

Nunc Maxisorp C bottom 96 well plates were coated with 20 μg/ml DWEYSVWLSN or scrambled versions of this peptide - SDYVWLNESW and KWRYSVWLSN (Cambridge Peptides) at room temperature for one hour in a coating buffer of 0.05M Carbonate-Bicarbonate, pH 9.6. The plate was then emptied and washed five times (this was done between each step) with wash buffer (50 mM Tris, 0.14 M NaCl, 0.05% Tween 20, pH 8.0). Wash steps were performed between all steps. The plate was then blocked for an hour at room temperature with blocking buffer (5% BSA in PBS). Samples were diluted in sample buffer (PBS 0.2% BSA and 0.05% Tween) at 1:500 for plasma and 1:1 for CSF and incubated for an hour at room temperature; secondary incubation was carried out at room temperature with DAKO anti-human/mouse HRP 1:2000. TMB (Bethyl) was used to develop the reaction which was

quenched after 15-20 minutes with 0.18 M H_2S0_4. Absorbance was read within 20 minutes on a plate reader at 450nm.

4.2.3 IFN-α SIMOA

The IFN-α SIMOA was carried out at the Institute Pasteur using the method published in Rodero et al.[171] Briefly, the protocol used a Quanterix Homebrew SIMOA assay, a form of digital ELISA technology. Two patient derived monoclonal antibodies specific for IFNα were used, the first, as capture antibody (8H1) antibody by coating it onto paramagnetic beads (0.3mg/ml) and a second (12H5) was used as a detector antibody and biotinylated (biotin:antibody ratio = 30:1). Patient sample was added to capture antibody labelled paramagnetic beads, at dilutions of between 1:3 and 1:30. Then detector antibody was added and beads were spun down into arrays of 50,000 individual 46 femtoliter sized wells. A streptavidin-β-galactosidase conjugate was then used to label the biotinylated detector molecule (150pM) and a fluorogenic enzyme substrate was finally added (resorufin-β-D-galactopyranoside). With the beads in single-molecule arrays, the decreased reaction volume allows a high local concentration of fluorescent signal and more accurate quantification at an individual immunocomplex level, giving an output in average numbers of enzymes per bead (AEB), which could be quantified by microwell. Recombinant IFNα17/αI (PBL assay science) was used to generate a standard curve and give a quantitative readout in fg/ml. The cut-off for positivity was based on mean plus three standard deviation of all blank runs.

4.3 Cohort description

Clinical details were collected by Dr Frederik Piehl and Dr Magnus Andersson from the Karolinska Institute, Sweden. The demographics in terms of age and sex are typical for SLE.

The cohort intentionally contained a mixture of patients with active SLE (65.7%) or NPSLE (42.9%) at time the paired plasma and CSF was collected. During all experiments we were blinded to the clinical features of the patients. In those with NPSLE, in keeping with current evidence, there were broad and overlapping neurological features described. The most predominant symptoms being headache (46.7%), cranial nerve deficit (46.7%) and cognitive symptoms (33.3%) respectively. MRI and EEG data were not widely available but as expected the majority of patients had positive anti-nuclear antibodies (ANA) (87.9%), whilst a smaller proportion had antibodies to dsDNA, (41.7%). The majority were on immunotherapy and this was primarily prednisolone (70.6%) and hydroxychloroquine (41.2%), as would be expected in a cohort of SLE patients. Only three were on a form of biologic therapy (Belimumab [n=2] and Rituximab [n=1]).

Characteristic	SLE patients (n=35)
Female (number, %)	34 (97.1%)
Age (median, range)	41 (18-77)
Active SLE	23 (65.7%)
Active NPSLE	15 (42.9%)
Neurological features • Headache • Cranial nerve deficit • Cognitive • Stroke • Psychiatric • Seizures • Movement disorder • Aseptic meningitis • Sensory deficit	 7/15 (46.7%) 7/15 (46.7%) 5/15 (33.3%) 3/15 (20.0%) 2/15 (13.3%) 1/15 (6.7%) 1/15 (6.7%) 1/15 (6.7%) 1/15 (6.7%)
MRI Abnormal	4/6 (66.7%)
EEG Abnormal	0/1 (0%)
Immunotherapy • Prednisolone • Hydroxychloroquine • ASA • AZA • MMF • Biologic • Ciclosporin • Methotrexate	32/34 (94.1%) 24/34 (70.6%) 14/34 (41.2%) 13/34 (38.2%) 9/34 (26.5%) 5/34 (14.7%) 3/34 (8.8%) 2/34 (5.9%) 1/34 (2.9%)
Positive ANA	29/33 (87.9%)
Positive dsDNA	10/24 (41.7%)

Table 4-2 Description of SLE cohort from Karolinska Institute Sweden

Demographic, clinical and paraclinical data of patients in our cohort. Where denominator is less than 35, the number represents the number of patients where that data was available.

4.4 Screening for binding on native conformational epitopes

4.4.1 Antibodies in cohort plasma or CSF do not bind extracellular domains of natively expressed NR1, NR2A or NR2B on CBA

As the DWEYS peptide sequence is located on the extracellular portion of both the NR2A and NR2B subunits of the NMDAR heterodimer, CBAs utilising both NR2A and NR2B in

combination with the obligate NR1 subunit were used to screen both paired CSF and plasma from our SLE cohort. No binding was found based on two repeated screenings (Figure 4-2), positive controls from serum of a patient with NMDAR-AbE worked in all assay used.

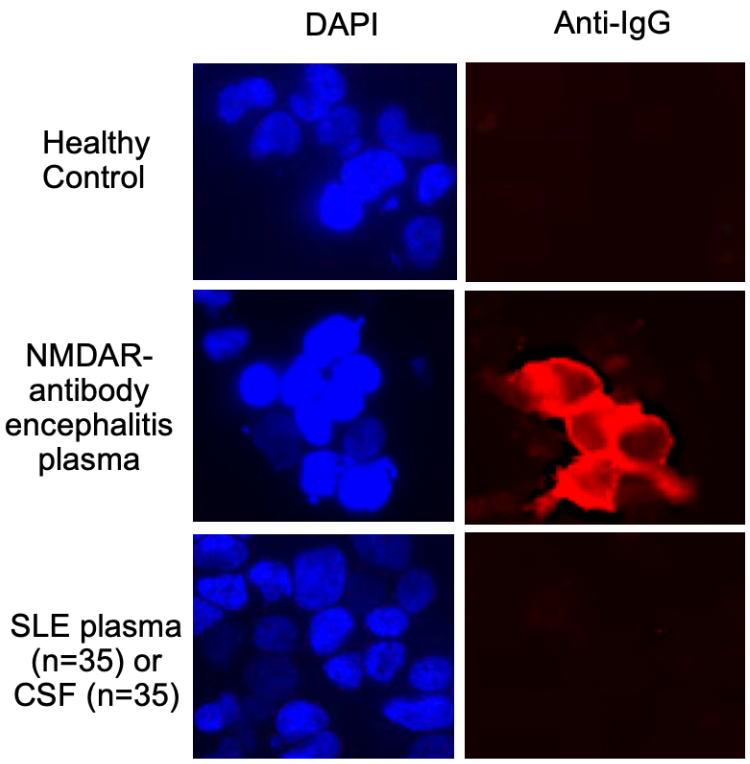


Figure 4-2 Cell based assay of serum and CSF from patients with NPSLE and SLE

Paired plasma and CSF from our SLE cohort did not bind CBAs expressing NR1 and NR2A heterodimers or NR1 and NR2B heterodimers on two repeated assays. Serum from a patient with clinically definite NMDAR-AbE bound these cells expression either NR1/NR2A or NR1/NR2B. DAPI in blue labelling nuclei, Anti-human IgG secondary antibody is shown in red.

4.4.2 SLE plasma/CSF does not bind cultured primary rodent hippocampal neurons

Using NMDAR CBA, with relevant NMDAR expressed in its native conformation, no binding could be detected. An alternative system was therefore trialled. Rodent neurons were cultured for 13 days and then used as a source of NMDARs not induced by plasmid transfection of a cell line. Patient plasma and CSF was assayed whilst the neurons were live and therefore the antigen is in its natural, three-dimensional conformation, before the

addition of any fixative, as previously described.[81] Using this method no binding was observed with any of the SLE plasma or CSF. A patient with NMDAR-AbE was used as positive control and this demonstrated reproducible binding (Figure 4-3). At this point, we could find no evidence of plasma or CSF from patients with SLE/NPSLE binding NMDARs in their native, conformational state in vitro.

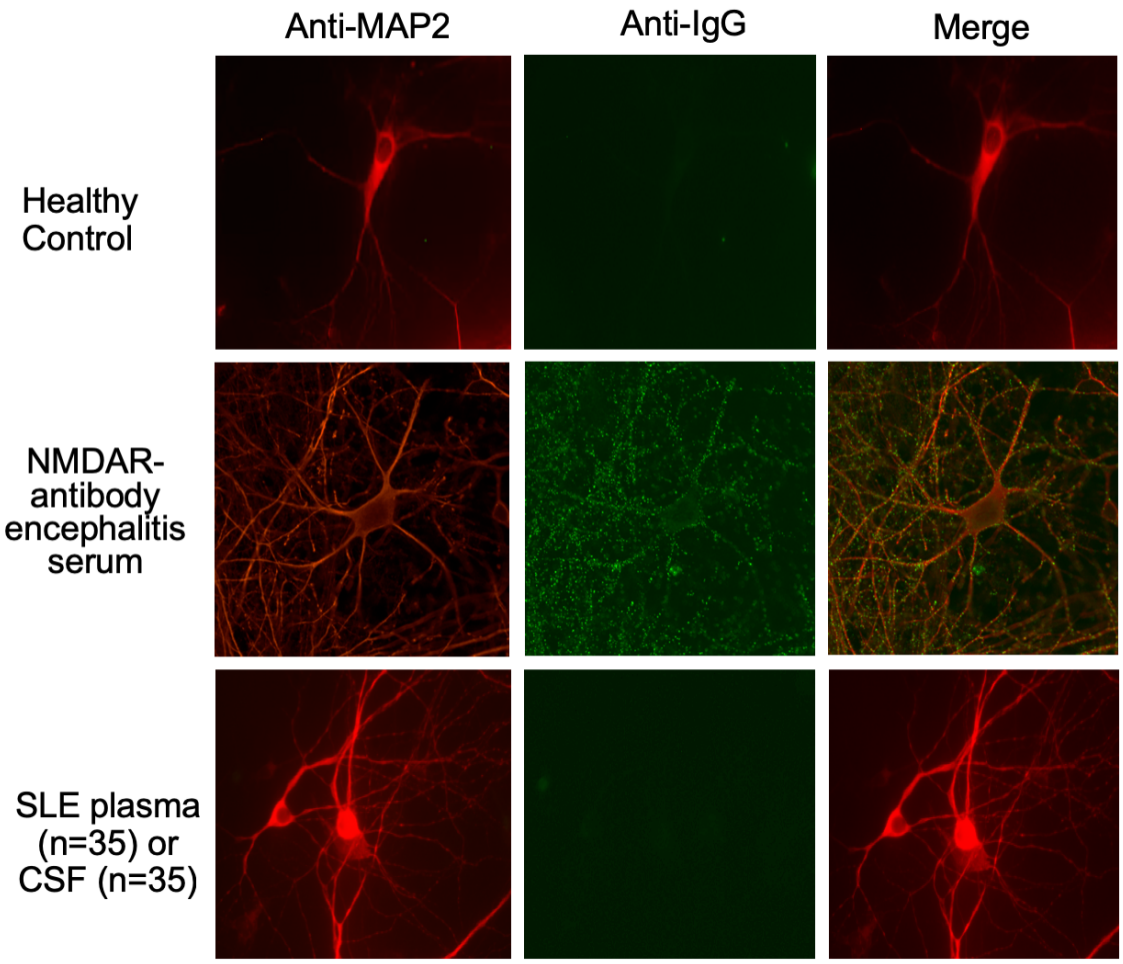


Figure 4-3 Antibodies in SLE plasma and CSF do not bind primary rodent hippocampal neurons

Primary rodent hippocampal neurons assayed at DIV 13 and stained with MAP2 (red) did not show any binding of patient antibody (IgG anti-human secondary in green) in either CSF or plasma. A patient with NMDAR-AbE was used as a positive control and showed excellent, reproducible binding. The positive control image was kindly provided by Dr Antonio Berretta, Oxford Autoimmune Neurology group, all other images my own work.

4.5 DWEYS ELISA assay experiments

4.5.1 DWEYS ELISA set up and optimisation

As no SLE patient antibody binding was observed to NMDAR (NR1 and either NR2A or NR2B), the next step was to replicate the DWEYS IgG ELISA set up by Diamond et al when they originally described the DWEYS antibodies in SLE.[155] In collaboration with this group, we obtained their monoclonals: the R4A clone, a murine isotype control - MPC, and a humanised DWEYS monoclonal - G11, and its isotype control - B1. Their shared and published exact assay protocol was replicated and successfully optimised both in terms of concentration of monoclonal antibody to demonstrate binding, which was 2μg/ml, and the concentration of DWEYS peptide used to coat the ELISA plate, which was 20μg/ml (Figure 4-4). Binding of R4A and G11 with no binding of isotype controls was achieved with low background.

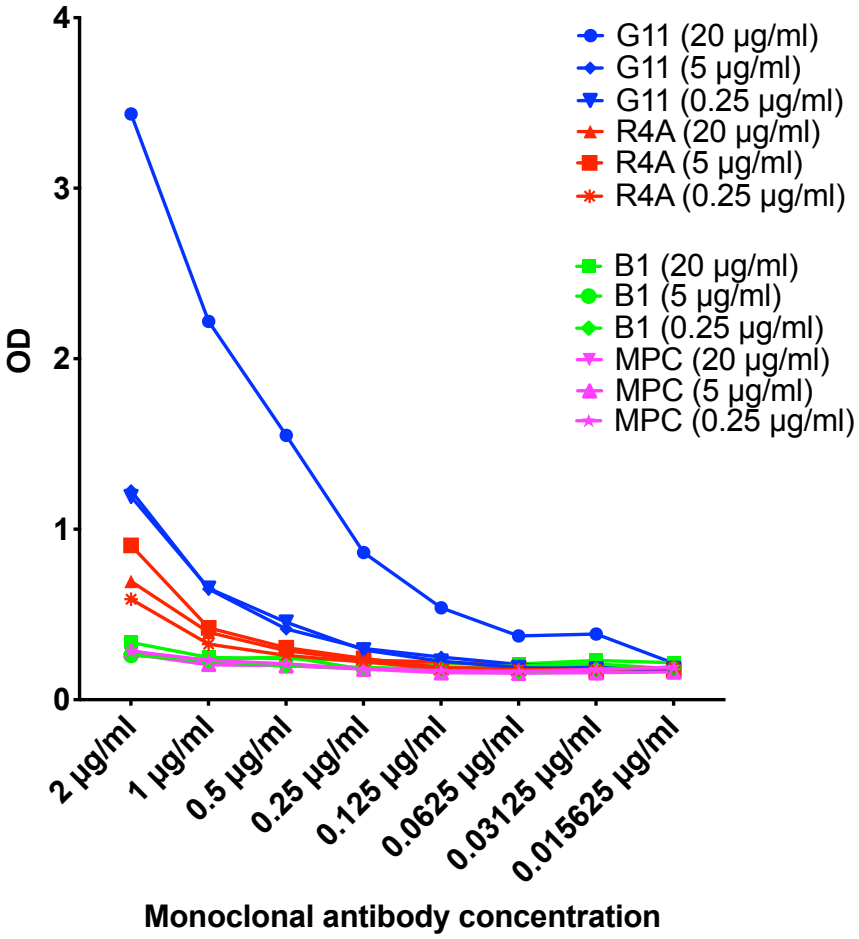


Figure 4-4 Optimisation of DWEYS IgG ELISA

ELISA coated with varied amounts of DWEYS peptide (displayed in figure legend of each monoclonal replicate) across of a range of concentration of monoclonal antibodies. Binding of B11 and R4A but not their isotype controls was achieved, at an optimal DWEYS coating concentration of 20µg/ml, as used by the Diamond laboratory.

4.5.2 DWEYS ELISA Plasma/CSF results in cohorts

Plasma from 35 SLE patients, 36 healthy controls (HC), 36 disease controls (DC) and 36 antibody controls (AC) were screened using the optimised DWEYS ELISA assay (Figure 4-5-A). Mean plus 3 standard deviations of the healthy controls was taken as the cut-off for positivity. The data from the different cohorts overlapped significantly: 8 SLE patients, 2 HCs and 2 DCs were positive. This translates as a sensitivity of 22.9% for SLE and specificity of 96.3%.

There was a significant difference between ODs of SLE patients versus HCs (p=0.007, Kruskal Wallis with post-hoc Dunn's) and ACs (p=0.0005, Kruskal Wallis with post-hoc Dunn's), suggesting there may be a population-based difference between them. DWEYS IgG ELISA in CSF from the same patients was not able to distinguish between SLE and HC and 6 patients and 1 HC were above the cut-off for positivity (Figure 4-5-B), giving a sensitivity of 17.1% and specificity of 97.2%.

After unblinding, within the SLE group, a comparison was made between patients with active NPSLE and those without. Based on these results in plasma, no difference could be seen (Figure 4-5-C) and in CSF only a small statistical difference was observed (p=0.02, Mann Whitney U, Figure 4-5-D). Sensitivity for NPSLE was 26.7% and 26.7% and specificity was 80.0% and 90.0% in plasma and CSF respectively. Taken together these results suggest that using this assay there may be a disease-related signature detectable in CSF of those with NPSLE.

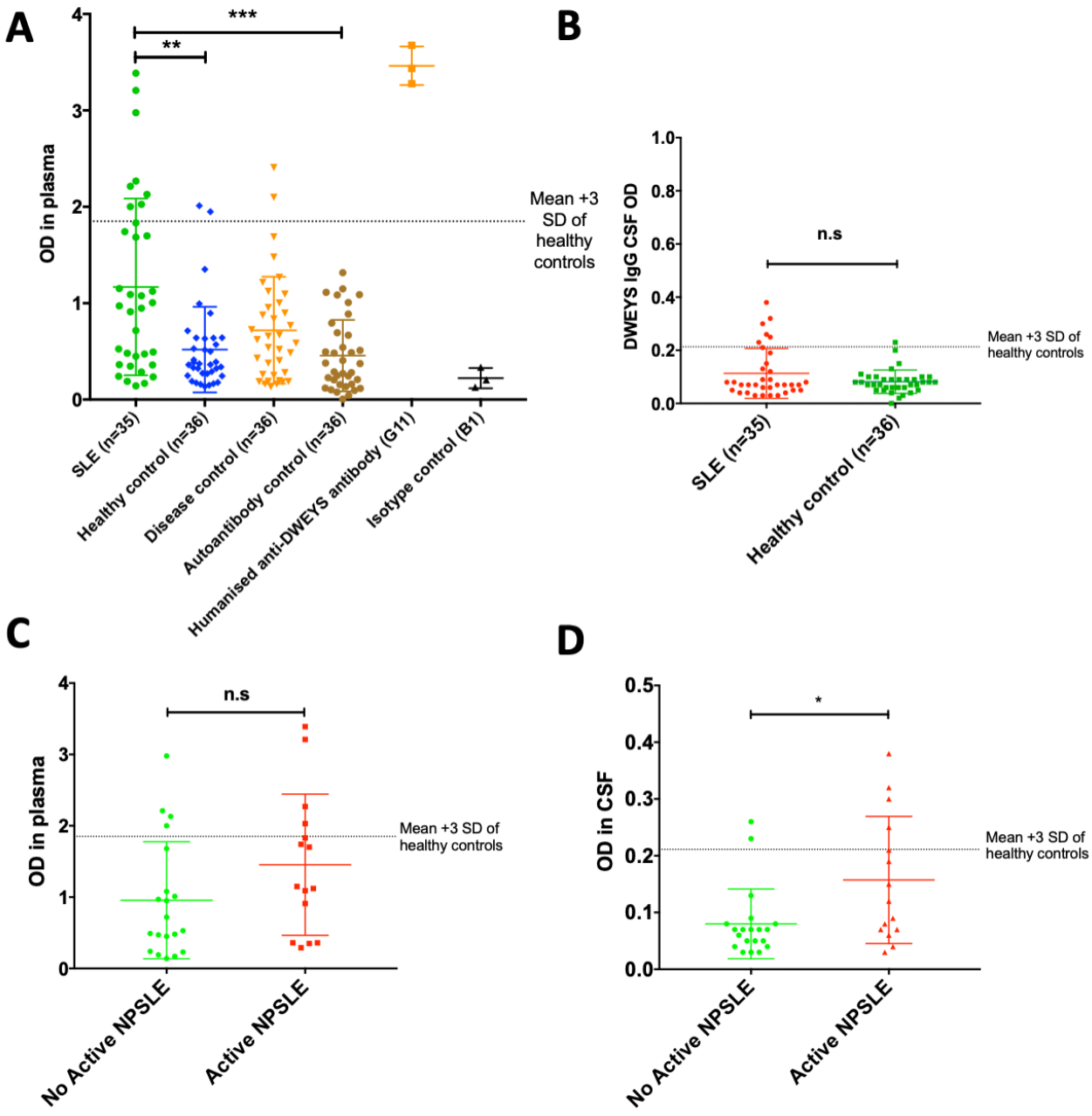


Figure 4-5 Plasma and CSF DWEYS IgG ELISA results from cohorts

*A) ELISA results based on the mean of two repeats in patients with SLE, healthy controls (HC), disease controls (DC) and autoantibody controls (AC). Mean plus 3 SD of HC used as the cut-off for positivity. Patients with SLE, HC and DC were identified above this cut-off but there were significant population differences. Kruskal Wallis with post hoc Dunn's correction for multiple comparisons B) DWEYS IgG ELISA in CSF, no difference between SLE and HCs, Mann Whitney U. C) Plasma DWEYS IgG OD not able to distinguish between active NPSLE or no active NPSLE. D) CSF DWEYS OD demonstrates a small statistical difference between active NPSLE and not. Statistical tests employed were Mann Whitney U tests for comparisons between two groups and for more than two groups, Kruskal Wallis with post-hoc Dunn's to correct for multiple comparisons was used. (**p<0.01, ***p<0.001). Mean plus standard deviation shown by line and error bars.*

4.5.3 Cohort plasma/CSF results on IgG ELISA without peptide coating and on scrambled peptide

Due to the detection of differences in DWEYS IgG between SLE patients, HCs and ACs in plasma and between NPSLE and no NPSLE in CSF, the robustness of this signature was examined. The same patient samples were retested without any DWEYS peptide coating of the ELISA plate and binding was almost identical (Figure 4-6) in both plasma (r=0.85, p<0.0001, Spearman's) and CSF (r=0.79, p<0.0001, Spearman's).

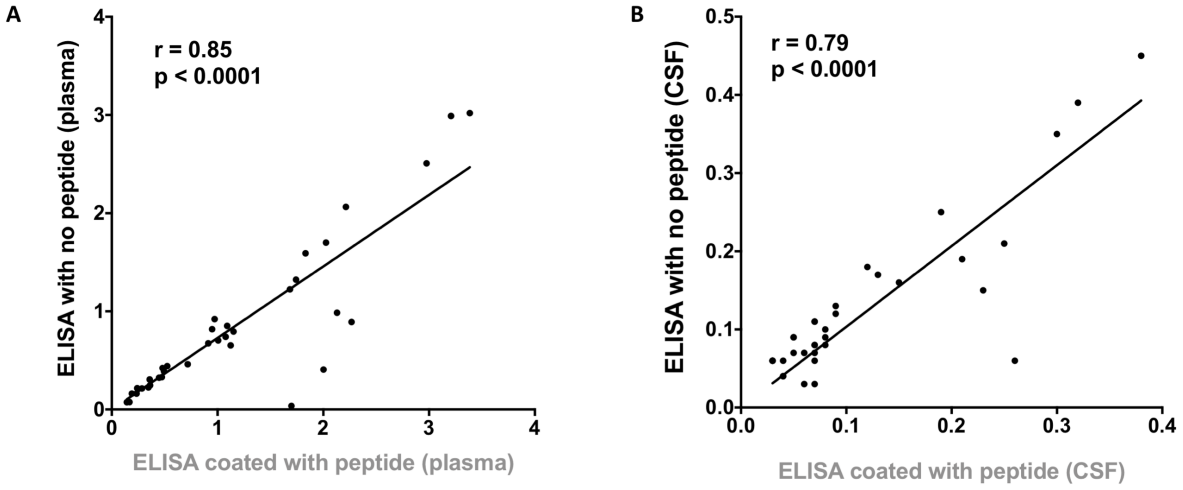


Figure 4-6 Cohort binding on uncoated ELISA plates vs DWEYS coated ELISA plates

SLE patient samples were run in duplicate on ELISA plates coated without peptide and compared to results obtained when run with peptide in both plasma (A) and CSF (B), an excellent correlation was observed between the runs in both plasma and CSF with or without peptide coated onto the ELISA plate. Correlation calculated using Spearman's r to two decimal places.

As it appeared that patient samples were not specifically binding DWEYS, two different decapeptides were used in place of DWEYS (full sequence DWEYSVWLSN); a random scramble of the same amino acids: SDYVWLNESW and a peptide where the negatively charged amino acids, aspartic acid (D) and glutamic acid (E) were substituted for positively charged ones, lysine (K) and arginine (R), to make KWRYSVWLSN. The aim was to determine whether

the negative charge of the DWEYS peptide was affecting patient antibody binding. Again, it was observed that despite the scrambled peptide, binding of patient samples matched closely the binding seen with the DWEYS coated assay, regardless of active or no active NPSLE, for both KWRYS (r=0.72, p<0.0001) and SDYVW (r=0.73, p<0.0001) (Figure 4-7).

Finally, to see if the anti-DWEYS peptide signal detected in patients was physiologically relevant, the plasma DWEYS ELISA results in SLE patients were correlated with the same patient's CSF results (Figure 4-8). There was not a strong correlation (r=0.34, p=0.04), suggesting that the signal observed does not relate to a property which is diffusible across the blood-brain barrier. This figure also displays that the four patients with active NPSLE that were above the cut-off for positivity on plasma DWEYS, are not the same four patients with active NPSLE above the cut-off for CSF DWEYS.

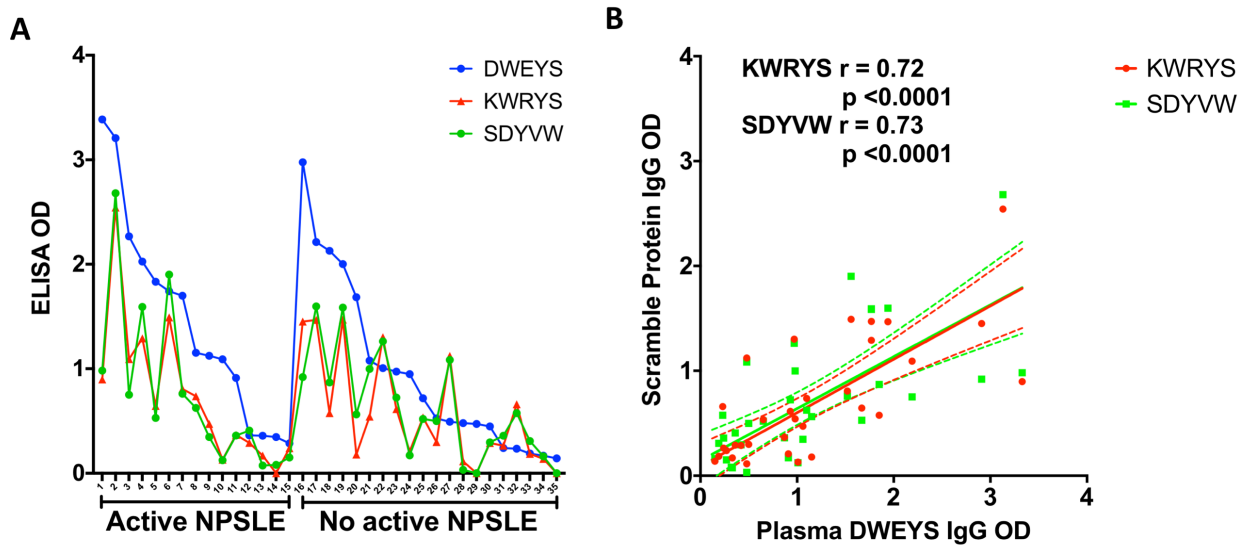


Figure 4-7 Scrambled peptide ELISA results using cohort SLE samples

A) SLE patient plasma run on ELISA coated with DWEYS or two scrambled versions of DWEYS; KWRYS and SDYVW in duplicate. Patients separated into active NPSLE and inactive NPSLE, demonstrating that similarity between runs not different in either group. B) Correlation between KWRYS/SDYVW IgG OD and DWEYS IgG OD in plasma is very good, Spearman's r. In B dotted lines are 95% confidence interval of linear regression.

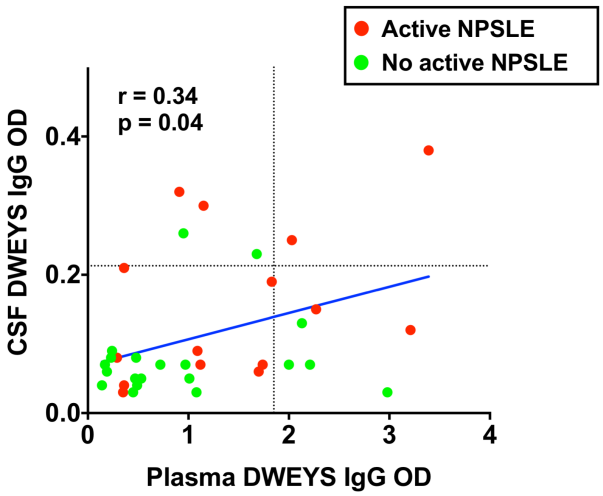


Figure 4-8 Plasma vs CSF DWEYS

Correlation of plasma DWEYS results versus CSF IgG results is not strong, Spearman's r=0.34, p=0.04. Patients with active NPSLE are shown in red and no active NPSLE are shown in green. Mean +3SD cut-off for positivity is plotted as a dotted line for plasma on the x axis and CSF on the y axis. The line in blue is linear regression plot.

4.6 IFN-α in SLE and NPSLE

4.6.1 IFN-α SIMOA results in plasma and CSF

Due to the significant plate binding artefact observed in our DWEYS ELISA data, an alternative methodology was employed in order to try and find a reliable biomarker of NPSLE. Via a collaboration with the Pasteur institute, our samples were tested on their pan-IFNα SIMOA assay. IFNα has been shown to diffuse across the blood-brain barrier[173] and therefore a good correlation between plasma and CSF IFNα is expected and a good initial test of the physiological validity of the results. This was indeed observed (r=0.68, p<0.0001, Figure 4-9).

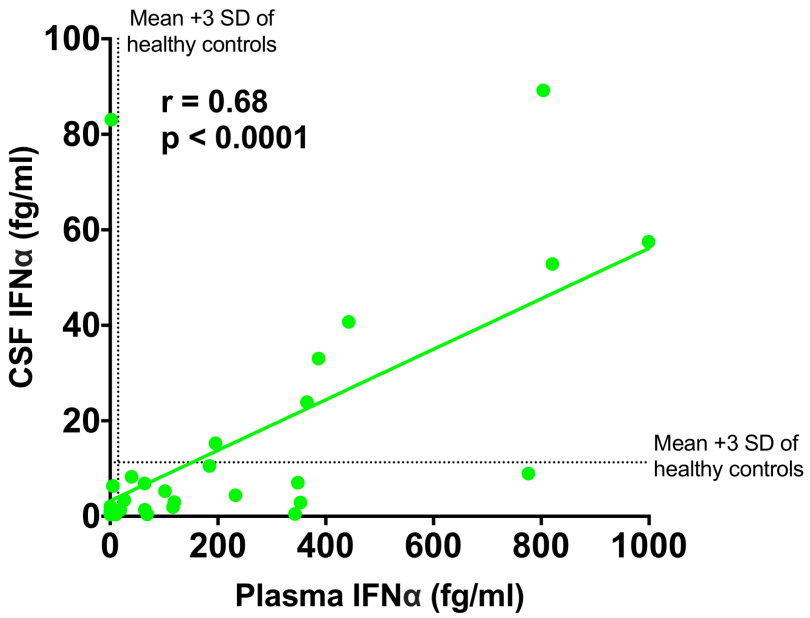


Figure 4-9 IFNα SIMOA results from SLE cohort: correlation between plasma and CSF

From our cohort of 35 SLE patients, paired plasma and CSF IFNα was tested, a cut-off for positivity was established from mean plus 3 standard deviation of 20 healthy controls (dotted line on each axis). A very good correlation is observed between plasma and serum IFNα, Spearman's r.

Comparing IFNα across cohorts (Figure 4-10), levels were markedly higher in the plasma of patients with SLE compared to HC (n=20, p<0.0001, Kruskal Wallis with post-hoc Dunn's) and DC (n=32, p<0.0001, Kruskal Wallis with post-hoc Dunn's)) (Figure 4-10-A). A similar, non-significant trend, was seen in a comparison between CSF IFNα in SLE vs DC (n=32, p=0.0056, Kruskal Wallis with post-hoc Dunn's) and difference with HCs (n=20, p=0.7729, Kruskal Wallis with post-hoc Dunn's) (Figure 4-10-B). Using mean plus three standard deviations of HC as a cut-off for positivity, 22 SLE patients, one HC and one DC would be positive in plasma and eight SLE patients and one DC in CSF. This translates as a sensitivity of 62.9%, and specificity of 97.2% for SLE IFNα in plasma. In CSF sensitivity is 22.86% and specificity is 98.6%. Importantly, however, IFNα levels were not able to distinguish between active NPSLE and non-NPSLE in either plasma or CSF (Figure 4-10-C and D). When the correlation between

plasma and CSF IFNα is separated into active NPSLE and non-NPSLE the slopes are not significantly different (p=0.03123) nor are the elevations/intercepts (p=0.7975) and both correlate, active NPSLE (r=0.76, 0=0.0021) and no active NPSLE (r=0.59, p=0.0066) (Figure 4-10-E).

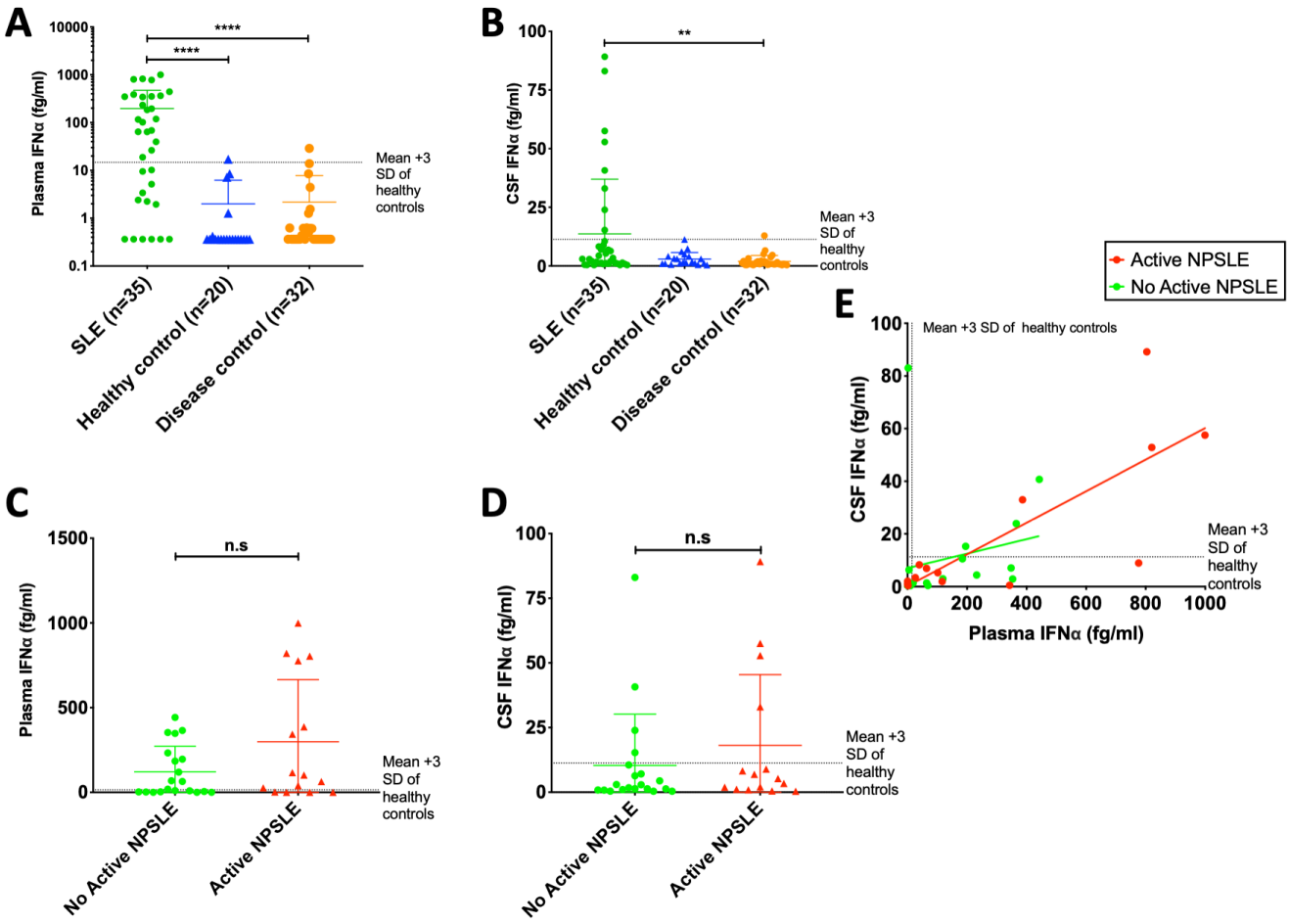


Figure 4-10 IFNα full cohort results, plasma and CSF

*A) Plasma IFNα results in SLE patients, HC and DC, demonstrate a marked difference between SLE and HC and DC, note log scale on Y-axis. B) CSF IFNα results from same cohorts, significant difference only between SLE patients and DC. C) Plasma and D) CSF IFNα in active NPSLE versus no active NPSLE, no significant difference. E) Correlation and linear regression of plasma versus CSF IFNα, compared between active NPSLE versus no active NPSLE; comparison of linear regressions revealed no difference in slope or intercept, both correlated (Spearman's r). For comparison between two groups Mann Whitney U was used, for comparisons between more than two groups, Kruskal Wallis with post-hoc Dunn's to correct for multiple comparisons was used. (**p<0.01, ****p<0.0001). Mean and standard deviation represented by line and error bars.*

There is a weak correlation between IFNα and DWEYS in CSF (r=0.3624, p=0.0324) but not in plasma (r=0.2258 (95% CI -0.1425 to 0.5153), p=0.23) (Figure 4-11).

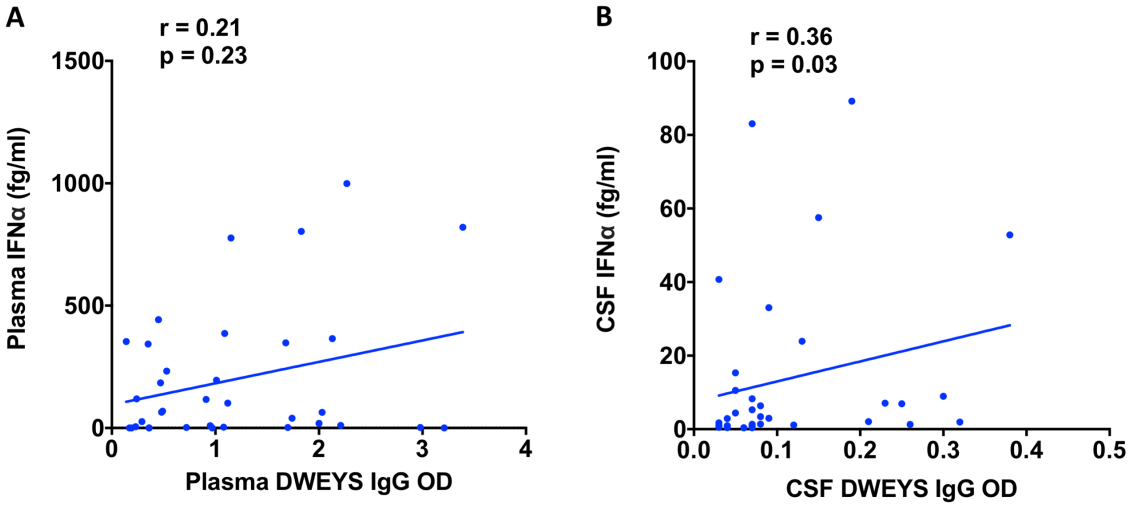


Figure 4-11 Correlation between plasma and CSF DWEYS and IFNα

Final DWEYS ELISA results are compared to IFNα SIMOA results in the 35 SLE patients with paired plasma and CSF. Poor correlation noted in CSF and none observed in plasma.

4.6.2 Clinical and paraclinical correlations with IFNα results

The relationship between plasma and CSF IFNα and available clinical and paraclinical parameters was examined. There was no significant difference between plasma IFNα in active versus inactive SLE (p=0.24, Figure 4-12-A), CSF IFNα was significantly higher, however (p=0.02, Figure 4-12-B). Quantification of disease activity was not available, so no assessment of correlation could be made. Plasma dsDNA did not correlate with plasma (r=0.01, p=0.96) or CSF IFNα (r=0.02, p=0.90) and there was no significant difference between groups if divided into low, medium and high IFNα protein levels (Figure 4-12-C and D). Plasma ESR correlated with CSF IFNα (r=0.53, p=0.002) but not plasma IFNα (r=0.29, p=0.1) and there was a significant difference in between groups divided by CSF but not plasma IFNα (Figure 4-12-E and F). No correlation (plasma r=-0.02, p=0.9, CSF r=0.09, p=0.61) or difference between groups was seen between CRP and IFNα.

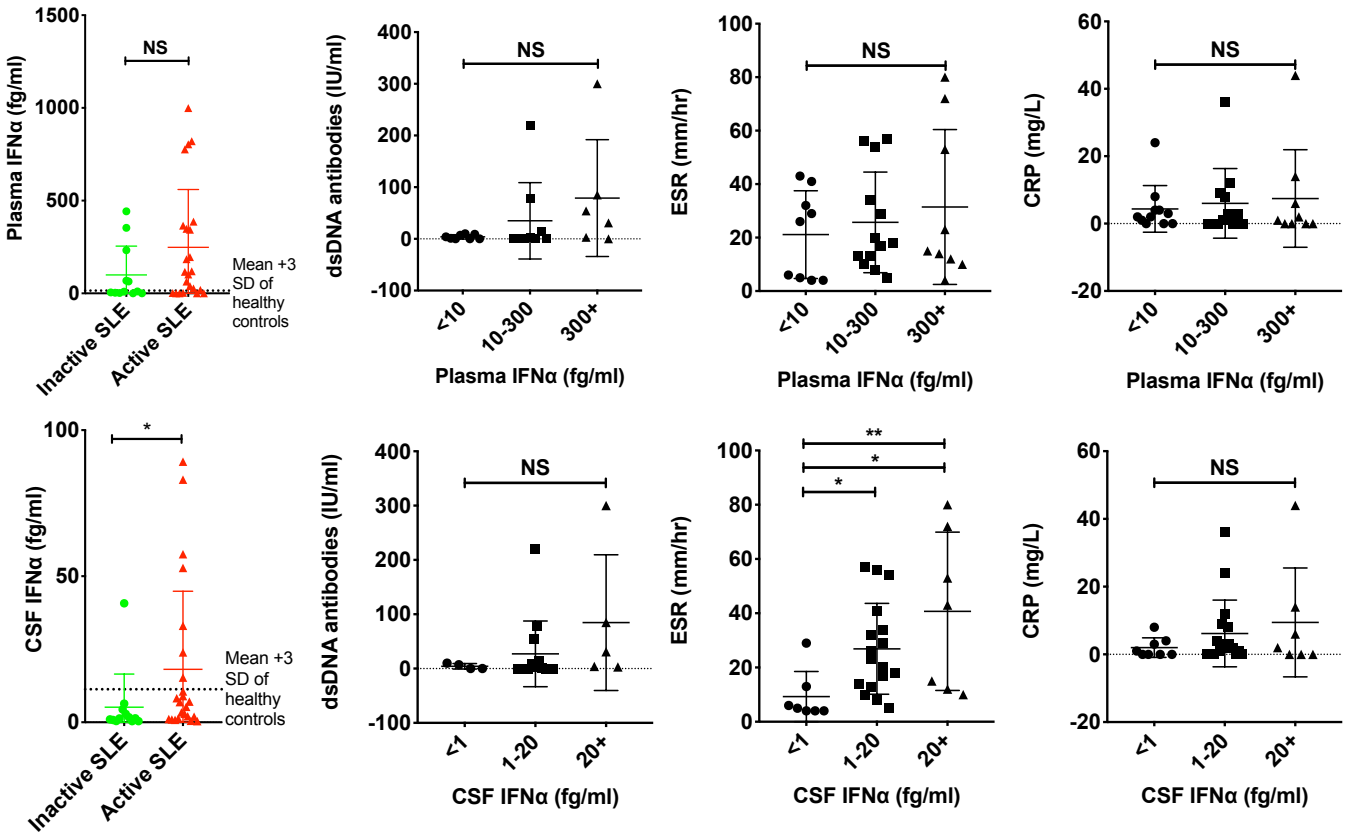


Figure 4-12 Clinical and paraclinical associations of plasma and CSF IFNα.

Patients were defined by their treating clinicians as either having active or inactive SLE and comparison was then made between plasma (A) and CSF (B) IFNα*, with a difference noted in CSF. Plasma dsDNA was compared in plasma (C) and CSF (D) groups divided into low, medium and high levels of* IFNα*, the same was done for ESR (E and F) and CRP (G and H). For comparison between two groups Mann Whitney U was used, for comparisons between more than two groups, Kruskal-Wallis with post-hoc Dunn's to correct for multiple comparisons was used. (*p<0.05, **p<0.01). Mean and standard deviation represented by line and error bars.*

4.7 Discussion

The aim of this study was to see if reliable biomarkers for NPSLE could be identified using contemporary techniques, routinely used in our laboratory. These methods allow detection of antibodies to native, conformationally intact antigen. No such antibodies were found. Furthermore, it has been demonstrated that the DWEYS ELISA is not a reliable way to test for NPSLE and that measurement of IFNα by SIMOA appears to distinguish between SLE and other diseases but not between SLE and NPSLE.

NSAbs to the NMDAR are well established in association with the distinct clinical entity of NMDAR-AbE, with a novel consensus description of the MD undertaken in chapter three of this thesis.[26, 28] The rationale of looking for these antibodies in NPSLE is that a large, albeit contradictory, literature, based on linearised antigen testing, exists to support a role for antibodies targeting the extracellular portion of NR2A and NR2B in this condition. These antibodies were not found using gold-standard methodology, using conformational antigen-based assays, including CBA and live cultured neurons. This is a finding that is corroborated by a large study of 174 patients with a mixture of SLE and NPSLE, demonstrated no binding on NMDAR CBA.[174] Taken together, these results argue against the presence of antibodies to NMDAR in NPSLE.

In order to address the existing literature on NMDAR antibodies in NPSLE, the linearised antigen DWEYS IgG ELISA was reproduced as faithfully as possible, using reagents from the laboratory responsible for developing this assay. The results were highly instructive. On an individual basis, the assay has a low sensitivity and imperfect specificity in both plasma and CSF. Nevertheless, significant population differences between SLE and control cohorts were observed in plasma and there was a small, statistically significant difference between active NPSLE and non-NPSLE patients, a result reported by other groups.[156, 175]

On further investigation, it was demonstrated that IgG from both plasma and CSF exhibited a capacity to bind the uncoated ELISA plate. This signal similarity was also observed in the presence of scrambled or intentionally charge-altered coating peptides. While the SLE patients exhibited greater propensity to bind the plate, this characteristic is not limited to SLE patients and therefore is not a useful biological marker to distinguish between SLE and other conditions. It may, however, reflect the heterogeneity of the antibody milieu in SLE, with

patients known to have antibodies to a wide range of proteins. It may also explain the reason why so many contradictory studies using DWEYS IgG ELISA exist.

Type 1 interferon in SLE represents a promising field. In addition to the IFNα protein and genetic signatures, microglia in brains of patients with SLE have been shown to have an activated IFNα signature with no evidence of lymphocytic infiltration.[176] In mice, microglia were found to be activated in response to IFNα, with evidence of engulfing synaptic material on electronic microscopy and lower synapse numbers, a defect reversed by an IFNα neutralising antibody.[176] Interferon production is thought to be triggered by immune complexes containing CNS antigens stimulating innate PPRs. SLE CSF has been demonstrated to be a highly potent inducer of a type 1 IFN response compared to MS or autoimmune control CSF.[177]

As there is evidence of IFNα contributing to brain pathology in SLE, quantification in SLE cohorts could yield vital information. Measuring IFNα via SIMOA is a relatively novel technique. The direct quantification of type 1 IFN has been challenging due to the large number of molecules in this family and the presence of endogenous IFNα antibodies.[178] Previous assays have instead used IFNα gene expression in PBMCs as a proxy readout. The digital ELISA SIMOA, utilising high-affinity antibodies from patients with homozygous AIRE mutations allows detection of all 13 IFNα subtypes, with protein measured at attomolar concentrations, correlating well with functional and genetic assays.[171] The results from our cohort are in keeping with the only other published comparison of SLE and HCs using IFNα SIMOA,[171] with excellent ability to separate SLE from HC and DC in plasma and novel data demonstrating a difference only between SLE and DC in CSF. Disappointingly, however, there was no significant difference between NPSLE and non-NPSLE patients IFNα in plasma or CSF.

Previous work using IFNα SIMOA demonstrated higher SLE disease activity index (SLEDAI), ESR, a-RNP antibodies and lower complement activity in patients with a higher level of serum IFNα, with no difference was seen in dsDNA antibodies or CRP.[171] This suggested the assay may have utility in detecting active disease. Our cohort showed a significant difference in CSF IFNα in active versus inactive SLE and a correlation with ESR, with highest serum ESR seen in those with the highest levels of CSF IFNα. In contrast to the previous study, no differences were seen between active and inactive SLE in plasma, with the caveat that full SLEDAI scores, ribonucleotide antibody reactivity and complement activity were not available. Similar to Rodero et al, no differences were seen in dsDNA and CRP in plasma and finally, novel CSF data showed no difference.

A potential reason for the limited correlation between IFNα and disease activity in SLE, and lack of any association with NPSLE could be explained by the nature of the signal detected. Serum IFNα protein quantification by SIMOA showed excellent correlation with IFN1-stimulated genetic expression when originally described.[171] In adults the IFN1-genetic signature is seen in 60-80% of adults with SLE [179] and in a range of cell types, including B and T cells. In contrast to the rapid and short lived IFN response to viruses, this genetic signature is a chronic response, with persistence over time and an inconsistent relationship to disease flares. [180-183] Interestingly 63% of patients with SLE in our cohort had raised IFNα protein in their plasma, a frequency similar to those with an increased genetic IFN-1 signature, with formal testing not available in these patients. Longitudinal samples were not available, but one conclusion is that IFNα protein levels, similar to the genetic signature, are chronically produced and therefore poorly related to disease flares.

As NPSLE is so broadly defined clinically[172], including 19 syndromes, a single unifying pathological entity defining them as a cohort is unlikely. In fact, the neuropathology points to

predominant vascular and ischaemic pathology with rare evidence of inflammation.[184] This may explain why anti-phospholipid antibodies appear to associate more robustly with NPSLE in certain studies,[185, 186] with complement activation being more key to pathology than immune complex deposition.[187]

In summary, the brain disease associated with SLE is likely to have a broad and varied pathological driver and the aim should be to describe disorders in these terms as much as possible and not based on symptomatology. It has been demonstrated in this study that brain antibodies, as they are currently defined, do not appear to make a significant contribution to NPSLE. IFNα is elevated in SLE patients, often significantly so, but this does not convincingly correlate with either disease activity or NPSLE and may reflect a chronic and ongoing process which may still prove to be important to both SLE and NPSLE.

5 HLA associations in LGI1- and CASPR2-antibody mediated neurological diseases

5.1 Introduction

The key findings of this thesis so far have been that NMDAR-AbE has a distinctive and characteristic associated MD and that conformational NMDAR antibodies appear to have no current role in NPSLE. Focus, therefore, shifted to another group of patients with established pathogenic brain antibodies.

A large proportion of patients seen in the Oxford autoimmune neurology clinic have antibodies to either LGI1 or CASPR2. A clear and consistent observation in patients with LGI1-antibodies was a high rate of adverse dermatological reaction to phenytoin and carbamazepine. This reaction was often severe, with numerous instances of the dermatological emergency, Stevens-Johnson syndrome, reported.[87] HLA alleles have been associated with a propensity to severe reaction to AEDs and immunotherapies[188, 189] and this led member of the laboratory to suspect an HLA association in LGI1-antibody patients. Whilst this work was being undertaken and analysed, it was reported in two small cohorts of LGI1-antibody patients that an HLA association did indeed exist.[190, 191]

HLA molecules are encoded by a highly variable region on chromosome six. Class I HLA molecules are expressed on most nucleated cells in the body and present intracellular proteins to CD8+ T cells. Class II HLA molecules are expressed on antigen presenting cells (APCs), B cells and activated T cells and present extracellular antigen to CD4+ T cells. HLA molecules are described by their gene (A,B,C for class I and DP, DQ, DR for class II), then two first-field digits signifying allele group and then, depending on depth of sequencing, two second-field digits describing a specific HLA protein.[192]

While there are distinguishing features in both LGI1- and CASPR2-antibody patients, particularly FBDS which only occur in association with LGI1 antibodies, there is clinical overlap between these patients.[86] They both occur mainly in older men and are characterised by predominant IgG4-subclass antibodies and associate in a single patient more often than would be expected by chance, often with the ultra-rare Morvan's syndrome.[77, 91, 193] These shared clinical and immunological features, as well as the fact that both proteins complex with VGKCs and are contained in mammalian CNS-membrane complexes,[81] could suggest they are directly involved in a break of tolerance and autoimmunisation. An *in vivo* example to validate this supposition is the report that abattoir workers, working in an environment with aerosolised brain protein, have been shown to develop autoantibodies against VGKC-complexes as well as, less frequently, CASPR2.[194] How VGKC-complex proteins are processed and presented by APCs in combination with existing B and T cell repertoires could, therefore, define the resultant dominant antigen and therefore dictate antibody specificity. HLA variants play a key role in antigen presentation and given the description of a strong HLA association in patients with LGI1-antibodies, it was hypothesised that an association may exist in patients with CASPR2-antibodies. The following is a clinicogenetic study of these patients, most of which has been published[195] and the data presented below are derived from this work.

5.2 Methods

5.2.1 Patients

A total of 111 Caucasian patients were recruited. These were identified from a number of sources including previous studies (n=51) [76, 83, 85], referral to our specialist clinic (n=49) or via collaborators at the University of California, San Francisco (n=11). They had the following antibody reactivities; LGI1 only (n=68), CASPR2 only (n=31), LGI1 and CASPR2 double positive (n=3) or intracellular aspects of VGKCs (n=9), as determined by previously described antigen-

specific CBAs.[81, 83] Patients were selected on the basis of positive binding to LGI1- or CASPR2-CBA and low positive patients were included. Two further non-Caucasian CASPR2-antibody patients were identified via referrals to the Oxford Autoimmune Neurology group. Clinical information was collected via direct patient and relative interviews and review of case-notes. All patients provided written informed consent (REC16/YH/0013 or the IRB 10-04905 approvals).

5.2.2 Genotyping, HLA imputation, verification and multi-locus haplotype-block construction

The Infinium Global Screening Array-24+v1.0 BeadChip with Illumina Infinium HTS custom markers was used for genotyping. This technology allowed HLA alleles imputation to two-field resolution (four digit typing, for example, HLA DRB1*07:01) using SNP2HLA at eight classical class I and class II loci (HLA-A, HLA-B, HLA-C, HLA-DPA, HLA-DPB, HLA-DQA1, HLA-DQB1 and HLA-DRB1).[196, 197] As a complementary and confirmatory technique, DRB1- , DRB4- and DQ-alleles underwent intermediate-resolution HLA-typing using polymerase chain reaction (PCR)-sequence specific primers (SSP).[198] This was carried out by Mian Chen, from Dr Martin Barnardo's laboratory at the Oxford transplant centre. Based on available primers, the PCR-SSP elucidated the first-field plus a range of second-field possibilities: the highest frequency allele in Caucasians was selected as the final result. In the case of discordant data, PCR-SSP was accepted as the final result. To act as a control cohort, HLA alleles from 5553 Caucasian healthy controls (HC, from Oxford Biobank) were available having been imputed using the same platforms, and with confirmatory checks made in 70 individuals by PCR-SSP.[197] Haplotype-blocks were calculated by a Bayesian algorithm using PHASE V2 software with 10,000 iterations for three haplotype-blocks: HLA-C-B, -DRB1-DQA1-DQB1, and -DPA1-DPB1.[199, 200]

5.2.3 Statistical analyses

Fisher's exact test (two-tailed) was used to compare the HLA allele and haplotype carrier frequencies between patients and the HC dataset. Multiple comparisons were corrected with Hochberg's method. Corrected p-values <0.05 were considered significant. Odds ratios (ORs) were calculated using the median-unbiased estimation method. Fisher's exact test was also used for clinical comparisons between antibody groups as well as comparisons within antibody groups by allele or haplotype. Mann-Whitney U was used for comparisons of ordinal values between two groups.

5.3 CASPR2-, LGI1- and VGKC-antibody patient clinical description

A cohort of 33 patients, selected from the Oxford autoimmune neurology clinic, who were uniquely positive for CASPR2-antibodies on live CBA were collected and are described in Table 5-1. Consistent with previous cohorts, patients were nearly all older males with a predominant clinical presentation of encephalitis. The majority of patients (n=26, 79%) had seizures as part of their presentation, with partial seizures the main phenotype (generalised seizures n=11, 33%) but none with FBDS. Isolated epilepsy was rare (n=2, 6%) as was isolated neuromyotonia (n=3, 9%) but a large proportion of patients had involvement of peripheral nerves in the form of neuromyotonia (n=10, 30%) or neuropathic pain (n=15, 45%). There were high rates of other autoimmune diseases (n=8, 24%), including pernicious anaemia, coeliac disease, Raynaud's, congenital adrenal hyperplasia, hypothyroidism, psoriasis, polymyalgia rheumatica and most interestingly pemphigus, an autoimmune disease driven by IgG4 antibodies. A range of associated tumours were present (n=4, 12%), including prostate (n = 2), pancreatic (n = 1) and thymic cyst (n = 1). This cohort was predominantly white British (n = 31) but also included one south Asian and one black British person.

	Number
Number of patients	33
Median age at onset (range)	68 (19-82)
Female	3 (9%)
Clinical Syndrome	
Epilepsy	2 (6%)
Encephalitis	19 (58%)
Morvan's	3 (9%)
Isolated Neuromyotonia	3 (9%)
Other[a]	6 (18%)
Clinical Features	
Any seizure	26 (79%)
Faciobrachial dystonic seizures	0 (0%)
Generalised seizure	11 (33%)
Amnesia	24 (73%)
Neuromyotonia	10 (30%)
Neuropathic pain	15 (45%)
Other features	
Other autoimmune disease	8 (24%)
Corticosteroid side effects[b]	5 (15%)
Other drug rash	1 (3%)
Mean improvement in mRS (range)	1.6 (0 to 4)
Tumour (%)[c]	4 (12%)

Table 5-1 Clinical features of recruited CASPR2-antibody cohort, all ethnicities included.

[a]Other diagnoses included movement disorders (n = 4, generalized chorea, hemifacial spasm, cervical dystonia and cerebellar ataxia), axonal neuropathy (n = 1) and psychosis (n = 1).
[b]Corticosteroid-related complications, sometimes multiple, in CASPR2-antibody patients [n = 5: marked weight gain (n = 1), rash (n = 2), striae/thin skin/bruising (n = 2), and hallucinations (n = 1)].
[c]Tumour types were prostate (n=2), pancreatic (n=1) and thymic cyst (n=1).

In order to make informative clinical and HLA comparisons, a cohort of patients with antibodies to LGI1 and to intracellular aspects of VGKCs only were collected by Dr. Sophie Binks, a researcher in the Oxford autoimmune neurology laboratory. Patients with antibodies to both LGI1 and CASPR2 were jointly recruited by Dr. Binks and I. All patients are described in Table 5-2. Our Oxford biobank HC cohort was Caucasian only and therefore to make accurate comparison all non-Caucasians (n=2) were excluded from analyses from this point forward. The resultant CASPR2-antibody patient (n=31) clinical details are therefore presented with these exclusions applied in Table 5-2.

Through comparison of the LGI1- and CASPR2-antibody positive groups the following observations were made; FBDS was seen only in patients with LGI1-antibodies (P<0.0001, Fisher's exact test) who also more often had seizures as part of their presentation (P = 0.01) compared to patients with CASPR2 antibodies. CASPR2-antibody patients, as expected, more often presented with involvement of the peripheral nerves, including neuromyotonia (P = 0.0003) and neuropathic pain (P<0.0001). The nine patients with antibodies to VGKC only had heterogeneous, often non-immune, clinical presentations. By way of comparison, non-immune syndromes were seen in only one patient with LGI1-antibodies (stroke) and in four with CASPR2-antibodies (axonal neuropathy, cervical dystonia, hemifacial spasm and psychosis). A marked distinction between the two groups was the 47% rate of corticosteroid side effects in patients with LGI1-antibodies (P = 0.004; 16% with CASPR2-antibodies) and a significantly higher rate of drug-induced rashes (35% versus 3% in CASPR2-antibody patients, P = 0.0004). The rashes were predominantly attributed to AEDs (n = 13: including carbamazepine [n = 6], phenytoin [n = 4], lamotrigine [n = 2] and valproate [n = 1]), antibiotics (n = 6: penicillins [n = 5] and metronidazole [n = 1]) and immunosuppressants (n = 5: azathioprine [n = 2], corticosteroids [n = 2] and methotrexate [n = 1]). These data provide

clear evidence of a clinical distinction between these two groups, on top of the established biochemical distinction. The next step was to determine if there were HLA differences.

	LGI1-Ab	CASPR2-Ab	LGI1-Ab and CASPR2-Ab	Cytosolic VGKC-Ab only
Number of patients	68	31	3	9
Median age at onset (range)	63 (41-85)	68 (19-82)	56 (52-65)	43 (33-71)
Female (%)	20 (29%)	2 (6%)	1 (33%)	4 (44%)
Clinical Syndrome (%)				
Epilepsy	8 (12%)	2 (6%)	0 (0%)	4 (44%)
Encephalitis	58 (85%)	18 (58%)	1 (33%)	2 (22%)
Morvan's	1 (2%)	3 (11%)	2 (67%)	0 (0%)
Isolated Neuromyotonia	0 (0%)	2 (6%)	0 (0%)	0 (0%)
Other[a]	1 (2%)	6 (19%)	0 (0%)	3 (33%)
Clinical Features (%)				
Any seizure	66 (97%)	25 (81%)	2 (67%)	7 (78%)
Faciobrachial dystonic seizures	47 (69%)	0 (0%)	1 (33%)	0 (0%)
Generalised seizure	26 (38%)	10 (32%)	2 (67%)	6 (67%)
Amnesia	58 (85%)	23 (74%)	3 (100%)	5 (56%)
Neuromyotonia	1 (2%)	8 (26%)	2 (67%)	0 (0%)
Neuropathic pain	5 (7%)	14 (45%)	2 (67%)	0 (0%)
Other features (%)				
Other autoimmune disease[b]	19 (28%)	7 (23%)	0 (0%)	0 (0%)
Corticosteroid side effects[c]	32 (47%)	5 (16%)	0 (0%)	1 (11%)
Other drug rash	24 (35%)	1 (3%)	0 (0%)	0 (0%)
Mean change in mRS (range)	1.6 (-3 to 4)	1.5 (0 to 4)	1.7 (0 to 3)	1 (0 to 2)
Tumour (%)[d]	9 (13%)	4 (13%)	2 (67%)	1 (11%)

Table 5-2 Clinical features of Caucasian patients with antibodies to LGI1, CASPR2, both LGI1 and CASPR2 and VGKC only. Adapted from Binks, Varley, Lee et al[195]

[a]Other syndromes included movement disorders (n = 4, CASPR2-antibodies; generalised chorea, hemifacial spasm, cervical dystonia and cerebellar ataxia), psychogenic amnesia (n = 2, VGKC-antibodies), widespread non-neuropathic pain (n = 1, VGKC-antibodies), axonal neuropathy (n = 1, CASPR2-antibodies), psychosis (n = 1, CASPR2-antibodies) and stroke (n =

1, LGI1-antibodies). Two patients with VGKC-only antibodies had epilepsy secondary to structural lesions.
[b]Autoimmune diseases in LGI1-antibody patients: [n = 19: hyper- and hypothyroidism and Hashimoto's thyroiditis (n = 8), psoriasis (n = 6), neuromyelitis optica (n = 1), multiple sclerosis (n = 1), optic neuritis (n = 1), myasthenia gravis (n = 1), Raynaud's disease (n = 1), diabetes (n = 1), pernicious anaemia (n = 1), heparin-induced thrombocytopaenia (n = 1) and ulcerative colitis (n = 1)] and CASPR2-antibody patients [n = 7: pemphigus, Raynaud's disease, psoriasis, hypothyroidism, pernicious anaemia, polymyalgia rheumatica and congenital adrenal hyperplasia (all n = 1)].
[c]Corticosteroid-related complications, occasionally multiple, in LGI1-antibody patients [n = 32: marked weight gain (n = 12), behavioural disturbance (n = 5) and diabetes (n = 5), or worsened diabetes (n = 1), insomnia (n = 4), fracture (n = 3), myopathy or muscle weakness (n = 3), skin thinning/easy bruising (n = 3), perforated abdominal viscus (n = 2), poor wound healing or abscess (n = 2), mania/hypomania (n = 2), ophthalmic infections (n = 2; keratitis and ophthalmic shingles), and one each of: cerebral venous sinus thrombosis, avascular necrosis of the hip (AVN), high INR and steroid-induced psychosis] and in CASPR2-antibody patients [n = 5: striae/thin skin/bruising (n = 2), rash (n = 2), marked weight gain (n = 1) and hallucinations (n = 1)].
[d]Tumours in LGI1-antibody patients (n = 9) were: basal cell carcinoma (n = 3), other skin – subtype not known (n = 2), prostate (n = 1), breast (n = 1), bladder (n = 1), dysplastic colonic polyp (n = 1) and in 4 CASPR2-antibody patients were: prostate (n = 2), pancreatic (n = 1) and thymic cyst (n = 1).

5.4 CASPR2- and LGI1-antibody patient HLA associations

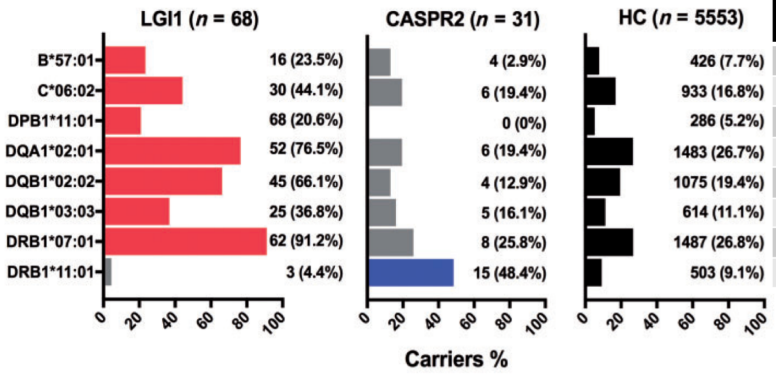
5.4.1 HLA allelic associations in LGI1-, CASPR2-, VGKC- and double-antibody positive patients.

As an HLA association was described in patients with LGI1-antibodies[190, 191] previously, we sought to confirm this in a larger cohort and look for HLA associations in patients with CASPR2-antibodies.

Statistical analysis of allele and haplotype frequency versus healthy controls was carried out by Dr. Wanseon Lee, from Professor Julian Knight's group in the Wellcome centre for human genetics, Oxford. We confirmed the strong association between HLA-DRB1*07:01 and patients with LGI1 antibodies, with 91% carrying this allele, compared to a 26% frequency in healthy controls (OR 27.6 [95% confidence interval, (CI) 12.9–72.2], $p = 4.1 \times 10^{26}$). Other over-represented alleles were HLA DQA1*02:01, HLA-DQB1*02:02, HLA-DQB1*03:03 and HLA-DPB1*11:01 (Figure 5-1, in red), all of which are known to often form haplotypes with

HLA-DRB1*07:01.[201] Nine (13%) patients with LGI1-antibodies were homozygous for DRB1*07:01, compared to 2% (115/5553) of healthy controls (OR 7.3 [95% CI 3.3–14.4], p = 3 $\times$ 10^4). Furthermore, an association was seen with two class I HLA alleles; HLA-B*57:01 (OR = 3.7 [95% CI 2.0–6.5]; p = 0.014) and HLA-C*06:02 (OR = 3.9 [95% CI 2.4–6.3]; p = 4.6 $\times$ 10^5). The DRB1 paralogue DRB4 had been reported in all patients with LGI1-antibodies in a previous cohort from a different country,[190] in our cohort it was expressed in 57/68 (83.8%) of the LGI1-antibody cohort, compared to 2578/5133 (50.2%) healthy controls. No difference in DRB4 frequencies compared to controls was seen in CASPR2-antibody patients (12/31, 38.7%) or VGKC-antibody only patients (5/9, 55.5%).

In what was an entirely novel finding, patients with CASPR2-antibodies exhibited overrepresentation of a single class II HLA allele; HLA-DRB1*11:01 (Figure 5-1, in blue). This was seen in 48% of our CASPR2-antibody cohort compared to only 4% of the LGI1-antibody cohort and 9% of healthy controls (OR 9.4 [95% CI 4.6–19.3]; P = 5.7 $\times$ 10^6). A single homozygous HLA-DRB1*11:01 CASPR2-antibody patient was identified. Four patients with CASPR2-antibodies were identified *a priori* as having non-immune conditions based on review of their clinical features; interestingly, none of these carried the HLA-DRB1*11:01 allele, increasing its frequency to 56% (15/27) in the remaining CASPR2-antibody patients.



OR	95% CI Lower	95% CI Upper	Fisher's Exact Test	Corrected (Hochberg) p-value
3.7	2.0	6.5	5.2×10^{-5}	1.0×10^{-2}
3.9	2.4	6.3	1.6×10^{-7}	4.6×10^{-5}
4.9	2.6	8.7	8.4×10^{-6}	2.0×10^{-3}
8.9	5.2	16.1	3.0×10^{-17}	8.7×10^{-15}
8.1	4.9	13.7	9.5×10^{-17}	2.8×10^{-14}
4.7	2.8	7.7	3.6×10^{-8}	1.0×10^{-5}
27.6	12.9	72.2	1.4×10^{-28}	4.1×10^{-26}
9.4	4.6	19.3	2.0×10^{-8}	5.7×10^{-6}

Figure 5-1 Comparison of HLA alleles between LGI1-, CASPR2-antibody and healthy control (HC) cohorts

Bar chart combined with table demonstrating statistically significant HLA allele associations in patients with LGI1-antibodies (n=68, red indicates statistical significance) and CASPR2-antibodies (n=31, blue indicates statistical significance), compared to HCs (black bars). Grey bars indicate non-significant associations. Numbers (%) of allele carriers next to bar and results of Fisher's exact test on corresponding row to bars displaying Odd's Ratio (OR), 95% confidence intervals (Cis), p value from Fisher's exact test and the Hochberg p value corrected for multiple comparisons.

Comparison to HCs was made with both the VGKC only patients and the patients positive for both CASPR2- and LGI1-antibodies and no significant overrepresentation of alleles was identified. The alleles associated with both LGI1- and CASPR2-antibody patients were not overrepresented in either of these populations (Figure 5-2). There was, however, a suggestion that these double positives may have their own signature as all carried HLA-B*44:02, HLA-C*05:01, HLA-DQA1*03:01 and HLA-DQB1*03:01, though none of these alleles reached significance due to small sample size. There was no pattern identifiable in the patients with VGKC-only antibodies.

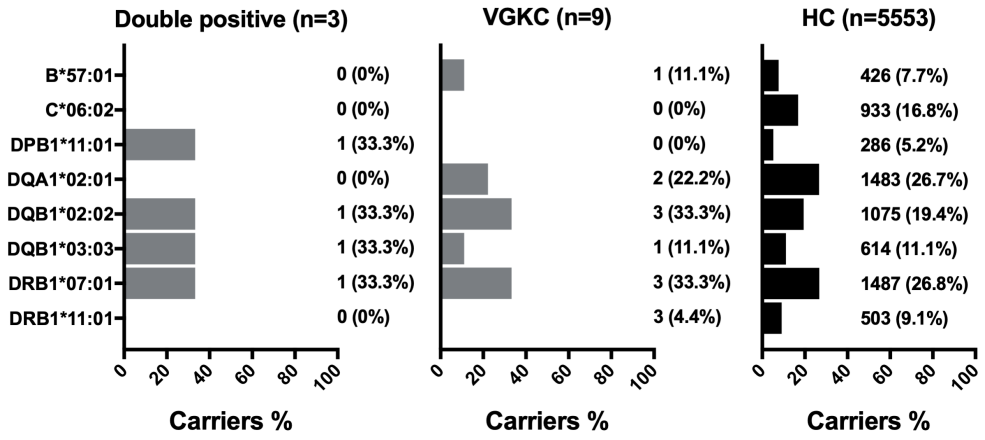
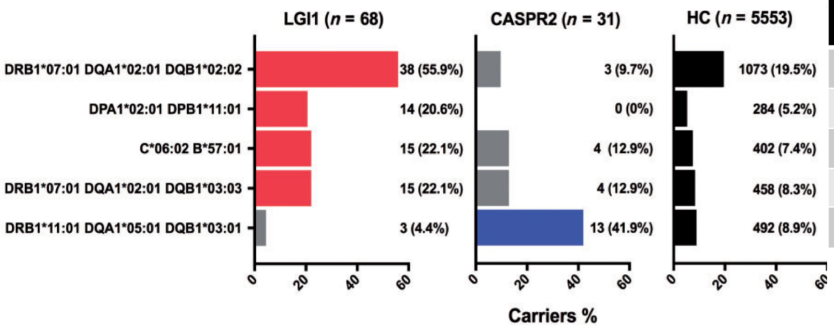


Figure 5-2 Comparison between LGI1- and CASPR2-antibody double positive antibody patients, VGKC only patients and HCs.

Comparison of double positive (LGI1- and CASPR2-antibody) patients, VGKC patients to HCs, grey bars indicate no statistical significance. Numbers (%) indicated next to bar relating to HLA allele.

5.4.2 HLA haplotype associations in CASPR2- and LGI1-antibody patients

In order to understand how alleles clustered together in patients, Dr Wanseon Lee carried out analysis of haplotype frequencies compared to healthy controls, in both LGI1- and CASPR2-antibody patients (Figure 5-3). The most frequently observed haplotypes in patients with LGI1-antibodies reflected those alleles known to associate with HLA-DRB1*07:01, as well as a class I haplotype consisting of the two previously associated class I alleles, HLA-C*06:02 and HLA-B*57:01. A single HLA class II haplotype was found in patients with CASPR2-antibodies (Figure 5-3): DRB1*11:01-DQA1*05:01-DQB1*03:01 (OR = 7.4 [95% CI 3.5–15.2], $P = 5.7 \times 10^{5}$).



OR	95% CI Lower	95% CI Upper	Fisher's Exact Test	Corrected (Hochberg) p-value
5.2	3.2	8.6	4.7×10^{-11}	2.3×10^{-9}
4.8	2.5	8.5	1.0×10^{-5}	3.8×10^{-4}
3.6	1.9	6.2	1.3×10^{-4}	8.8×10^{-3}
3.1	1.7	5.5	4.4×10^{-4}	2.1×10^{-2}
7.4	3.5	15.2	1.1×10^{-6}	5.7×10^{-5}

Figure 5-3 Comparison of HLA haplotypes between LGI1-, CASPR2-antibody and healthy control (HC) cohorts

As for Figure 5-1*, but comparison by HLA haplotype.*

5.5 Associations between HLA and clinical features in CASPR2- and LGI1-antibody patients

Given the clear and divergent HLA associations both at an allele and haplotype level in patients with CASPR2- and LGI1- antibodies, the presence of a clinical association to HLA expression was examined for. No disease relevant associations were seen in patients with LGI1-antibodies.[195] In patients with CASPR2-antibodies the effect of HLA allele and haplotype on the following was assessed: disease-phenotype (limbic encephalitis, epilepsy, non-immune), symptoms (seizures, neuromyotonia, neuropathic pain), severity (peak mRS), response to treatment (change in mRS – number presented is peak mRS minus mRS at most recent follow up), adverse drug reactions, association with autoimmune disease and the presence of a tumour (Table 5-3). No significant HLA allele or haplotype associations were found. Notably, however, as mRS change is an ordinal value, a quantitative comparison could be made between both allele and haplotype groups (Figure 5-4). There was no significant difference between groups (allele [p=0.11, Mann-Whitney U], haplotype [p=0.40, Mann-Whitney U]) but if the patients with non-autoimmune diseases are excluded, on the basis of not having immunotherapy responsive or relevant disease, then there is greater recovery

seen in those without the HLA allele (p=0.02, Mann-Whitney U). This was not seen when patients were grouped by haplotype (p=0.16, Mann-Whitney U). A similar difference was not seen when the same analysis was undertaken using peak mRS (all p values > 0.05, Mann-Whitney U).

Finally, it is worth emphasising that the same HLA alleles were present in LGI1- and CASPR2-antibody patients both with and without tumours.

	DRB1*11:01 Positive	**DRB1*11:01 Negative**	**Fisher's Exact**	**Haplotype Positive**	**Haplotype negative**	**Fisher's Exact**
LE	11/15 (73.3%)	7/16 (43.8%)	p=0.15	10/13 (76.9%)	8/18 (44.4%)	p=0.14
Morvan's	1/15 (6.7%)	3/16 (18.8%)	p=0.60	0/13 (0%)	3/18 (16.7%)	p=0.25
Seizures	13/15 (86.7%)	12/16 (75.0%)	p=0.65	11/13 (84.6%)	14/18 (77.8%)	p>0.99
Neuromyotonia	5/15 (33.3%)	3/16 (18.8%)	p=0.43	4/13 (30.8%)	4/18 (22.2%)	p=0.69
Neuropathic pain	7/15 (46.7%)	7/16 (43.8%)	p>0.99	5/13 (38.5%)	9/18 (50.0%)	p=0.72
Non-autoimmune	0/15 (0%)	4/16 (25.0%)	p=0.10	0/13 (0%)	4/18 (22.2%)	p=0.12
Peak mRS <1	0/15 (0%)	4/16 (25%)	p=0.10	0/13 (0%)	4/18 (22.2%)	p=0.12
Peak mRS >2	15/15 (100%)	12/16 (75%)		13/13 (100%)	14/18 (77.8%)	
mRS change <1	9/15 (60.0%)	7/16 (43.7%)	p=0.48	7/13 (53.8%)	9/18 (50.0%)	p>0.99
mRS change >2	6/15 (40.0%)	9/16 (56.3%)		6/13 (46.2%)	9/18 (50.0%)	
Drug rash	0/15 (0%)	1/16 (6.3%)	p>0.99	0/13 (0%)	1/18 (5.6%)	p>0.99
Associated autoimmune disease	2/15 (13.3%)	5/16 (31.3%)	p=0.39	1/13 (7.7%)	6/18 (33.3%)	p=0.19
Tumour	1/15 (6.7%)	3/16 (18.8%)	p=0.60	1/13 (7.7%)	3/18 (16.7%)	p=0.62

*Table 5-3 Clinical associations of both CASPR2-antibody associated HLA allele (DRB1*11:01) and haplotype (DRB1*11:01-DQA1*05:01-DQB1*03:01) expression.*

Fisher's exact test was used to test for differences between groups based on the following parameters; presentation as either LE, Morvan's syndrome or a non-immune syndrome (defined blinded to allele/haplotype by two clinicians), the presence of seizures, neuromyotonia or neuropathic pain at any point in disease course, peak mRS or improvement in mRS (defined as difference between peak mRS and mRS at latest follow up, median length

of time between disease onset and latest follow up - 44 months, range 5-160). No differences were noted between any parameters based on these analyses.

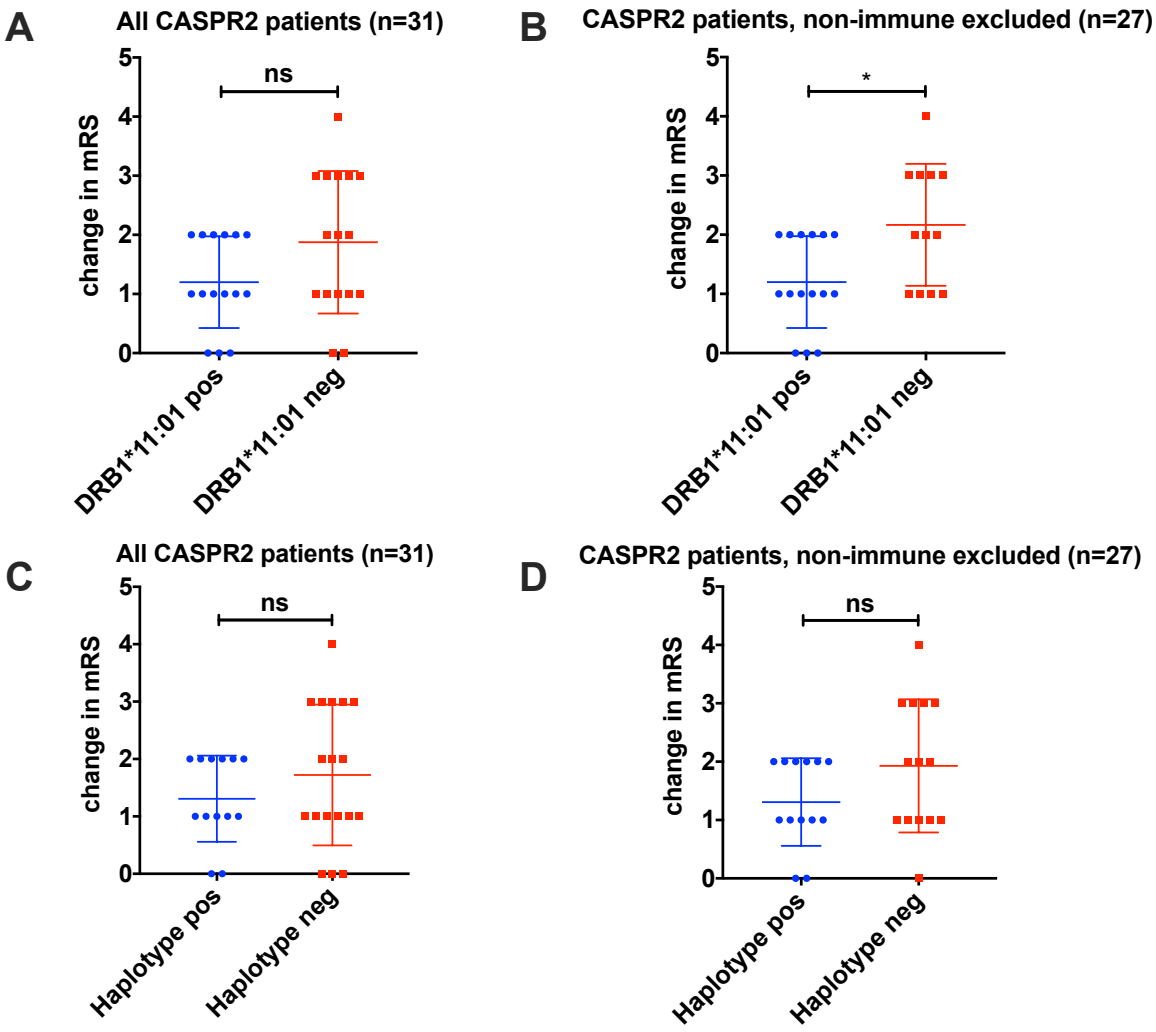


Figure 5-4 Improvement in mRS compared between CASPR2-antibody associated HLA allele and haplotypes

*(A and B) Difference in change in mRS between those with CASPR2-antibody associated allele (DRB1*11:01) and (C and D) haplotype (DRB1*11:01-DQA1*05:01-DQB1*03:01) from peak mRS to latest follow up. (A and C) Results for the whole cohort included in the HLA analysis, (B and D) Results for the cohort with patients non-immune mediated syndromes excluded. Two-tailed Mann-Whitney U-test used to test significance of difference, *p<0.05.*

5.6 Associations between HLA and biochemical features in patients with CASPR2-antibody mediated neurological disease

5.6.1 CASPR2-antibody live CBA

Given the limited clinical correlation between risk allele or haplotype in patients with either CASPR2- or LGI1-antibody mediated neurological diseases, the next assessment made was of any biochemical relationships, specifically in the CASPR2-antibody patients. From this point forward the full cohort of 33 patients, including non-Caucasians, were included as no further comparisons with Caucasian-only groups were required. For one Caucasian patient, no serum samples were available so 32 samples were used. The current gold standard of specific NSAb antibody quantification is end-point titration on CBA and this was carried out on the 32 serum samples available. I performed the titration on half of the patients with the remainder carried out by Selina Thompsen, a group member in the autoimmune neurology group, Oxford. A significantly higher titre was present in patients with both the HLA risk allele and haplotype (Figure 5-5-B+C) (allele, p=0.005; haplotype, p=0.0004; Mann-Whitney U). These differences remained when patients with non-immune syndromes were excluded (allele, p=0.03; haplotype p=0.003; Mann-Whitney-U). As higher CASPR2-antibody end-titre was seen in patients with the DRB1*11:01 allele and extended haplotype, a theoretical possibility existed that the poorer recovery seen in carriers of HLA*DRB1*11:01 might be due to higher amounts of CASPR2-antibody. There was, however, no difference in CASPR2-antibody end-titre if groups were divided by mRS change (Figure 5-5-D, p=0.6306, Mann-Whitney U), even if non-immune patients were excluded (p=0.8647, Mann-Whitney U).

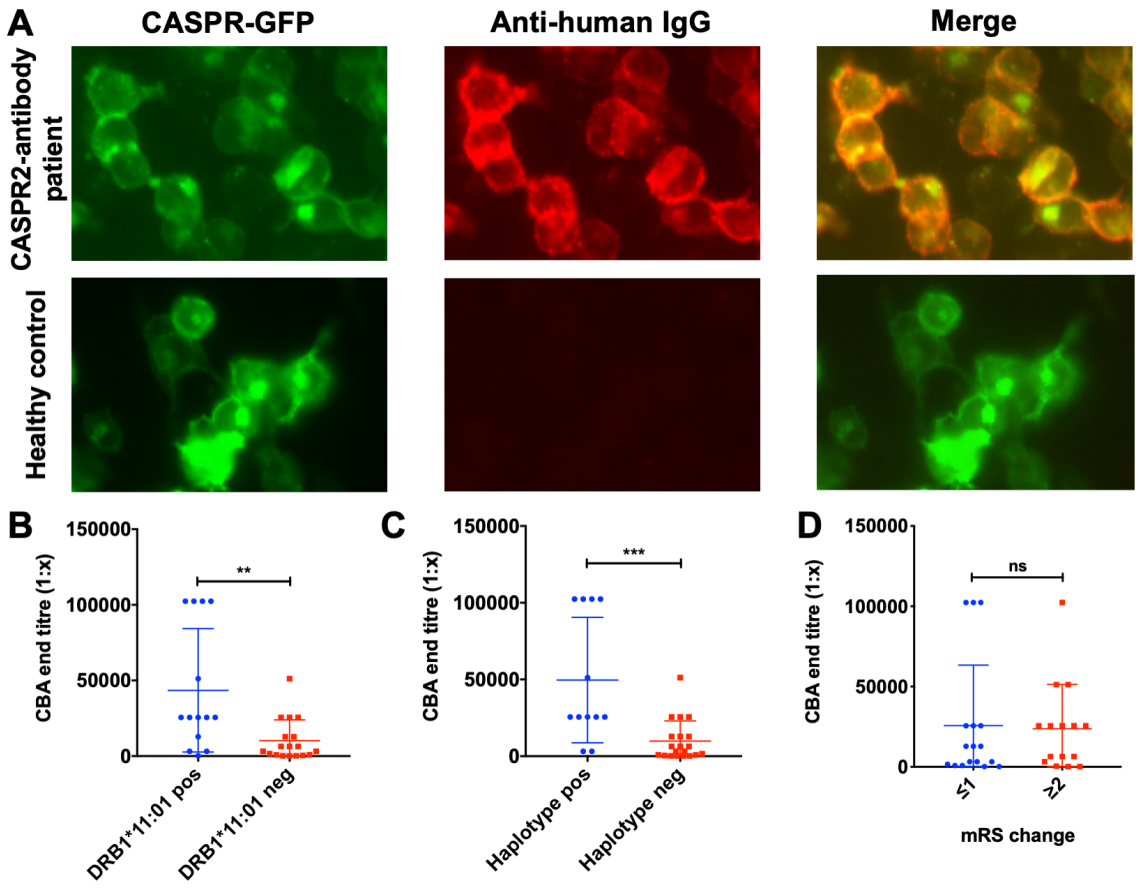


Figure 5-5 Cell based assay end titre in CASPR2-antibody patients, compared by HLA risk allele or haplotype expression

*(A) An example of a result from a CBA using serum from a CASPR2-antibody patient and healthy control on HEK293T cells transfected with CASPR2-eGFP (green), Alexafluor 594 anti-human IgG Fc (red) is then added. There is excellent colocalisation in the merged image (orange), suggesting patient antibody is binding specifically to expressed CASPR2. (B) CASPR2 CBA end titre of serum from CASPR2-antibody patients (n=32), divided by expression of DRB1*11:01 risk allele or risk haplotype (C). (D) Change in mRS divided by titre alone, no significant difference. Statistical comparison was undertaken using Mann-Whitney-U, **p<0.01, ***p<0.001.*

Due to the limited clinical differences between allele and haplotype positive patients and non-carriers, it is unlikely that the difference in CASPR2-antibody titre is caused by clinical differences between the two groups. Timing of the sample post onset of disease could have potentially interfered, but no significant difference was seen between DRB1*11:01 positive and DRB1*11:01 negative sample dates post onset (p=0.05 [Mann-Whitney-U], median 1796 days [range 68-4894] and median 706 [range 23-3317] respectively). A small but significant

difference was seen when date post onset of haplotype positive patients was compared to haplotype negative patients (p=0.03 [Mann-Whitney-U], median 2061 days, range 68-4894 and median 777, range 23-3317 respectively). This difference does not explain the higher titres seen in risk haplotype positive patients as they had, on average, later dates of sampling. Previously published longitudinal data suggests CASPR2-antibody decreases over time from disease onset,[110] rather than the increase observed.

5.6.2 FIPA

In order to confirm the difference in amounts of CASPR2-antibody seen in patients with the disease associated DRB1*11:01 allele or haplotype, an alternative method of antibody quantification was employed: the FIPA. This is a technique often used in this laboratory.[81] Briefly, HEK293T cells were transfected with CASPR2-eGFP and allowed to grow in a flask, then washed and lysed with FIPA buffer with 1% triton X-100 and protease inhibitors, creating a cell extract enriched for CASPR2-eGFP. This was then used as an immunoprecipitation substrate for patient CASPR2-antibodies in an in-solution assay. If human antibody bound CASPR2-eGFP, this was then immunoprecipitation with anti-human IgG antibodies and fluorescence units from precipitated CASPR2-eGFP was used as a readout (FU). The first step of establishing this assay was to optimise the amount of extract as well as patient serum dilution to use, in order to give the most effective assay (Figure 5-6-A). Using less than 12.5µl of cell extract, there appeared to be saturation of binding, with FUs actually increasing once serum was diluted below 1:100 and then consequently decreasing, whereas using 25µl or 12.5µl of extract gave excellent positivity at a CASPR2-antibody patient-serum dilution of 1:100, with 25µl having a higher signal at this dilution. At dilutions of 1:200 onward, however, there was limited separation between these 25 and 12.5µl of extract, both going negative at a serum dilution 1:12800, suggesting similar sensitivities to small amounts of

CASPR2-antibody (Figure 5-6-A). Combining these observations with the logistical practicalities of making and diluting CASPR2-eGFP extract, 10µl of extract was used with patient serum at 1:100, similar to previous set-ups. Primary incubation overnight at four °C (two-day) or for two hours at four °C (one day) was compared, with the two-day assay giving higher signal at 1:100 and higher positivity to lower dilutions. This was therefore used as our assay methodology of choice (Figure 5-6-B).

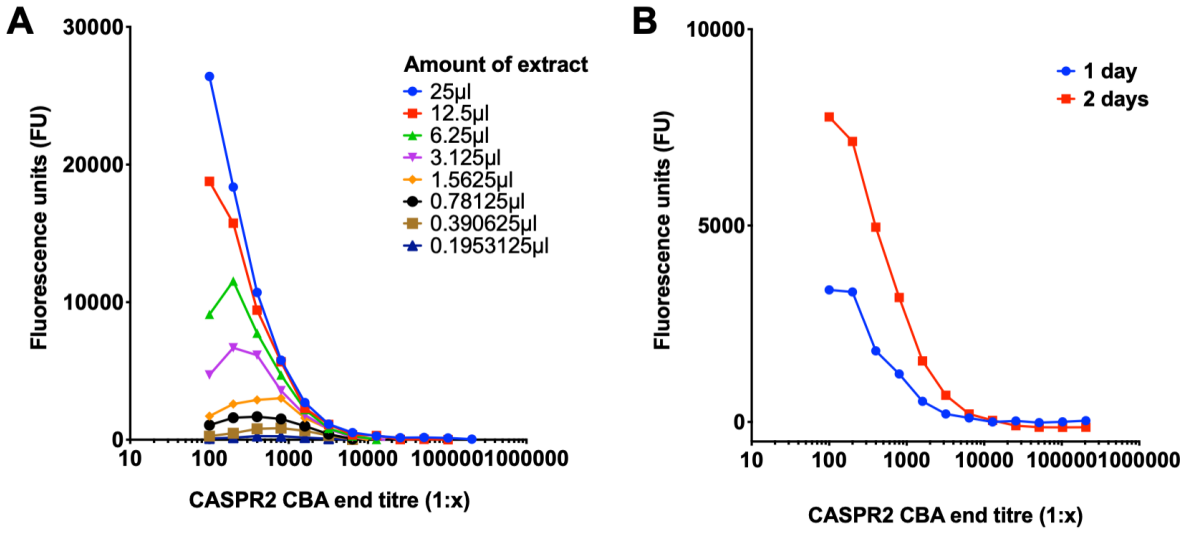


Figure 5-6 Optimisation of CASPR2-antibody fluorescent immunoprecipitation assay (FIPA)

(A) Optimisation of amount of extract (represented by different coloured lines – legend on graph) titrated against dilution of the serum from a patient with high titre CASPR2-antibodies (1:100, diluted serially to 1:204,800 – plotted on x axis), y axis represents fluorescence readout of immunoprecipitated samples in fluorescence units with background subtracted (FU). 25µl (blue) and 12.5µl (red) of extract were the only amounts not saturated by patient serum at 1:100, as evidenced by no increase once serum was further diluted, both remained positive to similar dilution amounts. (B) Comparison of one day assay, with two-hour primary incubation, versus two days, with overnight primary incubation, values presented are mean values of all extract amounts used in (A) titrated against the CASPR2-antibody patient serum (not the same serum as used in A), for the one- and two-day assays. The two-day assay clearly gives higher FU and also stays positive to a lower dilution.

The same CASPR2-antibody patient serum (n=32) was therefore tested using the optimised FIPA. This quantitative assay correlated well with CBA end-titre (r=0.8319, [95%CI 0.6748 to 0.9169], p<0.0001), suggesting it is a valid method of CASPR2-antibody

quantification (Figure 5-7-A). FIPA also confirmed the higher amounts of CASPR2-antibody seen in patients with the DRB1*11:01 risk allele (Figure 5-7-B,p=0.045, Mann-Whitney U) and with the associated risk haplotype (Figure 5-7-C, p=0.012, Mann-Whitney U).

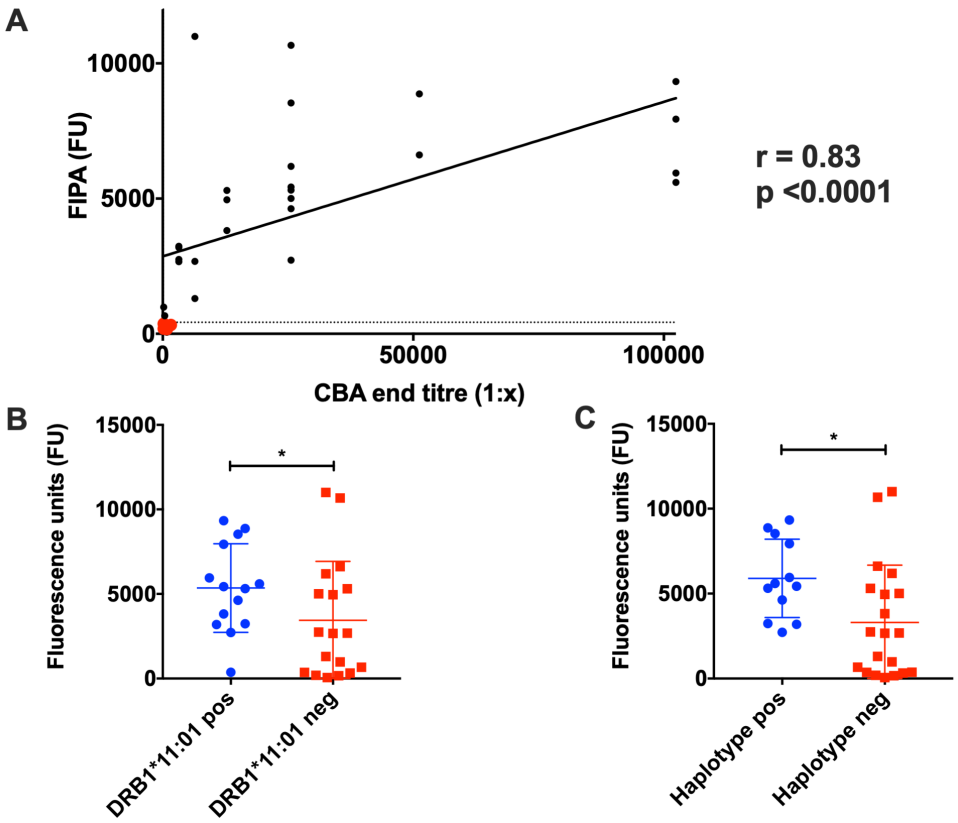


Figure 5-7 CASPR2-antibody FIPA correlation with CBA and comparison of quantification by HLA allele and haplotype

*(A) Correlation between quantification by FIPA (FU – y axis, based on mean of two tests) and CBA end titre (x-axis) on the 32 CASPR2-antibody patient serum samples, very good correlation noted, validating FIPA as a method of quantification, Spearman's r. Cut-off for positivity on FIPA based on 8 HCs mean plus three standard deviations represented by the dotted line on the y axis, dots in red are non-immune patients. (B) FIPA values for DRB1*11:01 allele carrying patients versus those without and (C) Patients with the risk associated haplotype versus those without. Line represents mean and error bars represent standard deviation. Mann-Whitney U test for significance, *p<0.05*

The threshold for positivity in the FIPA was calculated as mean plus three standard deviations of FU measurements from 8 healthy controls and is plotted as a dotted line on the y-axis in Figure 5-7-A. Based on four patients repeated on two assays, the mean inter-assay coefficient of variation was 15.4%, an acceptable figure. Four dots pertaining to patients who

were classed as having non-immune syndromes are highlighted as red dots on this graph. They were all positive on CBA using 1:100 as a cut-off for positivity with titres of 1:200, 1:200, 1:800 and 1:1600 respectively. None of them were above the cut-off for positivity on FIPA. All patients with the risk haplotype were positive on FIPA (12/12, 100%), while 14 out of 20 patients (70%) without were positive. 13/14 (92.9%) of DRB1*11:01 carrying patients were positive on FIPA compared to 13/18 (72.2%) of those without. As previously mentioned, none of the non-immune patients carried DRB1*11:01 and if these patients are excluded then only one patient from each group is negative on FIPA, and the significant difference between each group disappears (allele, p=0.2649; haplotype, p=0.0661; Mann-Whitney U), suggesting the syndrome, as opposed to the HLA difference, may be driving the difference seen in this assay.

Looking in more detail at the low titre patients (Figure 5-8), the patients with non-immune syndromes had lower titres but there are patients with similarly low titres who are clearly positive on FIPA. This suggests perhaps that the observed difference is due to an intrinsic difference in the antibodies made by these patients, rather than titre alone.

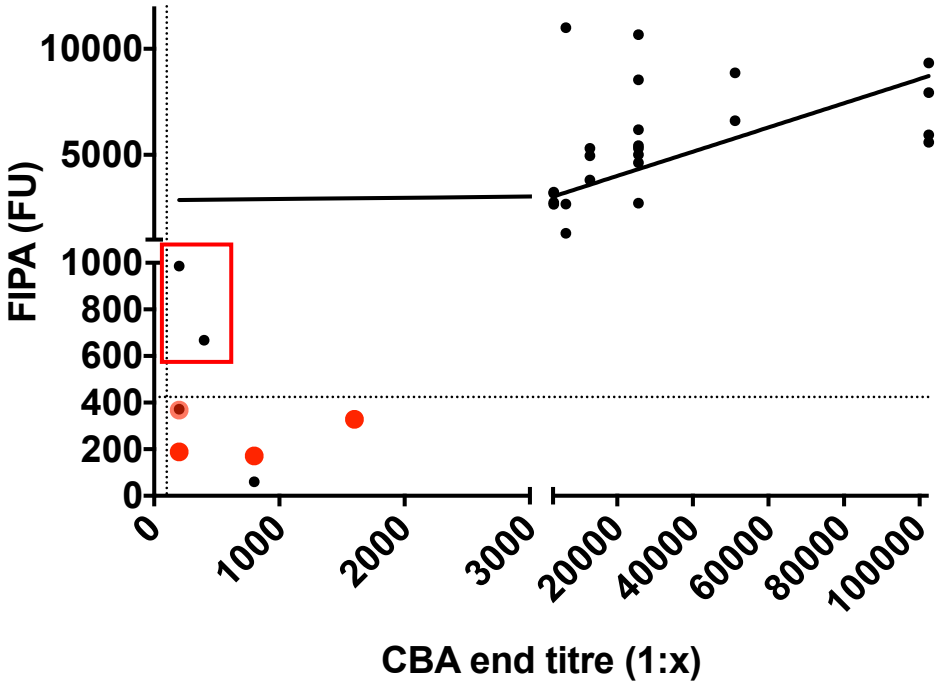


Figure 5-8 CBA end titre versus FIPA FU in low positive or non-immune patients

Correlation data from Figure 5-7*-A, with axis split to allow focus on low positive patients. FIPA cut-off for positivity is dotted line on y-axis, CBA cut-off for positivity of 1:100 is dotted line on x-axis. Red dots represent patients with non-immune syndromes, one dot has been made translucent in order to see overlapping data-point underneath. All non-immune patients are negative on FIPA despite in some instances having titres higher than patients with immune phenotypes who are positive on FIPA (highlighted by red box).*

5.7 Discussion

This study was the first to compare HLA alleles between patients with LGI1-and CASPR2-antibody mediated diseases. It confirmed the dominant HLA association in patients with LGI1-antibodies and revealed a novel and separate HLA association in patients with CASPR2-antibodies. As these antigens are co-expressed in VGKC complexes and the associated clinical features frequently overlap, with some notable distinctions, the dichotomous HLA associations may explain the differential generation of LGI1- versus CASPR2-antibodies. As the associations described are predominantly in class II alleles, T-helper cells are strongly implicated in disease initiation and propagation.

The association between HLA DRB1*07:01 and LGI1-antibody patients was very strong, seen in over 90% of patients. This was not seen at all in CASPR2-antibody patients, where expression of HLA DRB1*07:01 was similar to background healthy control rates and instead there was a strong association with single, distinct, class II allele: HLA DRB1*11:01. In LGI1-antibody patients, in contrast to a previous study,[190] DRB4 expression was less frequent than DRB1*07:01, there was an enrichment in homozygosity for HLA-DRB1*07:01 and two weaker class I associations were observed: HLA-B*57:01 and HLAC*06:02. An entirely separate complement of HLA alleles was observed in patients with both LGI1- and CASPR2-antibodies, though these patients are rare and the numbers consequently do not meet significance. It could represent, however, a further divergent molecular mechanism which defines whether a patient generates both autoantibody specificities in response to a break in tolerance to the VGKC-complex proteins.

The frequencies (9–27%) of these risk-associated HLA alleles in healthy Caucasians are significantly higher than disease prevalence, suggesting this HLA association is only one link in the chain of events leading to the manifestation of antibody production and disease, with other factors including environmental or lifestyle factors playing a role. Our findings also extend the HLA associations often seen in autoimmune diseases defined by predominant IgG4-related diseases,[202] but here, with a DR1 association as opposed to DQ5. In disagreement with a previous report,[190] the same HLA risk alleles were shared between tumour and non-tumour LGI1- and CASPR2-antibody patients. This suggests that a unique paraneoplastic signature is less of a factor in these diseases, in sharp contrast to Lambert-Eaton myasthenic syndrome where an HLA association is only seen in non-tumour associated cases.[203] Tumours observed were predominantly of skin or prostate, tumour types with a high background rate in the older population predominantly affected by LGI1- and CASPR2-

antibodies and therefore may simply reflect this background rate, rather than a distinct immune mechanism.

The predominant class II HLA associations implicate processing of extracellular antigen and CD4+ T helper cells.[204] In combination with recent translational B cell work which suggests T cells are important in the development of antibody mediated brain diseases,[12, 38] this provides an impetus to expand disease-specific T cells in vitro, an approach discussed in chapter seven. The weaker the class I associations found here in patients with LGI1-antibodies are different to previously described class I associations (HLA-B*44:03 and HLA-C*07:06) reported in seven patients.[191] This may suggest a role for intracellular antigen presentation in disease, including viruses and drugs. The differences in observed class I alleles between studies can be explained by varied ethnicity, sample size and relatively weak associations.[191]

Clinically the HLA associations do not distinguish between sub-phenotypes, symptoms, disease severity, drug rashes or association with an immune disease. There was a suggestion that, in CASPR2-antibody patients, those who did not express HLA-DRB1*11:01 had a better response to immunotherapy, despite disease severity being similar. The reason for this was not clear. A parallel biochemical observation was made that there were more serum CASPR2-antibodies in patients carrying DRB1*11:01 compared to those without, when tested by two different quantitative methods. This may provide a possible explanation. It has been demonstrated in 250 patients with NMDAR-antibody encephalitis that both higher serum and CSF titre predicts poorer outcome.[205] This was not seen in our cohort of CASPR2-antibody patients, though our data may be limited by a smaller sample size and variable timing of the serum sample used; this retrospective cohort was not designed to answer this question.

The robustly higher amounts of antibody observed in DRB1*11:01 carrying patients could be due to more efficient antigen presentation to CD4+ T helper cells, with consequently

more potent activation of T cells, allowing these cells to offer more help to CASPR2 specific B cells and promoting the observed increase in CASPR2-antibody secretion. It could be that in a larger, prospective cohort of CASPR2-antibody patients, higher titre at presentation may correlate with poorer outcome and this would explain the difference observed here. Another intriguing possibility is that in this disease, quantity of specific antibody truly isn't a factor and the difference is driven by the T cells themselves. This could be due to varied ability to drive somatic hypermutation and class switching of B cells, thereby directing affinity, avidity or epitope spread of antibodies. Alternatively, it could be a direct T cell effector function. The possibility also remains that one of the many non-antibody secreting roles of B cells is important, including secretion of cytokines, presentation of antigen and formation of ectopic lymphoid follicles.[206] Particularly preferentially establishment of CNS follicles is a feasible mechanism, with evidence in LGI1-antibody patients that intrathecal production of specific antibodies is the key factor in poor prognosis.[207]

The observation that patients with CASPR2-antibodies and non-immune syndromes did not express DRB1*11:01 and also were not picked up by the FIPA provides further information. One possibility is that the FIPA is simply less sensitive and indeed, six patients positive on CBA were negative on FIPA, in keeping with the known superiority of the CBA over the FIPA.[208] The fact, however, that four of these patients had non-immune syndromes, with two 'immune' patients positive on FIPA with a lower CBA end-titre could suggest an intrinsic difference in the antibodies produced, a further prompt to examine this in more detail.

In summary, in addition to the known clinical and biochemical distinction between patients with LGI1- and CASPR2-antibodies, the novel description of distinct HLA associations supports an immunological dissociation in the generation of these autoantibody-mediated syndromes. The dominant class II HLA involvement offers potential to better understand the

likely initiating T–B cell interactions. Finally, the suggestion of poorer response to immunotherapy and the higher amounts of CASPR2-antibodies in HLA risk allele carrying CASPR2-antibody patients implies a clinico-immunological consequence of this HLA association that warrants further exploration.

6 The B cell immunology of patients with CASPR2-antibodies

6.1 Introduction

Since their original description,[81] knowledge has grown significantly about patients with antibodies to CASPR2. The clinical syndrome has been established to predominantly include LE, NMT or both combined with prominent sleep and autonomic dysfunction in the rare MoS. Alternative clinical presentations, such as ataxia or movement disorder, occur but are less frequent.[77, 86, 102, 110] Excellent work has been done to establish the pathogenicity of CASPR2-antibodies as well as their mechanisms *in vitro*[111] and *in vivo.*[209] However, the cellular immunology of CASPR2-antibody mediated neurological diseases remains unexplored.

As an antibody mediated syndrome, B cells are clearly likely to be central to the underlying immunology in patients with CASPR2-antibodies. A better understanding of the B cells responsible for initiation and ongoing synthesis of CASPR2-antibody, as well as the factors that drive this, could provide valuable insights in order to direct immunotherapy. Plasma cells are the main antibody secreting cells. They are terminally differentiated with decreased expression of classical B cell surface markers (CD19 and CD20), increased expression of CD138 and their intracellular composition is adapted to specialise in rapid production of antibody. These can be short-lived or long-lived in the bone marrow or lymph nodes and are termed plasmablasts when present in the circulation. As described in the general introduction, plasma cells or plasmablasts arise once naïve, antigen-inexperienced B cells encounter antigen, enter a germinal centre and undergo CSR, SHM and affinity maturation. Post germinal centre, the majority of B cells gain CD27+ expression. At this point cells either become plasmablasts or memory B cells. Memory B cells do not secrete antibody

at the profuse rate seen in plasmablasts but instead provide the substrate for a prompt and effective antibody response upon antigen re-encounter.[210, 211] This situation is likely to be more complicated in autoimmune disease where antigen, as something present in the human body, could potentially be constantly available. Therefore, further study into the NSAb autoimmune brain diseases are necessary and likely to be informative.

Two studies from our laboratory set out to explore this question by culturing circulating lymphocytes from patients with AQP4-antibodies and neuromyelitis spectrum disorder (NMOSD)[12] or NMDAR antibodies and NMDAR-AbE.[38] In both sets of patients, from bulk PBMCs, it was possible to induce secretion of disease specific antibody *in vitro*. The most effective conditions mimicked T-cell help. In both diseases the amount of antibody produced in culture correlated with the patient's serum specific antibody, suggesting these circulating cells make a relevant contribution to serum specific antibody. Antibody secretion in culture could, therefore, represent a proxy of the amount of circulating antigen specific B cells. In AQP4-antibody positive NMOSD patients, it was demonstrated that the main circulating cell type driving this antigen secretion in culture was the memory B cell and not plasmablasts, in opposition to a previous paper on the subject.[212] In a surprising observation, it was also discovered that naïve B cells could be induced to secrete AQP4 antibody, suggesting a pre-germinal centre failure in tolerance.[12] Finally, in NMDAR-AbE, ongoing germinal centres were implicated in autoantibody production because 60% of patients had serum NMDAR-IgM, which was highest at disease onset and often increased in relapse, this was also produced in culture.[38]

Based on these studies, our hypothesis was that patients with CASPR2-antibodies had circulating B cells capable of producing CASPR2 specific antibody. When selecting agents to stimulate B cell proliferation, cytokines (IL-2 and IL-21) and a toll-like receptor (TLR)-agonist

(R848) were used which had an optimal effect in the aforementioned studies. In addition, a number of cytokines not tested previously were included based on a literature review of cytokines associated with autoimmune encephalitis (Figure 6-1). These cytokines were used in a combinatorial matrix layout given the established evidence of an additive effect of a number of cytokines when used together.[213] In order to gain further insights into which cells are responsible for antibody secretion during an evolving autoimmune response, patients PBMCs were cultured over serial time points.

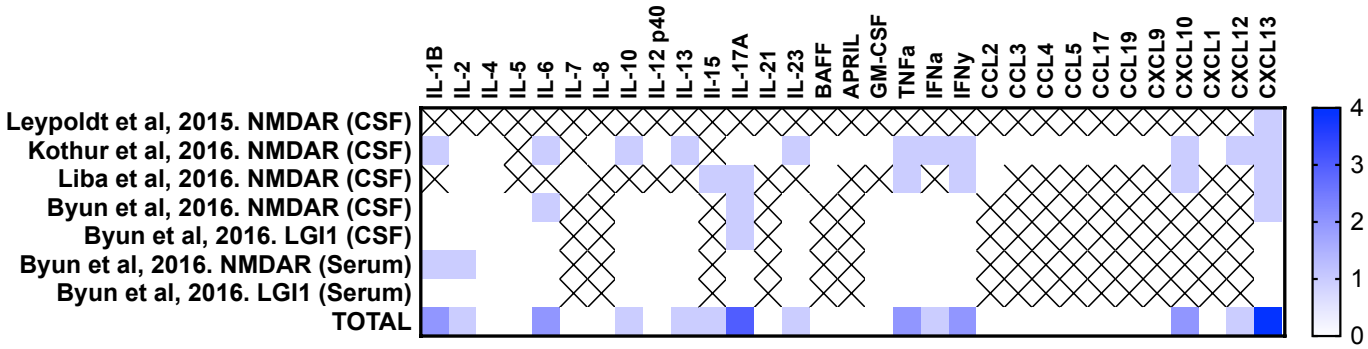


Figure 6-1 Literature review of cytokines associated with autoimmune encephalitis

A review of the existing literature comparing serum or CSF cytokines between patients with NSAb-mediated encephalitis and HCs was conducted. The results are presented, with each row pertaining to a single antibody group, in either CSF or serum from a single study.[214-217] A coloured box indicates a significant difference between patients and HC, a blank box means no significant difference and a cross means that cytokine was not tested in that study. Based on this review and excluding cytokines already tested, IL-10, IL-15, IL-17A, IL-23, CXCL10 and CXCL13 were included as novel cytokines.

In previous studies, no differences were seen in baseline flow cytometry quantification of patient circulating lymphocyte subsets and specific antibody production.[12, 38] Similarly, flow cytometry of culture stimulated PBMCs demonstrated only the expected development of plasmablasts which correlated with IgG secretion in supernatant (SN). Therefore, these experiments were not repeated in CASPR2-antibody patients.

Immunoglobulin G (IgG) is the most abundant immunoglobulin in blood (median concentration, IgG 1090 mg/dl, IgA 239mg/dl and IgM 134mg/dl)[218] and has four subclasses

in humans, numbered 1-4 in order of their average serum concentration.[219] CASPR2-antibodies in patients with CASPR2-antibody mediated neurological disease are predominantly of the IgG4 subclass.[102, 110] Given the previous close correlation between amounts of antibody produced in culture and serum specific antibody in NMDAR-AbE and AQP4-antibody positive NMOSD, IgG subclasses were quantified and compared between serum and cultured B cell supernatants from CASPR2-antibody patients. This was done with the expectation that they would be aligned. CASPR2-antibody epitopes were compared in the same way, with the hypothesis that there would similarly be a relationship. Finally, given the novel association of CASPR2-antibody patients and HLA DRB1*11:01, as well as the suggestion of the importance of T cell help in these cultures, we hypothesised that the expression of this allele would affect the production of CASPR2-antibody in culture.

6.2 Methods

6.2.1 Patients

Ten patients were recruited from the Oxford autoimmune neurology clinic or via referral from UK collaborators. Ten age matched healthy controls were recruited by Dr Sophia Michael and are included here with her permission. Bloods were taken for serum and PBMCs concomitantly. Clinical data was obtained from direct patient interview and from medical notes. This was carried out under the following ethical approvals: 16/YH/0013 and 16/SC/0224. Larger cohort serum CASPR2-antibody epitope testing (n=32) is based on patients described and recruited in chapter 5.

6.2.2 PBMC culture

For cell culture, 1-2$\times10^5$ unfractionated PBMCs per well were seeded in B-cell medium, comprised of RPMI 1640, supplemented with 5% IgG depleted foetal calf serum, 1%

penicillin-streptomycin, 1% L-glutamine, 0.1% IgG-depleted transferrin (20μg/ml) and 0.1% 2-mercaptoethanol. They were incubated in flat-bottomed 96-well plates with a matrixed layout, giving 72 wells tested per patient. Cytokines and mitogens included R848 (2.5 mg/ml Enzo Life Sciences), soluble CD40-ligand (sCD40L; 50 ng/ml, R&D Systems), interleukin-2 (IL-2; 50 ng/ml, PeproTech), interleukin-10 (IL-10; 20ng/ml, PeproTech), interleukin-15 (IL-15; 10 ng/ml, PeproTech), interleukin 17A (IL-17A; 10 ng/ml, R&D Systems) interleukin-21 (IL-21; 50 ng/ml, PeproTech), interleukin 23 (IL-23; 10 ng/ml, PeproTech), C-X-C motif cytokine 10 (CXCL10, 50 ng/ml, PeproTech) and C-X-C motif cytokine 13 (CXCL13; 10 ng/ml, PeproTech). Concentrations were based on literature review and previous experience in the laboratory. At day 13 cells were discarded and SN were collected and tested for total IgG, IgG subclass, CASPR2 IgG and CASPR2 IgG subclass.

6.2.3 B cell subclass sorting and culture

In order to sort B cells by subclass, HC PBMCS were sorted using BD FACS ARIA III. The following staining panel was used to isolate B cells: CD3 (clone UCHT1, Pacific Blue, BioLegend), CD14 (clone HCD14, Pacific Blue, BioLegend), CD19 (clone SJ25C1, APC-Cy7, BD Biosciences) and DAPI staining. IgG subclass antibodies used were as follows: IgG1 (clone SAG1, PE, Cytognos), IgG2 (clone SAG2, FITC, Cytognos), IgG3 (clone SAG3, FITC, Cytognos) and IgG4 (SAG4, APC, Cytognos). Once identified, B cells were sorted by subclass into BCM. Autologous PBMCs were B cell depleted using CD19+ beads (Dynabeads Pan-CD19 beads, Invitrogen). 5,000 sorted subclass specific B cells were plated onto 95,000 B cell depleted PBMCs and stimulated with R848, sCD40L and one of IL-10 or IL-21 in triplicate. Cultures were incubated for 13 days at which point the cells were discarded and SN were kept and tested for total IgG subclass. This work was carried out with the assistance of Dr Mateusz Makuch.

6.2.4 Pan IgG and subclass ELISAs

Total IgG was tested using an ELISA kit (Bethyl Laboratories kit, #E101), SN was tested at a dilution of 1:100-1:200, after 13 days culture in vitro. For subclass ELISA, a different kit was used (IgG subclass human ELISA kit, Thermofisher #991000), serum was tested at 1:2500 to 1:5000 and pooled SNs at 1:2-1:10.

6.2.5 Multiplex flow cytometry assay

This assay was based on the flow cytometry subclass CBA described previously.[87] Briefly, a CASPR2-eGFP expressing HEK293A cell line, developed by Dr Patrick Waters, was grown under geneticin selection (400 μg/ml) and used as the antigenic substrate. For epitope specific experiments, HEK293T cells were transfected as previously discussed with either construct specific for each domain (Figure 6-19). Cells were grown to 80% confluence, made into a single cell suspension with 1% trypsin and plated out at 10,000 cells per well, aiming to give 5,000 fluorescent cells per assay. If more than 50% of the cells were expressing CASPR2-eGFP, they were supplemented with untransfected HEK cells to act as an antigen negative population. These cells were then stained with patient serum at (1:100-1:400) or SN (1:5-1:20) for thirty minutes at 4 °C and then washed in FACS buffer (DPBS, 0.1% BSA, 2 mM EDTA). Next, cells were labelled with one of the following secondaries depending on the experiment; anti-human IgG Fab (PE-labelled, Fisher Scientific), for separate staining experiments; anti-human IgG1-4 subclass-specific antibodies (Alexa Fluor 647-labeled, Southern Biotech) and for multiplex experiments anti-human IgG1 (Alexa Fluor 647-labeled, Southern Biotech), anti-human IgG2 (APC-Cy7 labelled using Lighting-Link® Kit, Innova Biosciences, antibody from Southern Biotech), anti-human IgG3 (PE-Cy5, Lighting-Link® Kit, Innova Biosciences, antibody from Southern Biotech) and anti-human IgG4 (PE-labelled, Southern Biotech) or anti-human IgM (AF647, Southern Biotech – ran separately). After staining, cells were washed and stained

with DAPI for live/dead discrimination. Cells were analysed on LSR II (BD Biosciences). The gating strategy is described in the results section (Figure 6-3). To determine the relative quantities of different secondary antibodies bound to human-CASPR2-antibodies, a calibration curve was derived from Quantum Simply Cellular anti-mouse IgG beads (Bangs Laboratories) coated with the same amount of secondary antibody used to stain for patient antibody on HEK cells.

6.2.6 CXCL13 ELISA

This assay was carried out by Dr Sophia Michael, PhD student in the Oxford autoimmune Neurology group, and the results are used with her permission. Serum was tested on the CXCL13 Quantikine ELISA Kit (R&D Systems) as per manufacturer's instructions.

6.2.7 Statistics

All statistical analysis and graphing carried out on GraphPad Prism 7.

6.3 CASPR2-antibody subclass flow cytometry assay optimisation and cohort results

6.3.1 Subclass flow assay optimisation

As a key aim was to characterise the IgG subclass of both serum and SNs in a quantitative way, a novel flow cytometry assay was optimised. The assay previously employed by our laboratory to quantify LGI1-antibody subclass by flow cytometry[87] made use of four mouse anti-human IgG clones with specificity for IgG1, IgG2, IgG3 and IgG4, all prelabelled with AF647. The advantage of this method is that as the same fluorophore is used, results for each IgG subclass can be directly compared. The disadvantage is that it requires each sample to be run in quadruplicate in order to obtain results. Because roughly 50μl of SN is required per test and only 200μl is produced in total by our cell culture method, an alternative method

was devised. This involved using the same anti-human IgG clones but all with different fluorophores in order to quantify IgG1-4 from a single experimental run (Figure 6-2).

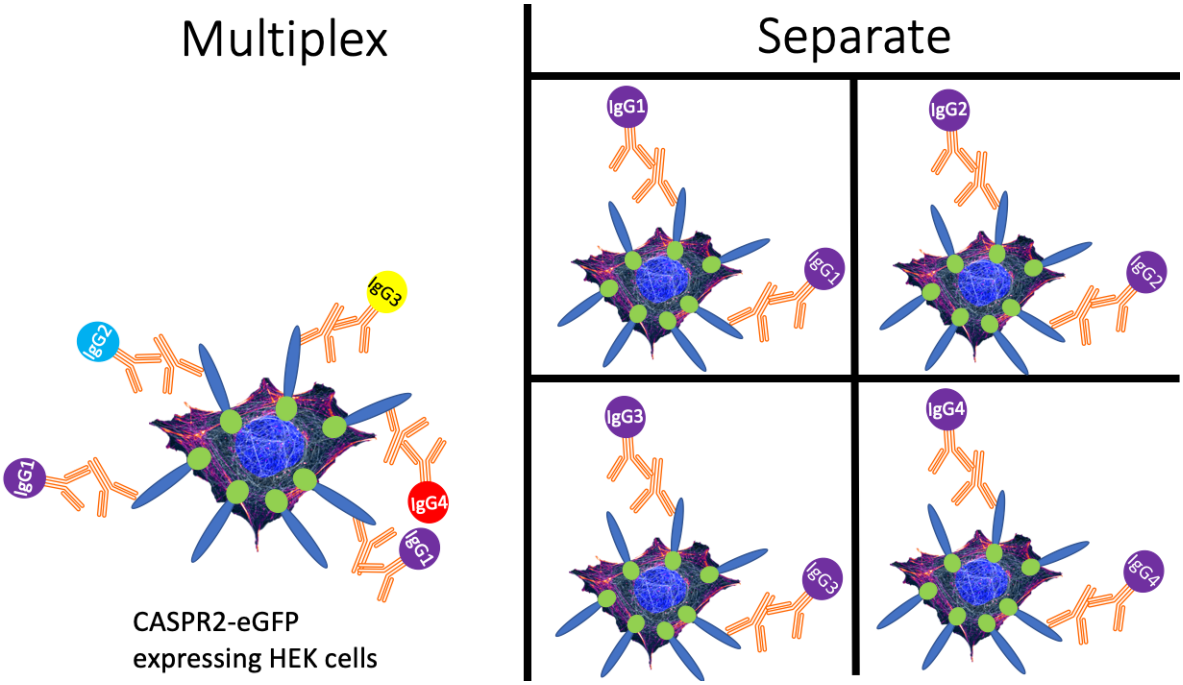


Figure 6-2 Multiplex versus separate IgG subclass flow cytometry assay

IgG subclass specific secondaries are used after primary incubation of patient serum with CASPR2-eGFP stable cells. In the multiplex assay the secondaries are all labelled with different fluorophores, so a sample needs only to be run once. In the separate assay they are all labelled with the same fluorophores, so the sample must be run four times to get a final result.

After staining, gating was carried out as shown in Figure 6-3. Briefly, HEK cells were gated for size on forward scatter area (FSC-A) and for granularity on side scatter area (SSC-A) and then for single cells on FSC-A and forward scatter height (FSC-H). They were then gated on the DAPI channel in order to exclude dead cells. Finally, live cells were displayed with eGFP on the x-axis to show degree of fluorescence which should directly relate to CASPR2 expression and the colour corresponding to each IgG subclass antibody on the y-axis. Delta median fluorescence intensity (ΔMFI) was calculated by subtracting the MFI of eGFP positive, CASPR2 expressing, cells from eGFP negative cells as per previous studies and shown in Figure 6-3.[12]

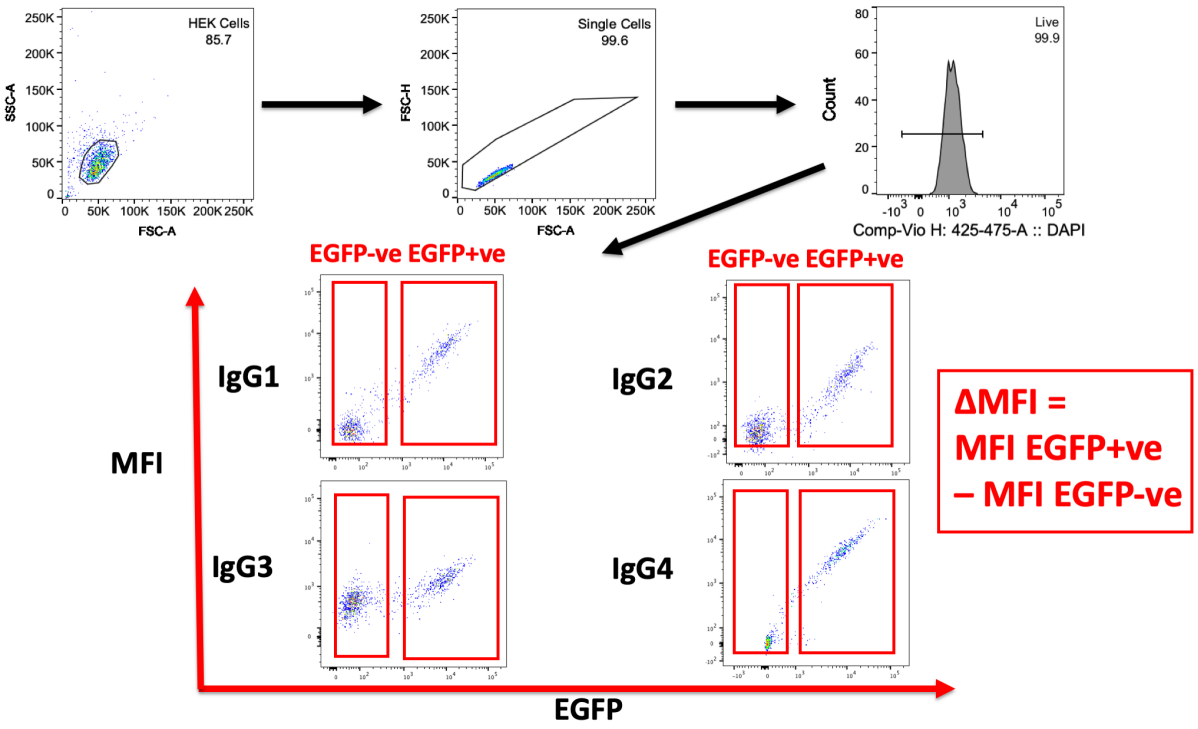


Figure 6-3 Multiplex IgG subclass flow cytometry assay gating example

Gating strategy for the multiplex flow cytometry assay, with the initial isolation of HEK cells, then single cells and then live cells. These live HEK cells are then plotted with eGFP along the x-axis and the fluorophore corresponding to each IgG subclass along the y-axis. ΔMFI *was calculated by subtracting MFI of the eGFP-ve (non-CASPR2 expressing) HEK cells from the MFI of eGFP+ve(CASPR2 expressing) HEK cells, representing a quantification with background subtracted.*

Labelled anti-human IgG secondary antibodies were titrated and optimal dilutions were obtained, very similar to the dilutions used in previous experience of these antibodies.[87] A key experiment was to ensure that the relative signals from each fluorophore were not blocked sterically by multiple labelled secondaries being in the dilution mix at once and therefore interfering with each other's capacity to bind to human IgG bound to CASPR2 (Figure 6-4). A slight reduction in ΔMFI was noted for IgG1, 2 and 4, with a mean percentage reduction, in all samples where antibody detected above cut off, of 18.3% (SD=20).

An issue in the IgG3 channel was noted, however. There was positive signal with all secondaries in the IgG3 channel but was most striking with IgG4 which had a ΔMFI greater

than IgG3 fluorophore in patient one (Figure 6-4-C). The IgG4 fluorophore was PE labelled and IgG3 was PE-Cy5 and it was discovered that the overlap was caused by the significant predominance of CASPR2 IgG4 antibodies in these samples, leading to an off-scale MFI which could not be compensated for and was bleeding into the PE-Cy5 channel. In order to avoid this, the decision was made to either run the IgG4 as a separate sample at a lower dilution or at a much lower voltage to give a lower MFI in situations where less sensitivity was required.

.

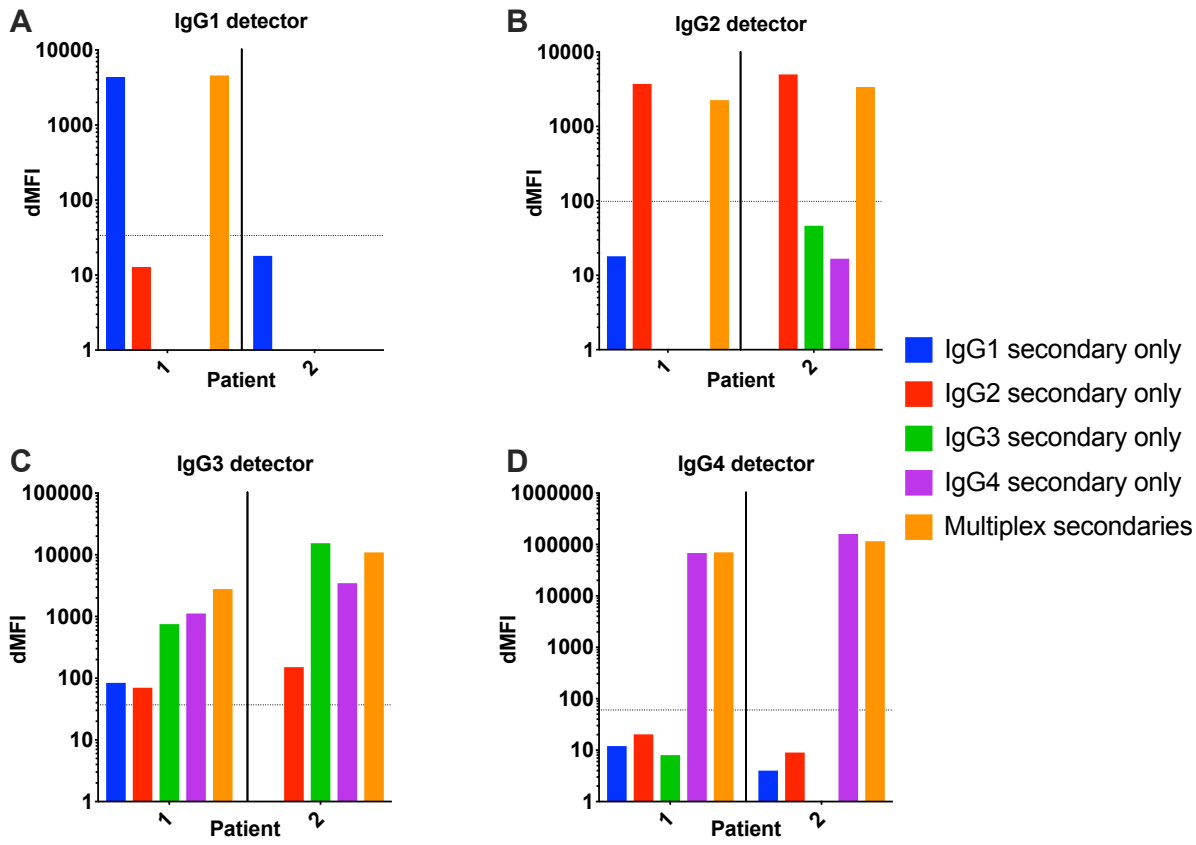


Figure 6-4 Multiplex flow cytometry assay optimisation – assessment of steric inhibition of multiplexed IgG subclass secondaries.

Each laser pertaining to a specific subclass associated fluorophore represented by A-D, single stains of each secondary in different colours (IgG1 – blue, IgG2 – red, IgG3 - green, IgG4 – purple) and multiplex stain (all secondary antibodies in staining mix - orange). Serum from two patients with CASPR2-antibody mediated encephalitis was used to optimise assay. The dotted line is mean plus three standard deviation cut off derived from HC samples run at same time. No significant decrease noted between single stains and multiplex stains of IgG1,2 and IgG4, bleed through of secondaries into IgG3 channel requiring a change in assay technique.

The next step was to titrate a serum sample against the number of CASPR2-eGFP stable HEK cells in the assay, to determine the optimal ratio of antigen allowing for highest sensitivity in the most reliable assay (Figure 6-5-A). 10,000 cells proved to the optimal number, giving enough events to generate a reliable curve and the highest ΔMFI figures for IgG4.

As there are inherent differences in the fluorescence of the four fluorophores used to label the IgG1-4 antibodies, they need to be normalised against a constant in order to allow comparison. To this end, for each assay, antibody binding capacity (ABC) was determined for each fluorophore by assaying each subclass secondary with a set of beads with a known range of capacities to bind secondary antibody, going from no binding to high binding. This then allowed the generation of a fitted four parameter curve where from ΔMFI, an ABC could be derived (Figure 6-5-B), allowing comparison between subclasses for each sample.

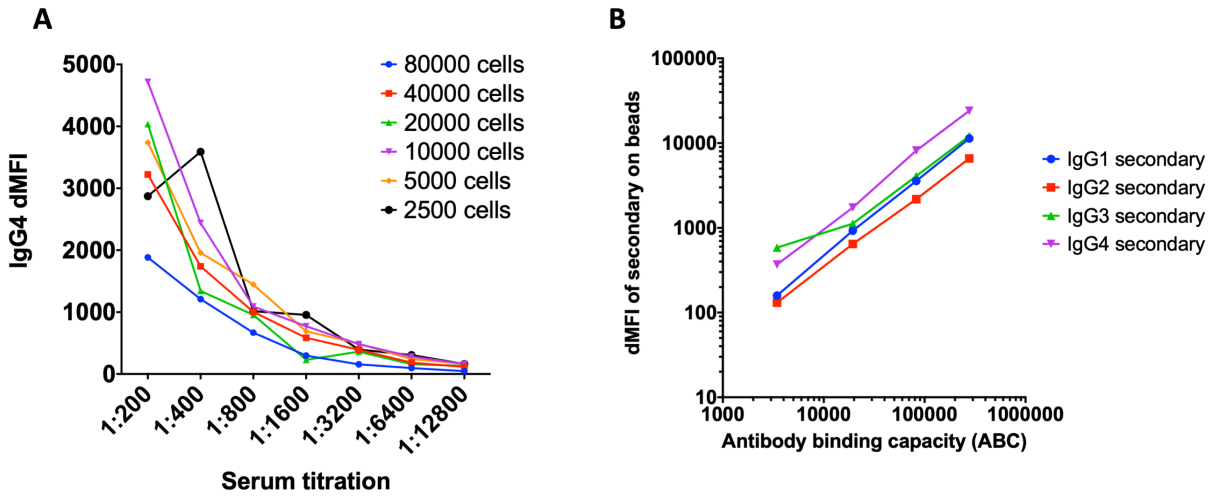


Figure 6-5 Multiplex flow cytometry assay - cell number and titration optimisation

(A) Serum from a patient with IgG4 CASPR2-antibodies only, used to titrate amount of serum used against number of CASPR2-eGFP expressing stable HEK cells, titration of serum antibody on x-axis, IgG4 only ΔMFI *on y-axis and each line represents the same titration with a different number of cells. As you can see, when many cells are used (eg 80,000 cells giving an excess of antigen), lower signal is observed (*ΔMFI*). Using 10,000 cells gave the best* ΔMFI *and most consistent curve so this was the number of cells used in the assay going forwards.*
(B) Example of how antibody binding capacity (ABC) is generated for each assay to allow comparison of quantification between each IgG subclass. A fitted four-parameter curve is derived from the binding of each IgG secondary to beads with a set range of capacities to bind mouse antibodies, this creates a reference curve to translate raw ΔMFI *into ABC for each fluorophore. This is done for every assay run to also control for inter-assay variation.*

Once this assay was established it was compared to already established methods of CASPR2-antibody quantification (Figure 6-6). There was an excellent correlation between the summed ABC for IgG1-4 from the multiplex assay versus the separate assay ($r=0.994$, $p<0.0001$) as well as the multiplex ABCs and an anti-human IgG Fab secondary, which binds all IgG subclasses ($r=0.9785$, $p<0.0001$). Mean coefficient of variation (%CV) across a three way comparison between multiplex flow cytometry, separate flow cytometry and IgG Fab was 22.6. In this experiment, the IgG Fab and separate flow cytometry assay had been run in the same batch but the multiplex flow cytometry results were from separate experimental runs. Reassuringly, mean %CV was 14.7 between the multiplex flow cytometry assay and the IgG Fab flow cytometry, suggesting acceptable variation between batches and methodologies.

In a further reassuring result, the correlation between multiplex flow and the current gold standard of CASPR2-antibody quantification, CASPR2-antibody end point titre on CBA, was excellent (r=0.8346, p<0.0001). Correlation with FIPA was less good but still reassuring (r=0.7146, p<0.0001).

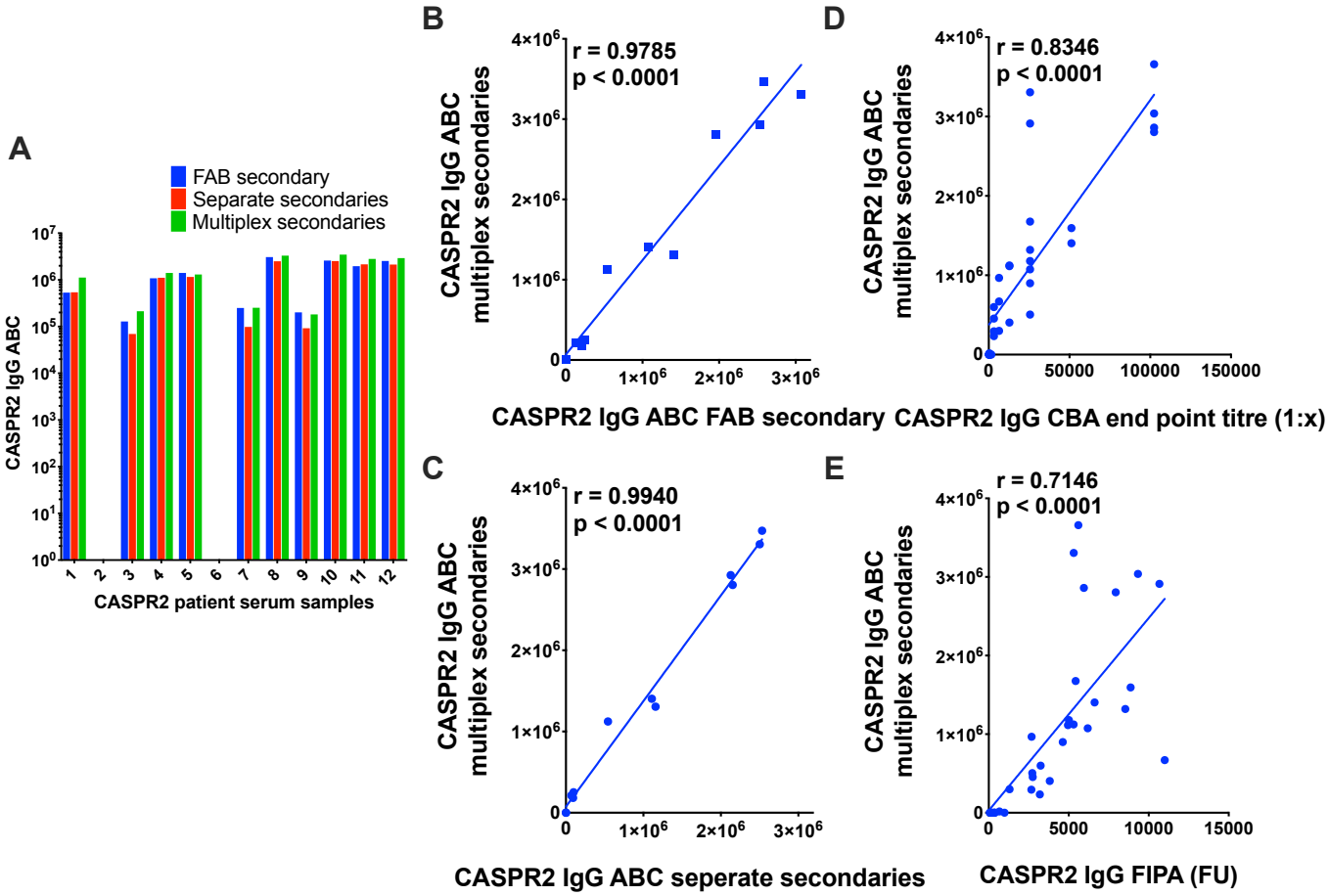


Figure 6-6 Comparison of multiplex flow cytometry assay to established methods of antibody quantification

(A) Comparison between multiplex flow cytometry ABCs (sum IgG1-IgG4 ABCs) and ABCs from the same 12 CASPR2-antibody patient sera obtained using the sum of IgG1-4 from the separate flow cytometry and a flow cytometry assay using a pan human-IgG Fab secondary. Results based on a single run. Good concordance was seen between all secondaries.
(B) Correlation between ABCs from n=12 patients run on the multiplex versus the IgG Fab secondary and between the multiplex and separate secondaries (C), near perfect correlation in both instances, Spearman's r.
(D) Correlation between ABCs obtained by multiplex flow cytometry assay and CASPR2-antibody CBA end point titre and FIPA (E) from n=32 CASPR2-antibody patient serum samples, correlation remained very good

6.3.2 CASPR2-antibody patient serum IgG subclass analysis

Having established a reliable CASPR2-IgG multiplex flow cytometry subclass assay, the subclass composition in the serum of the CASPR2-antibody patients (n=32) collected as part of the HLA study from chapter five was examined. A number of the patients had serial samples, taking the total number of samples to 62. A ΔMFI cut-off for each IgG subclass was generated from the mean plus six standard deviations from 10 healthy controls run in each assay contemporaneously. Sensitivity was 81.3% (26/32), with six patients negative by CASPR2-antibody multiplex flow cytometry who were positive on CASPR2-antibody CBA. CASPR2-antibody CBA end titres are compared between patient samples positive and negative on the multiplex flow cytometry assay (Figure 6-7-A). Five out of these six were also negative when tested on FIPA and four were non-immune. In terms of CASPR2 IgG subclasses in patients, results were in keeping with the literature (Figure 6-7-B-C) with IgG4 being the dominant subclass in terms of quantification of all CASPR2-antibody across the 62 samples (72.1%), with IgG2 second most common at 23.5% and IgG1 third at (4.1%). In terms of subclasses seen in individual patients (Figure 6-7-D), the most commonly identified CASPR2-antibody specific subclass were IgG4 antibodies (IgG4 25/32, 78.1%), with a high rate of positivity for IgG2 (24/32, 75%) and IgG3 antibodies (24/32, 75%), despite the small amounts of these CASPR2 IgG3 antibodies. IgG1 antibodies were seen in 13/32 patients (40.6%).

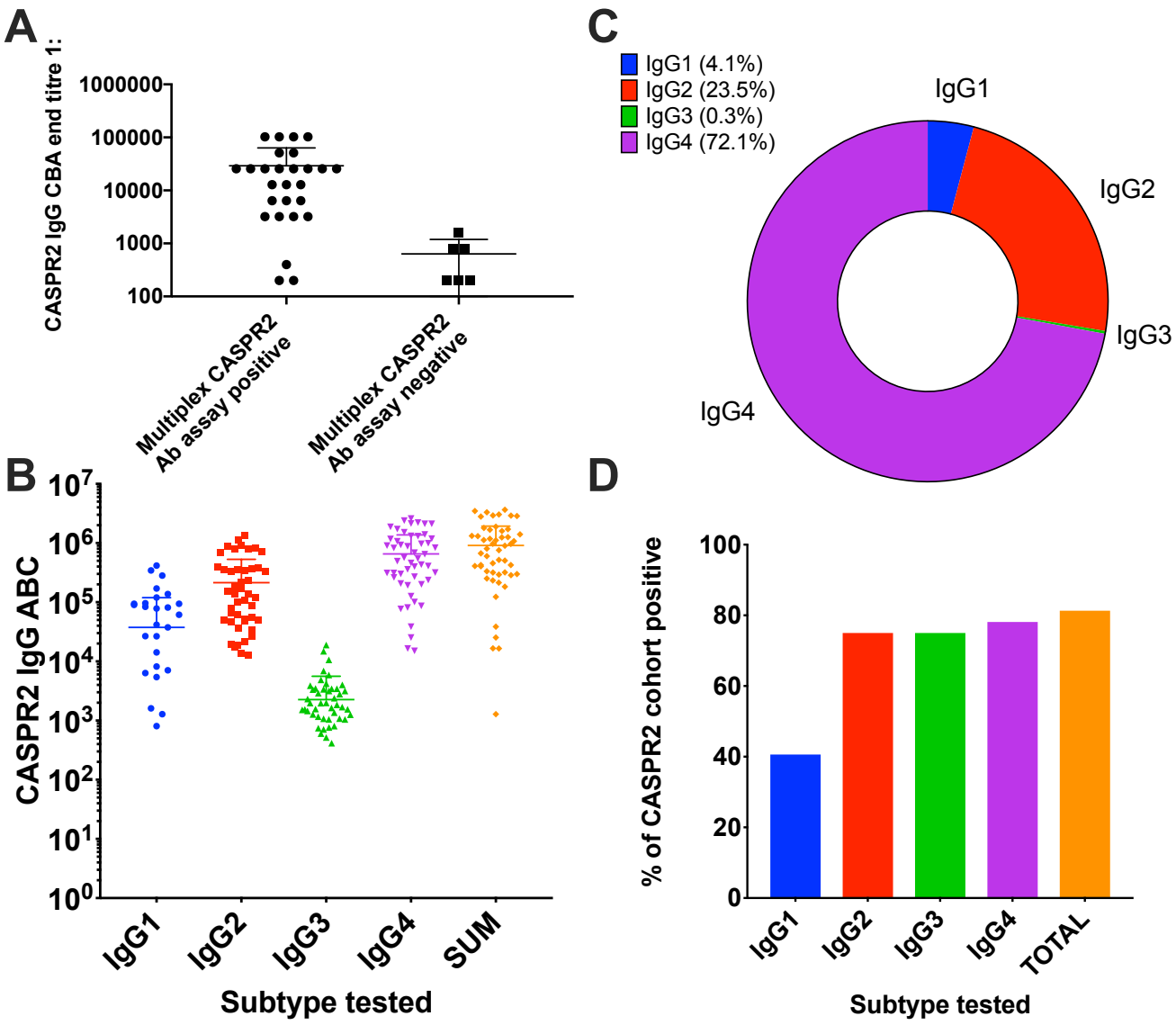


Figure 6-7 Cohort serum CASPR2-IgG subclasses

(A) Comparison of CASPR2 IgG CBA end-titre between patients positive on multiplex flow cytometry assay and those who were negative. Flow cytometry negative patients were mostly lower titre patients though patients with comparable titres were positive on multiplex flow cytometry assay.
(B) CASPR2-antibody ABC for each IgG subclass measured by multiplex flow cytometry assay from n=62 sera from n=32 CASPR2-antibody patients across a variety of time points. ABC values are only generated for patients above the ΔMFI cut-off derived from 10 HCs.
(C) Representations of the summed amounts of the values in A to give an idea of the proportions of each subclass relative to one another. CASPR2 IgG4 is predominant, followed by IgG2, then IgG1 and finally, minimal quantities of IgG3.
(D) Positivity for each subclass in serum defined as mean plus six standard deviations from the ΔMFIs of 10 HCs run contemporaneously in each assay. Based on this, in individual patients - IgG1 13/32 (40.6%) IgG2 24/32 (75%) IgG3 24/32 (75%) IgG4 25/32 (78.1%) with the total number positive on flow cytometry being 26/32 (81.3%). Of the 6 negative, 4 were non-immune and 5/6 were also negative on FIPA.

6.3.3 CASPR2-antibody patient serum IgM and IgE antibodies

A flow cytometry assay for CASPR2 specific IgM was also developed to enable comparison of the amounts of CASPR2 IgM specific antibody in serum with the observations made in patients with NMDAR-AbE.[38] Flow cytometry is a particularly good tool when it comes to working with high background as it allows subtraction of MFI from eGFP positive and negative cells, correcting for any increased background and allowing false negatives to be excluded in a quantitative manner. This is an advantage over the qualitative manner of visual CBA scoring, particularly in cases of high background and poor localisation of secondary binding with the eGFP signal.

The same stable cell line expressing CASPR2-eGFP used in the multiplex flow cytometry assay was assayed in solution with patient serum from our CASPR2-antibody cohort (n=32) across a number of time points post disease onset (n=57 serum samples). A mouse anti-human AF647 IgM secondary was used at an optimised dilution of 1:200. Gating was carried out as for the multiplex flow cytometry assay and is shown in Figure 6-8. This also demonstrates a negative flow cytometry plot, a positive one and a negative with high background.

In terms of positivity, a cut-off was derived from mean plus six standard deviations of the ΔMFIs from eight healthy controls from the same assay run. Based on this, 4/32 (12.5%) of the CASPR2-antibody cohort were positive for CASPR2 IgM antibodies in their serum, significantly less than the observed frequency of NMDAR IgM antibodies in NMDAR-AbE patients (60%). Quantification of CASPR2 IgM (ABC) against time from disease onset was plotted for all positive patients (Figure 6-9-A) and showed higher levels early in disease and then a decline with some long term persistence, similar to the observations made in NMDAR-

AbE. Serum CASPR2 IgG was plotted against serum CASPR2 IgM in a single patient in whom serial serum samples containing CASPR2 IgM were available (Figure 6-9-B) and this showed CASPR2 IgG and IgM largely mirroring each other over time, as seen in patients with NMDAR-AbE. The presence of CASPR2 IgE antibodies was also assessed via a flow cytometry assay and none were found.

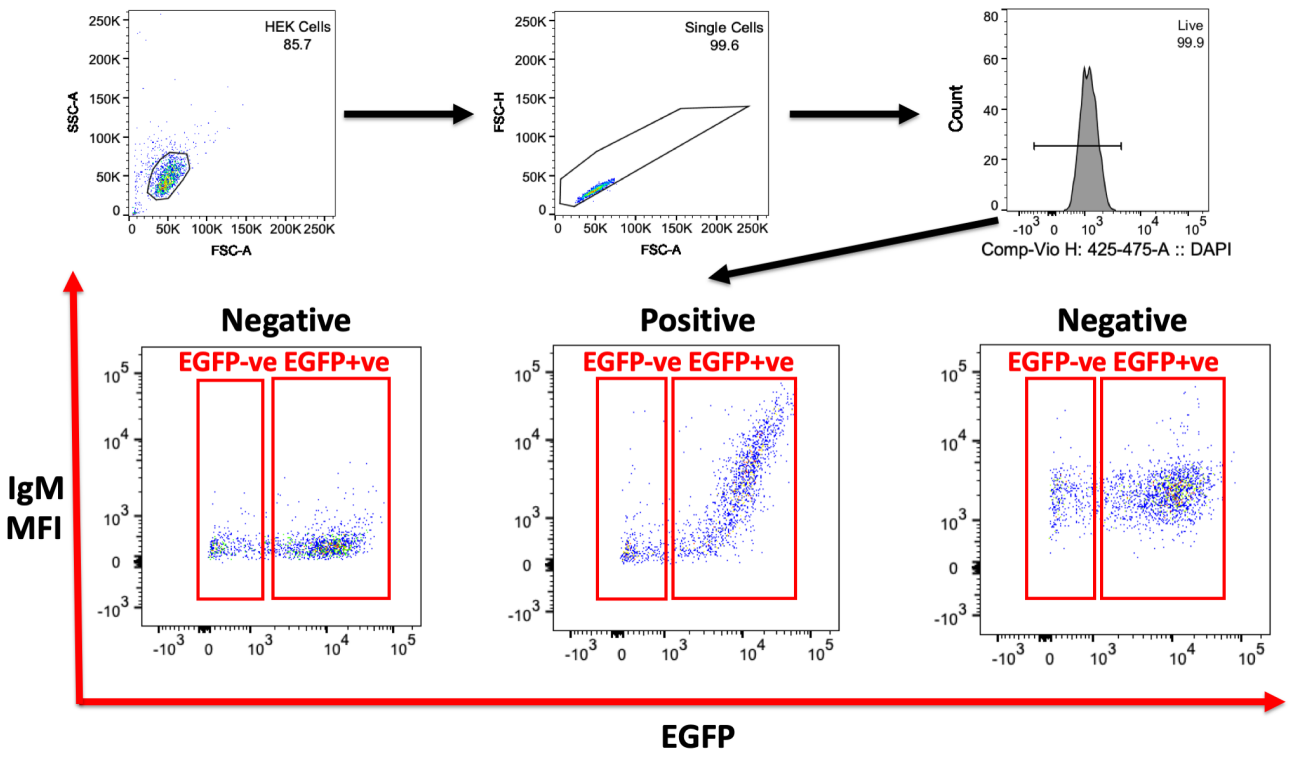


Figure 6-8 CASPR2 IgM flow cytometry assay gating and example plots

Gating strategy is the same as for as for multiplex flow cytometry assay. Three example plots are shown with eGFP on the x-axis and IgM secondary fluorescence on the y axis. From left to right they show a negative serum sample, a strong positive serum sample and a negative serum sample with a high amount of background binding (demonstrated by high IgM MFI for $eGFP^{low}$, non-CASPR2 expressing cells).

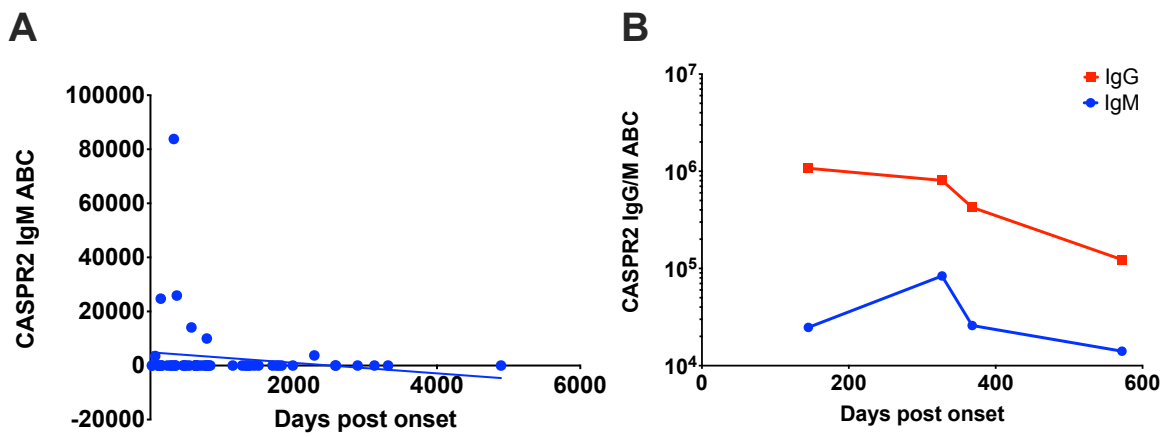


Figure 6-9 Serum CASPR2 IgM over time

(A) Plot of CASPR2-antibody patient serum samples tested for CASPR2-IgM by flow cytometry (n=57) and the time point post disease onset they are taken from. The minority of samples were positive, with 4/32 (12.5%) of patients positive. Linear regression shows a negative slope (slope -1) in CASPR2 IgM over time, with evidence of long term persistence.
(B) *Plot of CASPR2 IgG (red) and IgM (blue) in a single patient over time, this was the only patient with serially positive CASPR2 IgM antibodies and this plot demonstrates that CASPR2 IgG and IgM amounts broadly follow each other over time, with CASPR2 IgM at a lower level as expected.*

6.4 CASPR2-antibody patient PBMC matrix cultures – Total, specific IgG and clinical correlations

Having characterised the serum IgG and IgM subclasses from the CASPR2-antibody patient cohort, the next questions were whether these patients possessed circulating PBMCs which could be induced to generate specific IgG in culture, which cytokines were most stimulant for this and, if produced, what the IgG subclass characteristics of these *in vitro* antibodies were and how this related to the subclasses seen in serum.

To this end, 10 patients with CASPR2-antibodies were selected, based on availability of PBMC samples, representative disease manifestations, a range of HLA*DRB1*11:01 carrier status and immunotherapies. The characteristics of these patients and 10 age matched healthy controls (HC) are displayed in Table 6-1.

	CASPR2-Ab (n=10)	Healthy control (n=10)
Median age (range)	69.5 (27-80)	70.5 (46-81)
Male (%)	9 (90%)	8 (80%)
Clinical Syndrome (%)		
Epilepsy	1 (10%)	NA
Encephalitis	6 (60%)	NA
Morvan's	1 (10%)	NA
Isolated Neuromyotonia	2 (20%)	NA
Paraclinical details (%)		
Tumour[a]	2 (20%)	NA
Median days post onset[b]	976.5 (23-3317)	NA
Immunotherapy at time of sampling[c]	3 (30%)	NA
Median disease activity at time of sampling	1 (0-4)	NA
HLA alleles/haplotype (%)		
DRB1*11:01	5 (50%)	NK
DRB1*11:01,DQA1*05:01,DQB1*03:03	4 (40%)	NK

Table 6-1 Demographics and clinical characteristics of CASPR2-antibody patients and age matched healthy controls (HC) used in matrix cell culture experiments.

CASPR2-antibody patients were a subset of patients from the HLA study in chapter 5.
[a] tumour types were thymic cyst (n=1) and prostate cancer (n=1).
[b] Disease activity score is based on six core clinical features associated with patients with CASPR2-antibodies and neurological disease, a point is scored if any of the following were present at time of sampling: seizures, cognitive symptoms, psychiatric symptoms, peripheral nerve features, autonomic features or sleep disturbance. Maximum score of 6.
[c] Immunotherapies included steroids (n=2) and methotrexate (n=1).

PBMCs from the ten patients and ten HCs were cultured for 13 days in a combination of cytokines in a matrixed layout allowing for the combination of the eight selected cytokines with sCD40L alone or sCD40L and R848, a TLR-7 and 8 agonist which was highly stimulant for specific and total IgG production in our previous B cell culture models.[12, 38] This gave a total of 72 wells of cultured PBMCs per patient. Harvested SNs were tested for total IgG via ELISA

and specific IgG by CASPR2-antibody CBA, with CASPR2-antibody positive SNs then quantified by multiplex flow cytometry assay.

Strikingly, all patients made CASPR2-antibodies in culture detectable by CBA (median positive wells 10.5/72, range 1-35), confirming that circulating antigen specific B cells exist in sufficient numbers in these patients to create detectable amounts of specific antibody *in vitro*. The number of positive wells per patient correlated closely with patient serum titre, ($r=0.6712$, $p=0.0398$, Figure 6-10-A), with one notable outlier (highlighted in red): a patient on methotrexate and a serum titre of 1:102,400 and limited CASPR2-antibody production in culture. A trend towards a similar correlation was seen when serum CASPR2 IgG ABC was plotted against summed SN CASPR2 IgG ($r=0.6364$, $p=0.0544$, Figure 6-10-B). The lack of significant correlation is likely caused by the MTX-treated outlier and the fact that the different method of quantification enhances the difference between this patient and others. Total IgG production was stimulated most by R848, IL-2, IL-15 and IL-21 in patients and HCs. Despite being stimulated to produce comparable amounts of total IgG in culture, none of the HCs SNs tested positive for CASPR2 IgG on CBA. R848, IL-2, IL-15 and IL-21 were also the most stimulant for CASPR2 specific antibody production in the patients, with IL-21 most notable in its ability to produce large amounts of specific antibody without the proliferative aid of R848 (Figure 6-10-C).

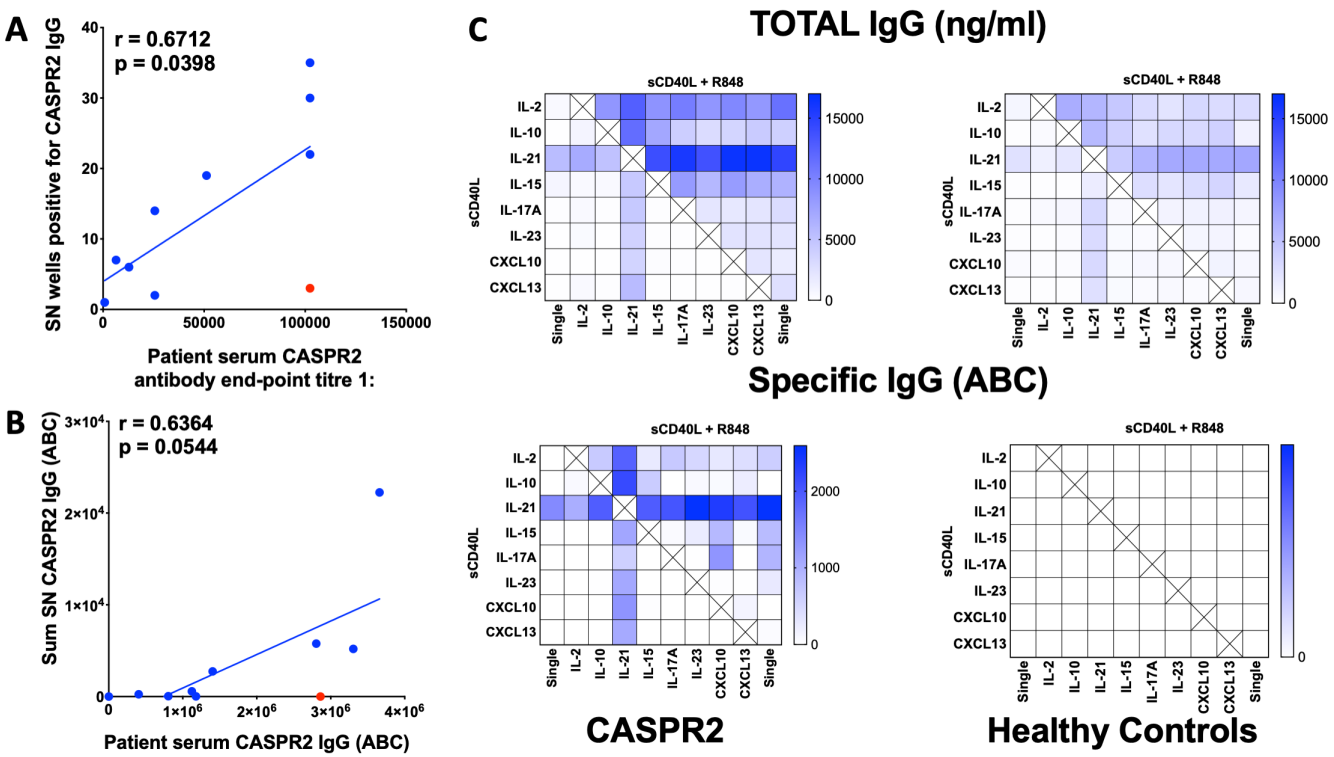


Figure 6-10 Production of CASPR2 IgG from cultured PBMCs

(A) Correlation between the number of culture wells positive for CASPR2 IgG per patients and their serum CASPR2 IgG CBA end point titre, inset text is Spearman's r with p value. Patient on MTX with high serum CASPR2-antibody titre but limited specific antibody production in culture shown in red.
(B) Correlation between summed SN CASPR2 IgG (ABC) as measured by multiplex CASPR2-antibody flow cytometry assay and serum CASPR2 IgG ABC. Correlation showed a trend towards significance. MTX-treated patient shown in red.
(C) Total IgG amounts (ng/ml) and CASPR2-antibody production (ABC) for CASPR2-antibody patients (n=10) and HCs (n=10). The heatmap shows culture layout, with combinations of eight cytokines in a matrix layout, all wells on the bottom left of the dividing line contain sCD40L in addition, all wells on the top right contain sCD40L and R848. Most stimulant cytokines were IL-2, IL-15, IL-21 and R848, none of the HCs made any specific antibody despite producing good amounts of total IgG.

The CASPR2-antibody patient treated with MTX was the only patient on a steroid-sparing agent. It was therefore theorised that, similar to the observed effect of Rituximab in AQP4-antibody positive NMOSD,[12] this drug was preventing the proliferation of B cells in culture. Increasing amounts folinic acid (FA), a known inhibitor of MTX, were added to PBMCs cultures in order to test this hypothesis. The MTX-treated CASPR2-antibody patient's PBMCs were cultured for 13 days in triplicate with a combination of sCD40L, R848 and either IL-21

alone, IL-2 and IL-21 and CXCL13 and IL-21. FA was added at a range of concentrations. A statistically significant, likely drug-toxicity induced, reduction of total IgG production of 10 mM FA versus all other conditions was observed (Kruskal-Wallis with post hoc Dunn's, Figure 6-11-A). No other statistically significant results were seen but at 100 μM of FA there was a peak in total and CASPR2-specific IgG production, giving a weak suggestion of an effect of this treatment and explaining the lack of CASPR2 IgG production observed in culture.

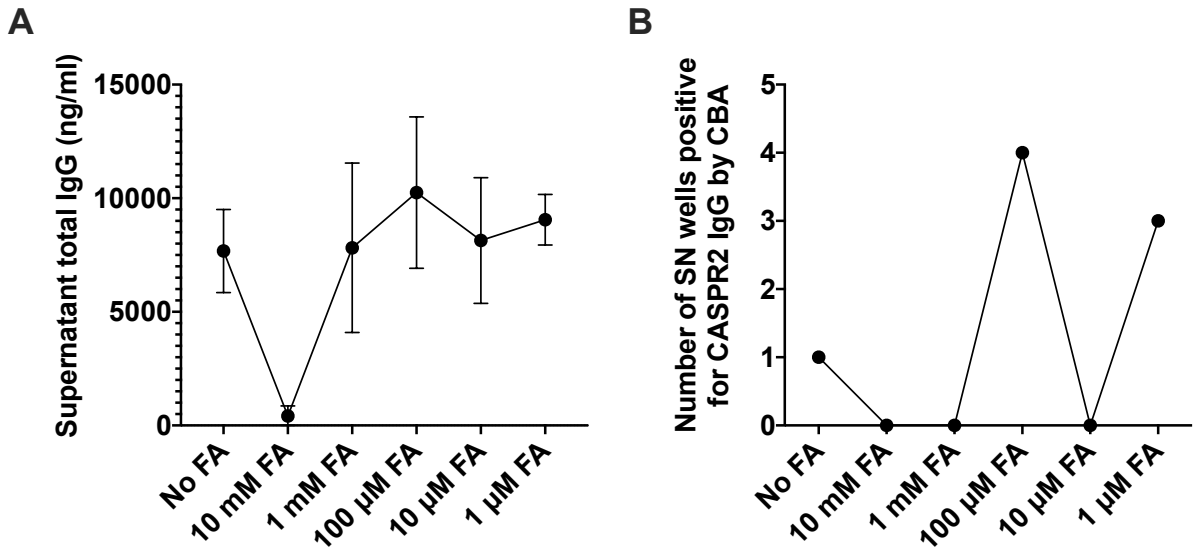


Figure 6-11 The effect of In vitro inhibition of MTX using folinic acid (FA) on the production of total IgG and CASPR2 specific IgG MTX-treated CASPR2-antibody patient's PBMCs.

(A) MTX-treated CASPR2-antibody patient PBMCs cultured with a range of cytokines and varied concentrations of FA. Measurement of SN total IgG showed significant reduction when incubated with 10 mM FA (Kruskal-Wallis with post hoc Dunns, 10 mM vs No FA p=0.0076, 10 mM vs 1 mM p=0.0458, 10 mM vs 100 μM p<0.0001, 10 mM vs 10 μM p=0.0177 and 10 mM vs 1 μM p=0.0003). No other significant differences were seen though the highest mean and (B) The highest number of positive SN wells for CASPR2 were seen at a FA concentration of 100 μM.

It was also noted that patients seemed to make more total IgG in culture than HCs, with the difference being statistically significant (p=0.0007, Mann-Whitney U, Figure 6-12-A). There was only a moderate correlation between the amount of total IgG made and CASPR2 specific antibody (r=0.463, p<0.0001, Spearman's r, Figure 6-12-B). This suggests that

stimulation of IgG production is important to the generation of CASPR2 specific antibody but that there are other factors, such as perhaps antigen specific cell frequency, which play a significant role. Finally, while the CASPR2-antibody patient SNs which produced specific antibody had significantly more total IgG compared to CASPR2-antibody patient SNs with no specific antibody and healthy control SNs (Kruskal Wallis $p<0.0001$, post-hoc Dunn's for individual comparisons), there was significant overlap between the groups (Figure 6-12-C). 25% of HC SNs produced over 3024 ng/ml of IgG, an amount at which specific antibody is made often in CASPR2-antibody patients. This suggested that enough total IgG was produced in HCs to generate specific antibody if CASPR2 antigen specific cells were present; the fact they were not is reassuring about the specificity of the technique.

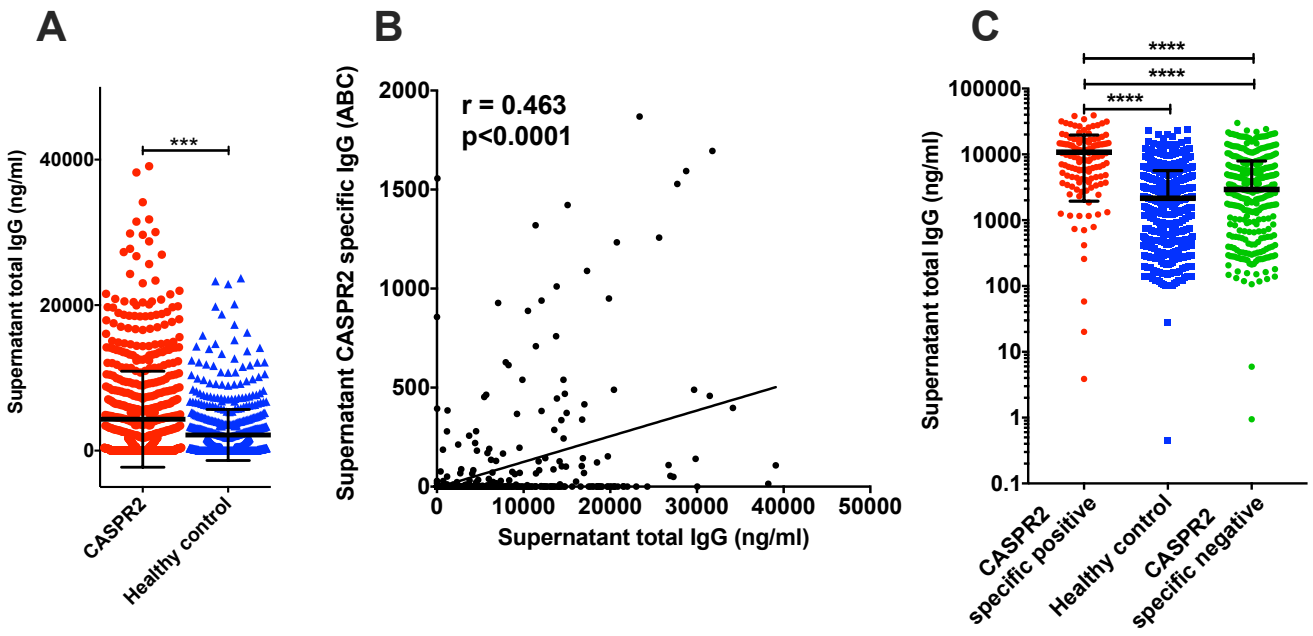


Figure 6-12 Comparison of total IgG production in culture between CASPR2-antibody patients and HCs

(A) Comparison of total IgG (ng/ml) between all wells of CASPR2 (red) and HC (blue) patients (n=720 each), CASPR2-antibody patients produced more total IgG (p=0.0007, Mann-Whitney U), line and error bars (black) represent mean with SD.
(B) Correlation between supernatant (SN) total IgG (x-axis) and SN CASPR2 specific IgG (y-axis), moderate correlation noted, Spearman's r.
*(C) Comparison of SN total IgG production between CASPR2 SNs which produced specific IgG (as measured by CASPR2-antibody CBA), HC SNs and CASPR2-antibody SN which did not produce specific IgG. Significant difference noted across all groups (p<0.0001, Kruskal Wallis) and between CASPR2-antibody producing SN and HC (p<0.0001, Kruskal Wallis with post-hoc Dunn's) and CASPR2-antibody patient SN which did not produce specific antibody (p<0.0001, Kruskal Wallis with post-hoc Dunn's). ***p<0.001, ****p<0.0001, line and error bars (black) represent mean with SD.*

The next step was to see if there were any clinical correlations with the production of CASPR2 specific antibody in culture, further to the relationship to serum CASPR2-antibody end titre. As was observed in previous studies,[12, 38] no correlation was seen between the amount of CASPR2 IgG made (sum of all CASPR2-antibody ABC) and disease activity, days post disease onset, number of immunotherapies or relapse at the time of sampling (Figure 6-13).

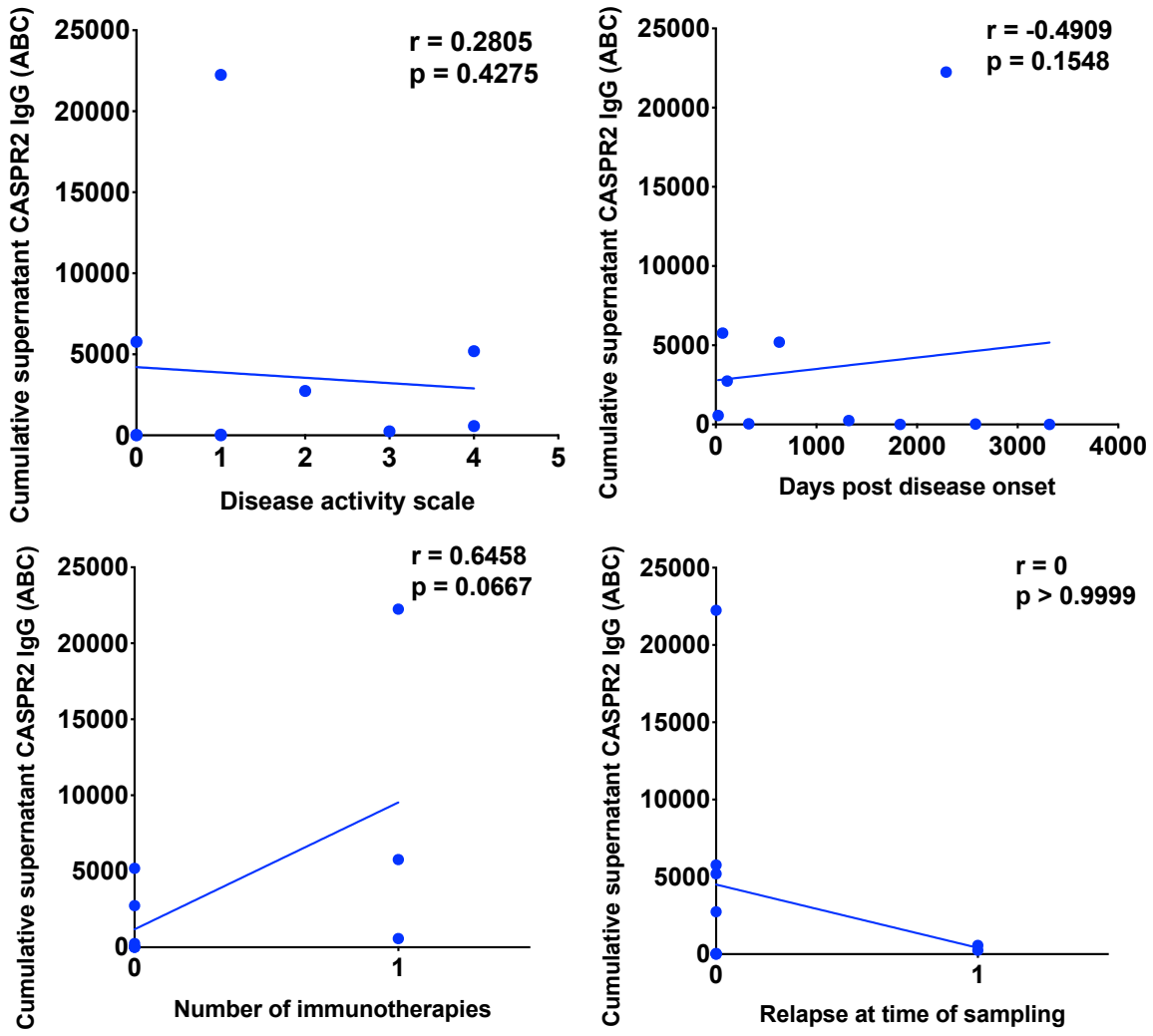


Figure 6-13 Clinical correlations of CASPR2 IgG production in vitro

Amount of CASPR2-antibody (ABC) was summed for each patient and correlated with disease activity, days post disease onset, number of immunotherapies and if the patient was relapsing at time of sampling. No correlations were identified using this method, Spearman's r.

6.5 CASPR2-antibody patient PBMC matrix cultures – IgG subclass characteristics and comparisons

Given the established relationship between patient serum CASPR2 end-titre and production of CASPR2-antibodies from circulating B cells, suggesting meaningful physiological contribution, we further hypothesised that the CASPR2 antibodies produced in culture would have IgG subclasses closely related to serum CASPR2 antibodies. From the 10 CASPR2-antibody patients used in culture experiments, CASPR2 specific IgG2 (30.4%) and IgG4 (66%)

were dominant in serum. CASPR2 IgG from culture on initial analysis appeared to have a different IgG subclass composition: IgG4 made up a greater proportion, 83.6% of CASPR2 specific IgG detected, followed by IgG1 at 15.6% and most surprisingly IgG2 at 0.7%, with expected minimal amounts of CASPR2 specific IgG3 detected (Figure 6-14-A).

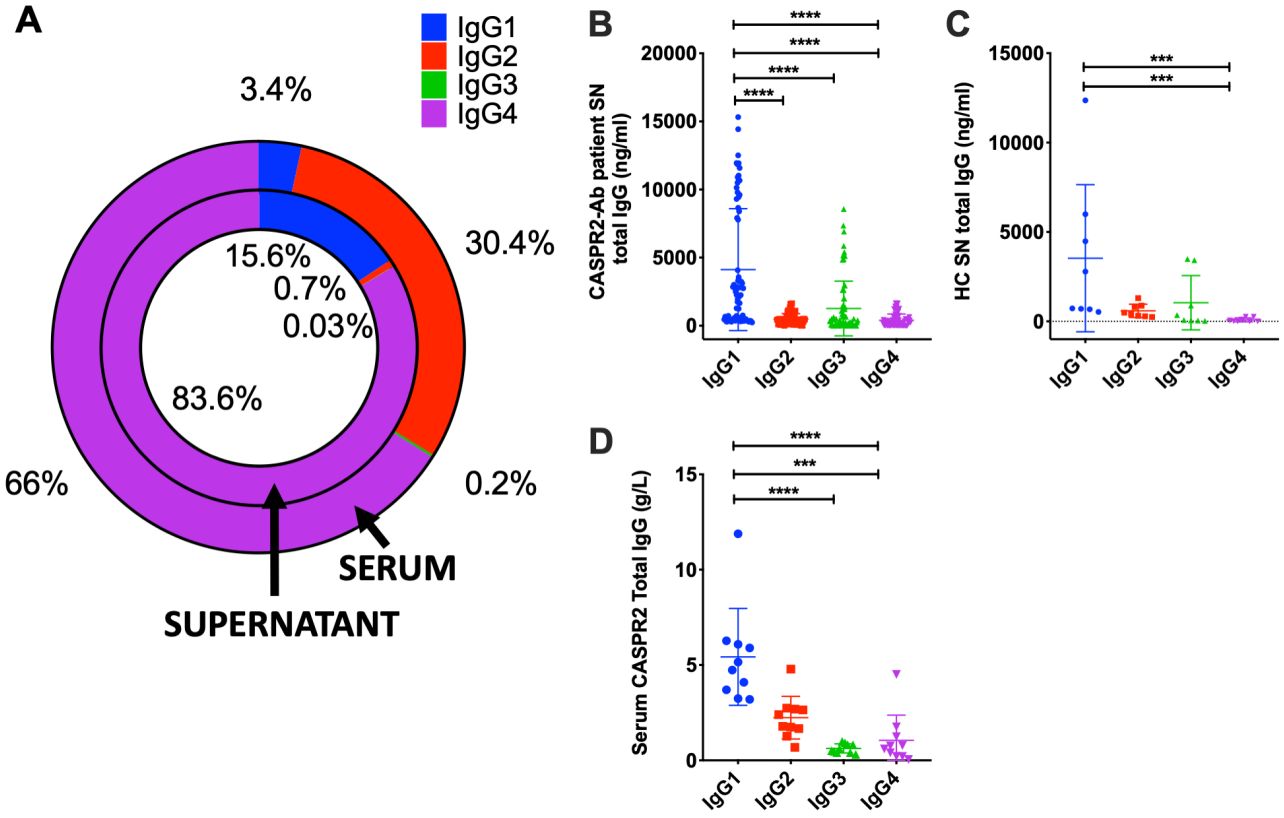


Figure 6-14 Subclass comparison between serum and supernatant produced CASPR2 specific IgG and total IgG

(A) In patients with CASPR2-antibody (n=10) sum of all CASPR2 specific IgG subclasses in ABC across all serum and all SN compared by percentage. Note the stark difference in CASPR2-specific IgG2 between the two compartments.
(B) All CASPR2-antibody patient (n=10) SNs were pooled by condition (n=72) and tested for total subclass IgG using subclass specific sandwich ELISA, output in ng/ml. As expected IgG1 was most highly produced vs all subclasses ($p<0.0001$, Kruskal-Wallis with post hoc Dunn's) but surprisingly IgG2 was underproduced.
(C) Pooled SN from HC (n=10) across single cytokine plus sCD40L and R848 conditions only (n=8 SN). Fewer wells tested for logistical reasons. Similar distribution of mean IgG subclass quantities to that seen in CASPR2-antibody patients, albeit with lower levels of IgG4 seen in HC compared to patients.
(D) CASPR2-antibody patient serum total IgG subtypes (g/L) showed the expected subclass quantity distribution and fell within normal ranges for serum, apart from an elevated IgG4 level being noted in three patients.

The minimal amounts of CASPR2 specific IgG2 detected was a surprising result. In order to understand this further, the IgG subclass composition of total IgG was measured in the pooled SNs from the 10 CASPR2-antibody patients, across 72 conditions, using an IgG subclass ELISA (Figure 6-14-B). In terms of total IgG detected in culture, these results showed an excellent relationship to the results for the same SNs obtained via a pan-IgG ELISA ($r = 0.9632$, $p<0.0001$, Spearman's, mean CoV 34.1%). As expected, IgG1 was the predominant subclass of total IgG detected and was produced at significantly higher levels than other IgG subclasses ($p<0.0001$, IgG1 vs IgG2/3/4, Kruskal Wallis with post-hoc Dunn's). Total IgG2 was lower than expected, with mean IgG1 being 2259 ng/ml (SD, 4479 ng/ml), mean IgG2 480 ng/ml (SD 411 ng/ml), mean IgG3 1263 ng/ml (SD 2005 ng/ml) and mean IgG4 392.9 ng/ml (SD 474.1 ng/ml). A similar pattern was seen in a sample of 8 HC sups (Figure 6-14-C), selected to represent PBMCs stimulated with sCD40L, R848 and the full range of eight utilised cytokines. In these mean IgG1 was 3531 ng/ml (SD 4116 ng/ml), mean IgG2 588 ng/ml (SD 372 ng/ml), mean IgG3 1043 ng/ml (SD 1516 ng/ml) and mean IgG4 85.5 ng/ml (SD 110.3ng/ml). All standards on the kit worked well and from measured patient serum (Figure 6-14-D) IgG1-4 amounts followed predicted patterns, with no issue detecting IgG2, suggesting this was a genuine result of the culture method.

Given that it had been established that our culture system as a whole was producing less than expected IgG2, the next question was how individual cytokines were affecting total IgG subclass production. To this end, a ratio was generated of IgG2 production divided by IgG1, IgG3 and IgG4 and then plotted across all 72 cytokine conditions based on the pooled SNs from the 10 CASPR2-antibody patients (Figure 6-15). This demonstrated the ratio of IgG2 to all subclasses is maximally skewed away from IgG2 production by cytokines which are most stimulant for both total and specific IgG (IL-2, IL-15, IL-21 and R848). This may explain why an

under-representation of CASPR2 specific IgG was seen in our system, requiring the data to be presented with this correction in mind.

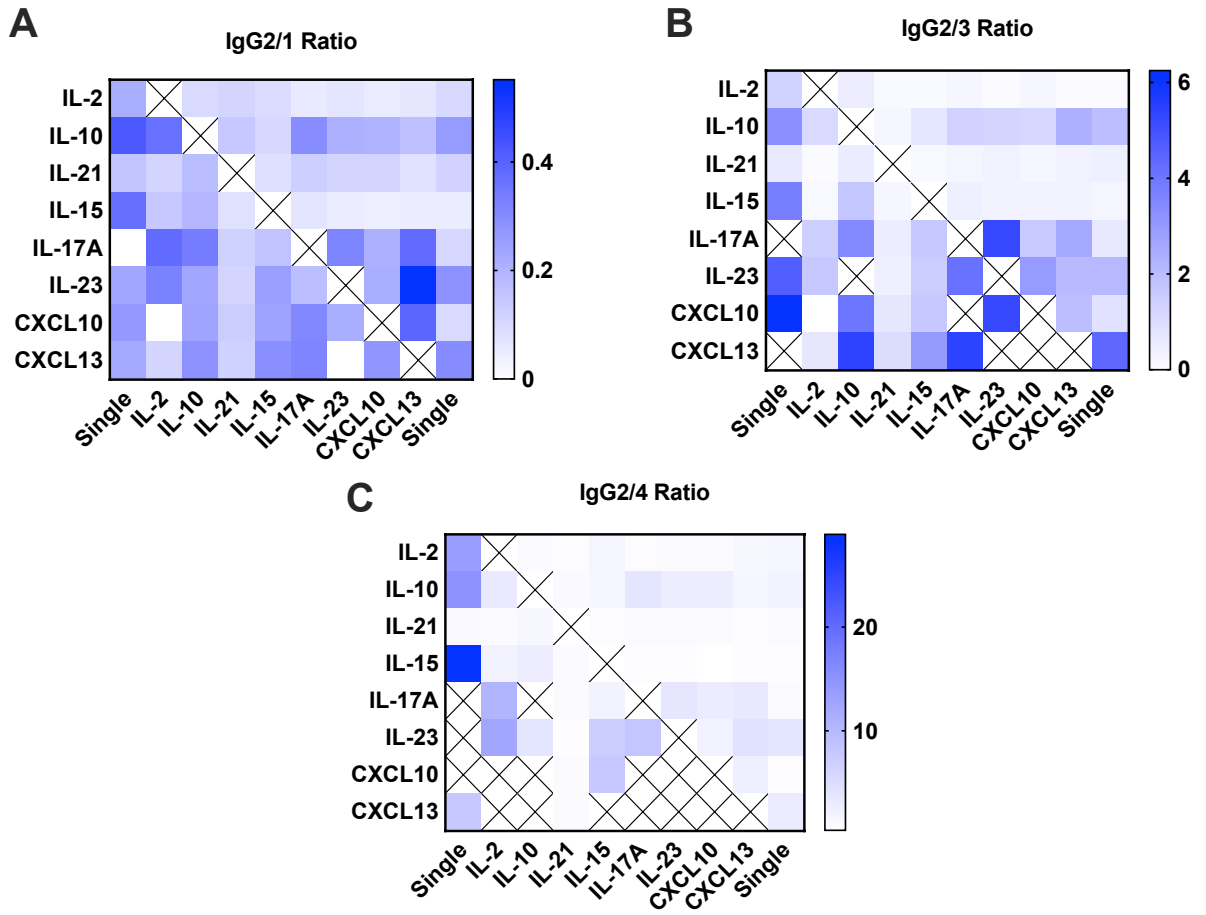


Figure 6-15 Total IgG subclass ratio across different stimulating cytokine conditions

(A) Total IgG2 was divided, across the 72 conditions by IgG1 to give a ratio of IgG2/IgG1, as well as IgG2/IgG3 (B) and IgG2/IgG4 (C). As IgG2 is the numerator and the colour scale is more blue with an increase in the ratio, therefore the more white a cell is, the more skewed away from IgG2 the ratio is. It is clear that in conditions which produced most specific and total IgG (R848, IL-2, IL-15 and IL-21) there is consistent skewing away from IgG2 in all subclasses (more white), perhaps explaining the underrepresentation of IgG2 in our system.

At this point, the question arose as to what the source of the skew away from IgG antibody production was. Several possibilities existed. First, it could be that there are less IgG2 circulating B cells in the PBMCs isolated. Second, IgG2 B cells could be out-competed by other subclass specific B cells. Third, cytokines were preferentially driving class switch away

from IgG2 *in vitro* and finally, it could be that IgG2 B cells simply do not proliferate and produce IgG as effectively as other subclass B cells in this culture method. In light of these questions, PBMCs from two HC were sorted on B cell markers and then by IgG subclass. 5,000 subclass specific B cells were then seeded on top of autologous, B cell depleted PBMCs and stimulated in triplicate (where sorted cell numbers allowed) in either R848, sCD40L and IL-21 or R848, sCD40L and IL-10 for 13 days. IL-10 and IL-21 were selected because IL-21 induces class switch to IgG1 and IgG3 subclasses[220] whereas IL-10 is thought to augment IgG4 production.[221] After 13 days, cells were discarded and SN was kept and tested for total IgG subclass.

Across both patients, subclass frequency of B cells in PBMCs was as expected: IgG1 class switched B cells were most common, followed in order by IgG2, IgG3 and IgG4 B cells. In humans, class switching of IgG subtypes occurs by excision of constant region DNA which is organised in the following way: IgG3, IgG1, IgG2 and IgG4. As can be seen in Figure 6-16, the subclass upon which the B cell was sorted was the predominant IgG subclass detected in SN from those cultures, suggesting limited class switching occurred in our cultures. Across all subclasses, the wells from PBMCs stimulated with IL-21 produced the most IgG, including IgG4, with IL-10 exhibiting no preferential secretion of IgG4. This suggested minimal cytokine-induced class switching. Finally, for each subclass sorted population it can be seen that different mean amounts of 'dominant' antibody are produced (i.e. how much IgG1 was produced by IgG1 sorted B cells etc), with IgG2 and IgG4 B cells producing least IgG (IgG1 – 82086 ng/ml, IgG2-43156 ng/ml, IgG3-96583 ng/ml and IgG4-48425ng/ml). As these different subclass specific B cells are cultured separately from each other, the difference seen is not due to competition between them. At this point, three out of four of our initial suppositions to explain this observation have been ruled out: namely lower numbers of IgG2 B cells,

competition between B cell subclasses and cytokine-induced class switching. This could, therefore, either be due to an intrinsic property of these B cells or due to the way they interact and receive help from other lymphocytes in our culture system. These data provide some explanation as to why IgG2 seems to be under-represented in our culture system and allowed for confidence in applying a correction based on IgG2-under representations for the purpose of comparison to serum subclasses.

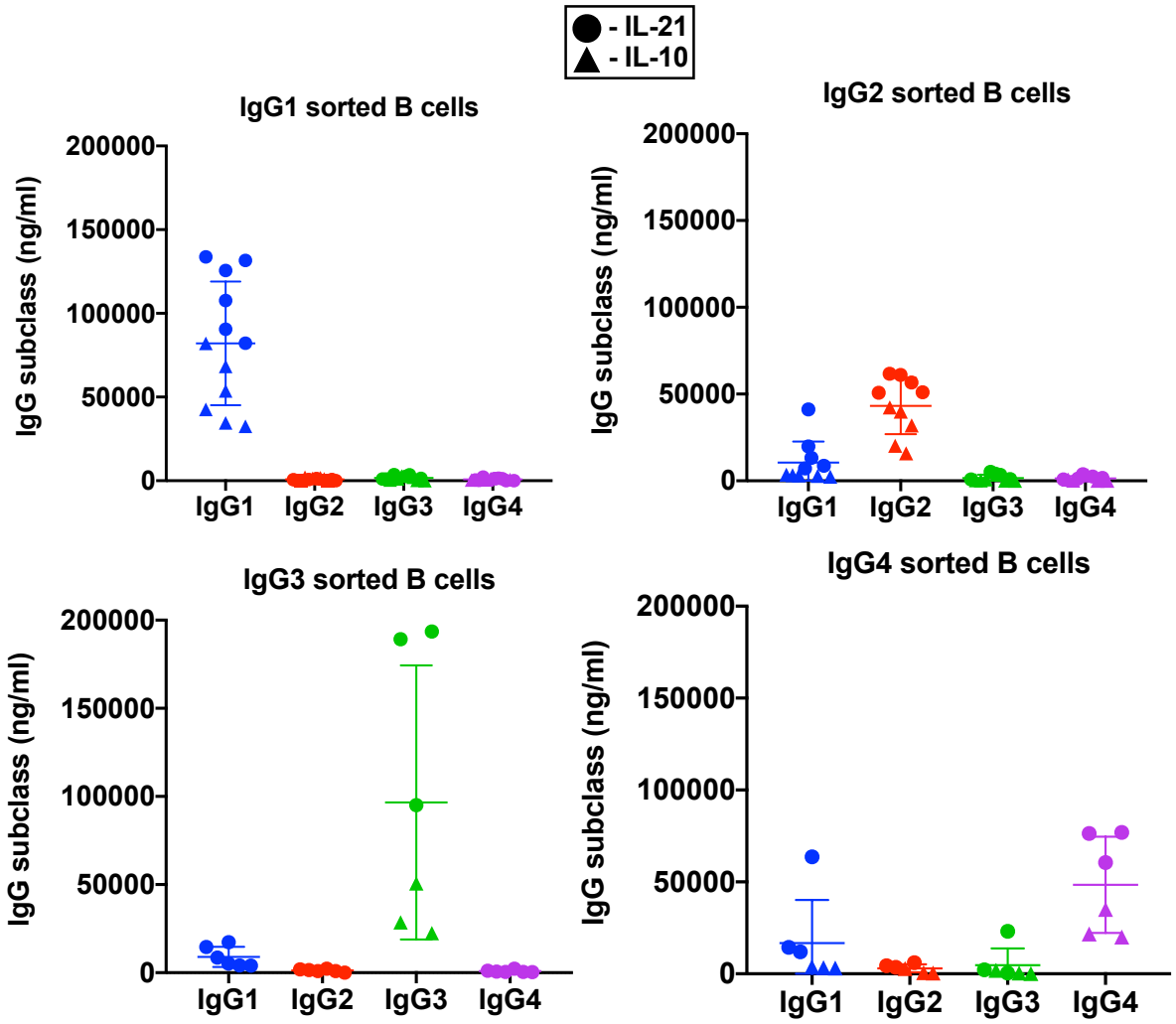


Figure 6-16 Total IgG subclass production from subclass sorted B cells

PBMCs from HC (n=2) were FACS sorted into B cells expressing IgG1-4, then recombined with autologous B cell depleted PBMCs and cultured for 13 days in R848, sCD40L and either IL-10 (triangle) or IL-21 (circle). After 13 days, culture SN were tested for total IgG subclasses on ELISA. Each graph represents the IgG1-4 quantity in ng/ml for each batch of IgG subclass sorted B cells.

As it had been established that the PBMC culture method utilised was skewing away from total IgG2, in order to make a meaningful comparison between serum and SN CASPR2 IgG subclasses, a correction was applied. Each positive well yielding a CASPR2 specific IgG subclass result was divided by its individual total IgG subclass from the same well (Figure 6-17-A) to yield a corrected ratio. This allowed for detection of CASPR2 specific IgG, with a correction made for the demonstrated effect of the culture system on subclass production. With this correction applied, it could be seen that CASPR2 IgG found in serum was mirrored by subclass representation in SN in patients (Figure 6-17-B). As displayed in Figure 6-14-D, 3/10 (30%) CASPR2-antibody patients had total IgG4 levels outwith normal limits. This suggests perhaps an increased propensity to class switch to IgG4 subclasses. However, given this only seen in the minority of patients and the amounts of total IgG1 are considerably higher in all, this doesn't explain the huge predominance of IgG4 CASPR2-specific antibodies on its own.

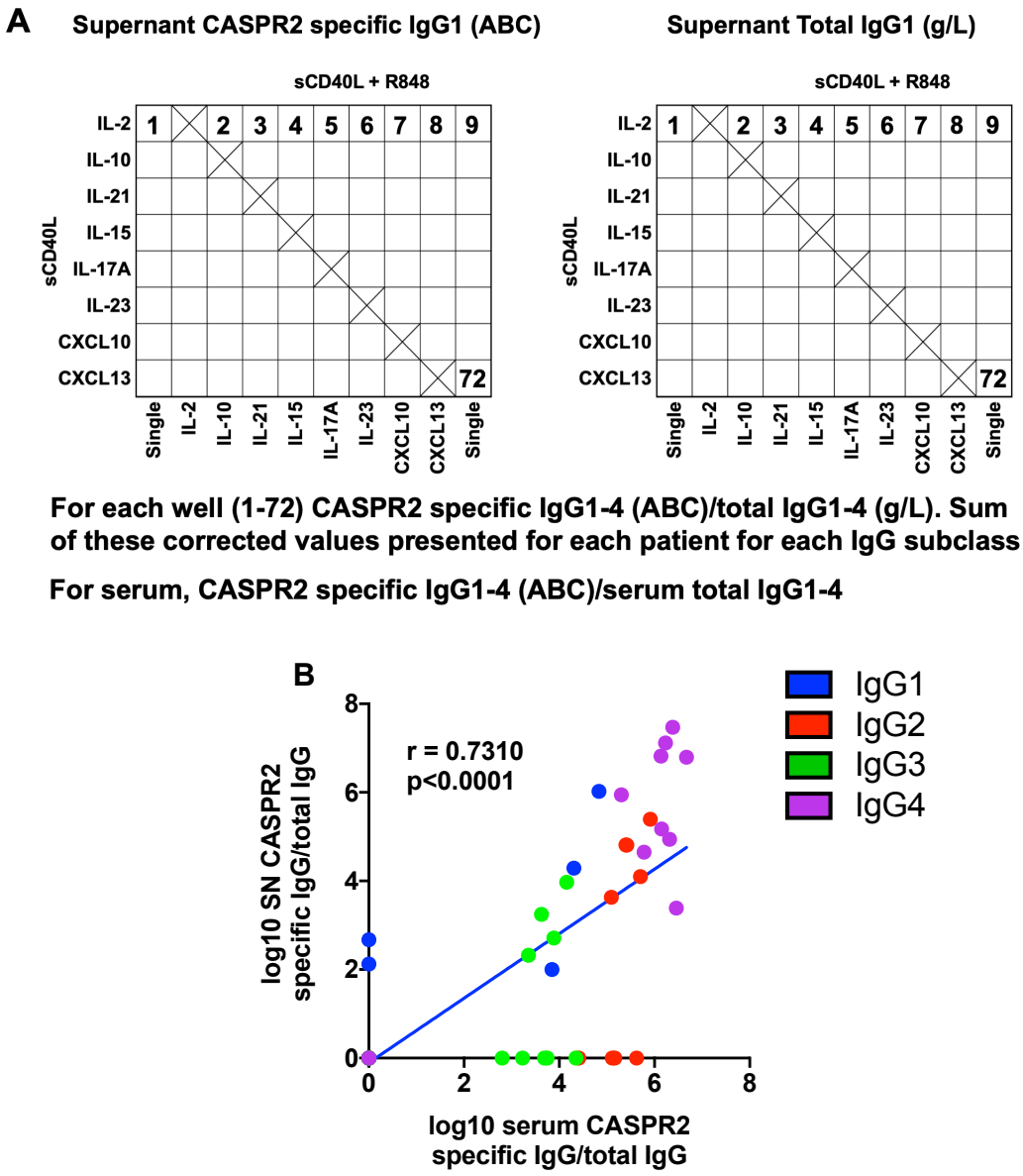


Figure 6-17 CASPR2 IgG subclass comparison between serum and SN, corrected for total subclass IgG

(A) From CASPR2-antibody patient PBMCs cultured (n=10), amount of CASPR2 IgG for each subclass detected in serum and SN was corrected for total subclass IgG. Serum specific/total IgG was derived by dividing CASPR2 specific IgG1-4 amount (ABC) by IgG total subclass amounts (g/L) for IgG1-4. SN specific/total IgG ratio was calculated by dividing SN specific IgG1-4 (ABC) for each of the 72 conditions by the results of the total IgG subtyping ELISA from the pooled SN of all ten patients across 72 conditions (g/L),
(B) These ratios from the patients (n=10, four subclasses) were then compared in serum (x-axis) to SN (y-axis) as log10 of their value as IgG4 was so predominant. The correlation between these two was excellent (Spearman's r=0.7310, p<0.0001 [95%CI 0.5364-0.8518]) The key conclusion is that CASPR2 specific antibody subclasses present in serum are represented in a significantly proportional way by the subclasses produced by cultured PBMCs. There are outliers, including the patient on MTX who produced very little CASPR2 specific antibody in culture, but on the whole, this representation appears matched.

6.6 CASPR2-antibody patient PBMC matrix cultures - Serial cultures

By this point, it had been established that PBMCs from CASPR2-antibody patients produce CASPR2 specific IgG in amounts that correlated with serum titre and appeared representative in terms of IgG subclass. With some notable exceptions, patient serum NSAb-titres fall with treatment and can increase with relapse. Given the relationship between serum titre and CASPR2 antibody production in cultured PBMCs it was hypothesised that this relationship would hold true longitudinally, with CASPR2-antibody production from cultured PBMCs falling with treatment and increasing in relapse. As an additional measure, serum CXCL13, a reported marker of germinal centre activity, was assayed[222] to see how this related to ongoing capacity to produce specific antibody. Four out of ten patients were selected, on whom serial PBMC samples were available; three who had a relapse and one who was immunotherapy naïve. Results are presented in Figure 6-18.

The first observation was that in all treated patients, the amount of CASPR2 IgG in serum, as well as produced by cultured PBMCs (measured by both number of wells positive for CASPR2 IgG as well as total CASPR2 IgG ABC) decreased rapidly, suggesting an effect of immunotherapy not observed in cross-sectional analyses. By comparison, in the untreated patient, there was a very gradual fall in serum and SN CASPR2 IgG. The next observation was that in the three patients with samples around the time of relapses, two (patient one and three) had an increase in serum CASPR2-antibody level without a corresponding increase in the amount of CASPR2 specific IgG produced from culture. Patient two had a relapse without a rise in either serum or SN CASPR2 specific IgG and was treated based on symptoms with PLEX, to good effect. A final thing to note was in patient one, serum CASPR2 specific (ABC) at onset was 1.4×10^7 which plateaued with treatment at 1.8×10^6. However, over a year, serum

CASPR2-antibodies increased progressively, and without symptoms, back up to 9.7×10^6 in the final sample taken before his relapse.

Subclasses over time appeared relatively stable in serum and SN, with one marked exception. In patient one, there was a trough in the amount of CASPR2 specific IgG in serum just after day 200, then there was a gradual but consistent increase prior to relapse. During this increase in CASPR2 specific IgG, the IgG1 subclass of CASPR2 antibodies were a larger proportion of the total CASPR2 IgG pool than during illness presentation, something mirrored by the subclasses detected in SN.

Serum CXCL13 levels did not show a consistent relationship to either serum CASPR2 specific IgG levels or production of CASPR2 IgG in culture. In patient one they followed the trajectory of the decrease in capacity to produce CASPR2 specific IgG in culture over time and did not rebound with increased serum CASPR2 specific IgG prior to relapse. In patient two, CXCL13 levels were inverse to the amount of CASPR2 specific IgG in serum and SN and in patients three and four, levels are consistently below the cut-off for positivity, despite significant ongoing amounts of CASPR2 specific IgG in serum and cultured PBMCs. CASPR2 IgM was only detectable in one patient (patient 3) at presentation and then became undetectable, with no rise associated with relapse. The disconnection between CXCL13 activity and CASPR2 specific IgG production in serum and SN, coupled with the isolated increase in serum CASPR2 specific IgG without corresponding increase in SN production of CASPR2 specific IgG in relapse, as well as the CASPR2 IgM data, yield little support for the idea of ongoing germinal centre reactions contributing to production CASPR2 antibodies in these patients, in contrast to patients with NMDAR-AbE.[38]

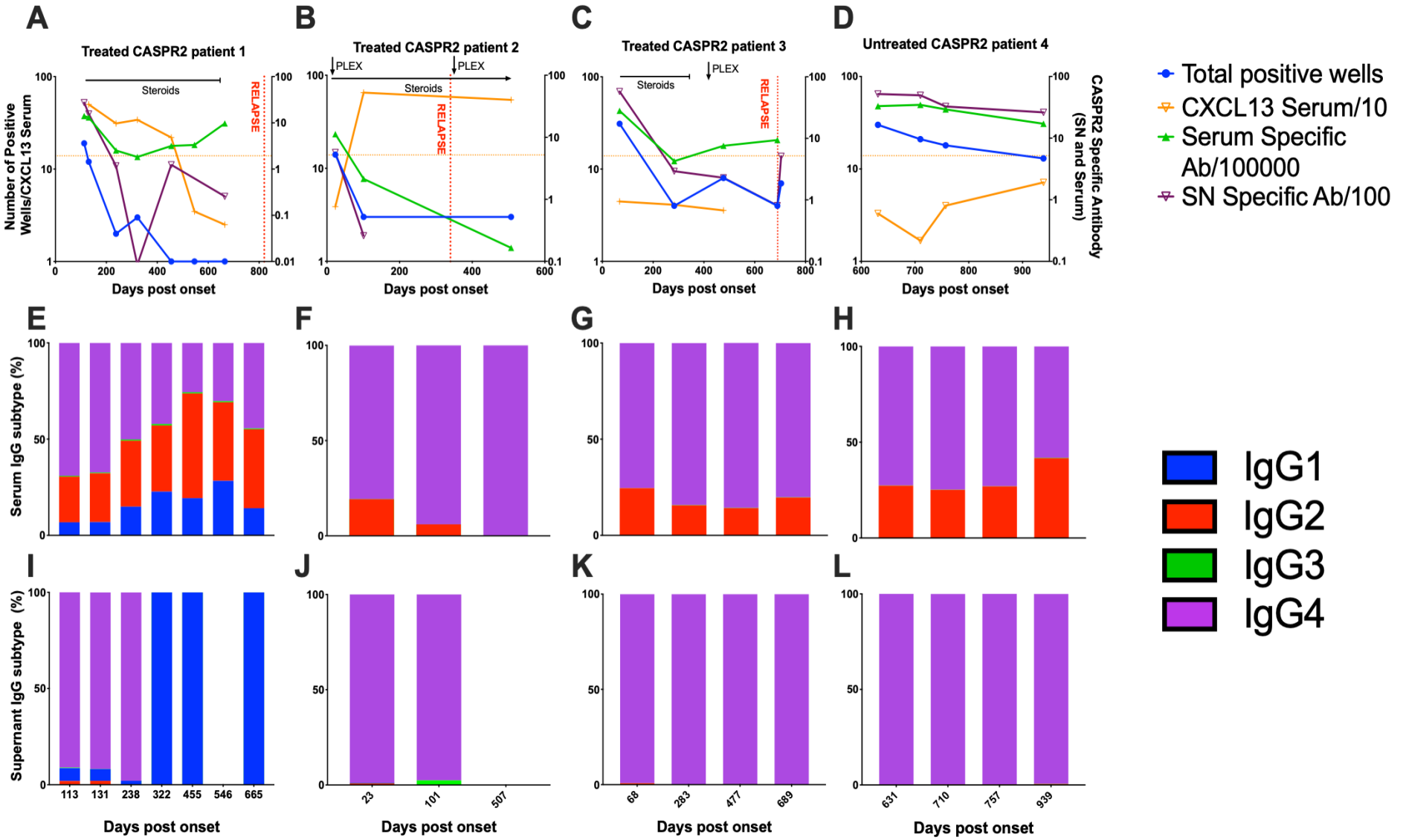

A
Treated CASPR2 patient 1
Steroids
RELAPSE
Number of Positive Wells/CXCL13 Serum
Days post onset
B
Treated CASPR2 patient 2
PLEX
PLEX
Steroids
RELAPSE
Days post onset
C
Treated CASPR2 patient 3
PLEX
Steroids
RELAPSE
Days post onset
D
Untreated CASPR2 patient 4
CASPR2 Specific Antibody (SN and Serum)
Days post onset
Total positive wells
CXCL13 Serum/10
Serum Specific Ab/100000
SN Specific Ab/100
E
F
G
H
Serum IgG subtype (%)
I
J
K
L
Supernant IgG subtype (%)
113 131 238 322 455 546 665
23 101 507
68 283 477 689
631 710 757 939
Days post onset
IgG1
IgG2
IgG3
IgG4

Figure 6-18 Serial PBMC matrix cultures from CASPR2-antibody patients (n=4)

(A-D) on left Y axis is number of positive wells (blue) and CXCL13 (pg/ml)/10 in corresponding serum sample (orange – with dotted line for positivity cut-off based on mean + 3SD 20 HC serum plotted), on the right Y axis is CASPR2 specific IgG ABC/100000 for serum (green) and ABC/100 SN (purple). Steroid treatment is denoted by a black line, where there is an arrow at the end, steroids were ongoing, where there is a line they were stopped. Plasma exchange (PLEX) is denoted by an arrow pointing downwards. Notable trends are the precipitous fall in both serum and SN antibody in immunotherapy treated patients versus the untreated patient and the disconnection between specific antibody production and serum CXCL13 levels. Serum and SN CASPR2 specific IgG subclasses proportions are also charted over time (E-L), with proportions relatively stable in (G, H, K and L), a fall in IgG2 in line with an overall fall in CASPR2 specific IgG amount in (F) and in (E) a gradual increase in all CASPR2 specific IgG over time which is initially more IgG1 than presenting IgG subclass proportions, something that is reflected in the CASPR2 specific IgG subclasses detected in contemporaneous SN.

6.7 CASPR2-antibody patient PBMC matrix cultures - Epitope specificities and effect of HLA allele expression

As it had been demonstrated that patients with CASPR2-serum antibodies possess circulating PBMCs capable of making CASPR2 specific IgG in culture with a similar subclass composition between serum and SN CASPR2 antibodies, the next hypothesis was that CASPR2-antibody epitope specificities would also be reflected in SN CASPR2 antibodies. Up to this point, a full length (FL) CASPR2-eGFP construct had been utilised in flow cytometry assays. In order to assess epitope reactivities, two truncated CASPR2 constructs were used, one expressing predominantly the N-terminal domain of CASPR2 (NTD) and one expressing the C-terminal domain (CTD) (Figure 6-19). These constructs were designed to separate out epitopes based on the previously described preference for N-terminal epitopes in patients with CASPR2-antibodies and were obtained via collaboration with Professor David Bennett, from Oxford University.[112]

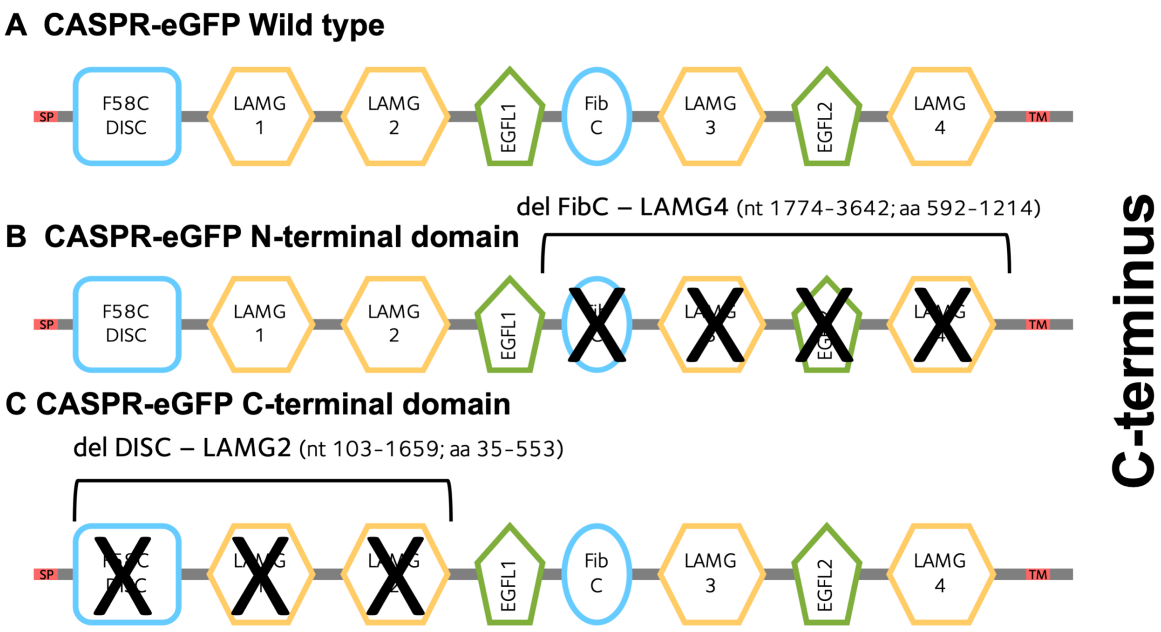


Figure 6-19 CASPR2 N-terminal domain and C-terminal domain mutant constructs

(A) Full length CASPR2 construct showing major domains as defined by consensus description of domains by homology to protein domains (http://www.uniprot.org/uniprot/Q9UHC6#section_seq).
(B) N-terminal domain only construct (NTD) with fibrinogen-like domain C (Fib C) to laminin-G 4 (LAMG 4) domain removed (nucleotides 1774-3642 deleted, amino acids 593-1214 deleted)
(C) C-terminal-domain only construct (CTD) with discoidin domain (F58C DISC) to laminin-G domain 2 removed (LAMG 2). Constructs were expressed in the same plasmids with same promoters and antibiotic resistances.

The multiplex flow cytometry assay was utilised with transfected HEK cells expressing either NTD or CTD CASPR2. Cell number and serum titrations were optimised and found to be the same as when using the CASPR2-eGFP FL stable cell line. Serum from the CASPR2-antibody patients used in the PBMC culture experiments was then tested and it was confirmed that the NTD was the preferred epitope, with 9/10 (90%) patients binding this construct (the same as with CASPR2-eGFP FL stable cell line), compared to 6/10 (60%) binding the CTD construct and with markedly higher ABCs seen when detecting CASPR2-antibodies to the NTD compared to the CTD (Figure 6-20-A).

The amount of either CTD or NTD specific CASPR2 specific IgG was then compared between the serum and SN of patients. For serum quantification multiplex flow cytometry

assay was used but for SNs only enough volume remained to carry out CBA, therefore number of wells positive for either CASPR2 antibodies per patient for either construct was determined (Figure 6-20-B). As can be seen, CASPR2 IgG CTD antibodies were only made in patients with CASPR2 IgG CTD antibodies in serum, and all but two patients made NTD antibodies, a good representation of epitope specificities between serum and SN. As patient CASPR2-antibody end-titre falls and, consequentially, amount of CASPR2 IgG made in culture falls, representation of epitope specificities is less complete. The fourth patient down was on MTX and generated only minimal amounts of SN CASPR2 specific IgG.

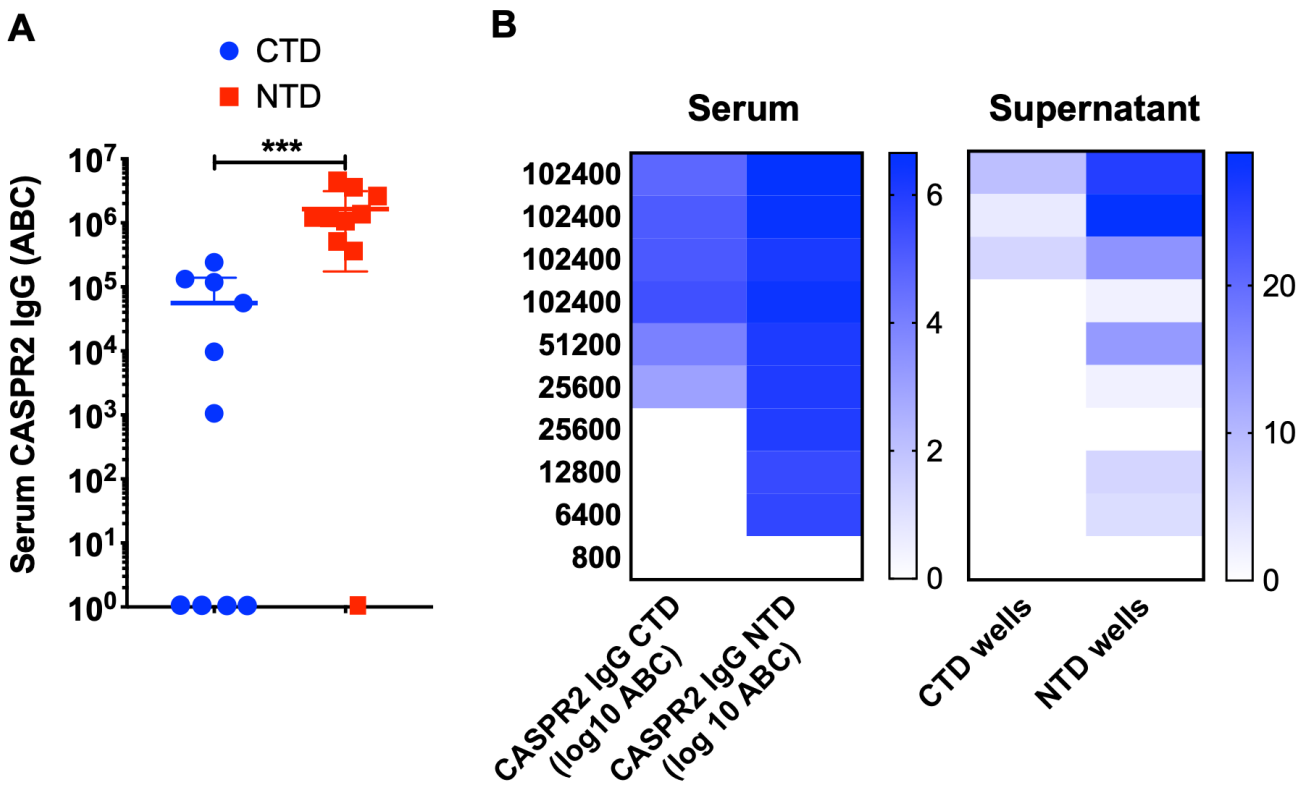


Figure 6-20 CASPR2 IgG N-terminal domain and C-terminal domain reactivity in serum and SN

A) Serum from CASPR2-antibody patients used in matrix culture experiments (n=10) tested on flow cytometry assay for CASPR2 CTD and NTD, antibodies, log10 scale. Significantly more CASPR2-antibodies to NTD identified than to CTD (p=0.0007, Mann-Whitney U), line and error bars represent mean and SD.
B) ABC values from same patients represented in a heatmap (log10 ABC) and ordered by serum FL CASPR2-antibody titre (1:x), compared to number of SN wells positive for CASPR2 CTD/NTD

antibodies (0-30). This shows proportional representation of epitopes from serum in SN, this relationship becomes less strong when titre falls as cultures produce less CASPR2 IgG.

Given the seemingly similar representation of serum CASPR2 IgG epitopes in SN, this relationship was next examined longitudinally in serially cultured patients. This demonstrated a close relationship between amounts of CTD and NTD antibodies in serum and SN (Figure 6-21-A). Of note, there was no skewing over time to either NTD or CTD epitopes. Finally, to confirm representation of serum specificities in SN, all samples, including serial samples were assessed for the correlation between serum CASPR2 IgG CTD/NTD ABC and the number of wells positive for CTD/NTD; there were good correlations with both, confirming the association between the two parameters (Figure 6-21-B).

It was noted that HLA subclass (blue dots on scatter plot) appeared to affect the amount of CASPR2 specific IgG produced in both serum and culture to both epitopes. This is an especially stark finding with reference to the CASPR2 CTD antibodies in culture and SN, with no patients without HLA DRB1*11:01 making antibody to the CTD in culture. This was therefore explored further in the next set of experiments.

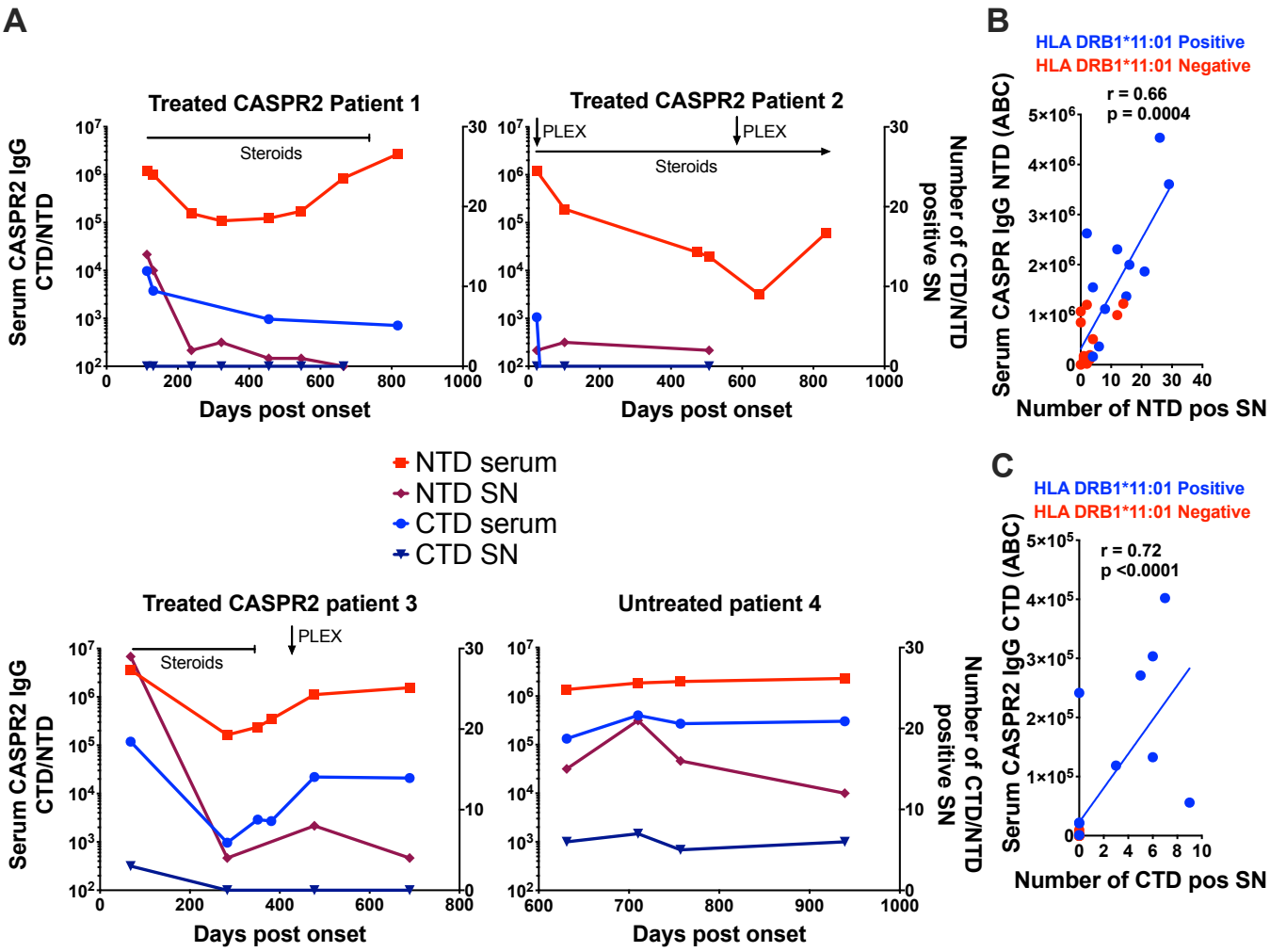


Figure 6-21 Relationship between CASPR2 IgG epitopes over time in individuals

(A) The four patients cultured serially previously had their serum CASPR2 specific IgG to NTD/CTD CASPR2 measured by flow cytometry (ABC – NTD in red, CTD in blue) and compared to number of wells positive for NTD (maroon) and CTD (dark blue) measured by CBA. A relationship between serum and SN epitopes was noted.
*(B) Correlation between serum CASPR2 IgG for NTD (ABC) and number of wells positive for NTD antibodies, a correlation was noted (Spearman's r), the same analysis for CASPR2 CTD antibodies was carried out with a similar good correlation seen (C). In both, it was observed that if patients were divided by whether they carried HLA DRB1*11:01, patients with the CASPR2-antibody patient associated HLA produced more CASPR2 specific IgG in culture, this was especially true in CASPR2 CTD antibodies, where only patients with DRB1*11:01 produced CASPR2 CTD antibodies in culture.*

6.8 CASPR2-antibody patient serum epitope quantification in the context of HLA allele expression

In chapter five it was observed that possession of the HLA*DRB1*11:01 CASPR2-antibody patient associated risk allele gave higher amounts of CASPR2-antibody in serum on CBA and FIPA, with a suggestion of a clinical effect. Testing for a similar effect was performed on the patients cultured as part of the matrix experiments, with serum CASPR2-antibody measured by multiplex flow cytometry on FL CASPR2, NTD CASPR2 and CTD CASPR2 (Figure 6-22). No clear significant difference was observed in this limited cohort though a trend towards significance was noted in all comparisons (Mann-Whitney U, FL p=0.0952, NTD p=0.0952 and CTD p=0.0635). To see if this was a function of sample size, the same question was asked in the full cohort of 32 patients.

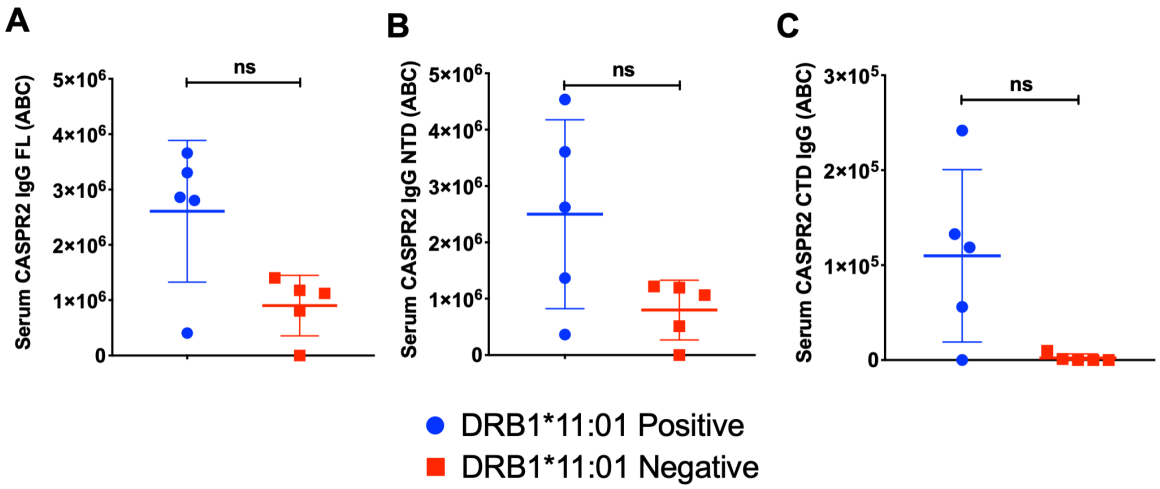


*Figure 6-22 HLA DRB1*11:01 associations and amounts of CASPR2-antibody in serum measured by multiplex flow cytometry assay.*

*In the CASPR2-antibody patients used in the matrix cell culture experiments (n=10), using CASPR2-antibody flow cytometry assay, to test for significant difference between HLA DRB1*11:01 carriers and non-carriers in serum antibodies to FL CASPR2 (A), NTD CASPR2 (B) and CTD CASPR2 (C). None noted. Mann-Whitney U. Line and error bars represent mean and SD.*

In this larger cohort, there were significantly more CASPR2-antibodies in HLA-DRB1*11:01 patients against all CASPR2 constructs; FL (p=0.0003), NTD (p=0.0011) and CTD (p<0.0001, Mann-Whitney U). The difference appeared to be most pronounced in the case of CTD antibodies (Figure 6-23-C). The correlations between FL-CASPR2 antibody ABC in serum to NTD/CTD CASPR2-antibody were plotted and separated by HLA risk allele expression (Figure 6-23-D-E). This showed no difference in slope between HLA-DRB1*11:01 positive and negative patients (p=0.1450) nor in the correlation between FL and NTD, with a good correlation seen in both instances (r=0.8409, p<0.0001 and r=0.9798, p<0.0001). However, the slope between CASPR2 CTD and FL antibodies in DRB1*11:01 carriers was more positive than in non-carriers (0.0742 [95% CI 0.0377-0.1107] versus 0.002 [95% CI -0.0011 to 0.0051]), a highly significant difference (p=0.0004), with both still correlating (r=0.5358, p=0.0016 and r=0.5606, p=0.0002 respectively). Put another way, in the absence of DRB1*11:01, despite patients having titres to FL CASPR2 as high as patients with DRB1*11:01, they made considerably less antibody to CTD CASPR2. This significant difference suggests that having the HLA DRB1*11:01 allele gave patients an increased ability to make antibodies to the CTD of CASPR2. This adds to the earlier finding that HLA DRB1*11:01 associates with higher levels of serum CASPR2 antibody, by demonstrating that it also confers a broader epitope repertoire, suggesting significant immunological relevance.

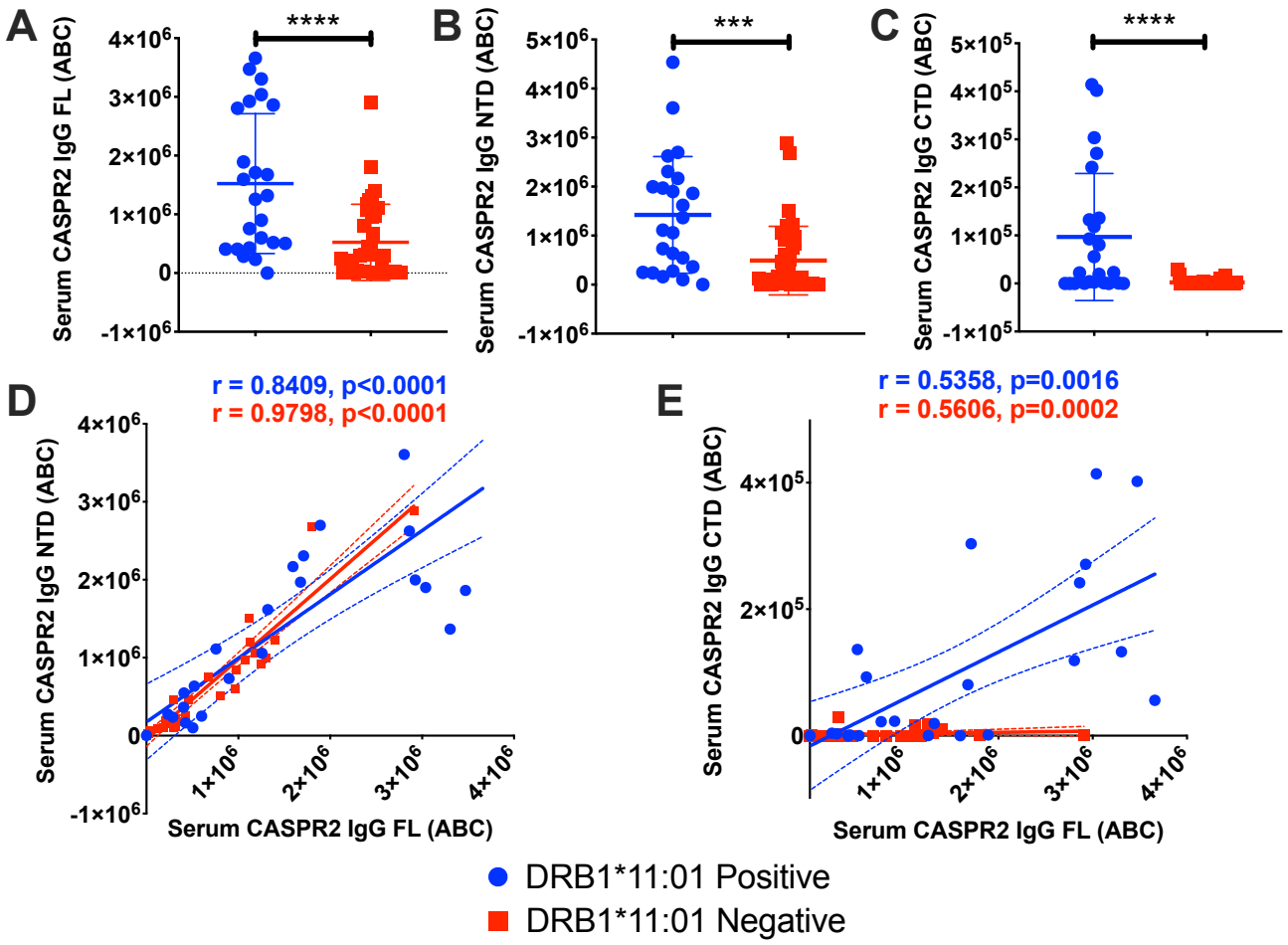


*Figure 6-23 CASPR2-antibody epitope specificities divided by HLA DRB1*11:01 carrier status against FL CASPR2, NTD CASPR2 and CTD CASPR2*

*(A) In the full cohort of CASPR2-antibody patients (n=32, 62 samples) comparison of the ABC to full length (FL) CASPR2 between patients carrying HLA DRB1*11:01 allele versus non-carriers. In keeping with the CBA and FIPA data, carriers have higher amounts of CASPR2-antibody (p<0.0001, Mann-Whitney U), lines and error bars represent mean and SD.*
(B) The same comparison testing for *N-terminal domain CASPR2 (NTD) antibodies and (C) C-terminal domain only CASPR2 (CTD) antibodies revealed significantly more of both in HLA DRB1*11:01 carriers (p<0.0001 and p=0.0001, Mann-Whitney U), lines and error bars represent mean and SD. ***p<0.001 and ****p<0.0001.*
(D) *Correlation of serum CASPR2 FL antibodies with CASPR2 NTD antibodies in HLA positive patients (blue) versus HLA negative patients (red) and (E) Serum CTD CASPR2 antibodies with the same patients. Comparison of linear regression between the two groups in D yields p=0.1450, illustrating no significant difference between the slopes, whereas in E the comparison gives p=0.0004, meaning the difference between the slopes is extremely significant. Spearman's correlation shown in related colours, all regressions are non-zero with the notable exception of that between FL and DRB1*11:01 negative patient CTD antibodies – suggesting the HLA association allows patients to make CASPR2-antibodies targeting these epitopes more readily, with slope in CTD DRB*11:01 positive patients equalling 0.0742 (95% CI 0.03777 to 0.1107, r^2=0.4474, p<0.0004) whereas in CTD DRB*11:01 negative patients it is 0.002 (95% CI -0.0011 to 0.0051, r^2=0.0432, p=0.1994).*

6.9 Discussion

The aim of this strand of study was to look at whether CASPR2-antibody patients carried antigen specific cells in their peripheral lymphocyte compartment at sufficient levels to produce CASPR2-antibodies in culture. If produced, the next questions were about which cytokines preferentially drove production of these antibodies, how the CASPR2 IgG subclasses and epitopes compared between serum and cultured derived CASPR2 IgG and how these properties changed over time. Given the novel class HLA II association described in chapter five, it was theorised this would affect cultures.

It was demonstrated, using a novel CASPR2-antibody multiplex flow cytometry assay, that the predominant CASPR2 IgG serum subclass is IgG4 in keeping with the literature,[102, 110] though we found IgG2 to be the next most dominant IgG subclass, not IgG1 as described by these two reports. One caveat is that neither study used quantitative methods and a study that used a quantitative method did corroborate our findings.[111]

All ten CASPR2-antibody patients cultured made CASPR2 IgG and no HCs made any CASPR2 IgG, despite producing enough total IgG in culture to give detectable levels of IgG by CBA. This is particularly noteworthy as previous PBMC culture systems from our laboratory were producing specific antibodies in diseases where the predominant autoantibody subclass was IgG1,[12, 38] the most abundant IgG subclass compared IgG4 which is the least. Similar to previous works, the amount of CASPR2-antibody made in culture correlated only with serum CASPR2 antibody titre. No other clinical correlations were seen when using cross-sectional analysis. One interpretation of this is that the number of circulating antigen specific cells relates to titre and further explains the only moderate correlation between culture total IgG and culture specific IgG production. The correlation between serum and culture CASPR2-

antibody amounts is a key way of supporting the relevance of this culture system to *in vivo* antibody production.

Another mechanism of proving the physiological relevance of culture derived CASPR2 IgG is to compare their subclass composition to serum CASPR2 IgG. It was noted that IgG2 was under-represented in our culture model, both in CASPR2 specific and total IgG. This underrepresentation of total IgG2 was particularly marked in conditions which are most trophic for specific IgG production. This has been noted by another group utilising a similar system.[223] The cytokines which produced the most specific and total antibody were IL-2, IL-15 and IL-21, as well as the TLR-agonist R848. This was a consistent finding across patients with no significant individual variation. IL-2, IL-15 and IL-21 all belong to the type I family of cytokines which bind to the common gamma-chain of the IL-2 receptor, as well as their own private receptors.[224] All have the capacity to induce IgG class switching: IL-2 has been reported to increase production of all IgG subclasses,[225] IL-15 only IgG1[226] and IL-21 to be a potent inducer of IgG1 and IgG3 subclass switch.[220] The human PBMC compartment contains roughly 80% naïve and 20% memory B cells and when bulk stimulated, memory B cells proliferate preferentially in response to IL-21 stimulation.[220] IgG+ memory B cells have been shown to demonstrate limited capacity for class switch while IgD+ memory B cells as well as naïve B cells class switch readily in vitro.[227] The observed subclasses are therefore likely an interaction between these groups, with a significant proportion of preferentially proliferating cells unable to class switch. Indeed, when B cells were sorted by subclass, limited class switch was noted *in vitro*. The net result was a skew away from IgG2 subclasses in total, requiring a correction to be made when comparing serum to SN IgG subclasses. With this correction applied, the cultured CASPR2 IgG subclasses correlated closely with serum CASPR2 IgG subclasses. This lends further credence to the notion that circulating antigen specific cells,

stimulated in our culture system, contribute significantly to overall autoantibody production *in vivo*.

It is worth, at this point, dwelling on the observation of the potency of IL-21 compared to other B cell activating factors, including IL-2 and IL-15, something demonstrated by a number of other studies.[228, 229] IL-21 has been shown to be a crucial factor in the B-cell proliferation induced by helper-T cells,[230] a role in which IL-2 and IL-15 have long been established,[226, 231] implying importance of T-cell help in the production of these antibodies. IL-21 is also is highly expressed by T-follicular helper cells[232] and IL-21R is upregulated on germinal centre B cells,[229] indicating a crucial role of the B and T cell interaction in the germinal centre as well as underlining the importance of this interaction to an antibody-driven response in general.

Germinal centres were postulated to be driving ongoing specific antibody production in patients with NMDAR-AbE.[38] Part of the reason for reaching this conclusion was the number of patients found to have NMDAR-IgM produced in an ongoing fashion, far longer than the serum half-life of IgM. In our cohort, using a novel flow cytometry assay, CASPR2 IgM was found much less often in CASPR2-antibody patients compared those with NMDAR-AbE, with limited evidence of long-term persistence. In order to ask further questions about the site of ongoing specific antibody production, four patients were cultured over serial time points, comparing serum and culture specific IgG production and subclasses, as well as CXCL13 levels, a marker of germinal centre activity.

In treated patients, amounts of CASPR2 IgG in serum and SNs fell dramatically with immunotherapy over time and in an untreated patient, there was no dramatic fall. In two patients, samples from around the time of relapse were associated with an increase in serum CASPR2-antibodies without an increase in capacity to generate CASPR2 specific IgG from

PBMCs. This suggested a lack of renewal of the circulating antigen specific memory B cell pool as one would expect with a new germinal centre reaction, as well as no relationship with serum CXCL13 or IgM production. It is important to highlight at this point that this relapse data is only based on two patients. The amount of CASPR2-antibody produced in culture correlated with serum CASPR2-antibody across the whole cohort. There was, however, one outlier: a patient treated with MTX, with a high serum CASPR2 titre (1:102,400) and only very limited capacity to produce CASPR2 antibodies in culture. This was similar to the dissociation seen in the relapse samples from serially cultured patients. Data has been presented which suggested that lack of IgG production in the patient treated with MTX was due to a reversible effect of MTX on circulating PBMCs. One possible conclusion based on these data is that in these contexts, serum CASPR2-antibody is not being made by circulating B cells but instead by niched plasma cells.

A close correlation between circulating antigen specific memory B cells and serum specific antibody has been observed by other groups,[233] using tetanus toxin (TTX). This correlation broke down after TTX booster was given, an observation also reported elsewhere.[234] Once TTX booster was given, serum specific antibody rose sharply in conjunction with a rapid rise in short lived-plasma cells while the circulating antigen specific memory B pool remained constant, as was seen in two of our relapsing patients. This rapid rise in specific antibody then plateaued and fell as the effect of the antigenic challenge faded. Ongoing antibody production was theorised to be due to a lower level 'polyclonal activation', mediated by TLR agonisation and by non-cognate T cell help via CD40L and cytokine secretion. Polyclonal activation was proposed as the ongoing stimulus to the circulating memory pool, driving differentiation into long-lived plasma cells and trafficking to bone marrow niches, perhaps explaining the slight decrease over time of antibody made in culture in our untreated

patient. The close relationship between serum and SN CASPR2 IgG subclasses and epitopes over time lends further strength to the argument that these circulating cells are contributing to the serum antibody pool in a meaningful way. One possibility as to how they are doing this is by providing a constant low-level differentiation into plasmablasts which then traffic to bone marrow niches and terminally differentiate, allowing long term and large volume secretion of CASPR2-specific antibody. There was little evidence of an ongoing germinal centre reaction in these patients.

Germinal centres clearly remain important in disease initiation, however, given the large amounts of class-switched CASPR2 specific antibody detected and the observed potency of IL-21. The sample size is limited and it may be true that there is heterogeneity within patients in terms of the relative contributions of germinal centres and niched plasma cells to serum antibody levels, explaining why some patients with NSAbs have very dramatic falls in titre to anti-CD20 monoclonal antibodies, which target circulating B cells, and some do not.[235] Lymph nodes contain germinal centres and niched memory B cells whilst the bone marrow contains plasma cells. Neither are sampled in this study and future work addressing the relative contributions of each compartment could involve comparisons between IgG subclasses, epitopes, cytokine secretion and, if able to isolate antigen specific cells, lineage analysis of heavy and light chain IgG sequences to determine the directionality of evolution.

Germinal centres are a key site of B-T cell interaction. After antigen encounter, naïve B cells undergo affinity-based selection for entry into germinal centres. This selection is carried out by T cells and is determined by the ability of a naïve B cell to take up antigen and present it via a peptide-HLA complex to a T cell. B cells which take up most antigen, as determined by BCR affinity for antigen, and present it in the most stimulant way, as determined by antigen processing and presentation, are most likely to gain entry into a

germinal centre and achieve a fully-formed antigen response.[8] HLA allele is a key factor in antigen processing and presentation and therefore has an influence not only on entry into a germinal centre but also on SHM and affinity maturation, a process that is also heavily dependent on the B-T cell interaction.

In previous chapters, it was established that CASPR2-antibody patients carrying HLA DRB1*11:01 produced more serum CASPR2 antibody than those with other class II alleles. It was confirmed again, using a third method to quantify CASPR2 IgG, that CASPR2 IgG in serum was higher in patients with HLA DRB1*11:01 to FL CASPR2 but also CTD and NTD CASPR2. It was further noted that the HLA DRB1*11:01 allele was noted to affect capacity to produce antibodies in culture, with perhaps some relationship to epitope as well. Patients carrying HLA DRB1*11:01 had significantly more serum antibodies to CTD of CASPR2 and CASPR2 CTD antibodies were detectable in PBMC cultures whereas DRB1*11:01 negative patients had far lower levels of CASPR2 CTD antibodies and produced none in culture. Further to the suggestion that HLA DRB1*11:01 is clinically relevant, this provides convincing evidence of its immunological relevance, giving patients higher levels of CASPR2-antibodies targeting a wider range of epitopes.

A few key examples of a similar effect exist in the literature. In type-1 diabetes mellitus, varied class II HLA associations has been shown to influence antibody epitope specificity to insulinoma-associated protein 2[236] and in a large case-control study of systemic sclerosis, there was evidence of an influence of class II allele on antibody epitopes and clinical phenotype.[237] Finally, in transplantation, epitope spread of the host response correlates with rejection of allografts.[238, 239]

A number of points arise as a result of this observation in CASPR2-antibody patients. First, this could be seen to provide further evidence of the importance of the B and T cell

interaction in this disease. Second, as germinal centres are a key site of B-T interaction, this data can be seen to further underline the importance of these structures in the initiation of this disease. This is despite finding limited evidence of an ongoing contribution to the production of specific antibody in these patients. Finally, the question arises as to how the difference in CASPR2-CTD antibody production occurs and what this tells us.

One possibility is that this is due to epitope spread (ES) driven by DRB1*11:01. ES can occur within a molecule (intramolecular), with proteins that complex together (intermolecular) or between proteins which are not linked but present in the same molecular site (intrastructual). With reference to CASPR2-antibodies, intermolecular spread may explain the presence of double positive LGI1- and CASPR2-antibody patients, as well as development of antibodies to intracellular aspects of VGKCs. ES can occur indirectly, when tissue is damaged, releasing cytokines and other antigens which aid this process. In situations where there is less prominent tissue destruction a direct interaction between antigen presenting cells and T cells becomes more relevant, as is likely to be the case in patients with CASPR2 antibodies. T cells are activated by APCs and then provide help to antigen specific B cells. This interaction can occur between cells targeting different epitopes on the same polypeptide.[240] Protein is endocytosed by APCs, cleaved and loaded onto MHC class II for trafficking to the cell surface. Class II HLA expression is thought to allow varied epitope specificities by presenting epitopes not otherwise available via binding preferences within the class II complex. The argument against ES in this condition is that in our longitudinal epitope data we did not see new development of antibodies to either the CTD or NTD over time, though it may be possible that this occurs during the initiation of the immune response and does not develop further once disease manifests.

An alternative could be that of a threshold effect. CASPR2-reactive naïve B cells could exist as was demonstrated in NMOSD AQP4-antibody patients[12] and after antigen encounter, traffic to lymph nodes in an attempt to form germinal centres. NTD-specific naïve B cells may have higher affinity for antigen and therefore gain entry to a germinal centre more easily. Lower affinity, CTD-specific naïve B cells, however, require the extra help of an HLA allele which allows for a more stimulant presentation of CASPR2 peptides to a T cell in order to enter a germinal centre and establish a propagating immune response. The HLA DRB1*11:01 allele could be a key determinant allowing these naïve B cells to cross this threshold. Finally, it could be that the specificity of the B cell affects the antigens presented, with HLA DRB1*11:01 allowing more efficient presentation of C-terminal regions of CASPR2 and therefore a more efficient B-T interaction.[241]

Chapter 7 in this thesis looks into antigen specific T cell and their epitopes in patients with LGI1- or CASPR2-antibody mediated neurological diseases. Isolation of antigen specific T cells would be a very useful tool in understanding the mechanisms of this observation and work should be done on this in the future. Nevertheless, the observation that HLA DRB1*11:01 expression in CASPR2-antibody patients gives broader epitope specificity and more CASPR2 specific antibody may also explain the poorer response to immunotherapy seen in these patients. This immunological insight could, therefore, offer clinical assistance by highlighting DRB1*11:01 carrying CASPR2-antibody patients as needing more potent immunotherapy, perhaps in the form of cyclophosphamide or Rituximab. It also perhaps provides a more specific target for immunotherapy in the form of the B-T cell interaction.

In trying to achieve a unifying hypothesis of how CAPSR2-antibody mediated disease arises, a final relevant observation was the very gradual increase in CASPR2-antibodies to significant levels prior to relapse in one patient. This slow rise in antibody has also been

observed in patients with NMO and AQP4 antibodies. [242] As previously discussed, there is a clear difference in kinetics between the rapid antibody titre rise seen with antigenic re-stimulation and the more gradual and indolent process driven by polyclonal activation. In the patients reported, this makes it unlikely that a single catastrophic exposure to brain antigens, for example by acute failure of the blood-brain barrier, is driving a rapid rise in production of CASPR2 antibodies. Indeed, the degree of exposure of brain antigens to the circulating immune system is unclear, with the example of acute brain tissue injury in the form of HSVE leading to NMDAR-AbE[42], evidence that rapid antigen efflux can overwhelm tolerance mechanisms in this paradigm. CASPR2 is expressed peripherally, however, with human CASPR2-antibodies able to bind CASPR2 in the dorsal root ganglia of mice but not the spinal cord.[209] This provides a possible source of immunising antigen to the peripheral immune system. As noted previously, CASPR2 is expressed at low levels in the parathyroid gland and at an RNA level in the adrenal and prostate gland,[107] providing further sources of antigen. Another possible source is via CNS draining lymphatics.[243]

Either way, the possibility exists that CASPR2 protein is encountered by the immune system of all humans at low levels. As IgG4 antibodies tend to be the result of prolonged immunisation[244] one hypothesis is that there is a constant, low level antigenic stimulation caused by a break in tolerance causing the observed gradual rise in CASPR2-antibodies. With age, one study has reported higher frequencies of memory B cells with higher levels of SHM and expression of more activation markers, utilising more downstream-located IgHG genes, including IGHG2 and IGHG4.[245] A unifying hypothesis of disease causation, therefore, is that CASPR2-antibody mediated neurological disease arises when there is a combination of a potentially age-related failure of tolerance, low-level antigenic stimulation, predisposing genetic factors, such as the HLA DRB1*11:01 allele, allowing for effective B-T interaction and

germinal centre formation. Ongoing CASPR2-antibody production could be underpinned by circulating antigen-specific B cells undergoing polyclonal activation and renewing CASPR2-antibody secreting plasma cell niches. Many of these processes could be modulated by hitherto unexplored variations in individuals such as VDJ gene usage, defective immune clearance and exaggerated cytokine production, all which could be explored in the future. The fact that a number of failures need to occur in order for disease to manifest, explains the rarity of this disease.

This study has a number of limitations. First, sample size is limited by availability of PBMCs from patients with CASPR2-antibody mediated disease, especially samples early in their presentation and free of immunotherapy. Larger numbers, particularly over serial time points would allow more definitive conclusions to be made. Second, IgG subclasses were skewed by using a range of conditions in bulk PBMCs which contain a mixture of cells with varied abilities to class switch *in vitro*. Given certain cytokines, for example IL-21, are the most effective at producing specific antibody but appear to skew towards IgG1 and IgG3, to an extent this is unavoidable.

In terms of the epitopes, relative expression of NTD and CTD CASPR2 constructs on HEK cells is not quantified or corrected for. However, NTD ABC values are similar to FL, suggesting equivalent expression and the preference of patient serum to NTD CASPR2 as opposed to CTD is well established in the literature.[112] The stark difference in serum and SN CTD antibodies in patients with and without HLA DRB1*11:01 are comparisons made within the same construct, therefore the relative expression of CASPR2 CTD compared to NTD becomes irrelevant: there is a clear difference regardless. Finally, the differences observed between patients with HLA*DRB1:11:01 may be due to non-HLA genes which are in linkage

disequilibrium with this allele, though this appears unlikely given the biologically plausible effect of this allele demonstrated in this chapter.

In summary, we have carried out the first in-depth study of the immunology of patients with CASPR2-antibody mediated disease. Their predominant IgG4 serum antibody subclasses and NTD epitope preference are represented by their circulating antigen specific B cells, suggesting relevance of these cells to overall serum CASPR2-antibodies seen *in vivo*. Evidence points away from ongoing germinal centres and towards lymph node or bone marrow niched cells for ongoing antibody secretion, though their renewal by this representative circulating population is likely crucial. Finally, expression of the HLA DRB1*11:01 allele gives greater production of CASPR2-antibodies, to a greater range of epitopes, perhaps explaining the inferior response to immunotherapy observed in these patients and underlining the importance of the B-T interaction in this disease. Future work could be to repeat this work in larger populations, explore other immunological compartments (spleen, lymph nodes or bone marrow) and mechanistic work on CASPR2-antibodies by subclass and epitope specificity could be informative.

7 CASPR2- and LGI1-antibody patient T cell immunology

7.1 Introduction

There is accumulating evidence pointing to the key role played by T cells in LGI1- and CASPR2-antibody mediated neurological diseases. First, there is maximal B cell activation by cytokines mimicking T cell help described in chapter six, similar to the results from studies in patients with diseases from the same paradigm.[12, 38] Second, there is a strong class II HLA association in both diseases described in chapter 5 and published in the literature.[190, 191, 195, 246] Third, immune checkpoint inhibitors which allow upregulation of T cell activity are increasingly being associated with B cell mediated neurological diseases as a side effect.[247] Finally, evidence from chapter 6 suggests an effect of the HLA DRB1*11:01 risk allele on both production and epitope specificity of CASPR2 antibodies. The next hypothesis-driven question, therefore, is whether there are T cells in these patients that respond to LGI1 and CASPR2 peptides in an antigen specific manner.

Peptides are presented to CD4+ T cell receptors (TCR) in complex with class II HLA molecules by APCs such as dendritic cells, macrophages and B cells. The HLA-peptide complex is formed in endosomes where peptides, derived from extracellularly sampled and processed antigen, are combined with compatible class II HLA molecules (Figure 7-1). A key point is that the formation of a peptide-class II HLA complex is defined by the affinity of binding between antigen derived peptides and an individual's class II HLA haplotype. Based on systematic binding studies sequencing class II associated self-peptides [248, 249] and knowledge of the X-ray crystal structure of MHC-peptide complexes,[250, 251] optimal length of class II associated proteins has been established as 15-20 amino acids (AA). In order to determine the key CD4+ T cell expanding peptides derived from a full-length protein antigen, a common approach is

to use overlapping peptides where FL antigen is represented in 15-20AA peptide sections covering the whole molecule. As LGI1 and CASPR2 are large molecules, a more targeted approach based on *in silico* modelling of predicted binding of LGI1 and CASPR2 to associated HLA alleles was used. Peptides predicted to bind favourably to disease-associated HLA alleles were then selected and used to expand CD4+ T cells *in vitro*, with the results presented below. This work was done in partnership with Dr Melanie Ramberger, post-doctoral researched in the Oxford autoimmune neurology group and is included with her permission.

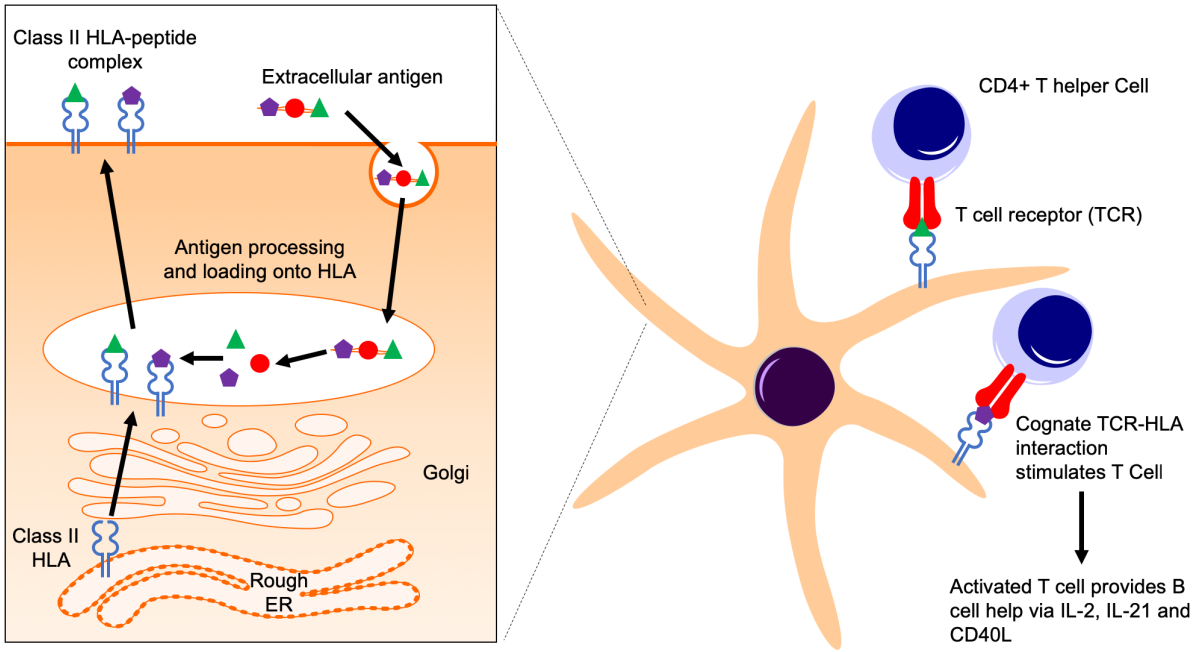


Figure 7-1 Dendritic cell uptake of antigen, processing and presentation to T cells via Class II HLA molecules

This diagram provides an overview of how a key professional APC, a dendritic cell, endocytoses extracellular antigen (protein with multiple peptide epitopes represented by purple, red and green shapes) and processes it intracellularly. This allow assembly of different peptide epitopes onto class II HLA molecules based on the affinity between these two entities. The class II HLA-peptide complex is then trafficked to the surface where it can bind the CD4+ TCR and cause activation and proliferation of these cells, which in turn provides B cell help and evolution of the immune response.

7.2 Methods

7.2.1 HLA-peptide binding prediction

The *in silico* analysis was carried out using the NetMHCIIpan 3.1 server model which is based on artificial neural networks.[252] Binding affinity was calculated between previously described disease associated HLA haplotypes, as well as consecutive overlapping peptides, 15 AA in length derived from LGI1 and CASPR2 protein sequences (UniProt O95970 and Q9UHC6, respectively). The output of this analysis was predicted peptide affinities (nM). In order to correct for the known property of HLA alleles to bind promiscuously to a number of peptides, the predicted affinities were compared to the predicted affinities of 200,000 random peptides of the same length to generate rank values. All peptides with a rank value of (%) <3 were considered strong binders. High rank peptides often clustered around core sequences, as expected. This worked was carried out by Dr Mateusz Makuch, post-doctoral researcher in the Oxford autoimmune neurology laboratory and is included with his permission.

7.2.2 Patient recruitment

Twenty-five patients were recruited for this section of the study, these included eight patients with CASPR2-antibodies and four with LGI1-antibodies from the HLA study discussed in chapter five. A further six patients with LGI1-antibodies and one patient with both LGI1- and CASPR2-antibodies were recruited prospectively from the autoimmune neurology clinic, Oxford. Six healthy control were recruited either from laboratory volunteers or from previous studies. Clinical datasets were collected via direct interview and review of the patient notes. All patients provided written and informed consent (REC16/YH/0013 or the IRB 10-04905 approvals).

7.2.3 T cell proliferation assay

This protocol was adapted from Ramberger et al.[253] Briefly, isolated PBMCs are washed in DPBS, counted and stained with CFSE at a density of 2×10^7 cells/mL in 0.4 μM carboxyfluorescein succinimidyl ester (CFSE - CellTrace CFSE, C34554, Fisher Scientific) as per the manufacturer's instructions. Three T cell expansion media were trialled; X-Vivo 15 (Lonza, BE02-061Q), RPMI-1640 (Gibco, 11875085) supplemented with 5% human serum (Sigma, H4522) and CTS:TS OpTimizer T Cell Expansion SFM (Gibco, A10221-01). CFSE stained cells were plated into T cell expansion media and stimulated with either pooled LGI1 or CASPR2 derived peptide (10μg/ml), dimethyl sulfoxide (DMSO – Sigma Aldrich) vehicle control, a tetanus toxin (TTX) positive control (10μg/ml, peptides ordered from Peptides & Elephants) or phytohaemagglutinin (PHA - Sigma, L4144), a general mitogen. Cells were then plated out in six repeats per condition, with 2×10^5 cells per well, in a 96 well, round bottom plate. At day 3-5, PHA stimulated cells were harvested and stained to ensure cell viability, success of CFSE stain and proliferation. At day seven or eight, PBMCs were restimulated with fresh peptides (10μg/ml) and 100μL of the cell culture medium was replaced with fresh medium and supplemented with IL-2 (20U/mL, Peprotech). Finally, three days after re-stimulation, all cells were harvested, pooled by condition and stained for flow cytometric analysis with the following antibodies; CD3 (PE labelled, 300408, Biolegend) CD4 (APC labelled, clone M-T466, Milltenyi), CD8 (PE-Cy7 labelled, 557746, BD) and DAPI for live-dead discrimination. Analysis was carried out on LSR II (BD Biosciences). In the experiment where HLA antibody was used, the mouse anti human HLA-DR antibody L243 was added to CFSE stained cells and incubated for an hour at 37 °C, then washed prior to the addition of stimulating peptides.

7.3 In silico peptide prediction

LGI1 and CASPR2 are 557 and 1331 amino acids (AA) long respectively (www.uniprot.org). As class II molecules preferentially bind peptides between 15 and 20 AA long, creating an overlapping peptide library for both molecules would have been a significant undertaking. *In silico* modelling of predicted binding of peptides to HLA alleles is an established technique in the literature and allows prediction of peptides which are likely to bind at high affinity to HLA alleles of interest. Peptides derived from this system can then be targeted as likely candidates to complex with specific HLA alleles and form peptide-MHC complexes likely to stimulate expansion of patient T cells *in vitro*. This analysis was carried out by Dr Mateusz Makuch, post-doctorate researcher in the Oxford autoimmune neurology laboratory and is included here with his permission.

The output from this analysis was a rank value, essentially the capacity of a 15 AA peptide to bind predicted HLA haplotypes, normalised for the intrinsic promiscuity of the HLA alleles. A large number of peptides for haplotypes in LGI1- and CASPR2-antibody patients were above our cut-off for likely relevant binding and as expected, centred around core sequences along the LGI1 and CASPR2 molecules (Figure 7-2). A number of peptides were predicted to bind HLA variants associated with both LGI1- and CASPR2-antibody cohorts and were therefore not treated as disease relevant. This included a previously identified peptide, identified using similar methodology, and argues against its relevance in disease.[191] However, 9/13 LGI1-derived core peptides sequences and 7/13 CASPR2 core sequences demonstrated high rank, entirely specific to the HLA variants associated with the appropriate antibody cohort (Figure 7-2, B and D, pink circles). These peptides were therefore used as the basis to select candidate peptides for use in the experimental system. Peptides selected were 15-

20mers and designed to give overlapping coverage of a core region and are displayed, along with their affinity and HLA allele specificity in Table 7-1.

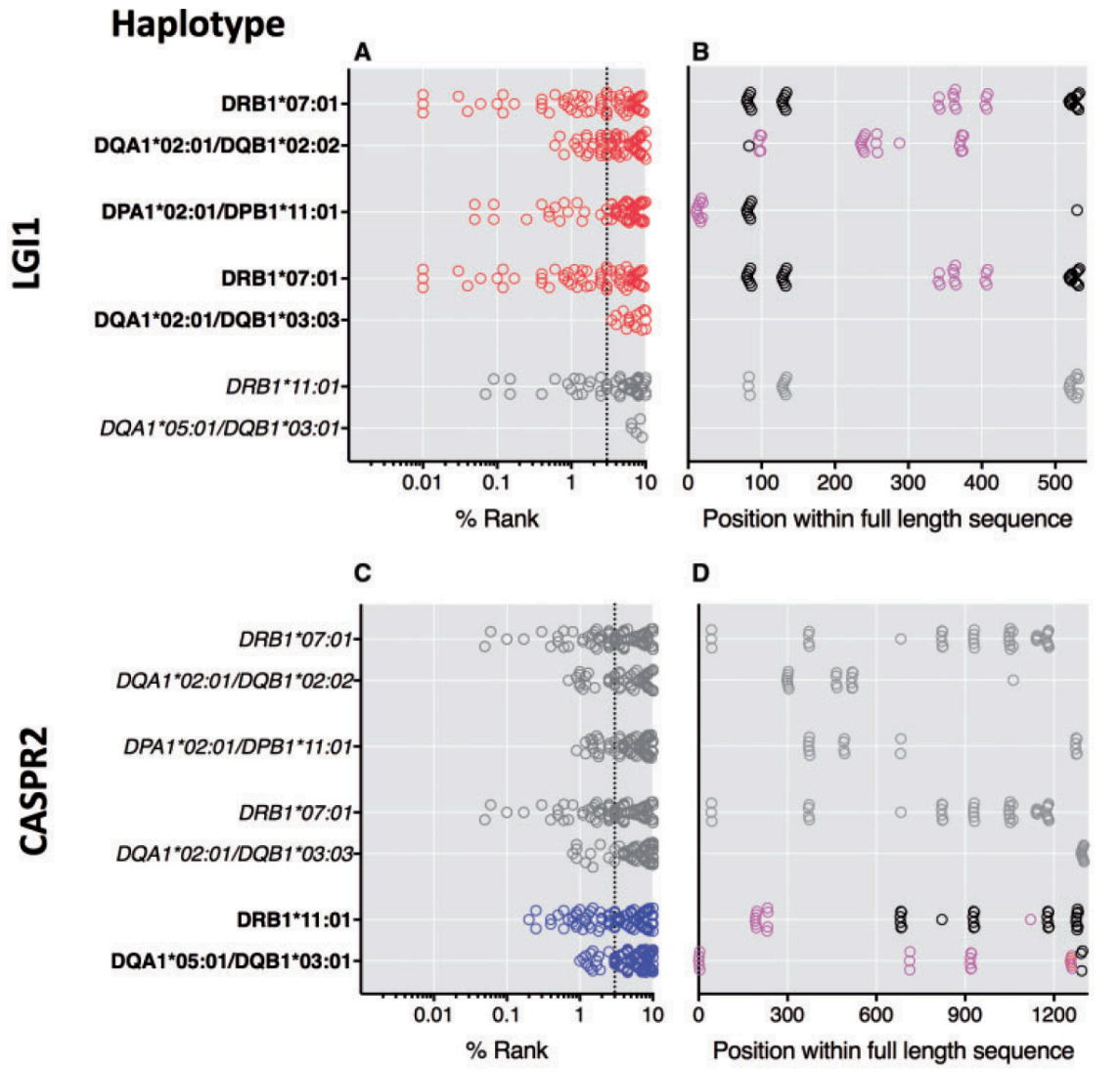


Figure 7-2 In silico LGI1 and CASPR2 peptide-HLA associations

Using the in silico method described, 15mers were derived from full-length LGI1 and CASPR2 with a high predicted binding to MHC-dimers encoded by disease-associated HLA haplotypes. Rank was derived by comparing predicted affinity (IC50, nM) of peptides from LGI1 (A) and CASPR2 (C) to 200 000 random peptides of the same length. A cut off of 3 was used to define significantly high binding proteins by rank (dotted line) and their position along FL LGI1 (B) and CASPR2 (D) is displayed. The displayed haplotypes correspond to the disease associated haplotypes described in chapter 5 and when in bold correspond to those observed in patients with antibodies to the relevant protein. LGI1-antibody patient cohort in red and CASPR2-antibody patient cohort in blue. Grey circles and italicised haplotypes relate to peptides from the other antigenic protein (i.e. CASPR2 in A and B; and LGI1 in C and D). Within B and D, pink circles represent peptides specific to that disease associated HLA variant, black circles represent peptides with some predicted promiscuity across LGI1- and CASPR2-associated HLA alleles. This figure has been adapted from Binks, Varley and Lee, at al.[195]

	Abbreviated name	15-mer start position	Extended core	LGI1 allele(s) binding	Highest affinity [nM]	CASPR2 allele(s) binding	Peptides in pool
LGI1	L1	12-21	KRIAYFLCLLSALLL	DPA1*02:01/DPB1*11:01	14.07	-	4
	L2	81-87	FLFTPSLQLLL	DRB1*07:01; DPA1*02:01/DPB1*11:01; DQA1*02:01/DQB1*02:02	5.79	DRB1*11:01	4
	L3	97-101	FDVISDDAF	DQA1*02:01/DQB1*02:02	722.35	-	3
	L4	289	LYVIVAQLF	DQA1*02:01/DQB1*02:02	924.59	-	1
	L5	342-344	FVVADSSKA	DRB1*07:01	36.94	-	1
	L6	362-366	FYSHQSLHA	DRB1*07:01	25.49	-	3
	L7	371-376	WYRDTDVEY	DQA1*02:01/DQB1*02:02	440.50	-	3
	L8	362-376	FYSHQSLHAWYRDTDVEY	DRB1*07:01	N/A	-	1
	L9	406-409	YQWNKATQL	DRB1*07:01	26.51	-	1
	Abbreviated name	**15-mer start position**	**Extended core**	**CASPR2 allele(s) binding**	**Highest affinity [nM]**	**LGI1 allele(s) binding**	
CASPR2	C1	1-5	PRAGCGAALLL	DQA1*05:01/DQB1*03:01	15.65	-	3
	C2	192-197	YRFRNKKMK	DRB1*11:01	21.90	-	3
	C3	232-235	YITLELKKAKLV	DRB1*11:01	27.15	-	1
	C4	713-715	WGGSGPGIQ	DQA1*05:01/DQB1*03:01	23.53	-	1
	C5	918-923	FVGGAGGQQG	DQA1*05:01/DQB1*03:01	12.95	-	3
	C6	1000-1004	VGAFFEEGM	DQA1*01:01/DQB1*05:03	189.36	-	3
	C7	1122	FLKLDHYPS	DRB1*11:01	36.97	-	1
	C8	1257-1262	IIGGVIAVV	DQA1*05:01/DQB1*03:01	13.39	-	3

Table 7-1 LGI1 and CASPR2 derived peptides selected for use in T cell stimulation experiments

Based on in silico modelling, nine core sequences for LGI1 and eight for CASPR2 were selected as appropriate targets. The table above details the abbreviated name used for peptides targeting the extended core in this study. The position of the peptide clusters within the full-length molecule (15-mer starting position), amino acids of the extended core, HLA allele predicted to bind and the highest affinity of the peptides in the cluster (nM) are all listed, as well as if the allele is promiscuous for either CASPR2- or LGI1-patient HLA alleles. Finally, the number of peptides used to target this pool is listed. Peptide L2 was included, despite its promiscuity for both LGI1 and CASPR2 as a control and because it has been highlighted by a previous study. L8 is a composite of the L6 and L7 cores, making an 18-mer that was not a result of in silico modelling as the analysis was based on 15mers, it is included on the basis of it being a biologically feasible stimulating peptide as it contains two cores. C6 is included as a control as it was not predicted to bind disease associated HLAs.

7.4 Clinical description of cohort

Patients recruited included those with antibodies to LGI1 (n=10), those with antibodies to CASPR2 (n=8), those with antibodies to both LGI1 and CASPR2 (n=1) and age-matched healthy controls (n=6), key details are included in Table 7-2. LGI1- and CASPR2-antibody

patients were predominantly older men as expected and healthy controls matched this well. The double positive patient was younger and female. The majority (70%) of patients with LGI1-antibodies were on immunotherapy at time of sampling, perhaps reflective of the fact they were sampled earlier in disease than patients with CASPR2-antibodies, in whom only a minority were on immunotherapy when sampled (25%). Clinical presentations were in keeping with respective antibody mediated diseases as were HLA associations, where available.

	LGI1-Ab (n=10)	**CASPR2-Ab (n=8)**	**Double Positive (n=1)**	**Healthy control (n=6)**
Median age (range)	71 (60-78)	71.5 (64-78)	46	73 (26-74)
Male (%)	7 (70%)	8 (100%)	0 (0%)	4 (66.7%)
Median days post-disease onset (range)	533 (62-2150)	1632 (238-4894)	1391	NA
Immunotherapy at time of sampling (%)	7 (70%)[a]	2 (25%)[b]	1 (100%)[c]	NA
Clinical presentation (%)				
Limbic Encephalitis	10 (100%)	6 (75%)	0 (0%)	NA
Neuromyotonia	0 (0%)	1 (12.5%)	1 (100%)	NA
Movement disorder	0 (0%)	1 (12.5%)	0 (0%)	NA
HLA risk alleles (%)				
DRB1*11:01	0 (0%)	5 (62.5%)	0 (0%)	0/3 (0%)
DRB1*07:01	10 (100%)	3 (37.5%)	0 (0%)	1/3 (33%)

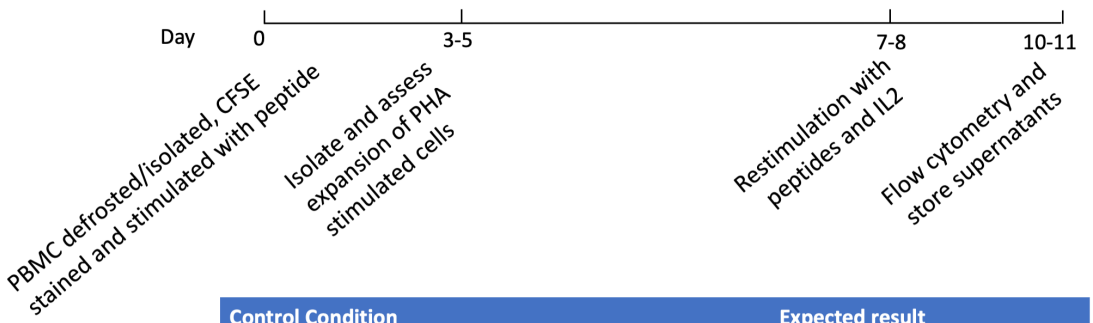
Table 7-2 Characteristic of cohort used for T cell stimulation experiments

*In HC, sequencing only available on three out of six patients. No DRB1*07:01 homozygotes in LGI1-antibody patients and no DRB1*11:01 homozygotes in CASPR2-antibody patients.*
a – corticosteroids (n=4), corticosteroids and plasma exchange (n=1), corticosteroids and mycofenolate mofetil (n=1) and methotrexate (n=1).
b – steroids (n=1) and mycofenolate mofetil (n=1)
c – steroids (n=1)

7.5 Optimisation of T cell proliferation assay

7.5.1 T cell proliferation protocol – optimisation

The T cell proliferation protocol is outlined in Figure 7-3. The flow cytometry panel was optimised in terms of antibody dilutions, set up and gating. A representative example, delineating our gating strategy is displayed in Figure 7-4. A key optimisation was selection of T cell expansion media. Based on the literature, three media were selected as possible options: X vivo, RPMI supplemented with 5% human serum and CTS media. Staining and culture in DMSO only was carried out as described in all three types of media and at day ten, cell numbers were compared between condition. X-vivo yielded the highest number of viable cells and was therefore used going forwards (Figure 7-5-A). Finally, an assessment was made on the effect of DMSO on the proliferation assay as it was used to resuspend lyophilised peptides. The maximum amount of DMSO in a stock was 6% and all solutions were used at 1:1000, therefore cells could be expected to encounter 0.006% DMSO. A range of DMSO concentrations were used therefore on the same protocol and no effect was seen on cell viability (Figure 7-5-B).



Control Condition		Expected result
DMSO	Vehicle control	Non-specific expansion
Tetanus peptide pool (TTX)	Pooled bacterial antigens	Memory T cell expansion

96 well plates: 6 wells per condition ($2x10^5$ cells each)
Flow panel: CFSE, DAPI, CD3 (PE), CD4 (APC), CD8 (PE-Cy7)

Figure 7-3 T cell proliferation assay protocol

Timeline of the experimental procedure of the T cell proliferation assay. PBMCs were either used fresh or frozen, washed in DPBS, CFSE stained, stimulated with peptide and plated out at 6 wells per condition. PHA stimulated cells were taken out and stained at day 3-5 to assess for cell viability, CFSE staining and expansion under mitogenic conditions. At day 7/8, media was changed and supplemented with IL-2 and fresh peptides. Finally, three days after re-stimulation, cells from each peptide condition were spun down, pooled and stained.

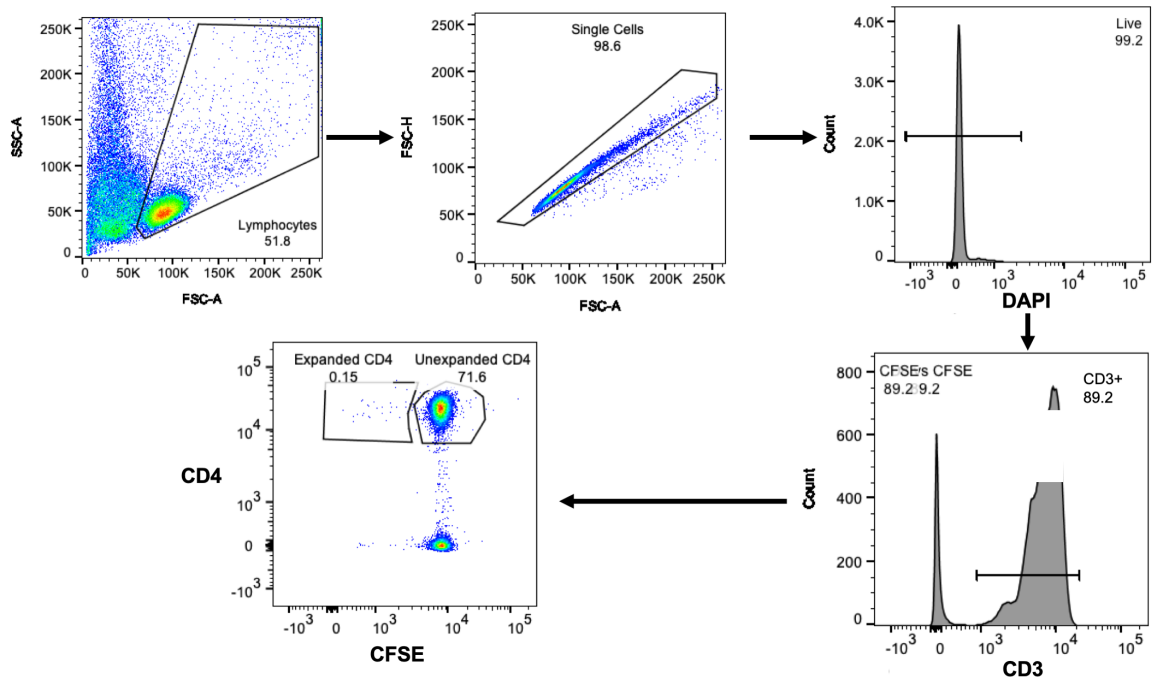


Figure 7-4 Gating strategy for flow cytometry analysis of proliferated T cells

Pooled, stimulated, PBMCs are stained at day 10/11 and gated for lymphocytes, then single cells, then on DAPI as a live/dead marker and finally on CD3. Therefore, single, live T cells are displayed in the final gate, with CFSE staining on the x-axis and CD4 on the y, the group of interest is expanded ($CFSE^{low}$), memory T cells (CD4+) and the percentage of this group from the final gate is compared to the non-expanded CD4+ cells.

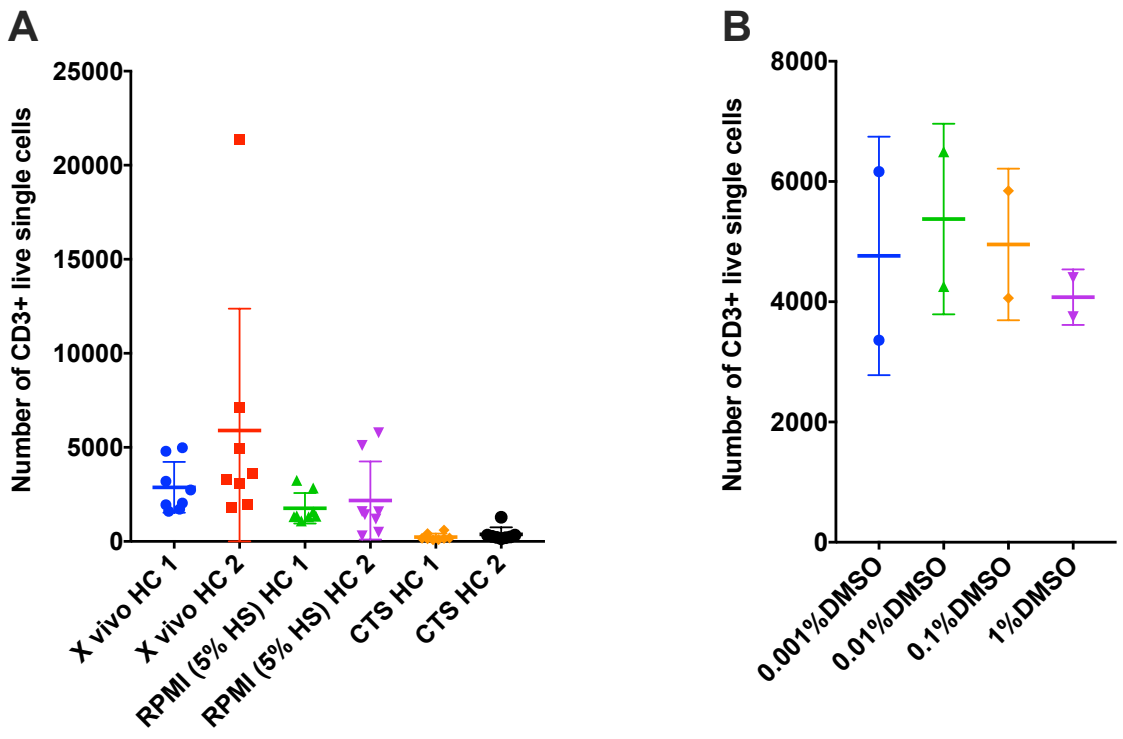


Figure 7-5 Optimisation of media used for T cell proliferation assay and assessment of the effect of DMSO on cell viability

(A) Count of viable, single CD3+ cells present at day 10 of T cell proliferation assay, gating as described in Figure 7-4. Two HC used in three different media: X-vivo, RPMI with 5% human serum (HS) and CTS. This shows some variability between individuals and most cells available using X vivo.
(B) Assessment of the effect of increase concentrations of DMSO used in X vivo culture medium as part of T cell proliferation assay, no effect on viability at day 10 up to 1% DMSO (n=2 HC PBMC samples), far exceeding the amount of DMSO used in our culture system.

7.5.2 Successful T cell proliferation to LGI1 peptides in an LGI1-antibody patient

Having optimised the assay on healthy control samples, the next step was to apply it to patients. Fresh PBMCs from LGI1-antibody patients were stimulated with the L1-9 peptides and Figure 7-6 demonstrates successful expansion of CD4+ T cells by LGI1 derived peptides. Four panels are shown and PBMCs are gated as live T cells. CD4+ cells are identified as they represent the population affected by peptide presentation via a class II HLA molecule, CFSE staining becomes dimmer with progressive cell division with decreasing values on the x-axis, therefore, pertaining to increased proliferation. With DMSO only there is limited expansion

of T cells. TTX stimulation gives massive expansion, with 7403/27935 (26.5%) of live CD4+ T cells having divided at day ten. Most interestingly though, is the reaction to an LGI1 peptide pool seen on the bottom right panel, with 2505/18284 (13.7%) cells falling within the proliferated CD4+ gate. This is a property specific to certain LGI1 peptide pools as other pools gave next to no expansion whatsoever, as is seen in the bottom left panel. Cell division index (CDI) is used as a quantification of T cell proliferation and is derived from the percentage of cells in the expanded CD4+ gate in the test condition divided by the number of expanded CD4+ cells in the DMSO control condition (Figure 7-6). This allows correction for background expansion in the absence of peptide stimulation, allowing for better comparison across samples.

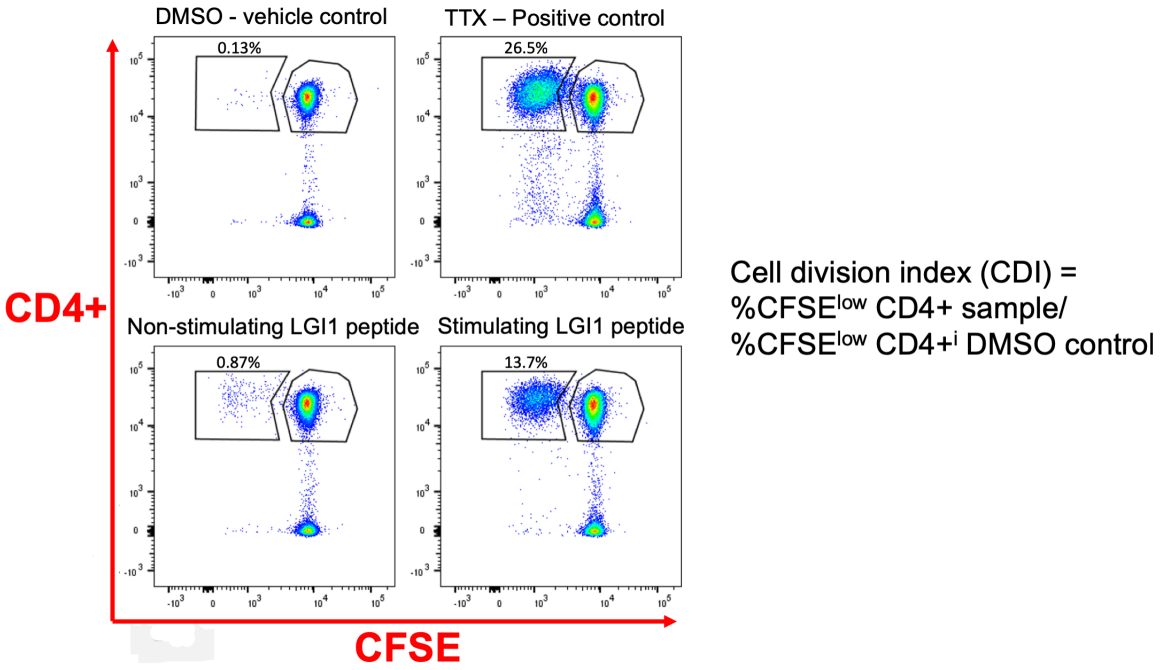


Figure 7-6 Successful expansion of CD4+ memory T cells with LGI1 peptides

LGI1-antibody patient PBMCs, stimulated with either DMSO, TTX or LGI1 peptides, collected at D10, stained and gated as previously described, displaying a successful expansion of CD4+ cells on the two panels on the right (TTX and LGI1 peptide), providing the first working example of the assay. Description of how CDI calculated provided to the right of panels.

Monocytes are important circulating APCs and are thought to be adversely affected by freeze-thawing of PBMCs, though some studies contradict this observation.[254] It was important, therefore, to compare CDI between PBMCs cultured fresh and after cryopreservation. This would furthermore serve as a test of assay repeatability. The LGI1-antibody patient from our initial successful experiment was re-run using cryopreserved cells from the same sample (Figure 7-7). Although a decrease in CDI was observed in a number of samples, the mean percentage change was 2.9 (SD 125.6) and the %CV was 71.6. Using a CDI greater than two as a cut-off, all peptides initially positive using fresh samples were positive when frozen samples. Given the logistical flexibility this allowed, as well as access to samples banked already in our laboratory, frozen PBMCs were utilised and are included in the final analysis.

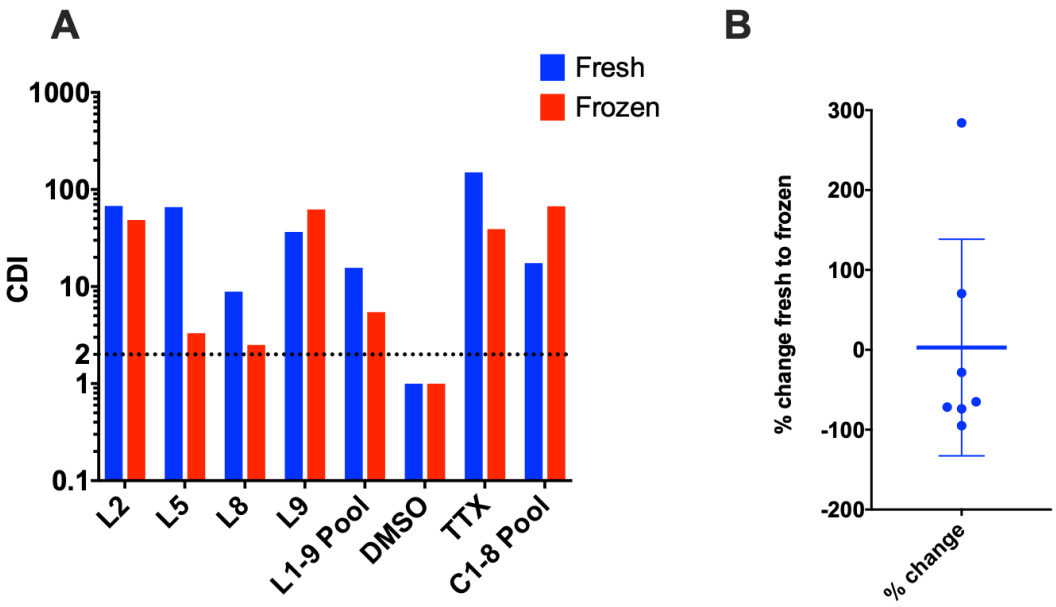


Figure 7-7 Fresh versus frozen PBMC T cell proliferation assay comparison

Comparison of the results of stimulation of the same patient PBMCs with the same peptides with the PBMCs used either fresh (blue) or frozen (red). A CDI of 2 was used as a positive cut-off (dotted line) and as you can see no CDI from the frozen sample fell below this line, mean percentage change was 2.9% (Standard deviation 125.6) and mean coefficient of variance was 71.6.

So far, it has been demonstrated that CD4+ T cells from LGI1-antibody patients could be induced to proliferate in response to certain peptides derived from the LGI1 protein. This response was reproducible and could be induced from fresh or frozen cells. In order to firmly conclude this expansion was taking place due to an interaction between class II-HLA peptide complexes and TCRs, a final experiment was performed where stained PBMCs were incubated with HLA-DR antibody prior to stimulation with peptide. In all instances where a positive expansion (CDI greater than 2) had been observed to a peptide, this was abrogated by the presence HLA-DR antibody (Figure 7-8), suggesting the peptide-HLA to TCR interaction is important to the expansion observed in patients.

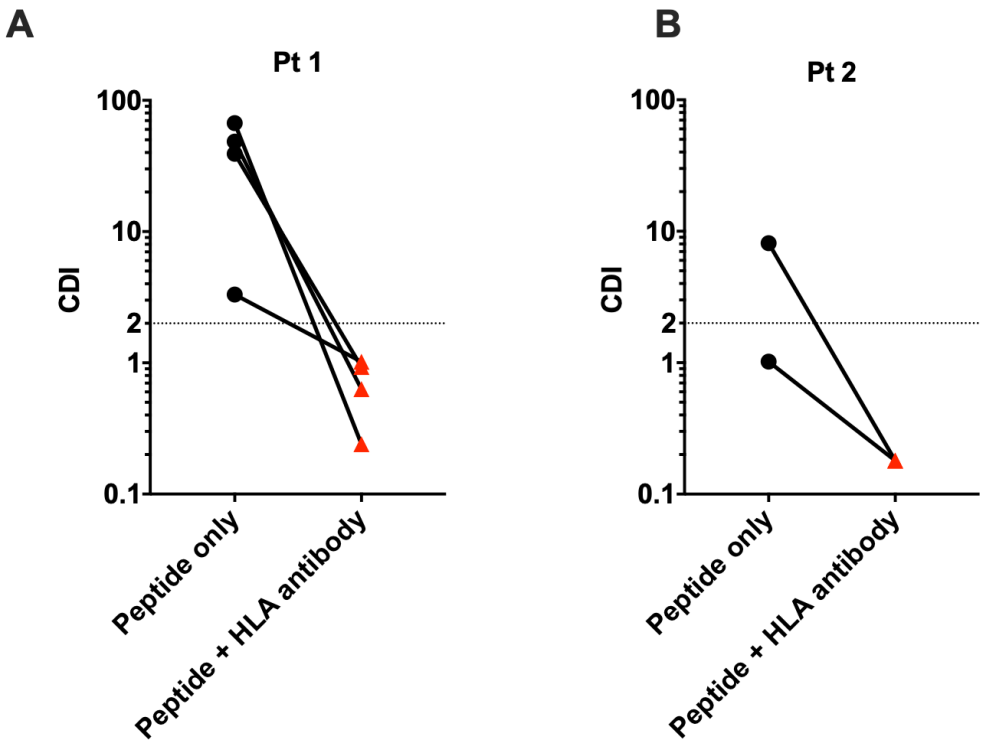


Figure 7-8 T cell proliferation in the presence of anti-HLA DR antibody

In the same assay, a comparison was made between stimulation of LGI1-antibody patient (n=2) PBMCs with peptides derived from full length LGI1, with or without preincubation with an HLA DR antibody for an hour at 37 ℃. In both patients, pre-incubation with the HLA DR antibody prevented any measurable proliferation.

7.6 Cohort-wide responses to relevant stimulating peptides

Having established a robust, reproducible T cell proliferation assay, screening was next undertaken on a range of LGI1-, CASPR2- and double positive antibody patients, as well as HCs. Peptides used to stimulate LGI1-antibody patients included all of the LGI1 peptides derived from the *in silico* modelling, with some of the CASPR2 peptides used as disease controls. To assess for a divergent effect of HLA-allele associations in the way peptides which complex together *in vivo* are processed, a similar logic was applied to CASPR2-antibody patients and the double positive patient. The HCs were assayed using both sets of peptides (Figure 7-9).

In the LGI1-antibody patients, 24/90 (26.7%) peptide pools targeting nine different core regions of the LGI1 protein induced CD4+ T cell expansion above assay cut-off for positivity. The cores reactive most often across patients were, in order, L9 (n=4), L7 (n=4), L8 (n=3) L6 (n=3) and L4 (n=3), with the rest all reactive in two patients each. 7/10 (70%) of patient T cells proliferated to TTX peptides. L4 and L7 were predicted to bind to HLA DQA1*02:01/DQB1*02:02 and L6, L8 and L9 to HLA DRB1*07:01. Patient HLA allele expression is displayed (Figure 7-9-A), with all patients carrying the DRB1*07:01 allele but no homozygous carriers.

In the CASPR2-antibody cohort, the situation is slightly different, as only 50% of these patients carry the HLA-DRB1*11:01 risk allele. 6/58 (10.3%) of CASPR2 derived peptide pools were positive and the most commonly reactive pool was C2 (n=2), with C3, C4, C6 and C7 all positive once (Figure 7-9-B). 5/6 of the positive expansions were seen in patient's carrying HLA DRB1*11:01, suggesting an effect of this allele, with C2, C3 and C7 predicted to associate with DRB1*11:01 and C4 with HLA DQA1*05:01/DQB1*03:01. C6 was included as a control, as it is not predicted to bind an HLA allele/haplotype associated with CASPR2-antibody

mediated disease (HLA DQA1*01:01/DQB1*05:03) but was positive in a patient with the following HLA DQ alleles: DQA1*05:01/03:01 and DQB1*03:01/03:02. This was an unexpected result and suggested an issue either with the *in silico* prediction or the assay itself.

The problem could be poor assay specificity, and indeed in LGI1-antibody patients 3/24 (12.5%) CASPR2 derived peptide pools provoke T cell expansions, and in CASPR2-antibody patients 2/33 (6%) LGI1 peptides did the same. It is worth noting, however, that the percentages are lower than the percentages of reactions to relevant peptides in both cases (LGI1 26.7% vs 12.5% and CASPR2 10.3% vs 6%, number of CD4+ expansions to antigen relevant peptide vs irrelevant peptide respectively). Most tellingly in HCs, 3/36 (8.3%) of LGI1- and 10/32 (31.3%) of CASPR2-derived peptides caused a positive expansion in these patients. Notably, the reaction to CASPR2 was seen in four healthy controls across all eight different CASPR2 peptide pools, suggesting it is a broad phenomenon, as opposed to being driven by a single patient or peptide.

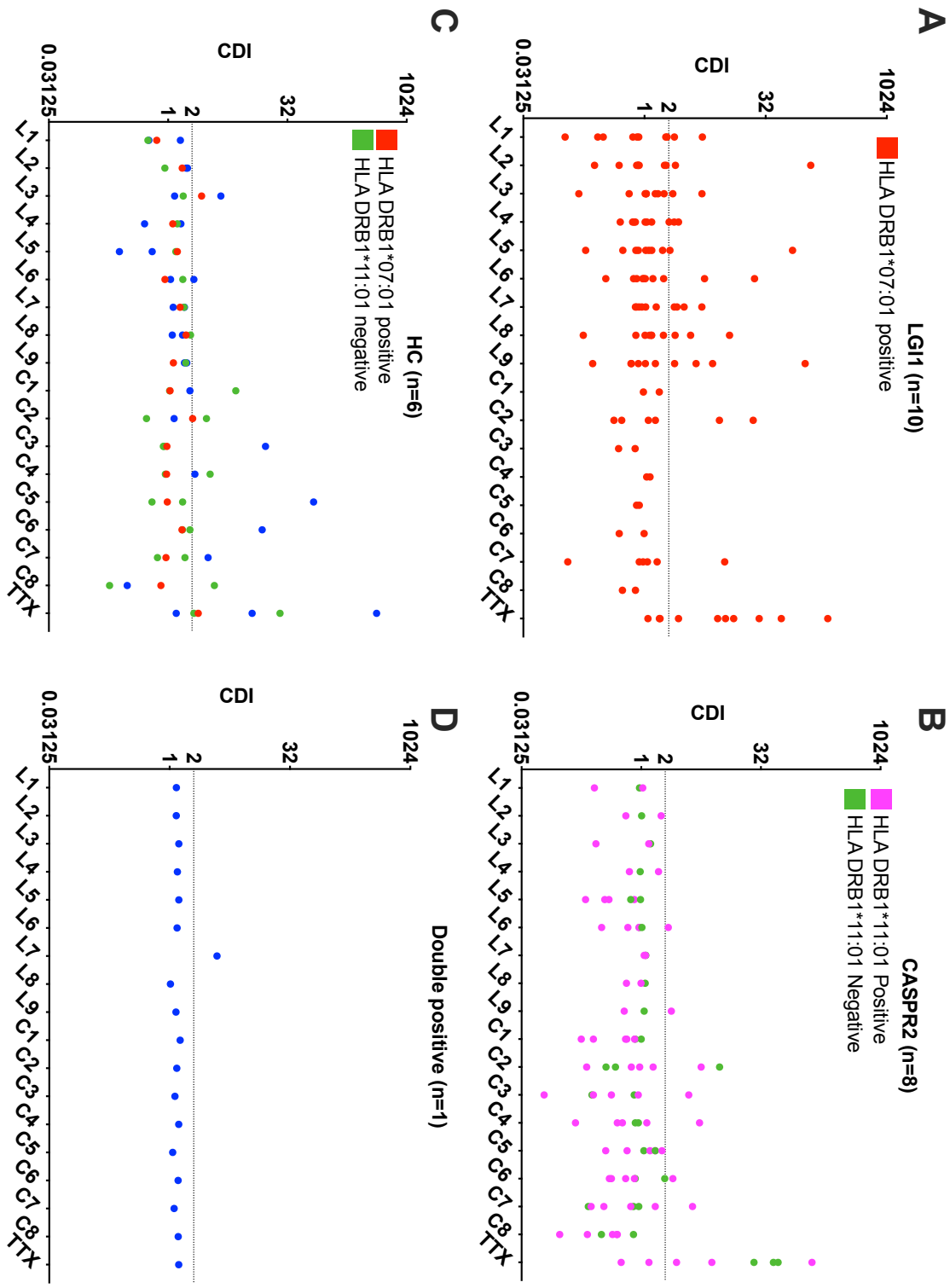


Figure 7-9 Cohort responses to stimulating peptides derived from FL LGI1 (L1-9) and CASPR2 (C1-8)

*CDI is plotted on a log2 scale on the y axis, on the x axis each peptide pool targeted to the relevant protein is represented. Dots represent the CDI of an individual patient derived from the pooled PBMCs from 6 wells for (A) LGI1-antibody patients, (B) CASPR2-antibody patients, (C) HCs and (D) A single double positive patient. Cut-off for positivity was a CDI greater than 2 and is represented by the dotted line. HLA DRB1*07:01 allele expression is represented by a*

*red dot in the LGI1-antibody patients and HCs (all were no carriers, no homozygotes), whereas, in the CASPR2-antibody and HC cohort, green represents confirmed non-carriers of HLA DRB1*11:01. The HC who carried HLA DRB1*07:01 did not carry DRB1*11:01, indeed none of the HC did. The double positive patient did not carry either disease associated HLA allele.*

One possibility is that patient CD4+ T cells are expanding non-specifically in the culture system, therefore the percentage of CD4+ T cells expanding in DMSO only (in the absence of peptide stimulation) was compared across patient groups and controls. No difference was seen, arguing against non-specific expansion driving observations ($p>0.05$, Kruskal Wallis, Figure 7-10). Next, the impact of clinical and specimen conditions on the ability of T cells to expand was assessed across all cohorts. No difference was seen if patients were on immunotherapy or not ($p=0.7401$, Mann-Whitney U, Figure 7-11-A) and no correlation was identified between when the sample was taken post disease onset and how many expansions to peptides were observed ($r= -0.0121$, 95% CI -0.4878 to 0.4691, $p=0.9619$, Spearman's r, Figure 7-11-B). Finally, no difference was seen in the number of expansions if the PBMCs were stained and stimulated from fresh or frozen ($p=0.9574$, Mann-Whitney U, Figure 7-11-C).

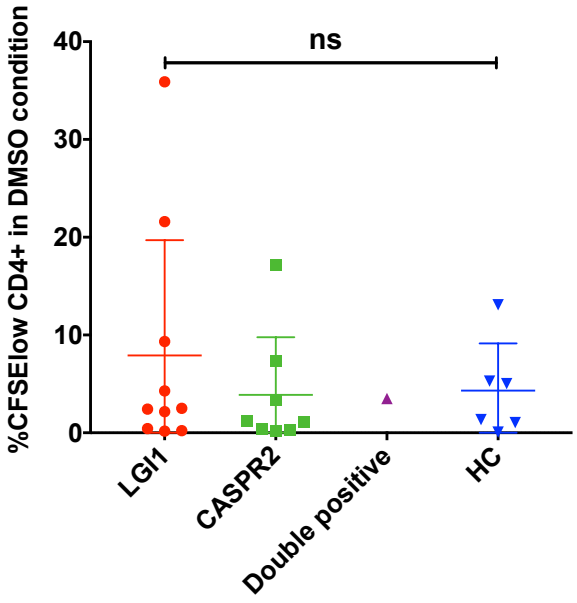


Figure 7-10 Comparison of the proliferation of CD4+ T cells in DMSO only conditions

The PBMCs incubated in only DMSO acted as our denominator when calculating CDI and some variability was noted between patients. This, % of expanded ($CFSE^{low}$) T helper (CD4+) in DMSO only conditions for individual patients is compared in the above graph between the four patients groups with no significant difference identified, p>0.05 (Kruskal Wallis).

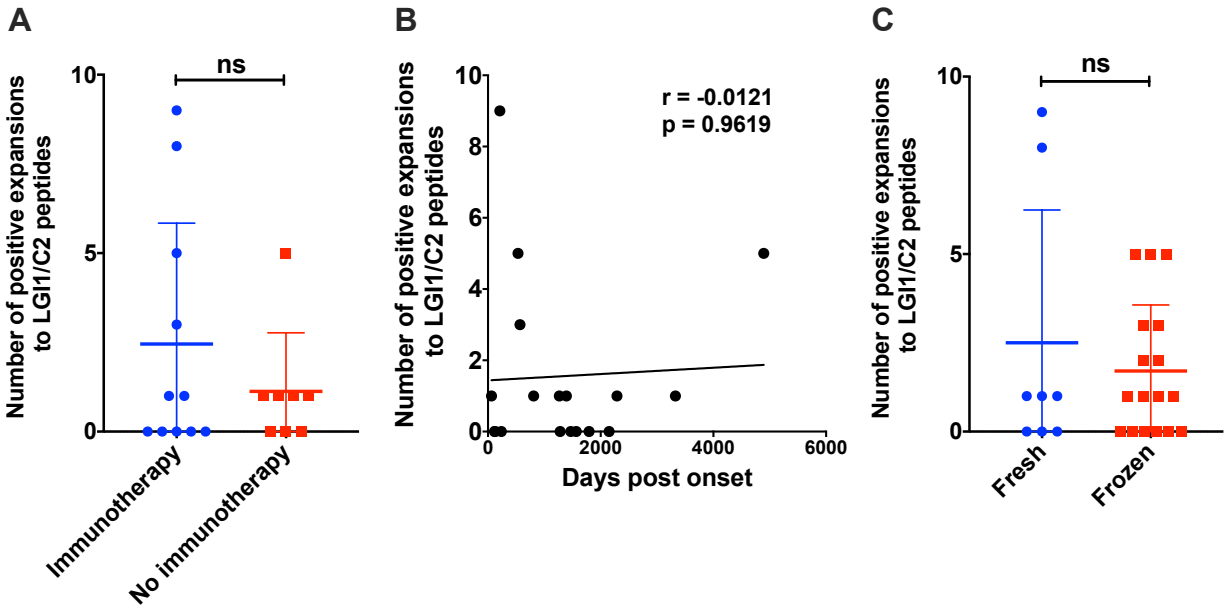


Figure 7-11 Effects of clinical and sample conditions on T cell proliferation

Comparison of the number of positive expansions above CDI cut-off for each patient by (A) on immunotherapy or not at time of sampling (no difference seen, p=0.7401, Mann-Whitney U) or (B) days post onset (Spearman's r). (C) Comparison of the number of positive expansions in patients and controls by whether sample stained and stimulated fresh or frozen, no difference seen (p=0.9574, Mann-Whitney-U).

7.7 Discussion

In order to further explore the significance of the class II HLA associations described in association with patients to CASPR2- and LGI1-antibodies, a T cell proliferation assay was developed using targeted *in silico* derived peptides from FL CASPR2 and LGI1. The *in silico* modelling highlighted peptides derived from CASPR2 and LGI1 which associated specifically with appropriate LGI1- and CASPR2-antibody associated HLA variants, as well as some peptides with a degree of promiscuity between both sets of variants, including HLA-DRB1*07:01 (Kim et al., 2017). This promiscuity may explain how immunisation with the same VGKC complex generates two distinct disease entities based on patient class HLA haplotype but also underlie the observed co-existence of both antibodies at a frequency significantly higher than would be expected by chance.[77] Peptides derived from both LGI1 and CASPR2 that were predicted to specifically bind to disease associated alleles were selected and used to develop a T cell proliferation assay from whole PBMCs.

The assay was optimised and it was determined in a LGI1-antibody patient that a proliferative response in CD4+ T cells could be induced by certain LGI1 derived-peptides over others. This expansion was found to be reproducible, with no significant difference noted using frozen over fresh samples. Furthermore, evidence supported this reaction as HLA-DR mediated as the addition of an HLA-DR antibody abrogated the previously observed expansions from two LGI1-antibody patients, suggesting presentation of peptide by an HLA molecule to a TCR was key to the observed expansion.

Preferential expansion of LGI1-patient CD4+ T cells was noted to LGI1 peptides and the same was seen in CASPR2-antibody patients with a strong suggestion that carrying HLA DRB1*11:01 was important for this expansion to take place in CASPR2-antibody patients.

LGI1-antibody patients were all HLA DRB1*07:01 carriers. With that in mind, of the four most proliferative pools, three were based on core sequences from the LGI1 protein predicted to bind favourably to DRB1*07:01 (L6, L8 and L9), again suggesting an effect of associated HLA on the proliferation of T cells. There was no dominant T cell epitope, with both patient groups expanding to peptides at various immunodominant positions along their respective antigenic molecules. This is similar to what is seen in narcolepsy[255] and myasthenia gravis.[256, 257]

There were issues with the dataset, most notably an expansion in CASPR2-antibody patient CD4 T cells to a peptide not predicted to associate with the HLA class II alleles carried by that patient and the high rate of reactivity to CASPR2-derived peptides in both LGI1-antibody patients and HCs. These observed differences were not driven by variations in immunotherapy, timing of sample to disease onset or whether samples were used fresh or frozen. Background expansion of T cells was noted to be varied across all patients but no disease specific differences were seen and this baseline reactivity is corrected for by the CDI calculation.

Some reactivity to disease-relevant peptides in HCs is often observed in studies based on CD4+ T cell proliferation, though it is usually less pronounced than in the disease cohort.[253, 255] In this study, CASPR2-antibody patient T cells responded to 10.3% of CASPR2 peptides while HCs responded to 31.25% of CASPR2 peptides. In marked contrast, the HC only responded to 8.3% of LGI1 peptides. The HCs are not fully genotyped and the expansion to CASPR2 peptides was across all pools and seen in a HC who was known HLA DRB1*11:01. This suggests HLA allele expression may not have a role in this observation. This could be a genuine phenomenon, as indeed CASPR2 is known to be expressed peripherally[209] and perhaps a certain level of reactivity to this peptide is common in HC CD4+ T cells.

A more fundamental issue could be that synthetically produced peptides which do not mirror physiologically processed and presented antigen were used. It is a consistent observation that T cells can be isolated which respond potently to synthetic peptide but not to full length protein of the same antigenic source.[255, 258, 259] From this observation two subsets of CD4+ T cells have been described; type A, which bind antigen when it has been processed intracellularly and loaded onto an HLA molecule in an endosome at pH 5 with the help of HLA-DM, and type B, which only bind the same antigen when it is loaded exogenously directly onto a plasma membrane class II HLA, without endosomal processing and HLA-DM editing.[260, 261] Type B T cells are a controversial entity in terms of their pathological relevance, though they have been described in mice with spontaneous diabetes.[262] The hypothesis is that by avoiding HLA-DM editing, unconventional peptides are presented which are not deleted by central tolerance and therefore provoke autoimmune disease.[263] The expanded cells seen may therefore not be disease relevant in every instance.

Other complicating factors include antigen specific T cell frequency. For each peptide, 1.2 million PBMCs were used and CD4+ T cells are thought to represent 60% of whole PBMCs.[264] This means roughly 700,000 CD4+ cells were used per peptide pool. Antigen specific memory T cell frequency has been estimated to be as low as 1-10 per million CD4+ cells,[255] and therefore may have been missed using this assay. A future experiment could use more PBMCs or an entirely different assay system. The *in silico* approach is inherently limited by the fact high affinity peptides are selected which are known to be more effectively deleted through central tolerance. Activation of T cells is an extremely complex interaction, influenced by the relative density of TCR and MHC-peptide complex, as well as the proximity and phenotype of interacting cells expressing co-receptors, adhesion molecules and co-stimulatory

molecules.[265, 266] Finally, peptides residues not in TCR binding positions can nevertheless affect the TCR and HLA-peptide complex interaction as well as the functional outcome.[267, 268]

The CD4+ T cells identified in this study appeared to be expanded in an HLA-DR dependent manner that was reproducible. In CASPR2-antibody patients, carriage of the DRB1*11:01 allele appeared to enhance T cell expansion and both LGI1- and CASPR2-antibody patients responded preferentially to their relevant peptides. The combination of these factors suggests these cells are disease relevant. This represents important *in vitro* evidence of the immunological contribution of CD4+ helper T cells, as well as CASPR2- and LGI1-associated class II HLA alleles, to disease. Future work should focus on validating the pathogenicity and relevance of the expanded T cells. This work could include in depth immunophenotyping, cloning and sequencing of TCRs (especially with comparison between patient and HC derived T cells), profiling of cytokines produced and further repeat sampling of individual samples to more firmly establish repeatability of these expansions. A final experiment could be to culture isolated antigen specific T cells with autologous B cell to assess their capacity to provide cognate help and stimulate antibody production *in vitro*.

8 Conclusions

NSAb-mediated neurological diseases are novel diseases where great strides have been made in terms of identifying new target antigens, defining phenotypes and proving the pathogenic potential of these antibodies. As with any new field, significant gaps remain, both in the clinical and basic science knowledge of these conditions. Through this thesis, translational work has been undertaken in an attempt to fill some of these gaps and improve

our understanding of how to diagnose NSAb mediated diseases as well as how they arise, from an immunological perspective.

The MD associated with NMDAR-AbE has been characterised in detail in a large cohort of patients, providing a consensus clinical description which will potentially aid diagnosis and recognition. This should lead to earlier treatment, with the well-described improvement in clinical outcome that this entails. The study also gives further insight into the underlying pathophysiology of this disease and serves to underline the key role that downregulation of NMDAR by autoantibodies play, providing further *in vivo* proof of NSAb pathogenicity.

No evidence supporting the existence of conformational NMDAR antibodies could be found in NPSLE. Further experiments suggested that antibodies to linear epitopes derived from the NMDAR may be artefactual and that biomarkers exist which may be useful in identifying SLE but not NPSLE. This helps to clarify a key area of controversy in the literature and should simplify the situation for clinicians dealing with these patients. The raised IFNα levels in SLE patients contributes to the growing literature highlighting interferon dysfunction as important in SLE, further underlining this as an important area of further exploration.

In order to better explain clinical observations made in patients with NSAbs, a hypothesis-driven driven question was asked about HLA associations and confirmed the description of a strong class II association in 92% of patients with LGI1-antibodies and found a novel association in 48% of patients with CASPR2-antibodies. These findings provide an explanation as to how immunisation with VGKC, complexed with other proteins, can give rise to different diseases based on individual genetic makeup. The class ll predominance, in combination with the worse response to immunotherapy and higher CASPR2-antibody titres in patients who carry HLA DRB1*11:01, suggests CD4+ T cells appear to have a significant role to play, despite these diseases being driven by pathogenic autoantibodies.

Investigations into whether patients with CASPR2-antibodies possessed circulating antigen specific B cells were fruitful, with experiments presented demonstrating their existence. It was also shown that production of these antibodies in culture correlates with serum CASPR2-antibody titre, suggesting a significant physiological contribution. Further evidence of their relevance was provided by the alignment between serum and supernatant CASPR2 IgG subclasses and epitopes. Most stimulant cytokines to CASPR2-antibody production in culture were those mimicking T cell help. Based on the measurement of proxy markers of germinal centre activity, little evidence of an ongoing contribution of germinal centres CASPR2-antibody patients was seen. The alternative explanation could be that circulating antigen specific B cells are tasked with renewing the bone marrow and other secondary lymphoid organs, allowing long term secretion of specific antibody. Finally, patients carrying the HLA DRB1*11:01 allele were found to make more CASPR2-antibody in culture against a wider range of CASPR2 epitopes. This reflected what was seen in serum, where CASPR2-antibody patients who did not carry HLA DRB1*11:01, had almost no circulating C-terminal specific CASPR2-antibodies. This suggested involvement of this allele in specific antibody production and also differentiation and maturation of the immune response, perhaps explaining the earlier observed difference in response to immunotherapy. Not only could this provide a clinical message, with risk allele carrying patients perhaps more appropriate targets for aggressive immunotherapy, it also provides an insight into potentially effective immunotherapy targets by underlining again the importance of the B and T cell interaction. The final branch of study, demonstrating that patients with LGI1- and CASPR2-antibodies appear to possess circulating antigen specific T cells, completes this supposition.

This thesis has therefore met its aim of advancing knowledge of NSAb-mediated neurological disorders, hopefully to the direct benefit of patients. A number of interesting

potential future directions have also arisen, particularly in terms of the cellular immunology of these disorders. Similar work based on circulating lymphocytes could be done in other NSAb mediated diseases, comparing specific antibody production, subclasses and epitopes longitudinally to see if further immunological differences emerge between this group of diseases. These studies could include sampling of alternate lymphocyte compartments, such as lymph nodes, spleen or bone marrow, in order to further address some of the questions raised in this thesis about the site of ongoing autoantibody production.

Isolation of either antigen-specific single B or T cells would inform a whole host of experiments. In CASPR2-antibody mediated disease, one possibility includes using antigen-specific B and T cell co-culture experiments to further probe the nature of their interaction. This could be done in the context of varied HLA carrier status, using naïve or memory cells and those with varied epitope specificity to further localise important points of contact which may represent novel and specific sites for design of immunotherapies. This could be complemented by molecular biology work on isolated antigen-specific B and T cells to analyse their phenotypes, VDJ gene usage and lineage to learn more about the key factors driving the onset and propagation of these diseases.

9 References

1. Janeway CA Jr TP, Walport M. Immunobiology: The Immune System in Health and Disease., 5th ed. New York: Garland Science, 2001.
2. Burnet FM. A modification of Jerne's theory of antibody production using the concept of clonal selection. *CA Cancer J Clin* 1976;26:119-121.
3. Anderson MS, Su MA. Aire and T cell development. *Curr Opin Immunol* 2011;23:198-206.
4. Shevach EM. Mechanisms of foxp3+ T regulatory cell-mediated suppression. *Immunity* 2009;30:636-645.
5. Yarkoni Y, Getahun A, Cambier JC. Molecular underpinning of B-cell anergy. *Immunol Rev* 2010;237:249-263.
6. Rosenblum MD, Remedios KA, Abbas AK. Mechanisms of human autoimmunity. *J Clin Invest* 2015;125:2228-2233.
7. Okada T, Miller MJ, Parker I, et al. Antigen-engaged B cells undergo chemotaxis toward the T zone and form motile conjugates with helper T cells. *PLoS Biol* 2005;3:e150.
8. Schwickert TA, Victora GD, Fooksman DR, et al. A dynamic T cell-limited checkpoint regulates affinity-dependent B cell entry into the germinal center. *J Exp Med* 2011;208:1243-1252.
9. Victora GD, Schwickert TA, Fooksman DR, et al. Germinal center dynamics revealed by multiphoton microscopy with a photoactivatable fluorescent reporter. *Cell* 2010;143:592-605.
10. Okazaki I, Yoshikawa K, Kinoshita K, Muramatsu M, Nagaoka H, Honjo T. Activation-induced cytidine deaminase links class switch recombination and somatic hypermutation. *Ann N Y Acad Sci* 2003;987:1-8.
11. Revy P, Muto T, Levy Y, et al. Activation-induced cytidine deaminase (AID) deficiency causes the autosomal recessive form of the Hyper-IgM syndrome (HIGM2). *Cell* 2000;102:565-575.
12. Wilson R, Makuch M, Kienzler AK, et al. Condition-dependent generation of aquaporin-4 antibodies from circulating B cells in neuromyelitis optica. *Brain* 2018;141:1063-1074.
13. Arahata K, Engel AG. Monoclonal antibody analysis of mononuclear cells in myopathies. I: Quantitation of subsets according to diagnosis and sites of accumulation and demonstration and counts of muscle fibers invaded by T cells. *Ann Neurol* 1984;16:193-208.
14. Aharonov A, Abramsky O, Tarrab-Hazdai R, Fuchs S. Humoral antibodies to acetylcholine receptor in patients with myasthenia gravis. *Lancet* 1975;2:340-342.
15. Varley J, Vincent A, Irani SR. Clinical and experimental studies of potentially pathogenic brain-directed autoantibodies: current knowledge and future directions. *J Neurol* 2015;262:1081-1095.
16. Damato V, Balint B, Kienzler AK, Irani SR. The clinical features, underlying immunology, and treatment of autoantibody-mediated movement disorders. *Mov Disord* 2018;33:1376-1389.
17. Waters P, Reindl M, Saiz A, et al. Multicentre comparison of a diagnostic assay: aquaporin-4 antibodies in neuromyelitis optica. *J Neurol Neurosurg Psychiatry* 2016;87:1005-1015.

18. Armangue T, Leypoldt F, Dalmau J. Autoimmune encephalitis as differential diagnosis of infectious encephalitis. *Curr Opin Neurol* 2014;27:361-368.
19. Irani SR, Gelfand JM, Al-Diwani A, Vincent A. Cell-surface central nervous system autoantibodies: Clinical relevance and emerging paradigms. *Ann Neurol* 2014;76:168-184.
20. Lancaster E, Dalmau J. Neuronal autoantigens--pathogenesis, associated disorders and antibody testing. *Nat Rev Neurol* 2012;8:380-390.
21. Hoftberger R, Rosenfeld MR, Dalmau J. Update on neurological paraneoplastic syndromes. *Curr Opin Oncol* 2015;27:489-495.
22. Zhang L, Qian W, Chen Q, Yin L, Li B, Wang H. Imbalance in circulating T lymphocyte subsets contributes to Hu antibody-associated paraneoplastic neurological syndromes. *Cell Immunol* 2014;290:245-250.
23. Kim TJ, Lee ST, Shin JW, et al. Clinical manifestations and outcomes of the treatment of patients with GABAB encephalitis. *J Neuroimmunol* 2014;270:45-50.
24. Vitaliani R, Mason W, Ances B, Zwerdling T, Jiang Z, Dalmau J. Paraneoplastic encephalitis, psychiatric symptoms, and hypoventilation in ovarian teratoma. *Ann Neurol* 2005;58:594-604.
25. Dalmau J, Tuzun E, Wu HY, et al. Paraneoplastic anti-N-methyl-D-aspartate receptor encephalitis associated with ovarian teratoma. *Ann Neurol* 2007;61:25-36.
26. Dalmau J, Gleichman AJ, Hughes EG, et al. Anti-NMDA-receptor encephalitis: case series and analysis of the effects of antibodies. *Lancet Neurol* 2008;7:1091-1098.
27. Titulaer MJ, McCracken L, Gabilondo I, et al. Treatment and prognostic factors for long-term outcome in patients with anti-NMDA receptor encephalitis: an observational cohort study. *Lancet Neurol* 2013;12:157-165.
28. Irani SR, Bera K, Waters P, et al. N-methyl-D-aspartate antibody encephalitis: temporal progression of clinical and paraclinical observations in a predominantly non-paraneoplastic disorder of both sexes. *Brain* 2010;133:1655-1667.
29. Adang LA, Lynch DR, Panzer JA. Pediatric anti-NMDA receptor encephalitis is seasonal. *Ann Clin Transl Neurol* 2014;1:921-925.
30. Kleinig TJ, Thompson PD, Matar W, et al. The distinctive movement disorder of ovarian teratoma-associated encephalitis. *Mov Disord* 2008;23:1256-1261.
31. Baizabal-Carvallo JF, Stocco A, Muscal E, Jankovic J. The spectrum of movement disorders in children with anti-NMDA receptor encephalitis. *Mov Disord* 2013;28:543-547.
32. Mohammad SS, Fung VS, Grattan-Smith P, et al. Movement disorders in children with anti-NMDAR encephalitis and other autoimmune encephalopathies. *Mov Disord* 2014;29:1539-1542.
33. Duan BC, Weng WC, Lin KL, et al. Variations of movement disorders in anti-N-methyl-D-aspartate receptor encephalitis: A nationwide study in Taiwan. *Medicine (Baltimore)* 2016;95:e4365.
34. Finke C, Kopp UA, Scheel M, et al. Functional and structural brain changes in anti-N-methyl-D-aspartate receptor encephalitis. *Ann Neurol* 2013;74:284-296.
35. Schmitt SE, Pargeon K, Frechette ES, Hirsch LJ, Dalmau J, Friedman D. Extreme delta brush: a unique EEG pattern in adults with anti-NMDA receptor encephalitis. *Neurology* 2012;79:1094-1100.
36. Tabata E, Masuda M, Eriguchi M, et al. Immunopathological significance of ovarian teratoma in patients with anti-N-methyl-d-aspartate receptor encephalitis. *Eur Neurol* 2014;71:42-48.

37. Dabner M, McCluggage WG, Bundell C, et al. Ovarian teratoma associated with anti-N-methyl D-aspartate receptor encephalitis: a report of 5 cases documenting prominent intratumoral lymphoid infiltrates. *Int J Gynecol Pathol* 2012;31:429-437.
38. Makuch M, Wilson R, Al-Diwani A, et al. N-methyl-D-aspartate receptor antibody production from germinal center reactions: Therapeutic implications. *Ann Neurol* 2018;83:553-561.
39. Pruss H, Finke C, Holtje M, et al. N-methyl-D-aspartate receptor antibodies in herpes simplex encephalitis. *Ann Neurol* 2012;72:902-911.
40. Gascon GG, al-Jarallah AA, Okamoto E, al Ahdal M, Kessie G, Frayha H. Chorea as a presentation of herpes simplex encephalitis relapse. *Brain Dev* 1993;15:178-181.
41. Armangue T, Leypoldt F, Malaga I, et al. Herpes simplex virus encephalitis is a trigger of brain autoimmunity. *Ann Neurol* 2014;75:317-323.
42. Hacohen Y, Deiva K, Pettingill P, et al. N-methyl-D-aspartate receptor antibodies in post-herpes simplex virus encephalitis neurological relapse. *Mov Disord* 2014;29:90-96.
43. Mohammad SS, Sinclair K, Pillai S, et al. Herpes simplex encephalitis relapse with chorea is associated with autoantibodies to N-Methyl-D-aspartate receptor or dopamine-2 receptor. *Mov Disord* 2014;29:117-122.
44. Westman G, Studahl M, Ahlm C, et al. N-methyl-d-aspartate receptor autoimmunity affects cognitive performance in herpes simplex encephalitis. *Clin Microbiol Infect* 2016;22:934-940.
45. Armangue T, Moris G, Cantarin-Extremera V, et al. Autoimmune post-herpes simplex encephalitis of adults and teenagers. *Neurology* 2015;85:1736-1743.
46. Li J, Xu Y, Ren H, Zhu Y, Peng B, Cui L. Autoimmune GFAP astrocytopathy after viral encephalitis: A case report. *Mult Scler Relat Disord* 2018;21:84-87.
47. Xu F, Sternberg MR, Kottiri BJ, et al. Trends in herpes simplex virus type 1 and type 2 seroprevalence in the United States. *JAMA* 2006;296:964-973.
48. Lau CG, Zukin RS. NMDA receptor trafficking in synaptic plasticity and neuropsychiatric disorders. *Nature reviews Neuroscience* 2007;8:413-426.
49. Wenthold RJ, Prybylowski K, Standley S, Sans N, Petralia RS. Trafficking of NMDA receptors. *Annual review of pharmacology and toxicology* 2003;43:335-358.
50. Kreye J, Wenke NK, Chayka M, et al. Human cerebrospinal fluid monoclonal N-methyl-D-aspartate receptor autoantibodies are sufficient for encephalitis pathogenesis. *Brain : a journal of neurology* 2016;139:2641-2652.
51. Moscato EH, Peng X, Jain A, Parsons TD, Dalmau J, Balice-Gordon RJ. Acute mechanisms underlying antibody effects in anti-N-methyl-D-aspartate receptor encephalitis. *Ann Neurol* 2014;76:108-119.
52. Hughes EG, Peng X, Gleichman AJ, et al. Cellular and synaptic mechanisms of anti-NMDA receptor encephalitis. *J Neurosci* 2010;30:5866-5875.
53. Tüzün E, Zhou L, Baehring JM, Bannykh S, Rosenfeld MR, Dalmau J. Evidence for antibody-mediated pathogenesis in anti-NMDAR encephalitis associated with ovarian teratoma. *Acta neuropathologica* 2009;118:737-743.
54. Martinez-Hernandez E, Horvath J, Shiloh-Malawsky Y, Sangha N, Martinez-Lage M, Dalmau J. Analysis of complement and plasma cells in the brain of patients with anti-NMDAR encephalitis. *Neurology* 2011;77:589-593.
55. Bien CG, Vincent A, Barnett MH, et al. Immunopathology of autoantibody-associated encephalitides: clues for pathogenesis. *Brain* 2012;135:1622-1638.

56. Planagumà J, Leypoldt F, Mannara F, et al. Human N-methyl D-aspartate receptor antibodies alter memory and behaviour in mice. *Brain : a journal of neurology* 2015;138:94-109.
57. Wright S, Hashemi K, Stasiak L, et al. Epileptogenic effects of NMDAR antibodies in a passive transfer mouse model. *Brain* 2015;138:3159-3167.
58. Hilderink M, Titulaer MJ, Schreurs MW, Keizer K, Bunt JE. Transient anti-NMDAR encephalitis in a newborn infant due to transplacental transmission. *Neurol Neuroimmunol Neuroinflamm* 2015;2:e126.
59. Nolt MJ, Lin Y, Hruska M, et al. EphB controls NMDA receptor function and synaptic targeting in a subunit-specific manner. *J Neurosci* 2011;31:5353-5364.
60. Mikasova L, De Rossi P, Bouchet D, et al. Disrupted surface cross-talk between NMDA and Ephrin-B2 receptors in anti-NMDA encephalitis. *Brain* 2012;135:1606-1621.
61. Planagumà J, Haselmann H, Mannara F, et al. Ephrin-B2 prevents N-methyl-D-aspartate receptor antibody effects on memory and neuroplasticity. *Annals of neurology* 2016;80:388-400.
62. McCarron MM, Schulze BW, Thompson GA, Conder MC, Goetz WA. Acute phencyclidine intoxication: incidence of clinical findings in 1,000 cases. *Ann Emerg Med* 1981;10:237-242.
63. Marco LA, Joshi RS. A ketamine-induced rat model of tardive dyskinesia. *Prog Neurobiol* 1992;38:571-600.
64. Curran HV, Morgan C. Cognitive, dissociative and psychotogenic effects of ketamine in recreational users on the night of drug use and 3 days later. *Addiction* 2000;95:575-590.
65. Moghaddam B, Javitt D. From revolution to evolution: the glutamate hypothesis of schizophrenia and its implication for treatment. *Neuropsychopharmacology* 2012;37:4-15.
66. Pathmanandavel K, Starling J, Merheb V, et al. Antibodies to surface dopamine-2 receptor and N-methyl-D-aspartate receptor in the first episode of acute psychosis in children. *Biol Psychiatry* 2015;77:537-547.
67. Zandi MS, Irani SR, Lang B, et al. Disease-relevant autoantibodies in first episode schizophrenia. *J Neurol* 2011;258:686-688.
68. Lennox BR, Palmer-Cooper EC, Pollak T, et al. Prevalence and clinical characteristics of serum neuronal cell surface antibodies in first-episode psychosis: a case-control study. *Lancet Psychiatry* 2017;4:42-48.
69. Dahm L, Ott C, Steiner J, et al. Seroprevalence of autoantibodies against brain antigens in health and disease. *Ann Neurol* 2014;76:82-94.
70. Steiner J, Teegen B, Schiltz K, Bernstein HG, Stoecker W, Bogerts B. Prevalence of N-methyl-D-aspartate receptor autoantibodies in the peripheral blood: healthy control samples revisited. *JAMA Psychiatry* 2014;71:838-839.
71. Oviedo-Salcedo T, de Witte L, Kumpfel T, et al. Absence of cerebrospinal fluid antineuronal antibodies in schizophrenia spectrum disorders. *Br J Psychiatry* 2018;212:318-320.
72. Al-Diwani A, Handel A, Townsend L, et al. The psychopathology of NMDAR-antibody encephalitis in adults: a systematic review and phenotypic analysis of individual patient data. *Lancet Psychiatry* 2019.
73. Thieben MJ, Lennon VA, Boeve BF, Aksamit AJ, Keegan M, Vernino S. Potentially reversible autoimmune limbic encephalitis with neuronal potassium channel antibody. *Neurology* 2004;62:1177-1182.

74. Vincent A, Buckley C, Schott JM, et al. Potassium channel antibody-associated encephalopathy: a potentially immunotherapy-responsive form of limbic encephalitis. *Brain* 2004;127:701-712.
75. Irani SR, Buckley C, Vincent A, et al. Immunotherapy-responsive seizure-like episodes with potassium channel antibodies. *Neurology* 2008;71:1647-1648.
76. Irani SR, Michell AW, Lang B, et al. Faciobrachial dystonic seizures precede Lgi1 antibody limbic encephalitis. *Ann Neurol* 2011;69:892-900.
77. Irani SR, Pettingill P, Kleopa KA, et al. Morvan syndrome: clinical and serological observations in 29 cases. *Ann Neurol* 2012;72:241-255.
78. Shillito P, Molenaar PC, Vincent A, et al. Acquired neuromyotonia: evidence for autoantibodies directed against K+ channels of peripheral nerves. *Ann Neurol* 1995;38:714-722.
79. Kleopa KA, Elman LB, Lang B, Vincent A, Scherer SS. Neuromyotonia and limbic encephalitis sera target mature Shaker-type K+ channels: subunit specificity correlates with clinical manifestations. *Brain* 2006;129:1570-1584.
80. Klein CJ, Lennon VA, Aston PA, et al. Insights from LGI1 and CASPR2 potassium channel complex autoantibody subtyping. *JAMA Neurol* 2013;70:229-234.
81. Irani SR, Alexander S, Waters P, et al. Antibodies to Kv1 potassium channel-complex proteins leucine-rich, glioma inactivated 1 protein and contactin-associated protein-2 in limbic encephalitis, Morvan's syndrome and acquired neuromyotonia. *Brain* 2010;133:2734-2748.
82. Lai M, Huijbers MG, Lancaster E, et al. Investigation of LGI1 as the antigen in limbic encephalitis previously attributed to potassium channels: a case series. *Lancet Neurol* 2010;9:776-785.
83. Lang B, Makuch M, Moloney T, et al. Intracellular and non-neuronal targets of voltage-gated potassium channel complex antibodies. *J Neurol Neurosurg Psychiatry* 2017;88:353-336.
84. Becker EB, Zuliani L, Pettingill R, et al. Contactin-associated protein-2 antibodies in non-paraneoplastic cerebellar ataxia. *J Neurol Neurosurg Psychiatry* 2012;83:437-440.
85. Irani SR, Stagg CJ, Schott JM, et al. Faciobrachial dystonic seizures: the influence of immunotherapy on seizure control and prevention of cognitive impairment in a broadening phenotype. *Brain* 2013;136:3151-3162.
86. Gadoth A, Pittock SJ, Dubey D, et al. Expanded phenotypes and outcomes among 256 LGI1/CASPR2-IgG-positive patients. *Ann Neurol* 2017;82:79-92.
87. Thompson J, Bi M, Murchison AG, et al. The importance of early immunotherapy in patients with faciobrachial dystonic seizures. *Brain* 2018;141:348-356.
88. van Sonderen A, Thijs RD, Coenders EC, et al. Anti-LGI1 encephalitis: Clinical syndrome and long-term follow-up. *Neurology* 2016;87:1449-1456.
89. Naasan G, Irani SR, Bettcher BM, Geschwind MD, Gelfand JM. Episodic bradycardia as neurocardiac prodrome to voltage-gated potassium channel complex/leucine-rich, glioma inactivated 1 antibody encephalitis. *JAMA Neurol* 2014;71:1300-1304.
90. Rocamora R, Becerra JL, Fossas P, et al. Pilomotor seizures: an autonomic semiology of limbic encephalitis? *Seizure* 2014;23:670-673.
91. Arino H, Armangue T, Petit-Pedrol M, et al. Anti-LGI1-associated cognitive impairment: Presentation and long-term outcome. *Neurology* 2016;87:759-765.
92. Navarro V, Kas A, Apartis E, et al. Motor cortex and hippocampus are the two main cortical targets in LGI1-antibody encephalitis. *Brain* 2016;139:1079-1093.

93. Malter MP, Frisch C, Schoene-Bake JC, et al. Outcome of limbic encephalitis with VGKC-complex antibodies: relation to antigenic specificity. *J Neurol* 2014;261:1695-1705.
94. Butler CR, Miller TD, Kaur MS, et al. Persistent anterograde amnesia following limbic encephalitis associated with antibodies to the voltage-gated potassium channel complex. *J Neurol Neurosurg Psychiatry* 2014;85:387-391.
95. Bettcher BM, Gelfand JM, Irani SR, et al. More than memory impairment in voltage-gated potassium channel complex encephalopathy. *Eur J Neurol* 2014;21:1301-1310.
96. Sirerol-Piquer MS, Ayerdi-Izquierdo A, Morante-Redolat JM, et al. The epilepsy gene LGI1 encodes a secreted glycoprotein that binds to the cell surface. *Hum Mol Genet* 2006;15:3436-3445.
97. Fukata Y, Lovero KL, Iwanaga T, et al. Disruption of LGI1-linked synaptic complex causes abnormal synaptic transmission and epilepsy. *Proc Natl Acad Sci U S A* 2010;107:3799-3804.
98. Ohkawa T, Fukata Y, Yamasaki M, et al. Autoantibodies to epilepsy-related LGI1 in limbic encephalitis neutralize LGI1-ADAM22 interaction and reduce synaptic AMPA receptors. *J Neurosci* 2013;33:18161-18174.
99. Petit-Pedrol M, Sell J, Planaguma J, et al. LGI1 antibodies alter Kv1.1 and AMPA receptors changing synaptic excitability, plasticity and memory. *Brain* 2018;141:3144-3159.
100. Irani SR, Gelfand JM, Bettcher BM, Singhal NS, Geschwind MD. Effect of rituximab in patients with leucine-rich, glioma-inactivated 1 antibody-associated encephalopathy. *JAMA Neurol* 2014;71:896-900.
101. Lancaster E, Huijbers MG, Bar V, et al. Investigations of caspr2, an autoantigen of encephalitis and neuromyotonia. *Ann Neurol* 2011;69:303-311.
102. van Sonderen A, Arino H, Petit-Pedrol M, et al. The clinical spectrum of Caspr2 antibody-associated disease. *Neurology* 2016;87:521-528.
103. Vincent A, Irani SR. Caspr2 antibodies in patients with thymomas. *J Thorac Oncol* 2010;5:S277-280.
104. Iwasaki Y, Kinoshita M, Ikeda K, Takamiya K, Shiojima T. Concurrence of myasthenia gravis and choree fibrillaire de Morvan. *Eur Arch Psychiatry Neurol Sci* 1990;239:335-336.
105. Poliak S, Salomon D, Elhanany H, et al. Juxtaparanodal clustering of Shaker-like K+ channels in myelinated axons depends on Caspr2 and TAG-1. *J Cell Biol* 2003;162:1149-1160.
106. Gu C, Gu Y. Clustering and activity tuning of Kv1 channels in myelinated hippocampal axons. *J Biol Chem* 2011;286:25835-25847.
107. Uhlen M, Fagerberg L, Hallstrom BM, et al. Proteomics. Tissue-based map of the human proteome. *Science* 2015;347:1260419.
108. Rodenas-Cuadrado P, Ho J, Vernes SC. Shining a light on CNTNAP2: complex functions to complex disorders. *Eur J Hum Genet* 2014;22:171-178.
109. van Sonderen A, Petit-Pedrol M, Dalmau J, Titulaer MJ. The value of LGI1, Caspr2 and voltage-gated potassium channel antibodies in encephalitis. *Nat Rev Neurol* 2017;13:290-301.
110. Bien CG, Mirzadjanova Z, Baumgartner C, et al. Anti-contactin-associated protein-2 encephalitis: relevance of antibody titres, presentation and outcome. *Eur J Neurol* 2017;24:175-186.
111. Patterson KR, Dalmau J, Lancaster E. Mechanisms of Caspr2 antibodies in autoimmune encephalitis and neuromyotonia. *Ann Neurol* 2017.

112. Olsen AL, Lai Y, Dalmau J, Scherer SS, Lancaster E. Caspr2 autoantibodies target multiple epitopes. *Neurol Neuroimmunol Neuroinflamm* 2015;2:e127.
113. Horresh I, Poliak S, Grant S, Bredt D, Rasband MN, Peles E. Multiple molecular interactions determine the clustering of Caspr2 and Kv1 channels in myelinated axons. *J Neurosci* 2008;28:14213-14222.
114. Ong E, Viaccoz A, Ducray F, et al. Dramatic improvement after rituximab in a patient with paraneoplastic treatment-refractory Morvan syndrome associated with anti-CASPR2 antibodies. *Eur J Neurol* 2013;20:e96-97.
115. Honorat JA, Komorowski L, Josephs KA, et al. IgLON5 antibody: Neurological accompaniments and outcomes in 20 patients. *Neurol Neuroimmunol Neuroinflamm* 2017;4:e385.
116. Gresa-Arribas N, Planaguma J, Petit-Pedrol M, et al. Human neurexin-3alpha antibodies associate with encephalitis and alter synapse development. *Neurology* 2016;86:2235-2242.
117. Florance NR, Davis RL, Lam C, et al. Anti-N-methyl-D-aspartate receptor (NMDAR) encephalitis in children and adolescents. *Ann Neurol* 2009;66:11-18.
118. Byrne S, Walsh C, Hacohen Y, et al. Earlier treatment of NMDAR antibody encephalitis in children results in a better outcome. *Neurol Neuroimmunol Neuroinflamm* 2015;2:e130.
119. Stamelou M, Plazzi G, Lugaresi E, Edwards MJ, Bhatia KP. The distinct movement disorder in anti-NMDA receptor encephalitis may be related to Status Dissociatus: a hypothesis. *Mov Disord* 2012;27:1360-1363.
120. Graus F, Titulaer MJ, Balu R, et al. A clinical approach to diagnosis of autoimmune encephalitis. *Lancet Neurol* 2016;15:391-404.
121. Bayreuther C, Bourg V, Dellamonica J, Borg M, Bernardin G, Thomas P. Complex partial status epilepticus revealing anti-NMDA receptor encephalitis. *Epileptic Disord* 2009;11:261-265.
122. McCarthy A, Dineen J, McKenna P, et al. Anti-NMDA receptor encephalitis with associated catatonia during pregnancy. *J Neurol* 2012;259:2632-2635.
123. Poloni C, Korff CM, Ricotti V, et al. Severe childhood encephalopathy with dyskinesia and prolonged cognitive disturbances: evidence for anti-N-methyl-D-aspartate receptor encephalitis. *Dev Med Child Neurol* 2010;52:e78-82.
124. Wong-Kisiel LC, Ji T, Renaud DL, et al. Response to immunotherapy in a 20-month-old boy with anti-NMDA receptor encephalitis. *Neurology* 2010;74:1550-1551.
125. Xia C, Dubeau F. Teaching Video NeuroImages: dystonic posturing in anti-NMDA receptor encephalitis. *Neurology* 2011;76:e80.
126. Fasano A, Nardocci N, Elia AE, Zorzi G, Bentivoglio AR, Albanese A. Non-DYT1 early-onset primary torsion dystonia: comparison with DYT1 phenotype and review of the literature. *Mov Disord* 2006;21:1411-1418.
127. Goto S, Yamada K, Shimazu H, et al. Impact of bilateral pallidal stimulation on DYT1-generalized dystonia in Japanese patients. *Mov Disord* 2006;21:1785-1787.
128. Guehl D, Cuny E, Tison F, et al. Deep brain pallidal stimulation for movement disorders in neuroacanthocytosis. *Neurology* 2007;68:160-161.
129. Cimaz R, Gana S, Braccesi G, Guerrini R. Sydenham's chorea in a girl with juvenile idiopathic arthritis treated with anti-TNFalpha therapy. *Mov Disord* 2010;25:511-514.
130. Camargos S, Lees AJ, Singleton A, Cardoso F. DYT16: the original cases. *J Neurol Neurosurg Psychiatry* 2012;83:1012-1014.

131. Goldman S, Temudo T. Hand stereotypies distinguish Rett syndrome from autism disorder. *Mov Disord* 2012;27:1060-1062.
132. Kobylecki C, Damodaran D, Kerr B, Newton RW, Silverdale MA. Prominent Lower-Limb Involvement in a Family with Myoclonus-Dystonia. *Movement Disorders Clinical Practice* 2014;1:115-117.
133. Myers PJ, Kane KE, Porter BG, Mazzaccaro RJ. Sydenham Chorea: rare consequence of rheumatic fever. *West J Emerg Med* 2014;15:840.
134. Thompson S, Iyer A, Byrd P, Taylor M, Spinty S. Dopa-Responsive Dystonia and Chorea as a Presenting Feature in Ataxia-Telangiectasia. *Movement Disorders Clinical Practice* 2014;1:249-251.
135. Carapito R, Paul N, Untrau M, et al. A de novo ADCY5 mutation causes early-onset autosomal dominant chorea and dystonia. *Mov Disord* 2015;30:423-427.
136. Cellini E, Vignoli A, Pisano T, et al. The hyperkinetic movement disorder of FOXG1-related epileptic-dyskinetic encephalopathy. *Dev Med Child Neurol* 2016;58:93-97.
137. Abdo WF, van de Warrenburg BP, Burn DJ, Quinn NP, Bloem BR. The clinical approach to movement disorders. *Nat Rev Neurol* 2010;6:29-37.
138. Varley JA, Webb AJS, Balint B, et al. The Movement disorder associated with NMDAR antibody-encephalitis is complex and characteristic: an expert video-rating study. *J Neurol Neurosurg Psychiatry* 2018.
139. Finke C, Kopp UA, Pruss H, Dalmau J, Wandinger KP, Ploner CJ. Cognitive deficits following anti-NMDA receptor encephalitis. *J Neurol Neurosurg Psychiatry* 2012;83:195-198.
140. Krzywinski M, Schein J, Birol I, et al. Circos: an information aesthetic for comparative genomics. *Genome Res* 2009;19:1639-1645.
141. Sanger TD, Chen D, Fehlings DL, et al. Definition and classification of hyperkinetic movements in childhood. *Mov Disord* 2010;25:1538-1549.
142. Tandon R, Heckers S, Bustillo J, et al. Catatonia in DSM-5. *Schizophr Res* 2013;150:26-30.
143. Edwards MJ, Lang AE, Bhatia KP. Stereotypies: a critical appraisal and suggestion of a clinically useful definition. *Mov Disord* 2012;27:179-185.
144. Jankovic J. Stereotypies. In: Marsden CD FS, eds. . Movement Disorders, 3rd ed1994.
145. Temudo T, Oliveira P, Santos M, et al. Stereotypies in Rett syndrome: analysis of 83 patients with and without detected MECP2 mutations. *Neurology* 2007;68:1183-1187.
146. Prioni S, Fetoni V, Barocco F, et al. Stereotypic behaviors in degenerative dementias. *J Neurol* 2012;259:2452-2459.
147. Mink JW. The Basal Ganglia and involuntary movements: impaired inhibition of competing motor patterns. *Arch Neurol* 2003;60:1365-1368.
148. Lemke JR, Geider K, Helbig KL, et al. Delineating the GRIN1 phenotypic spectrum: A distinct genetic NMDA receptor encephalopathy. *Neurology* 2016;86:2171-2178.
149. Marco LA, Pendleton R, Reed TF, Brigham TE, Aldes LD, Chronister RB. Ketamine-induced tongue protrusions in rats. *Comp Biochem Physiol C* 1989;94:29-33.
150. Rosch RE, Wright S, Cooray G, et al. NMDA-receptor antibodies alter cortical microcircuit dynamics. *Proc Natl Acad Sci U S A* 2018;115:E9916-E9925.
151. Somers EC, Marder W, Cagnoli P, et al. Population-based incidence and prevalence of systemic lupus erythematosus: the Michigan Lupus Epidemiology and Surveillance program. *Arthritis Rheumatol* 2014;66:369-378.
152. Popescu A, Kao AH. Neuropsychiatric systemic lupus erythematosus. *Curr Neuropharmacol* 2011;9:449-457.

153. DeGiorgio LA, Konstantinov KN, Lee SC, Hardin JA, Volpe BT, Diamond B. A subset of lupus anti-DNA antibodies cross-reacts with the NR2 glutamate receptor in systemic lupus erythematosus. *Nat Med* 2001;7:1189-1193.
154. Gaynor B, Putterman C, Valadon P, Spatz L, Scharff MD, Diamond B. Peptide inhibition of glomerular deposition of an anti-DNA antibody. *Proc Natl Acad Sci U S A* 1997;94:1955-1960.
155. Kowal C, Degiorgio LA, Lee JY, et al. Human lupus autoantibodies against NMDA receptors mediate cognitive impairment. *Proc Natl Acad Sci U S A* 2006;103:19854-19859.
156. Fragoso-Loyo H, Cabiedes J, Orozco-Narvaez A, et al. Serum and cerebrospinal fluid autoantibodies in patients with neuropsychiatric lupus erythematosus. Implications for diagnosis and pathogenesis. *PLoS One* 2008;3:e3347.
157. Gono T, Kawaguchi Y, Kaneko H, et al. Anti-NR2A antibody as a predictor for neuropsychiatric systemic lupus erythematosus. *Rheumatology (Oxford)* 2011;50:1578-1585.
158. Hanly JG, Robichaud J, Fisk JD. Anti-NR2 glutamate receptor antibodies and cognitive function in systemic lupus erythematosus. *J Rheumatol* 2006;33:1553-1558.
159. Steup-Beekman G, Steens S, van Buchem M, Huizinga T. Anti-NMDA receptor autoantibodies in patients with systemic lupus erythematosus and their first-degree relatives. *Lupus* 2007;16:329-334.
160. Gulati G, Iffland PH, 2nd, Janigro D, Zhang B, Luggen ME. Anti-NR2 antibodies, blood-brain barrier, and cognitive dysfunction. *Clin Rheumatol* 2016.
161. Tay SH, Fairhurst AM, Mak A. Clinical utility of circulating anti-N-methyl-d-aspartate receptor subunits NR2A/B antibody for the diagnosis of neuropsychiatric syndromes in systemic lupus erythematosus and Sjogren's syndrome: An updated meta-analysis. *Autoimmun Rev* 2017;16:114-122.
162. Chasset F, Arnaud L. Targeting interferons and their pathways in systemic lupus erythematosus. *Autoimmunity Reviews* 2018;17:44-52.
163. Gota C, Calabrese L. Induction of clinical autoimmune disease by therapeutic interferon-alpha. *Autoimmunity* 2003;36:511-518.
164. Hooks JJ, Moutsopoulos HM, Geis SA, Stahl NI, Decker JL, Notkins AL. Immune interferon in the circulation of patients with autoimmune disease. *N Engl J Med* 1979;301:5-8.
165. Shiozawa S, Kuroki Y, Kim M, Hirohata S, Ogino T. Interferon-alpha in lupus psychosis. *Arthritis Rheum* 1992;35:417-422.
166. Trysberg E, Carlsten H, Tarkowski A. Intrathecal cytokines in systemic lupus erythematosus with central nervous system involvement. *Lupus* 2000;9:498-503.
167. Kirou KA, Lee C, George S, et al. Coordinate overexpression of interferon-alpha-induced genes in systemic lupus erythematosus. *Arthritis Rheum* 2004;50:3958-3967.
168. Coit P, Jeffries M, Altorok N, et al. Genome-wide DNA methylation study suggests epigenetic accessibility and transcriptional poising of interferon-regulated genes in naive CD4+ T cells from lupus patients. *J Autoimmun* 2013;43:78-84.
169. Banchereau R, Hong S, Cantarel B, et al. Personalized Immunomonitoring Uncovers Molecular Networks that Stratify Lupus Patients. *Cell* 2016;165:551-565.
170. Hua J, Kirou K, Lee C, Crow MK. Functional assay of type I interferon in systemic lupus erythematosus plasma and association with anti-RNA binding protein autoantibodies. *Arthritis Rheum* 2006;54:1906-1916.

171. Rodero MP, Decalf J, Bondet V, et al. Detection of interferon alpha protein reveals differential levels and cellular sources in disease. *J Exp Med* 2017;214:1547-1555.
172. The American College of Rheumatology nomenclature and case definitions for neuropsychiatric lupus syndromes. *Arthritis Rheum* 1999;42:599-608.
173. Greig NH, Fredericks WR, Holloway HW, Soncrant TT, Rapoport SI. Delivery of human interferon-alpha to brain by transient osmotic blood-brain barrier modification in the rat. *J Pharmacol Exp Ther* 1988;245:581-586.
174. Probstel AK, Thanei M, Erni B, et al. Association of antibodies against myelin and neuronal antigens with neuroinflammation in systemic lupus erythematosus. *Rheumatology (Oxford)* 2018.
175. Arinuma Y, Yanagida T, Hirohata S. Association of cerebrospinal fluid anti-NR2 glutamate receptor antibodies with diffuse neuropsychiatric systemic lupus erythematosus. *Arthritis Rheum* 2008;58:1130-1135.
176. Bialas AR, Presumey J, Das A, et al. Microglia-dependent synapse loss in type I interferon-mediated lupus. *Nature* 2017;546:539-543.
177. Santer DM, Yoshio T, Minota S, Moller T, Elkon KB. Potent induction of IFN-alpha and chemokines by autoantibodies in the cerebrospinal fluid of patients with neuropsychiatric lupus. *J Immunol* 2009;182:1192-1201.
178. Morimoto AM, Flesher DT, Yang J, et al. Association of endogenous anti-interferon-alpha autoantibodies with decreased interferon-pathway and disease activity in patients with systemic lupus erythematosus. *Arthritis Rheum* 2011;63:2407-2415.
179. Becker AM, Dao KH, Han BK, et al. SLE peripheral blood B cell, T cell and myeloid cell transcriptomes display unique profiles and each subset contributes to the interferon signature. *PLoS One* 2013;8:e67003.
180. Chaussabel D, Quinn C, Shen J, et al. A modular analysis framework for blood genomics studies: application to systemic lupus erythematosus. *Immunity* 2008;29:150-164.
181. Feng X, Wu H, Grossman JM, et al. Association of increased interferon-inducible gene expression with disease activity and lupus nephritis in patients with systemic lupus erythematosus. *Arthritis Rheum* 2006;54:2951-2962.
182. Landolt-Marticorena C, Bonventi G, Lubovich A, et al. Lack of association between the interferon-alpha signature and longitudinal changes in disease activity in systemic lupus erythematosus. *Ann Rheum Dis* 2009;68:1440-1446.
183. Petri M, Singh S, Tesfasyone H, et al. Longitudinal expression of type I interferon responsive genes in systemic lupus erythematosus. *Lupus* 2009;18:980-989.
184. Sibbitt WL, Jr., Brooks WM, Kornfeld M, Hart BL, Bankhurst AD, Roldan CA. Magnetic resonance imaging and brain histopathology in neuropsychiatric systemic lupus erythematosus. *Semin Arthritis Rheum* 2010;40:32-52.
185. Afeltra A, Garzia P, Mitterhofer AP, et al. Neuropsychiatric lupus syndromes: relationship with antiphospholipid antibodies. *Neurology* 2003;61:108-110.
186. Sciascia S, Bertolaccini ML, Roccatello D, Khamashta MA, Sanna G. Autoantibodies involved in neuropsychiatric manifestations associated with systemic lupus erythematosus: a systematic review. *J Neurol* 2014;261:1706-1714.
187. Devinsky O, Petito CK, Alonso DR. Clinical and neuropathological findings in systemic lupus erythematosus: the role of vasculitis, heart emboli, and thrombotic thrombocytopenic purpura. *Ann Neurol* 1988;23:380-384.
188. McCormack M, Alfirevic A, Bourgeois S, et al. HLA-A*3101 and carbamazepine-induced hypersensitivity reactions in Europeans. *N Engl J Med* 2011;364:1134-1143.

189. Yip VL, Alfirevic A, Pirmohamed M. Genetics of immune-mediated adverse drug reactions: a comprehensive and clinical review. *Clin Rev Allergy Immunol* 2015;48:165-175.
190. van Sonderen A, Roelen DL, Stoop JA, et al. Anti-LGI1 encephalitis is strongly associated with HLA-DR7 and HLA-DRB4. *Ann Neurol* 2016.
191. Kim TJ, Lee ST, Moon J, et al. Anti-LGI1 Encephalitis is Associated with Unique HLA Subtypes. *Ann Neurol* 2016.
192. Choo SY. The HLA system: genetics, immunology, clinical testing, and clinical implications. *Yonsei Med J* 2007;48:11-23.
193. Binks SNM, Klein CJ, Waters P, Pittock SJ, Irani SR. LGI1, CASPR2 and related antibodies: a molecular evolution of the phenotypes. *J Neurol Neurosurg Psychiatry* 2018;89:526-534.
194. Meeusen JW, Klein CJ, Pirko I, et al. Potassium channel complex autoimmunity induced by inhaled brain tissue aerosol. *Ann Neurol* 2012;71:417-426.
195. Binks S, Varley J, Lee W, et al. Distinct HLA associations of LGI1 and CASPR2-antibody diseases. *Brain* 2018.
196. Jia X, Han B, Onengut-Gumuscu S, et al. Imputing amino acid polymorphisms in human leukocyte antigens. *PLoS One* 2013;8:e64683.
197. Neville MJ, Lee W, Humburg P, et al. High resolution HLA haplotyping by imputation for a British population bioresource. *Hum Immunol* 2017;78:242-251.
198. Bunce M, O'Neill CM, Barnardo MC, et al. Phototyping: comprehensive DNA typing for HLA-A, B, C, DRB1, DRB3, DRB4, DRB5 & DQB1 by PCR with 144 primer mixes utilizing sequence-specific primers (PCR-SSP). *Tissue Antigens* 1995;46:355-367.
199. Stephens M, Donnelly P. A comparison of bayesian methods for haplotype reconstruction from population genotype data. *Am J Hum Genet* 2003;73:1162-1169.
200. Stephens M, Smith NJ, Donnelly P. A new statistical method for haplotype reconstruction from population data. *Am J Hum Genet* 2001;68:978-989.
201. Gonzalez-Galarza FF, Takeshita LY, Santos EJ, et al. Allele frequency net 2015 update: new features for HLA epitopes, KIR and disease and HLA adverse drug reaction associations. *Nucleic Acids Res* 2015;43:D784-788.
202. Huijbers MG, Querol LA, Niks EH, et al. The expanding field of IgG4-mediated neurological autoimmune disorders. *Eur J Neurol* 2015;22:1151-1161.
203. Wirtz PW, Willcox N, van der Slik AR, et al. HLA and smoking in prediction and prognosis of small cell lung cancer in autoimmune Lambert-Eaton myasthenic syndrome. *J Neuroimmunol* 2005;159:230-237.
204. Trowsdale J, Knight JC. Major histocompatibility complex genomics and human disease. *Annu Rev Genomics Hum Genet* 2013;14:301-323.
205. Gresa-Arribas N, Titulaer MJ, Torrents A, et al. Antibody titres at diagnosis and during follow-up of anti-NMDA receptor encephalitis: a retrospective study. *Lancet Neurol* 2014;13:167-177.
206. Hoffman W, Lakkis FG, Chalasani G. B Cells, Antibodies, and More. *Clin J Am Soc Nephrol* 2016;11:137-154.
207. Gadoth A, Zekeridou A, Klein CJ, et al. Elevated LGI1-IgG CSF index predicts worse neurological outcome. *Ann Clin Transl Neurol* 2018;5:646-650.
208. Waters PJ, McKeon A, Leite MI, et al. Serologic diagnosis of NMO: a multicenter comparison of aquaporin-4-IgG assays. *Neurology* 2012;78:665-671; discussion 669.

209. Dawes JM, Weir GA, Middleton SJ, et al. Immune or Genetic-Mediated Disruption of CASPR2 Causes Pain Hypersensitivity Due to Enhanced Primary Afferent Excitability. *Neuron* 2018.
210. Dalakas MC. B cells as therapeutic targets in autoimmune neurological disorders. *Nat Clin Pract Neurol* 2008;4:557-567.
211. Caraux A, Klein B, Paiva B, et al. Circulating human B and plasma cells. Age-associated changes in counts and detailed characterization of circulating normal CD138- and CD138+ plasma cells. *Haematologica* 2010;95:1016-1020.
212. Chihara N, Aranami T, Sato W, et al. Interleukin 6 signaling promotes anti-aquaporin 4 autoantibody production from plasmablasts in neuromyelitis optica. *Proc Natl Acad Sci U S A* 2011;108:3701-3706.
213. Berglund LJ, Avery DT, Ma CS, et al. IL-21 signalling via STAT3 primes human naive B cells to respond to IL-2 to enhance their differentiation into plasmablasts. *Blood* 2013;122:3940-3950.
214. Liba Z, Kayserova J, Elisak M, et al. Anti-N-methyl-D-aspartate receptor encephalitis: the clinical course in light of the chemokine and cytokine levels in cerebrospinal fluid. *J Neuroinflammation* 2016;13:55.
215. Kothur K, Wienholt L, Mohammad SS, et al. Utility of CSF Cytokine/Chemokines as Markers of Active Intrathecal Inflammation: Comparison of Demyelinating, Anti-NMDAR and Enteroviral Encephalitis. *PLoS One* 2016;11:e0161656.
216. Byun JI, Lee ST, Moon J, et al. Distinct intrathecal interleukin-17/interleukin-6 activation in anti-N-methyl-d-aspartate receptor encephalitis. *J Neuroimmunol* 2016;297:141-147.
217. Leypoldt F, Hoftberger R, Titulaer MJ, et al. Investigations on CXCL13 in anti-N-methyl-D-aspartate receptor encephalitis: a potential biomarker of treatment response. *JAMA Neurol* 2015;72:180-186.
218. Gonzalez-Quintela A, Alende R, Gude F, et al. Serum levels of immunoglobulins (IgG, IgA, IgM) in a general adult population and their relationship with alcohol consumption, smoking and common metabolic abnormalities. *Clin Exp Immunol* 2008;151:42-50.
219. Schauer U, Stemberg F, Rieger CH, et al. IgG subclass concentrations in certified reference material 470 and reference values for children and adults determined with the binding site reagents. *Clin Chem* 2003;49:1924-1929.
220. Pene J, Gauchat JF, Lecart S, et al. Cutting edge: IL-21 is a switch factor for the production of IgG1 and IgG3 by human B cells. *J Immunol* 2004;172:5154-5157.
221. Jeannin P, Lecoanet S, Delneste Y, Gauchat JF, Bonnefoy JY. IgE versus IgG4 production can be differentially regulated by IL-10. *J Immunol* 1998;160:3555-3561.
222. Havenar-Daughton C, Lindqvist M, Heit A, et al. CXCL13 is a plasma biomarker of germinal center activity. *Proc Natl Acad Sci U S A* 2016;113:2702-2707.
223. Fecher P, Caspell R, Naeem V, Karulin AY, Kuerten S, Lehmann PV. B Cells and B Cell Blasts Withstand Cryopreservation While Retaining Their Functionality for Producing Antibody. *Cells* 2018;7.
224. Asao H, Okuyama C, Kumaki S, et al. Cutting edge: the common gamma-chain is an indispensable subunit of the IL-21 receptor complex. *J Immunol* 2001;167:1-5.
225. Jeannin P, Delneste Y, Lecoanet-Henchoz S, Gretener D, Bonnefoy JY. Interleukin-7 (IL-7) enhances class switching to IgE and IgG4 in the presence of T cells via IL-9 and sCD23. *Blood* 1998;91:1355-1361.

226. Armitage RJ, Macduff BM, Eisenman J, Paxton R, Grabstein KH. IL-15 has stimulatory activity for the induction of B cell proliferation and differentiation. *J Immunol* 1995;154:483-490.
227. Werner-Favre C, Bovia F, Schneider P, et al. IgG subclass switch capacity is low in switched and in IgM-only, but high in IgD+IgM+, post-germinal center (CD27+) human B cells. *Eur J Immunol* 2001;31:243-249.
228. Avery DT, Bryant VL, Ma CS, de Waal Malefyt R, Tangye SG. IL-21-induced isotype switching to IgG and IgA by human naive B cells is differentially regulated by IL-4. *J Immunol* 2008;181:1767-1779.
229. Good KL, Bryant VL, Tangye SG. Kinetics of human B cell behavior and amplification of proliferative responses following stimulation with IL-21. *J Immunol* 2006;177:5236-5247.
230. Bryant VL, Ma CS, Avery DT, et al. Cytokine-mediated regulation of human B cell differentiation into Ig-secreting cells: predominant role of IL-21 produced by CXCR5+ T follicular helper cells. *J Immunol* 2007;179:8180-8190.
231. Mingari MC, Gerosa F, Carra G, et al. Human interleukin-2 promotes proliferation of activated B cells via surface receptors similar to those of activated T cells. *Nature* 1984;312:641-643.
232. Chtanova T, Tangye SG, Newton R, et al. T follicular helper cells express a distinctive transcriptional profile, reflecting their role as non-Th1/Th2 effector cells that provide help for B cells. *J Immunol* 2004;173:68-78.
233. Bernasconi NL, Traggiai E, Lanzavecchia A. Maintenance of serological memory by polyclonal activation of human memory B cells. *Science* 2002;298:2199-2202.
234. Leyendeckers H, Odendahl M, Lohndorf A, et al. Correlation analysis between frequencies of circulating antigen-specific IgG-bearing memory B cells and serum titers of antigen-specific IgG. *Eur J Immunol* 1999;29:1406-1417.
235. Valentino P, Marnetto F, Granieri L, Capobianco M, Bertolotto A. Aquaporin-4 antibody titration in NMO patients treated with rituximab: A retrospective study. *Neurol Neuroimmunol Neuroinflamm* 2017;4:e317.
236. Richardson CC, McLaughlin KA, Morgan D, Feltbower RG, Christie MR. Influence of HLA-DR and -DQ alleles on autoantibody recognition of distinct epitopes within the juxtamembrane domain of the IA-2 autoantigen in type 1 diabetes. *Diabetologia* 2016;59:334-340.
237. Arnett FC, Gourh P, Shete S, et al. Major histocompatibility complex (MHC) class II alleles, haplotypes and epitopes which confer susceptibility or protection in systemic sclerosis: analyses in 1300 Caucasian, African-American and Hispanic cases and 1000 controls. *Ann Rheum Dis* 2010;69:822-827.
238. Ciubotariu R, Liu Z, Colovai AI, et al. Persistent allopeptide reactivity and epitope spreading in chronic rejection of organ allografts. *J Clin Invest* 1998;101:398-405.
239. Liu Z, Colovai AI, Tugulea S, et al. Indirect recognition of donor HLA-DR peptides in organ allograft rejection. *J Clin Invest* 1996;98:1150-1157.
240. Mitchison NA. The carrier effect in the secondary response to hapten-protein conjugates. II. Cellular cooperation. *Eur J Immunol* 1971;1:18-27.
241. Watts C, Lanzavecchia A. Suppressive effect of antibody on processing of T cell epitopes. *J Exp Med* 1993;178:1459-1463.
242. Leite MI, Coutinho E, Lana-Peixoto M, et al. Myasthenia gravis and neuromyelitis optica spectrum disorder: a multicenter study of 16 patients. *Neurology* 2012;78:1601-1607.

243. Louveau A, Smirnov I, Keyes TJ, et al. Structural and functional features of central nervous system lymphatic vessels. *Nature* 2015;523:337-341.
244. Nirula A, Glaser SM, Kalled SL, Taylor FR. What is IgG4? A review of the biology of a unique immunoglobulin subtype. *Curr Opin Rheumatol* 2011;23:119-124.
245. de Jong BG, H IJ, Marques L, et al. Human IgG2- and IgG4-expressing memory B cells display enhanced molecular and phenotypic signs of maturity and accumulate with age. *Immunol Cell Biol* 2017;95:744-752.
246. Mueller SH, Farber A, Pruss H, et al. Genetic predisposition in anti-LGI1 and anti-NMDA receptor encephalitis. *Ann Neurol* 2018;83:863-869.
247. Wilson R, Menassa DA, Davies AJ, et al. Seronegative antibody-mediated neurology after immune checkpoint inhibitors. *Ann Clin Transl Neurol* 2018;5:640-645.
248. Chicz RM, Urban RG, Gorga JC, Vignali DA, Lane WS, Strominger JL. Specificity and promiscuity among naturally processed peptides bound to HLA-DR alleles. *J Exp Med* 1993;178:27-47.
249. Vogt AB, Kropshofer H, Kalbacher H, et al. Ligand motifs of HLA-DRB5*0101 and DRB1*1501 molecules delineated from self-peptides. *J Immunol* 1994;153:1665-1673.
250. Ghosh P, Amaya M, Mellins E, Wiley DC. The structure of an intermediate in class II MHC maturation: CLIP bound to HLA-DR3. *Nature* 1995;378:457-462.
251. Stern LJ, Brown JH, Jardetzky TS, et al. Crystal structure of the human class II MHC protein HLA-DR1 complexed with an influenza virus peptide. *Nature* 1994;368:215-221.
252. Andreatta M, Karosiene E, Rasmussen M, Stryhn A, Buus S, Nielsen M. Accurate pan-specific prediction of peptide-MHC class II binding affinity with improved binding core identification. *Immunogenetics* 2015;67:641-650.
253. Ramberger M, Hogl B, Stefani A, Mitterling T, Reindl M, Lutterotti A. CD4+ T-Cell Reactivity to Orexin/Hypocretin in Patients With Narcolepsy Type 1. *Sleep* 2017;40.
254. Mata MM, Mahmood F, Sowell RT, Baum LL. Effects of cryopreservation on effector cells for antibody dependent cell-mediated cytotoxicity (ADCC) and natural killer (NK) cell activity in (51)Cr-release and CD107a assays. *J Immunol Methods* 2014;406:1-9.
255. Latorre D, Kallweit U, Armentani E, et al. T cells in patients with narcolepsy target self-antigens of hypocretin neurons. *Nature* 2018;562:63-68.
256. Moiola L, Karachunski P, Protti MP, Howard JF, Jr., Conti-Tronconi BM. Epitopes on the beta subunit of human muscle acetylcholine receptor recognized by CD4+ cells of myasthenia gravis patients and healthy subjects. *J Clin Invest* 1994;93:1020-1028.
257. Nagvekar N, Jacobson LW, Willcox N, Vincent A. Epitopes expressed in myasthenia gravis (MG) thymomas are not recognized by patients' T cells or autoantibodies. *Clin Exp Immunol* 1998;112:17-20.
258. Lovitch SB, Walters JJ, Gross ML, Unanue ER. APCs present A beta(k)-derived peptides that are autoantigenic to type B T cells. *J Immunol* 2003;170:4155-4160.
259. Barlow AK, He X, Janeway C, Jr. Exogenously provided peptides of a self-antigen can be processed into forms that are recognized by self-T cells. *J Exp Med* 1998;187:1403-1415.
260. Pu Z, Carrero JA, Unanue ER. Distinct recognition by two subsets of T cells of an MHC class II-peptide complex. *Proc Natl Acad Sci U S A* 2002;99:8844-8849.
261. Pu Z, Lovitch SB, Bikoff EK, Unanue ER. T cells distinguish MHC-peptide complexes formed in separate vesicles and edited by H2-DM. *Immunity* 2004;20:467-476.
262. Mohan JF, Petzold SJ, Unanue ER. Register shifting of an insulin peptide-MHC complex allows diabetogenic T cells to escape thymic deletion. *J Exp Med* 2011;208:2375-2383.

263. Sadegh-Nasseri S, Kim A. MHC Class II Auto-Antigen Presentation is Unconventional. *Front Immunol* 2015;6:372.
264. Corkum CP, Ings DP, Burgess C, Karwowska S, Kroll W, Michalak TI. Immune cell subsets and their gene expression profiles from human PBMC isolated by Vacutainer Cell Preparation Tube (CPT) and standard density gradient. *BMC Immunol* 2015;16:48.
265. Valitutti S, Lanzavecchia A. Serial triggering of TCRs: a basis for the sensitivity and specificity of antigen recognition. *Immunol Today* 1997;18:299-304.
266. Viola A, Lanzavecchia A. T cell activation determined by T cell receptor number and tunable thresholds. *Science* 1996;273:104-106.
267. Boehncke WH, Takeshita T, Pendleton CD, et al. The importance of dominant negative effects of amino acid side chain substitution in peptide-MHC molecule interactions and T cell recognition. *J Immunol* 1993;150:331-341.
268. Kersh GJ, Allen PM. Structural basis for T cell recognition of altered peptide ligands: a single T cell receptor can productively recognize a large continuum of related ligands. *J Exp Med* 1996;184:1259-1268.
269. Deuschl G, Bain P, Brin M. Consensus statement of the Movement Disorder Society on Tremor. Ad Hoc Scientific Committee. *Mov Disord* 1998;13 Suppl 3:2-23.
270. Albanese A, Bhatia K, Bressman SB, et al. Phenomenology and classification of dystonia: a consensus update. *Mov Disord* 2013;28:863-873.
271. Meyers R. Ballismus. In: Vinken PJ BG, editors. Handbook of clinical neurology. North-Holland, Amsterdam1968.
272. Barbeau A, Duvoisin RC, Gerstenbrand F, Lakke JP, Marsden CD, Stern G. Classification of extrapyramidal disorders. Proposal for an international classification and glossary of terms. *J Neurol Sci* 1981;51:311-327.
273. Baizabal-Carvallo JF, Cardoso F, Jankovic J. Myorhythmia: phenomenology, etiology, and treatment. *Mov Disord* 2015;30:171-179.
274. Yaltho TC, Jankovic J. The many faces of hemifacial spasm: differential diagnosis of unilateral facial spasms. *Mov Disord* 2011;26:1582-1592.
275. Averbuch-Heller L, Remler B. Opsoclonus. *Semin Neurol* 1996;16:21-26.
276. Daroff RB MJ. Neurology in Clinical Practice: Elsevier Health Sciences, 2012.
277. Liepmann H. Die perseveration. In: Liepmann H e. Ueber Storungen des Handelns bei Gerhirnkranken. Berlin: Karger, 1905.
278. Fung VS, Morris JG, Leicester J, Soo YS, Davies L. Clonic perseveration following thalamofrontal disconnection: a distinctive movement disorder. *Mov Disord* 1997;12:378-385.

10 Appendix

10.1 Appendix A

MD Glossary (Modified from Mohammad et al[6])

Tremor: The consensus statement of the movement disorder society on tremor defines it as "Tremor is a rhythmic back-and-forth or oscillating involuntary movement about a joint axis."[269]

Action tremor: Action tremor is any tremor that is produced by voluntary contraction of muscle, including postural, isometric, and kinetic tremor. The latter includes intention tremor (also known as terminal kinetic tremor).[269]

Dystonic tremor: A spontaneous oscillatory, rhythmical, although often inconstant, patterned movement produced by contractions of dystonic muscles often exacerbated by an attempt to maintain primary (normal) posture. The dystonic tremor may not be relieved by allowing the abnormal dystonic posture to fully develop without resistance ("null point"). Dystonic tremor may be difficult to distinguish from other types of tremor.[270]

Rest tremor: Rest tremor is defined by tremor that occurs in a body part that is not voluntarily activated and is completely supported against gravity.[269]

Athetosis: Athetosis is a slow, continuous, involuntary writhing movement that prevents maintenance of a stable posture. In contrast to chorea, in athetosis the same regions of the body are repeatedly involved.[141]

Ballism: Repetitive, but constantly varying, large amplitude involuntary movements of the proximal parts of the limbs. This activity is almost ceaseless and movements are often complex and combined.[271]

Chorea: The ad hoc Committee on Classification of the World Federation of Neurology has defined chorea as "a state of excessive, spontaneous movements, irregularly timed, non-repetitive, randomly distributed and abrupt in character. These movements may vary in severity from restlessness with mild intermittent exaggeration of gesture and expression, fidgeting movements of the hands, unstable dance-like gait to a continuous flow of disabling, movements with a continuum into ballism, where ballism is a more proximal form of chorea.[272]

Dystonia: A Consensus Committee was established under the auspices of the Dystonia Medical Research Foundation, the Dystonia Coalition, and the European Dystonia Cooperation in Science and Technology (COST) Action which proposed the following definition of Dystonia: “Dystonia is a movement disorder characterized by sustained or intermittent muscle contractions causing abnormal, often repetitive, movements, postures, or both. Dystonic movements are typically patterned, twisting, and may be tremulous. Dystonia is often initiated or worsened by voluntary action and associated with overflow muscle activation.”[270]

Myoclonus: Myoclonus is a sequence of repeated, often non-rhythmic, brief shock-like jerks due to sudden involuntary contraction (positive myoclonus) or relaxation (negative myoclonus or asterixis) of one or more muscles.[141]

Tics: Tics are repeated, individually recognizable, intermittent movements or movement fragments that are almost always briefly suppressible and are usually associated with awareness of an urge to perform the movement.[141]

Stereotypy: Stereotypy has been defined variably over the years. The latest proposed definition from Edwards et.al defines stereotypy as "a non–goal-directed movement pattern that is repeated continuously for a period of time in the same form and on multiple occasions, and which is typically distractible"[143.] However, a widely accepted definition from Jankovic defines stereotypy as: "involuntary or unvoluntary, coordinated, patterned, repetitive, rhythmic, purposeless but seemingly purposeful or ritualistic movement, posture or utterance."[144]

Myorhythmia: Is defined as a repetitive, rhythmic, frequently jerky movement with a slow (1-4Hz) frequency, primarily affecting cranial and limb muscles. It typically occurs at rest but can occur with maintenance of posture and voluntary movements, disappearing with sleep.[273]

Akathisia: Akathisia refers to a subjective feeling of inner restlessness, prompting movement in order to reduce to relieve this feeling. Motor corollary are often complex and repetitive and can involve almost any part of the body.

Myokymia: Myokymia is characterised by persistent undulating muscle quivering associated with non-rhythmic, irregular bursts of normal motor unit potentials usually occurring in doublets or triplets, with a broad range (5-150 Hz) of frequencies. Myokymia most often

involves the eyelids but can affect other facial muscles.[274]

Opsoclonus: Opsoclonus can be defined as the intrusion into fixation of involuntary, repetitive, rapid, multi-vectorial, conjugate ocular saccades that are irregular in amplitude and frequency and occur in all directions without intersaccadic interval.[275]

Perseveration: It can be defined as the inappropriate persistence of word, thought, or action in response to a given stimulus. *Motor perseveration* is the inability to stop a movement or a series of movements after the task is complete. In recurrent motor perseveration, the patient persistently returns to a previously completed motor program, and in afferent or continuous motor perseveration, the patient cannot end a recently completed motor program.[276]

Clonic perseveration: In clonic perseveration a performance, once initiated, is repeated indefinitely without interruption; for example, the patient may continuously repeat letters when writing a word or continue to draw circles though asked to draw only one.[277]

Intentional perseveration: In intentional perseveration a performance is repeated when, and only when, a new performance is intended. An example, cited by Liepmann, is the patient who has blown out a flame and in the subsequent performance of different duties repeats the blowing movement.

Tonic perseveration: Tonic perseveration refers to persistence of a muscle contraction once initiated in the absence of an ongoing cue. An example, cited by Liepmann is the patient who having grasped an object cannot voluntarily relax the hand although the effort is made to do so.[278]

Bradykinesia/Akinesia: Bradykinesia is characterized by slowness of movement and has been linked to Parkinson's disease and other disorders of the basal ganglia. Rather than being a slowness in initiation (akinesia), bradykinesia describes a slowness in the execution of movement and a decrease in its amplitude.

Akinesia is the inability to initiate movement due to difficulty selecting and/or activating motor programs in the central nervous system.

We use the term akinesia as an umbrella term similar to previous usage[137] to include bradykinesia (slowness of movement) and hypokinesia (poverty of movement, and movements that are smaller than intended), and the progressive fatiguing and decrement of repetitive alternating movements seen during finger or foot tapping[4].

Catatonia: This has recently been redefined in DSM-5[142] as the presence of three or more of:

- Catalepsy – passive induction of a posture held against gravity
- Waxy flexibility – slight and even resistance to positioning by examiner
- Stupor – no psychomotor activity; not actively relating to environment
- Agitation – not influenced by external stimuli
- Mutism – no, or very little verbal response – NB not applicable if established aphasia
- Negativism – opposing or not responding to instructions or external stimuli
- Posturing - spontaneous and active maintenance of a posture against gravity
- Mannerisms – odd caricature of normal actions
- Stereotypies – repetitive, abnormally frequent, non-goal directed movements
- Grimacing
- Echolalia/Echopraxia – mimicking another's speech/movements respectively

10.2 Appendix B

Data Collection Sheet

	video 1		video 2		video 3		video 4	
	dominant (D) or associated (A)?*	Distribution	dominant (D) or associated (A)?*	Distribution	dominant (D) or associated (A)?*	Distribution	dominant (D) or associated (A)?*	Distribu
dystonia								
chorea								
myoclonus								
clonic perseveration								
ballism								
tonic perseveration								
tremor								
stereotypies								
bradykinesia / akinesia								
other - please specify								
None								
Can you provide 3 alternative diagnoses which would be consistent with this movement disorder, in order of likelihood?	1. disorder X		1. disorder X		1. disorder X		1. disorder X	
	2. disorder Y		2. disorder Y		2. disorder Y		2. disorder Y	
	3. disorder Z		3. disorder Z		3. disorder Z		3. disorder Z	